ISSN: 2382-6533 (Print)
ISSN: 2424-810X (Online)
Volume 12· Issue 1
February 2026

Journal of Clinical and Translational Research

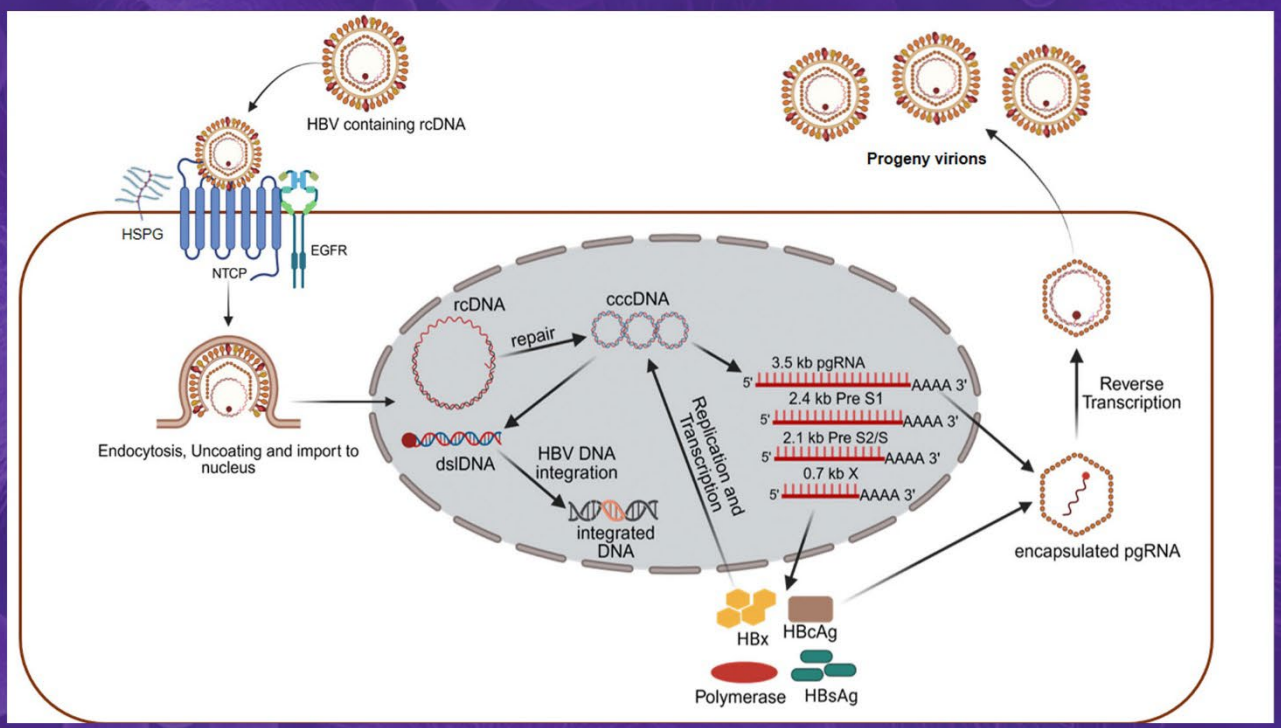

ACCSCIENCE PUBLISHING

ABOUT JCTR

Aims and scope

The Journal of Clinical and Translational Research (JCTR) is an open access, peer-reviewed, multidisciplinary scientific journal that publishes studies with at least an ex vivo, in vivo, or clinical component. The published research is centered on any clearly defined clinical problem, which may comprise a disease or the basis of disease, a form of therapy or intervention, and clinical diagnostics or prognostics. Articles (original research, reviews, technical reports, medical hypotheses, commissioned articles, special issue articles, and editorials) are published continuously online and bimonthly in print. Studies performed in cells only will generally not be accepted unless they contain critical data that are in line with the scope of the journal. Some examples of such studies include molecular pathways that lie at the basis of a disease, novel biotechnological approaches for e.g., the production of drugs, or new techniques that improve clinical diagnostics and prognostics. Articles that combine preclinical and clinical data are given priority. Contributions from academic institutions and industry are welcome.

The research areas that JCTR covers include but are not limited to:

Internal medicine (all branches)
Vascular medicine and phlebology
Oncology
Cardiology
Intensive care medicine
Ophthalmology
Neurology and neurosciences
Anatomy, physiology, and embryology
Pathology
Clinical physics
Epidemiology
Medical devices
Pharmacology
Microbiology
Parasitology
Biomedical spectroscopy and spectrometry
Gastroenterology and hepatology
Surgery and transplantation
Hematology
Nephrology
Dermatology
Endocrinology and metabolism
Anesthesiology
Radiology and nuclear medicine
Clinical chemistry
Genetics and epigenetics
Global health
Nutrition
Immunology
Virology
Biomedical engineering

Key features

- Open access
- Reputable international editorial board
- Easy and fast submissions - no formatting rules (“your paper, your way”)
- No word count or reference restrictions
- Double blind review process to minimize bias
- Rapid online publication of articles upon acceptance
- Outlet for academic institutions and industry

Indexing

The Journal of Clinical and Translational Research is currently indexed by Chemical Abstract Service, Google Scholar, CNKI, and Peking University Library, and is currently working towards being indexed (PubMed, Science Citation Index Expanded, BIOSIS, Scopus, etc.).

Volume 12 • Issue 1 • February 2026
ISSN 2382-6533 (print) ISSN 2424-810X (online)

JOURNAL OF CLINICAL AND TRANSLATIONAL RESEARCH

ACCSCIENCE PUBLISHING

Journal of Clinical and Translational Research

Editorial Board

ACCSCIENCE PUBLISHING

Volume 12 | Issue 1 | February 2026 | Page 1 – 94 |

Journal of Clinical and Translational Research

https://accscience.com/journal/jctr

CONTENTS

ACCSCIENCE PUBLISHING

Journal of Clinical and Translational Research

EDITORIAL

Recent progress in human embryology

Jacek Z. Kubiak[1,2*]

[1]Institute of Genetics and Development of Rennes, UMR 6290 CNRS/University of Rennes, Faculty of Medicine, Rennes, France

[2]Laboratory of Molecular Oncology and Innovative Therapies, Military Institute of Medicine-National Research Institute (WIM-PIB), Szaserow, Warszawa, Poland

1. (Pre)history of embryology

Human embryology has developed through several major periods, each marked by different philosophical approaches, technological advances, and scientific breakthroughs.

Hippocrates (460–370 BC) wrote the first recorded embryological research on obstetrics and gynecology, proposing that embryos developed by extracting moisture and breath from the mother. Aristotle (384–322 BC) advanced the field through observational science, opening bird eggs at different developmental stages and dissecting mammalian embryos. He proposed epigenesis—the theory that organisms develop progressively from undifferentiated material.

During the Renaissance, Leonardo da Vinci (1452-1519) made quantitative measurements and was the first to demonstrate that embryos undergo changes in weight, size, and shape over time. William Harvey (1578–1657) examined deer and chicken embryos with low-powered lenses, identifying the blastoderm as the origin of the embryonic body.

Until the 18th century, preformationism dominated. It was the belief that organisms developed from pre-existing miniature versions of themselves, including the idea of a tiny "homunculus" hidden in the sperm head. This view was challenged by Caspar Friedrich Wolff (1733–1794), who argued for epigenesis in his landmark 1759 work, "Theory of Generation."[1] Only Karl Ernst von Baer's (1792-1876) observations of the mammalian ovum, dated to the year 1827, marked the birth of modern embryology. Next, von Baer and Heinz Christian Pander (1794-1865) developed the germ layer theory, explaining how embryos develop in progressive steps.

2. Real human embryology

Wilhelm His (1880–1904), a Swiss anatomist considered the founder of human embryology, published detailed side views of human embryos from 15 days to 8.5 weeks. Franklin Mall (1862-1917) began collecting human embryos at Johns Hopkins University in 1887, creating the Carnegie Collection, which now holds over 10,000 specimens. The Carnegie Institution of Washington established the first research institution devoted specifically to embryology at Johns Hopkins in 1914. This period saw the first descriptions of human embryos from the first 2 weeks after fertilization and elucidation of ovulation timing.

After World War II, human embryology declined as developmental biology shifted its focus to model organisms, such as flies, frogs, sea urchins, and mice, where experimental manipulation was easier. Embryologists believed that by describing the embryonic development of mice, rats, sheep, and cows, they could obtain information

***Corresponding author:**
Jacek Z. Kubiak
(jacek.kubiak@univ-rennes1.fr)

Citation: Kubiak JZ. Recent progress in human embryology. *J Clin Transl Res.* 2026;12(1):1-3. doi: 10.36922/JCTR026050007

Received: January 28, 2026

Published online: February 20, 2026

that could easily be extrapolated to human development. This was a highly convenient way of thinking, as it allowed them to study human development *per procura*, thereby circumventing the religious taboo against interfering with the dignity of a human being, which lasted from natural conception to natural death. However, this was false thinking, as it quickly became clear that, despite striking similarities, each mammalian embryo also has its own unique characteristics, requirements, and cellular and molecular mechanisms. Full extrapolation turned out to be an illusion.

3. The *in vitro* fertilization (IVF) breakthrough

The birth of the first IVF baby in 1978, thanks to Robert Edwards, Patrick Steptoe, and Jean Purdy, revolutionized access to early human embryos. The 1990 United Kingdom Human Fertilisation and Embryology Act permitted research on donated embryos up to 14 days. Biobanks, such as the Human Developmental Biology Resource in Newcastle and London provided ethical supplies of post-implantation embryos from pregnancy terminations. Embryology returned to the era of Leonardo da Vinci, but this time the objects of research were real human embryos.

The discovery of DNA structure in the 1950s launched molecular developmental biology, and the establishment of human embryonic stem cell lines in 1998 revolutionized regenerative medicine research. Recent advances, including synthetic embryo models, optogenetic control of development, and Clustered Regularly Interspaced Short Palindromic Repeats gene editing in human embryos, have brought us to the cutting-edge achievements of recent years.

Human embryology has thus evolved from philosophical speculation to detailed molecular understanding over approximately 2,400 years of inquiry. From this perspective, let us look at the major recent achievements in human embryology.

4. First complete visualization of human embryo implantation and advanced synthetic embryo models

Researchers achieved the first real-time observation of the entire sequence of human implantation using artificial uterine tissue in microfluidic chips.[2-5] This breakthrough allowed scientists to observe embryos burrow into lab-recreated womb tissue, revealing previously hidden details about this critical early pregnancy stage. Researchers utilized synthetic embryo models (blastoids) derived from human embryonic stem cells to study implantation without using actual embryos. Multiple teams created increasingly sophisticated stem cell-based embryo models that replicate early human development without fertilization, improving both reproducibility and accuracy. These synthetic embryology models allow researchers to study developmental stages that were previously inaccessible due to ethical and technical restrictions, addressing a significant cause of infertility and miscarriage.

5. Optogenetic control of embryonic development

Scientists have developed light-controlled embryo models that revealed the fundamental interplay between mechanical forces and chemical signals during gastrulation.[6] Using engineered human embryonic stem cells that respond to specific light wavelengths, researchers discovered that chemical cues alone, such as bone morphogenetic protein 4 (BMP4), are insufficient; proper mechanical conditions are also essential for cells to organize into the body's basic structure. This work from Rockefeller University demonstrated that gastrulation requires both chemical signals (like BMP4) and mechanical forces, using light-activated synthetic embryo models.

6. Artificial intelligence (AI)-powered embryo selection

New AI algorithms can select embryos with the best developmental potential using only a single time-lapse image, surpassing the capabilities of contemporary embryologists. The two 2025 reviews show continued improvements with newer algorithms achieving 77–92% accuracy in clinical pregnancy prediction.[7,8] This technology promises to give couples undergoing IVF a much better chance of success.

7. Pre-implantation genetic testing success

Studies have demonstrated the successful use of pre-implantation genetic testing for monogenic disorders to prevent the transmission of inherited kidney diseases, including autosomal dominant polycystic kidney disease, Alport syndrome, and other monogenic kidney disorders, with live births of healthy children reported.[9,10] This highlights the growing potential to eliminate hereditary diseases before pregnancy. Such achievements collectively represent a transformative year for understanding early human development, with major implications for treating infertility, preventing miscarriages, and developing regenerative therapies.

While writing this editorial, I learned that the US National Institutes of Health (NIH) will stop funding research involving human fetal tissues.[11,12] This

announcement represents a significant hindrance to the development of human embryology, stem cell research, regenerative medicine, and the treatment of infectious, chronic, and neurodegenerative diseases and conditions. This marks another negative turn in the history of human embryology and developmental biology, at least in the USA.

Conflict of interest

Jacek Z. Kubiak is the Editor-in-Chief of this journal, but was not in any way involved in the editorial and peer-review process conducted for this paper, directly or indirectly. The author declared that he has no known competing financial interests or personal relationships that could have influenced the work reported in this paper.

References

1. Witt E. Form-a matter of generation: the relation of generation, form, and function in the epigenetic theory of Caspar F. Wolff. Sci Context. 2008;21(4):649-664.

   doi: 10.1017/s0269889708001993

2. Song J, Zhao R, Zhang Y, *et al*. 3D post-implantation co-culture of human embryo and endometrium. *Cell Stem Cell*. 2026;33(1):58-72.e7.

   doi: 10.1016/j.stem.2025.12.002

3. Li Q, Yuan Y, Zhao W, *et al*. A 3D *in vitro* model for studying human implantation and implantation failure. *Cell*. 2026;189(1):70-86.e20.

   doi: 10.1016/j.cell.2025.10.026

4. Molè MA, Elderkin S, Zorzan I, *et al*. Modeling human embryo implantation *in vitro*. *Cell*. 2026;189(1):87-105.e28.

   doi: 10.1016/j.cell.2025.10.027

5. Shibata S, Endo S, Nagai LAE, *et al*. Modeling embryo-endometrial interface recapitulating human embryo implantation. *Sci Adv*. 2024;10(8).

   doi: 10.1126/sciadv.adi4819

6. De Santis R, Jutras-Dubé L, Bourdrel S, Rice E, Piccolo FM, Brivanlou AH. Crosstalk between tissue mechanics and BMP4 signaling regulates symmetry breaking in human gastrula models. *Cell Stem Cell*. 2025;32(11):1691-1704.e6.

   doi: 10.1016/j.stem.2025.09.006

7. Olawade DB, Teke J, Adeleye KK, Weerasinghe K, Maidoki M, Clement David-Olawade A. Artificial intelligence in *in-vitro* fertilization (IVF): A new era of precision and personalization in fertility treatments. *J Gynecol Obstet Human Reprod*. 2025;54(3):102903.

   doi: 10.1016/j.jogoh.2024.102903

8. Shoham Z. Artificial intelligence in reproductive medicine: Transforming assisted reproductive technologies. *J IVF-Worldwide*. 2025;3(2):1-8.

   doi: 10.46989/001c.137620

9. Knoers NVAM. Prenatal and preimplantation genetic testing for monogenic kidney disorders. *Kidney Int*. 2025;107(2):255-261.

   doi: 10.1016/j.kint.2024.06.031

10. Liu X, Zhang Q, Cao K, *et al*. Preimplantation genetic testing for monogenic disorders (PGT-M) for monogenic nephropathy: A single-center retrospective cohort analysis. *Clin Kidney J*. 2024;18(1):sfae356.

    doi: 10.1093/ckj/sfae356

11. Ledford H, Chen E. NIH ends support for most human fetal-tissue research - dismaying some scientists. *Nature*. 2026.

    doi: 10.1038/d41586-026-00251-2

12. Now is not the time to defund human fetal tissue research. *Nature*. 2026;650(8100):8.

    doi: 10.1038/d41586-026-00308-2

ACCSCIENCE PUBLISHING

Journal of Clinical and Translational Research

REVIEW ARTICLE

Harnessing the gut microbiome for therapeutic interventions

Zoha Waheed Abbasi[1†], Sania Ikram[1†], Muneeb Ullah[2], Aftab Ahmad[1], Irfan Ali[1], and Muhammad Naeem[1*]

[1]Department of Biological Sciences, National University of Medical Sciences, Islamabad, Punjab, Pakistan

[2]College of Pharmacy, Pusan National University, Geoumjeong-gu, Busan, Republic of Korea

Abstract

Background: Gut microbiome comprises a diverse microbial community, including bacteria, viruses, and fungi, which play a crucial role in human health. These microbes contribute to host well-being by producing beneficial compounds such as short-chain fatty acids and other metabolites that help maintain microbial homeostasis. Recent advancements in high-throughput sequencing techniques have identified key microbes crucial for human health and revealed that an imbalance in these communities—known as dysbiosis—can lead to various diseases, including inflammatory bowel disease (IBD), Crohn's disease, colorectal cancer, type 2 diabetes, and liver diseases. **Aim:** This review aims to provide a comprehensive overview of emerging microbiome-based therapeutic strategies, including fecal microbiota transplantation (FMT), prebiotics, probiotics, next-generation probiotics, synthetic microbiome transplantation, and microbiome editing therapies, as potential interventions to restore gut microbial balance and improve health outcomes. **Relevance for patients:** Microbiome-based therapies have emerged as promising tools for restoring gut homeostasis and managing microbiome-associated diseases. Approaches such as FMT have shown clinical benefits in conditions such as IBD, *Clostridium difficile* infection, and cancer immunotherapy. Understanding these therapies may guide future personalized treatments aimed at improving patient outcomes through modulation of the gut microbiome.

Keywords: Synthetic microbiome transplantation; Microbiome editing therapies; Inflammatory bowel disease; Next-generation probiotics

†These authors contributed equally to this work.

***Corresponding author:**
Muhammad Naeem
(m.naeem@numspak.edu.pk)

Citation: Abbasi ZW, Ikram S, Ullah M, Ahmad A, Ali I, Naeem M. Harnessing the gut microbiome for therapeutic interventions. *J Clin Transl Res.* 2026;12(1):4-21. doi: 10.36922/JCTR025390067

Received: September 27, 2025

Revised: December 26, 2025

Accepted: January 19, 2026

Published online: February 6, 2026

1. Introduction

Humans have historically exploited microbes for a variety of purposes, from the fermentation of food to the heterologous synthesis of pharmaceutically useful substances such as insulin and antibiotics.[1-3] This long-lasting fascination eventually extended to the invisible microbial world within the human body, where the idea that microorganisms could shape human health sparked a new scientific frontier.[4] Reflecting how human curiosity often drives scientific discovery, this advancement led to a deeper understanding of the gastrointestinal (GI) tract, which was once viewed merely as the digestive system

but is now recognized as a significant contributor to human health and disease.[5] This shift in perspective stems from the recognition of the gut microbiome as a highly evolved and heterogeneous community of bacteria, fungi, viruses, and archaea that plays a major role in regulating physiological and metabolic processes by influencing both health maintenance and disease progression.[6]

Among the gut microbes, bacteria are the most prevalent, with the majority comprising obligate and facultative anaerobes. This dominant bacterial population is largely represented by four major phyla: Firmicutes (formerly Bacillota), Bacteroidetes (Bacteroidota), Actinobacteria (Actinomycetota), and Proteobacteria (Pseudomonadota), which together comprise approximately 90% of the total bacterial population in the gut.[7,8] These microbes perform diverse functions, ranging from digestion and nutrient metabolism to immune modulation and even the gut–brain axis communication. The metabolic capabilities of these microbes are particularly noteworthy, as they enable the breakdown of non-digestible carbohydrates to short-chain fatty acids (SCFAs), such as acetate, propionate, and butyrate.[9,10] SCFAs not only act as a source of energy but also play functions in gut integrity, immune system, cardiovascular system, metabolic homeostasis, and neurophysiological function. Beyond metabolic versatility, the gut microbiome also serves as a vital source of micronutrients essential for host physiology. It includes the synthesis of essential vitamins such as folate, riboflavin, cobalamin, niacin, pantothenate, and pyridoxine.[11-13] These micronutrients are important for essential processes, including DNA synthesis, energy metabolism, and neurotransmission, highlighting the vital role of the microbiome in sustaining health.[14]

Given the pivotal role of gut microbiota in maintaining homeostasis, any imbalance in its composition results in dysbiosis. Recent studies confirmed that dysbiosis is associated with the pathogenesis of numerous illnesses, including metabolic syndromes (obesity and diabetes), autoimmune diseases, GI disorders, and neuropsychiatric conditions.[15-17] This knowledge has brought a turnover in medicine, positioning the gut microbiome as a potential therapeutic target for the management and treatment of a variety of diseases. Scientists and clinicians have progressively discovered ways to harness this microbial community. Interferences range from simple strategies of dietary modifications and prebiotic or probiotic supplementation to complex approaches such as fecal microbiota transplantation (FMT) and microbiome-based drug development.[18,19] Whole genome analysis of bacterial species has recognized meanings attributed to strains, and integrating those strains in microbiome-based therapies has shown a noteworthy potential in enlightening health conditions.[20,21] Building on these discoveries, a major focus has shifted toward modified microbiome-based involvement. The probability of adapting treatments based on an individual's exceptional microbiome conformation heralds an era of precision medicine where interferences are custom-made to amplify efficiency and diminish side effects.[22,23]

The interaction between the host and the resident microorganisms has been increasingly elucidated with the advancement of molecular techniques, such as metagenomics, transcriptomics, and metabolomics, providing deeper insights into microbial communities and their molecular mechanisms.[24-27] Disruption in these microbial communities is characterized by alterations in microbial composition, including an increase in pro-inflammatory species and a decrease in anti-inflammatory species.[28-31] Restoration of a dysbiotic gut can be achieved through several approaches, including lifestyle modifications such as diet, exercise, and hygiene practices.[32] Beyond lifestyle modification, microbiome-based therapies have emerged as a promising candidate to restore microbial balance. These therapies involve the administration of prebiotics, probiotics, and post-biotics, as well as FMT.[33-35] Emerging therapeutic tools, such as the generation of probiotics and engineered microbial consortia, are gaining attention for their ability to more precisely target dysbiosis and modulate host health.[36-38] These innovative approaches represent a significant leap forward in tailoring microbiome intervention for specific health conditions. A general overview is illustrated in Figure 1. This review comprehensively overviews the microbiome-based therapies, signifying a transformative method in addressing some of the most interesting health problems. It aims to discuss the recent developments in the field of microbiome-driven therapeutics, highlight the challenges that must be overcome, and propose future directions. By addressing these gaps and fostering innovative approaches, microbiome-based therapies have the potential to become the keystone of precision medicine, offering personalized and sustainable solutions for a broad spectrum of diseases.

2. Microbiome-based therapeutic strategies

Microbiome-based strategies aim to restore microbial balance, enhance immunity, improve metabolism, and fight pathogens, moving toward personalized medicines. This leverages the gut–brain axis and immune system connections. Methods such as probiotics, prebiotics, and synbiotics administration, as well as FMT, gene editing,

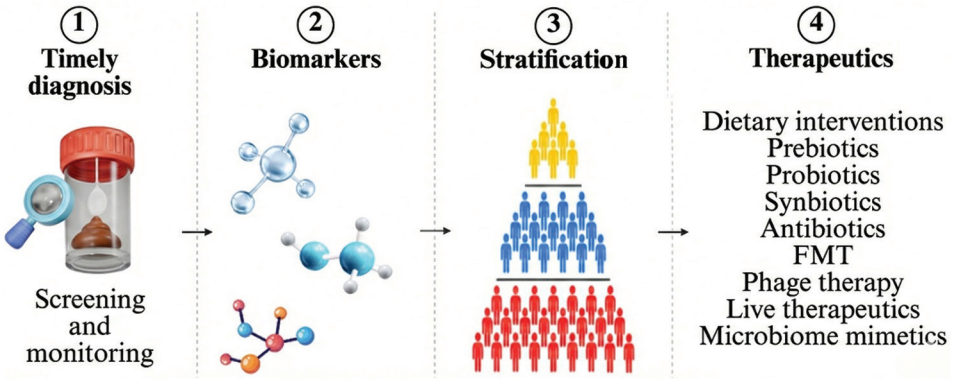

Figure 1. Summary of the various medical applications of the microbiome. Microbiota roles include serving as biomarkers for patient screening, monitoring, and stratification, as well as being used in therapeutic approaches. Created with BioRender.com. Ikram S. (2025).

engineered microbes, and personalized diets, aim to target specific diseases or enhance well-being.

2.1. Fecal microbiota transplantation

In recent studies, FMT has emerged as the ground-breaking therapy revolutionizing gut health by restoring microbial balance and offering hope where conventional treatment falls short. Originally rooted in traditional Chinese medicine, FMT was rediscovered by modern medicine in the 20th century.[39,40] This therapy involves transferring the entire fecal material from the donor to the patient through various routes, aiming to restore gut microbial diversity and treat various conditions.[41-43] It can be administered either through the upper GI tract, such as the duodenal tube, through oral capsule, or lower GI tract using colonoscopy or enema.[43,44] For FMT to be effective, the transplanted microbes must colonize and persist in the GI tract to achieve long-term therapeutic benefits. Donor selection and diet play a crucial role in determining microbial colonization, as a diverse and resilient microbiota enhances engraftment success.[45-47]

Studies on inflammatory bowel disease (IBD) patients have shown that FMT induces a significant shift in gut microbiota composition, increasing the abundance of *Bacteroides, Faecalibacterium*, and butyrate-producing bacteria, aligning the recipient microbiome more closely with that of the donor.[48] Butyrate, an SCFA produced by gut bacteria, plays a key role in gut health by exerting anti-inflammatory effects, strengthening gut-barrier integrity, and modulating immune response.[49-51] In patients with *Clostridium difficile* infection, a significant increase in alpha diversity is observed post-FMT. Notably, 92.1% of patients successfully resolved the infection, restoring normal bowel patterns. The microbial composition shifted toward the healthier state with a notable increase in key taxa, including *Bacteroides, Faecalibacterium, Blautia*, and *Enterobacter*, contributing to gut microbiome recovery.[52,53]

Beyond infections, gut dysbiosis can also promote tumorigenesis through multiple mechanisms, including chronic inflammation, DNA damage, and immune modulation.[54,55] Pathogenic bacteria such as *Escherichia coli* promote tumor progression by producing genotoxins (e.g., colibactin) and activating inflammatory pathways, including nuclear factor-kappa B (NF-κB), signal transducer and activator of transcription 3 (STAT-3), along with pro-inflammatory cytokines such as interleukin (IL)-17 and tumor necrosis factor-alpha (TNF-α).[56,57] These cations contribute to the creation of a tumor-promoting micro-environment through immune modulation, as represented in Figure 2.

Fecal microbiota transplantation has shown promise in cancer immunotherapy, particularly programmed cell death protein 1 (PD-1) inhibitors.[58,59] By modulating the gut microbiota, FMT enhances cytotoxic T-cells activation and their infiltration into the tumor microenvironment, thereby promoting anti-tumor immune response.[60-62] Phase 2 clinical trials have demonstrated that combining FMT with anti-PD-1 monoclonal antibody tislelizumab and vascular endothelial growth factor receptor (VEGFR) inhibitor fruquintinib improved survival in refractory microsatellite stable, metastatic colorectal cancer patients, with a median progression-free survival of 9.6 months and overall survival of 13.7 months.[63,64] Responders exhibited distinct gut microbiota signatures, including an abundance of Proteobacteria and Lachnospiraceae and lower levels of *Bifidobacterium* and Actinobacteriota, alongside unique T-cell receptor characteristics, highlighting FMT's potential to enhance immunotherapy efficacy.[65]

Preclinical studies have shown the effectiveness of FMT in treating cancer. One of the studies has demonstrated

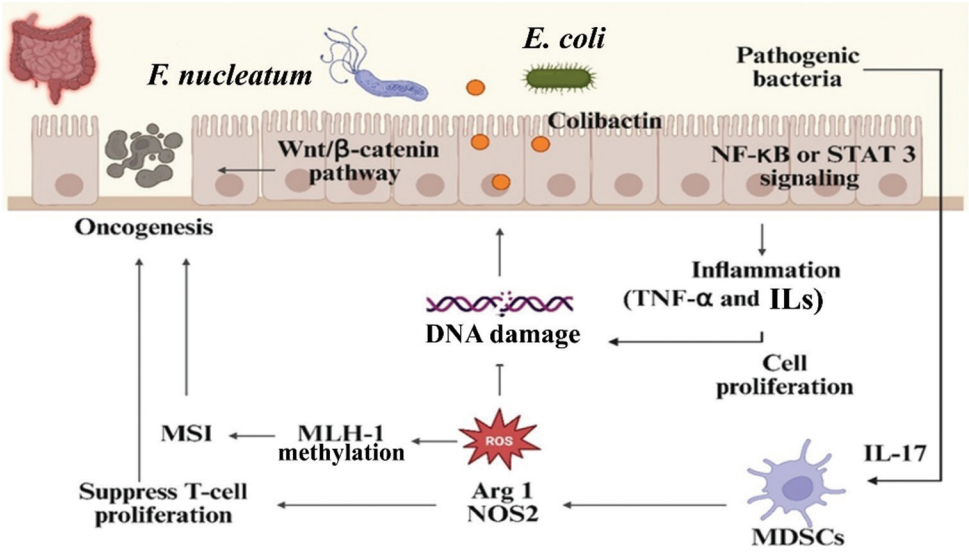

Figure 2. Mechanisms by which the gut microbiome drives cancer development and progression include activation of inflammatory pathways such as NF-κB and STAT-3, along with the induction of pro-inflammatory cytokines such as IL-17 and TNF-α. Created with BioRender. Ikram S. (2025). Abbreviations: Arg1: Arginase 1; *E. coli*: *Escherichia coli*; *F. nucleatum*: *Fusobacterium nucleatum*; IL: Interleukin; MDSC: Myeloid-derived suppressor cells; MLH-1: MutL homolog 1; MSI: Microsatellite instability; NOS2: Nitric oxide synthase 2; ROS: Reactive oxygen species; STAT3: Signal transducer and activator of transcription 3; TNF-α: Tumor necrosis factor-alpha.

that FMT reduced tumor size by nearly 40% and improved gut morphology in mice with colorectal cancer.[66] It restored microbial diversity along with downregulation of pro-inflammatory cytokines (e.g., IL-6 and TNF-α) and oncogenic markers (e.g., β-catenin and Ki-67), indicating suppressed tumor regression.[67] The therapeutic potential of FMT across various diseases is highlighted in Table 1.

One of the key challenges in this therapy is the selection of appropriate donors and the standardization of the FMT protocol. Significance and efficacy of FMT largely depend on the donor's microbiota composition, as transplants from different donors have resulted in varying clinical outcomes.[79] To improve FMT efficacy and consistency, standardized donor screening criteria and microbiome profiling should be established. In addition, long-term stability of FMT remains a concern, as it is unclear whether the transplanted microbes persist in the gut over an extended period or if periodic reinfusion is required to maintain therapeutic benefits.[80] While FMT is generally considered safe, potential risks include the transmission of opportunistic pathogens and unexpected immune responses of patients, underscoring the need for rigorous screening and regulatory oversight.

Table 1. Therapeutic potential of fecal microbiota transplantation across various diseases

Disease	Key outcomes	References
Ulcerative colitis	Clinical remission in 40–60% of patients, reduced pro-inflammatory cytokines	68,69
Immune checkpoint inhibitor-induced colitis	Clinical remission in 83–92% of patients, improved patient-reported outcomes	70,71
Graft-versus-host disease	Complete clinical response in 66–71% of patients, reduced immunosuppressant use	72,73
Colorectal cancer	Improved PFS and OS, increased beneficial bacteria, and enhanced anti-PD-1 efficacy	63,74
Metabolic syndrome	Improved insulin sensitivity and glucose metabolism	75,76
COVID-19	Alleviated diarrheal and depression symptoms	77,78

Abbreviations: OS: Overall survival; PD-1: Programmed cell death protein 1; PFS: Progression-free survival.

2.2. Probiotics

The World Health Organization defines probiotics as "live microorganisms which when administered in adequate amounts confer the health benefit to the host."[81(p22)] These microbes have been studied for their role in restoring gut microbiomes and have emerged as a keystone of microbiome-based therapies.[82,83] Probiotics help restore microbial balance by promoting beneficial microbes and maintaining gut homeostasis through the production of antimicrobial peptides, regulating inflammatory response by stimulating anti-inflammatory cytokines, and strengthening intestinal integrity to prevent

harmful substances from entering circulation.[55,84,85] These beneficial strains maintain intestinal homeostasis through competitive exclusion by promoting the growth of the endogenous desirable microbial population. Through competition, the probiotic strain uses the available nutrients and carbon source to reduce basic chlorine and oxygen in the microenvironment, helping them to occupy ecological niches and inhibit the growth of harmful bacteria (Figure 3). Certain probiotic strains, including *Lactobacillus* and *Bifidobacterium*, contribute to the biosynthesis of certain B vitamins, which are crucial for energy metabolism, immune regulation, and neurological function.[86,87] This vitamin production further enhances host health by preventing deficiencies and supporting metabolic processes. In addition, probiotics produce bioactive compounds such as SCFAs, bacteriocins, and neurotransmitters, supporting gut health and overall well-being.[88]

As a key component of the gut microbiome, probiotic strains are widely used to manage various health conditions, including GI disorders, metabolic diseases, neurodegenerative conditions, and immune dysfunction. Their influence on the gut–brain axis suggests potential therapeutic roles in cognitive health, including Alzheimer's disease and Parkinson's disease, by modulating gut inflammation and oxidative stress.[89] Probiotics influence both gut motility and mental health through modulation of microbiome-derived metabolites and serotonin pathways. The study on multistrand probiotics and sensi-biome (designed to target the sensitive and dynamic portion of the gut microbiome that responds rapidly to environmental changes) identified key microbiome-derived metabolites, including SCFAs (e.g., butyrate, iso-butyrate, propionate, and iso-valeric acid) for gut health, equal for anti-inflammatory benefits, and oleamide for potential neuroprotective effect.[90] The therapeutic potential of probiotics extends beyond GI disorders to metabolic and autoimmune disease. Probiotic strain *Klebsiella sp*. ARO112 treats IBD by displacing pathobiont adherent and invasive *E. coli* AIEC strain.[91,92] *Bifidobacterium* and *Lactobacillus*, termed as psychobiotic strains, have been shown to relieve symptoms of depression and anxiety through the production of neurotransmitters serotonin and dopamine, highlighting microbiome-based therapy as a promising approach for mental health disorders[93] (Table 2). The efficacy of probiotics is both disease-specific and site-specific, as different probiotic strains exhibit variable colonization, survival, and functional activities across the GI tract region, leading to different therapeutic outcomes in conditions such as irritable bowel syndrome, IBD, and antibiotic-associated diarrhea.[94] A pilot study using three probiotic strains (*Lactobacillus helveticus* MIMLh5, *Lacticaseibacillus paracasei* DG, and *Bifidobacterium bifidum* MIMBb23sg) revealed distinct colonization and site-specific effects of each strain on immune regulation, gut barrier integrity, and serotonergic signaling.[95] Further ongoing research continually uncovers new therapeutic potential.

2.3. Next-generation probiotics

Traditional probiotics, including *Lactobacillus* and *Bifidobacterium*, have been used to treat various diseases.

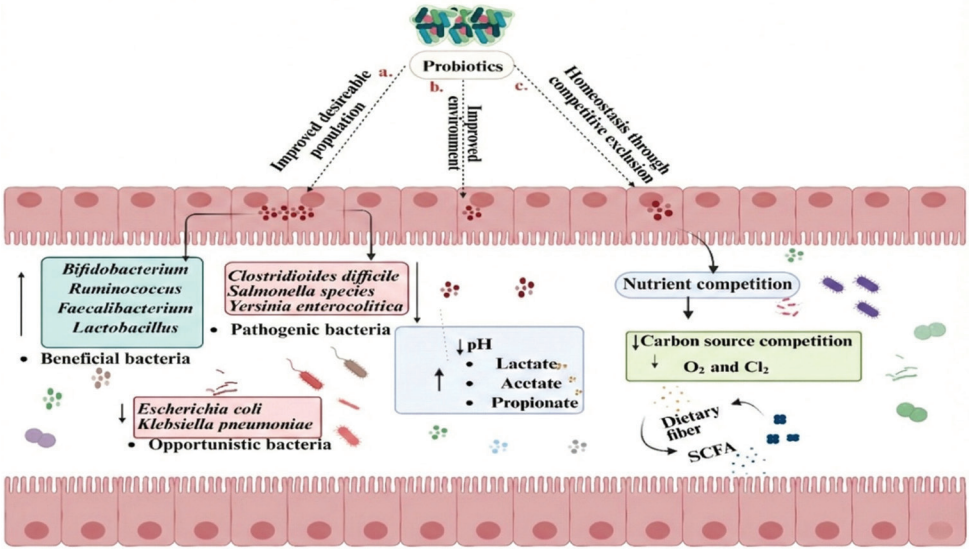

Figure 3. Probiotics maintain intestinal homeostasis by enhancing the growth of beneficial microbes, suppressing pathogenic and opportunistic bacteria, and promoting microbial balance through mechanisms such as nutrient competition and SCFA production. Created with BioRender. Ikram S. (2025). Abbreviation: SCFA: Short-chain fatty acid.

Table 2. Therapeutic applications of certain probiotic strains influencing gut motility and mental health

Probiotic strain	Therapeutic application/ diseases	References
Klebsiella sp. ARO112	Inflammatory bowel disease (IBD) and necrotizing enterocolitis	91
Lactobacillus rhamnosus	Gastrointestinal disorder and immune modulation	96
Akkermansia muciniphila	Metabolic disorder and obesity	97
Bifidobacterium animalis	Mental health, gut barrier function, and atopic dermatitis	98,99
Bifidobacterium longum	Gut–brain axis (reveals depression)	100
Pediococcus pentosaceus	Colorectal cancer therapy	101
Lactobacillus reuteri	Infantile colic	102
Lactobacillus rhamnosus, Lactobacillus plantarum, Escherichia coli Nissle 1917	IBD	103,104
Bifidobacterium spp., and Lactobacillus spp.	Irritable bowel syndrome, Parkinson's disease, Alzheimer's disease, type 2 diabetes, and functional constipation (pediatric)	105,106
Saccharomyces boulardii, Lactobacillus reuteri, and L. rhamnosus GG	Acute gastroenteritis (pediatric)	107
Lactiplantibacillus plantarum HY7712, Bifidobacterium animalis ssp. lactis HY8002, and Lacticaseibacillus casei HY2782	Inflammatory colitis, and atopic dermatitis	108

However, their effectiveness is limited by poor stability in harsh environments, lack of targeted action, and limited functionality (Table 3).[109] Advancements in genetic engineering and synthetic biology have led to the development of next-generation probiotics (NGP), designed to enhance viability, stability, and therapeutic potential, overcoming the limitations of traditional probiotics.[110,111] NGP employs advanced tools such as clustered regularly interspaced short palindromic repeats (CRISPR)–CRISPR-associated proteins (Cas) system and synthetic gene circuits to create customizable therapies personalized for individual microbiome profiles. To overcome the challenge of harsh environments, such as nutrient limitation, encapsulation technologies and bioadhesion platforms enhance the adhesion and persistence of probiotic strains in the gut.[112] Advancement of high-throughput sequencing techniques, functional annotation, and metabolic modeling has further facilitated

Table 3. Comparison of traditional probiotics and next-generation probiotics

Features	Traditional probiotics	Next-generation probiotics	References
Stability	Limited stability in a harsh environment	Enhanced stability and viability	112
Targeted Action	Broad non-specific effect	Targeted delivery and sensitivity	114
Therapeutic potential	Primarily for gastrointestinal health	Wide range of applications, including mental health and cancer	110,115
Personalization	Limited personalization	Tailored to the specific disease state and individual	114
Genetic engineering	Not genetically modified	Engineered using synthetic biology tools	116

the identification of new NGPs in the gut microbiome with potential health benefits.[111,113]

Many probiotic bacterial strains have been identified from the intestinal microbiome using novel next-generation sequencing techniques, and these NGPs have become potential sources of innovative therapeutics for various diseases.[117] Notably, NGPs such as *Faecalibacterium prausnitzii*, *Akkermansia muciniphila*, and *Bacteroides fragilis* have an impact on cancer incidence.[118] It has been shown that these NGPs enhance GI immunity, maintain intestinal barrier integrity, improve immunotherapy efficacy, and reduce complications associated with chemotherapy and radiotherapy. To reduce inflammation in the gut and to alleviate symptoms of IBD, *Lactobacillus* bacteria have now been engineered to produce anti-inflammatory compounds such as IL-10 and transforming growth factor-β.[119] Furthermore, to overcome the challenges of a harsh environment, researchers have used CRISPR/Cas9 to delete genes in *Lactobacillus* species, making them resistant to stomach acid, thereby increasing their survival rate through the digestive tract.[120] In a study including *Akkermansia muciniphila*, CRISPR/Cas9 was used to enhance its ability to produce mucin-degrading enzymes.[109] These enzymes improve the bacterium's ability to strengthen the gut barrier and reduce inflammation, making it more effective in treating metabolic disorders such as diabetes and obesity.

2.4. Prebiotics

Prebiotics have emerged as a promising component in microbiome-based therapies in treating various conditions. Prebiotics are non-digestible dietary fibers that serve as a substrate for beneficial gut bacteria, encouraging

their growth and action, thereby improving gut health. The integration of prebiotics into therapeutic strategies is gaining attention due to their potential to enhance the efficacy of treatments by targeting gut microbiota dysbiosis. This approach is being explored in various contexts, from enhancing drug delivery systems to supporting the function of NGPs.

Prebiotics-based nanoparticles have advanced to target drug delivery to the colon, showing potential in treating colonic diseases such as ulcerative colitis and colorectal cancer. These systems utilize prebiotic shells that degrade in response to gut microbiota to release therapeutic agents directly at the site of inflammation.[121] The use of prebiotics in these systems not only aids in drug delivery but also maintains intestinal homeostasis in maintaining the gut microbiota.[104,122] Prebiotics have shown promise in managing IBD by altering the gut microbiota composition, reducing inflammation, and supporting immune function. They induce the growth of beneficial bacteria, which, in turn, produce anti-inflammatory metabolites.[123] Clinical trials have demonstrated variable but generally positive outcomes, suggesting that prebiotics can be a valuable adjuvant in IBD treatment.[123,124]

Moreover, prebiotics are crucial in enhancing the viability and function of probiotics, specifically, NGPs, which are more sensitive to GI conditions.[99] They help improve the antioxidant capacity and probiotics resistance, thereby enhancing their therapeutic potential.[125,126] The combination of prebiotics with probiotics, also called symbiotics, has been explored for various disorders, including metabolic syndromes and central nervous system disorders, by promoting the survival and growth of beneficial bacteria (Figure 4).[127] The novel approach to symbiotics emphasizes microbial metabolism as a key mechanism for therapeutic benefits, focusing on targeted metabolite–microbe interactions to enhance health outcomes.[128] While prebiotics offer a significant potential in microbiome-based therapies, challenges remain in understanding their precise mechanism and interaction with the host microbiome. The variability in individual response to prebiotic intervention highlights the need for personalized approaches in their application.

2.5. Synthetic microbiome transplantation

Synthetic microbiome transplantation (SMT) represents an innovative approach to microbiome therapy, aiming to overcome the limitations of traditional FMT.[129,130] This treatment involves the use of defined microbial communities, known as SynComs, to restore the microbiome in a controlled and safe manner. SynComs are composed of selected, well-characterized microbial

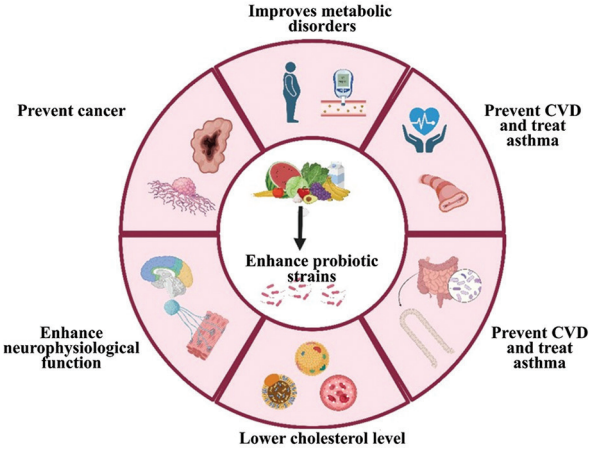

Figure 4. Prebiotics in combination with probiotics maintain overall body functions, from preventing cardiovascular disease (CVD), asthma, and cancer to enhancing neurological functions and lowering cholesterol levels. Created with BioRender. Ikram S. (2025).

strains, which can be derived from the mucosa and feces of human samples.[131] In the current era, the growing culturing capacity, along with reasonable sequencing and progressive computational modeling, has started a "golden age" for connecting the beneficial potential of SynComs to mitigate GI disorders such as infections and chronic IBD.[132,133] The development of SMT is driven by the need for more consistent, safe, and effective treatment for various diseases linked to microbiome dysbiosis. Some major advantages of SMT over FMT are its safety and consistency, which offer a controlled and known composition of microbial species, reducing the potential risk of infection and ensuring reproducibility in treatments.[134]

SynComs can be used in targeted therapeutics, such as restoring the microbial imbalance in conditions such as IBD and bacterial vaginosis, offering a more precise and personalized therapeutic approach. One of the studies has explored synthetic microbial consortia to combat bacterial vaginosis induced by *Gardnerella vaginalis* in germ-free mice to explore its effects on pro-inflammatory biomarkers in vaginal tissue.[135] It was found that key inflammatory regulator NF-κB and pro-inflammatory cytokines (IL-1 and IL-8) were suppressed by this treatment, along with increased abundance of *Lactobacillus* and reduction of *Escherichia*, *Shigella*, and *Vagococcus*. In addition, upregulation of anti-inflammatory cytokine (IL-10) suggests that SMT also helps modulate the immune system effectively. To combat the infection of multidrug-resistant *Klebsiella pneumoniae*, a SynCom of 15 microbial species isolated from the gut was tested across different settings. The successful engineering of this SynCom suppressed the resistant pathogen across various environments,

showcasing its versatility and robustness.[136,137] The engineered therapeutic microbes also act as therapeutic agents in reprogramming the microbial network to detect disease biomarkers and produce therapeutic molecules in response to the host's physiological state.[138,139] In conclusion, SynComs emerged as versatile and effective tools in addressing microbial imbalance, offering targeted therapeutic solutions across the range of conditions, showcasing their ability to restore microbial communities.

3. Microbiome-editing therapies

Recent progress in microbiome-editing therapies has opened new avenues for targeting microbial genes in the human gut with specificity. The new tools, primarily CRISPR and base editing, provide promising ways of editing the microbial populations they target with high accuracy and efficiency, and have immense potential to cure many diseases.[140] These *in situ* approaches edit the microbiome in its natural environment. Microbiome transplants can make dramatic changes, but are not specific; *in situ*-engineered microbes target specific bacteria with little effect on the rest of the microbial community. Base editing is a tool that can make single-base, precise modifications without inducing double-strand breaks or requiring homologous recombination.[141,142] A hybrid base-editing approach has been proposed that uses a catalytically impaired CRISPR-associated protein together with a nucleobase deaminase enzyme. A guide RNA directs the complex to the target DNA sequence, where the deaminase makes chemical modifications and introduces a point mutation. This approach enables precise genetic modifications with less likelihood of unwanted genomic alterations. These novel approaches offer a new means of manipulating the microbiome and have immense potential for addressing the challenges of antibiotic resistance and complex microbial communities.

Many research teams have proposed new gene-editing technologies for gut bacteria, including CRISPR-Cas9 and CRISPR interference. Moreover, scientists have designed viruses that infect bacteria with CRISPR-Cas systems to specifically target antibiotic-resistant bacteria, offering a new tool to address antibiotic resistance.[143] Clinical trials have recently tested whether microbiome modification can cure infections. Locus Biosciences has run a Phase 2 trial of CRISPR-enhanced viruses in urinary tract infection (UTI) patients caused by *E. coli*. Reported results indicated reductions in bacterial levels together with improvement in UTI symptoms, supporting the potential of CRISPR-enabled approaches for targeted antimicrobial strategies. Furthermore, scientists at the University of California have used CRISPR tools to edit the gut microbiota and alleviate childhood asthma by altering the composition of the microbiome.[21,144,145] These studies are promising for disease prevention by fixing microbial imbalances through microbiome modification.

Despite these encouraging steps forward, several challenges remain with microbiome-edited therapies. It is of the highest importance that genome-editing technologies are precise and safe to prevent unwanted side effects that would upset the sensitive balance of the microbiome. Moreover, the understanding of the intricate interactions of microbial communities and their influence on human health is critical to implement these therapies successfully. Future research should address these issues with better editing technologies and delivery strategies. The Innovative Genomics Institute is developing new CRISPR-based technologies to improve microbiome editing, making it safer and more precise, thereby allowing these therapies to reach their potential.[146] The Berkeley Initiative for Optimized Microbiome Editing is developing better CRISPR technologies to edit microbiomes in their natural environment,[146] aiming to identify safe and effective solutions to difficult problems by understanding and controlling the microbial ecosystems.

4. Multi-omics approaches in microbiome research

The human microbiome is a dynamic complex community of fungi, viruses, bacteria, small eukaryotes, and archaea that differ between individuals and locations.[147] The gut microbes help in vitamin synthesis, metabolism, immune system regulation, and resistance to infection.[148,149] Dysbiosis, or microbial imbalance, has been associated with metabolism, inflammation, and nervous system issues.[150]

Multi-omics has given insightful data on host–microbiome interaction, especially through diet. Deehan *et al.*[151] proved that higher fermentable fiber intake elevates propionate-producing bacteria, satiates the subject, and decreases obesity risk. Wang *et al.*[152] recognized lithocholic acid, a secondary bile acid derived from gut microbiota, as powerfully activating the body's heat production, supporting fat metabolism through farnesoid X receptor and Takeda G-protein-coupled receptor 5. However, Zeb *et al.*[78] and Caradonna *et al.*[153] reported that trimethylamine, a gut microbiota-derived metabolite generated from a protein-rich diet, contributes to atherosclerosis and cardiovascular disease. Likewise, Nageswaran[154] recognized imidazole propionate, a microbial metabolite, as a factor that impairs insulin signaling and exacerbates type 2 diabetes. Luo *et al.*[155] associated the production of toxic metabolites 2-butanone and 4-methyl-2-pentanone by microorganisms with non-alcoholic fatty liver disease,

whereas Tan *et al.*[156] delineated *K. pneumoniae*, an ethanol-producing bacterium, as perpetuating liver damage and inflammation.

New functional omics technologies have accelerated microbiome research. Ferrocino *et al.*[157] demonstrated how metagenomics and meta-transcriptomics profiling may reveal dysbiosis and gene expression changes in inflammatory and metabolic diseases. Meta-proteomics has the potential to yield absolute functional information but is limited by sampling depth. Han *et al.*[158] highlighted the function of metabolomics in identifying metabolites derived from the microbiome. They suggested that proton nuclear magnetic resonance spectroscopy can be used to identify common compounds, including short-chain fatty acids (SCFAs). Singer *et al.*[159] reported, however, that although many metabolite features are detected in microbial samples, more than 90% cannot be confidently annotated or assigned to known metabolites, thereby limiting our understanding of microbial functions.

These findings have driven the development of microbiome-directed therapies. Probiotics, prebiotics, and symbiotics have been highlighted by Kadam *et al.*[160] as a central part in restoring the balance of microbes. FMT has shown great success in the treatment of *C. difficile* infection and is additionally being researched into metabolic and inflammatory diseases.[15,161] Recent developments in precision microbiome medicine, such as engineered probiotics and targeted post-biotic treatments, offer potential for the prevention and treatment of diseases.

Scientists are striving to develop tailored treatments through enhanced functional omics approaches and improved interventions from the microbiome. These treatments aim to harness the power of the microbiome in promoting human health and combating disease.

5. Limitations and risks of microbiome-based therapies

Like most new technologies and therapies, microbiota transplants and treatments create challenges for regulators and raise ethical concerns for researchers and practitioners. Nonetheless, scientific research attempts to balance the safety of patients against promoting innovation and medical advancements.

5.1. Variability impact of an individual's microbiome

Our gut microbiome is influenced by factors such as what we eat, where we live, how we live, and even how tidy we are. Ethnicity is one factor, but geography, culture, routine, lifestyle, and exposure to environmental toxins or pathogens all shape the microbiome in different ways.[162] This variability made it complicated to develop universal microbiome-targeted treatments. More recent research suggests that a one-size-fits-all approach to diet therapies for metabolic diseases is likely to fail, as gut microbes play a major role in controlling how individuals metabolize key nutrients.[163] With all such variations, it is difficult to identify reliable microbial biomarkers to predict treatment outcomes. Individuals with the same illness respond differently to the same treatment due to the uniqueness of their microbiome.

5.2. Knowledge gaps in microbiome research

Even though microbiome information is important for treatment, it is still challenging to analyze and understand due to several reasons, including composition, which causes negative bias, sparsity, and collinearity.[164,165] The complexity of microbial communities has made it difficult to explore certain interactions between microbes and their hosts. At present, the effects of probiotics and symbiotics are not fully understood. The human microbiome has a complex mixture of microbes, and we still lack comprehensive data on the specific roles each species plays in human health. Our understanding remains limited regarding how effectively these microbes perform their functions and how they communicate with the host and with each other. Closing this knowledge gap through focused research is essential to unravel the complicated relationships within the microbiome.

5.3. Ethical and regulatory issues in microbiome research

Study of the human microbiome must justify a favorable risk–benefit ratio, indicating potential benefits outweigh disadvantages. However, balancing these benefits and risks is not always straightforward. Therapies involving living organisms, such as FMT, probiotics, and prebiotics, are subject to regulatory oversight regarding their safety and effectiveness.[166] Choosing the appropriate regulatory category (e.g., drug, biological product, or dietary supplement) can be difficult, as it governs the requirements and approval processes. Developers need to position their products within regulatory frameworks based on their function and biological nature.

To quantify safety and efficacy, thorough preclinical and clinical testing is essential, including assessments of adverse effects on the microbiome and host physiology. The manufacture, distribution, and storage of live biotherapeutic products must comply with Good Manufacturing Practice guidelines.[167] Ethical considerations, particularly for FMT, are critical to ensure patient protection and informed consent. Rigorous donor screening and careful recipient selection help minimize the risk of transmitting infections or diseases.[168] Informed consent remains a fundamental

element, involving the participant's voluntary agreement to clinical trial participation with full knowledge of the study's aims, risks, potential benefits, and safety measures. Ultimately, a comprehensive evaluation of safety and risk–benefit ratio is necessary to prevent adverse effects and ensure therapies are safe and effective.

6. Conclusion

The fast-growing area of microbiome-based therapies holds tremendous potential to revolutionize the treatment of various health conditions. From FMT to SMT, and the application of probiotics, prebiotics, and engineered microbial consortia, these approaches aim to restore microbial balance and treat diseases once considered difficult to treat. The research covered in this review emphasizes the various potent means through which manipulation of the gut microbiome can enhance health, influence disease prognosis, and even modulate immune responses, including in cancer therapy.

Treatments such as FMT and Syncoms, along with personalized and precision medicine, are leading the way for microbiome-based therapy. The ability to engineer microbial communities targeted specifically to correct dysbiosis provides new opportunities for treating multifactorial diseases, ranging from metabolic diseases to GI and neuropsychiatric disorders. Synthetic microbial consortia are particularly promising due to their controlled composition, which allows for more predictable and safer restoration of microbial communities compared to conventional FMT. However, challenges remain in fully understanding the complex interactions between the microbiome and the host.

In the future, microbiome-based treatments are poised to unlock some gripping prospects. Advances in genetic engineering, synthetic biology, and computational modeling will enhance the design and performance of NGPs and SMT. In addition, integrating microbiome data into personalized medicine strategies could result in more targeted and effective treatments, optimizing therapeutic benefits while reducing side effects. In summary, microbiome-based therapies are a revolutionary breakthrough in medical science, offering a promising new direction for the management of various diseases. Continued research, development, and deeper understanding of microbial dynamics will be critical to realize the potential of these therapies, enabling their widespread implementation in healthcare, personalized medicine, and disease prevention in the future.

Acknowledgments

The author would like to acknowledge the National University of Medical Sciences, Islamabad, Pakistan, for providing a guidance and supportive research environment.

Funding

None.

Conflict of interest

The authors declare that they have no competing interests.

Author contributions

Conceptualization: Zoha Waheed Abbasi, Sania Ikram, Muhammad Naeem
Visualization: Sania Ikram, Muneed Ullah
Writing-original draft: Zoha Waheed Abbasi, Sania Ikram
Writing-review & editing: Aftab Ahmad, Irfan Ali, Muneed Ullah

Ethics approval and consent to participate

Not applicable.

Consent for publication

Not applicable.

Availability of data

Not applicable.

References

1. Kapoor D, Sharma P, Sharma MMM, Kumari A, Kumar R. Microbes in pharmaceutical industry. In: *Microbial Diversity, Interventions and Scope*. Germany: Springer; 2020. p. 259-299.
   doi: 10.1007/978-981-15-4099-8_16
2. Dutta B, Lahiri D, Nag M, Ghosh S, Dey A, Ray RR. Fungi in pharmaceuticals and production of antibiotics. In: *Applied Mycology: Entrepreneurship with Fungi*. Germany: Springer; 2022. p. 233-257.
   doi: 10.1007/978-3-030-90649-8_11
3. Amara AAAF, Gupta A. An Overview About Pharmaceutical Grade Fungal Protein and Peptides. Prospects of Fungal Biotechnologies for Livestock. In: *Fungal Biotechnologies for Animal Cell Lines*. Vol. 2. Germany: Springer; 2025. p. 321-353.
   doi: 10.1007/978-3-032-06478-3_12
4. Bhatt B, Patel K, Lee CN, Moochhala S. *The Microbial Blueprint: The Impact of Your Gut onYour Wellbeing*. Singapore: Partridge Publishing; 2024. Available from: https://www.partridgepublishing.com/ensg/bookstore/bookdetails/851799-the-microbial-blueprint-the-impact-of-your-gut-on-your-well-being [Last accessed on 2025 Jul 12].
5. Welcome MO. History of development of gastrointestinal physiology: From antiquity to modern period and the birth of modern digestive physiology. In: Gastrointestinal Physiology: Development, Principles and Mechanisms of Regulation. Germany: Springer; 2018. p. 1-51.

doi: 10.1007/978-3-319-91056-7_1

6. Walter J, Ley R. The human gut microbiome: Ecology and recent evolutionary changes. *Ann Rev Microbiol*. 2011;65(1):411-429.

   doi: 10.1146/annurev-micro-090110-102830

7. Neiroukh D, Hajdarpasic A, Ayhan C, Sultan S, Soliman O. Gut microbial taxonomy and its role as a biomarker in aortic diseases: A systematic review and future perspectives. *J Clin Med*. 2024;13(22):6938.

   doi: 10.3390/jcm13226938

8. Mamo Z, Abera S, Tafesse M. Taxonomic and functional profiling of microbial community in municipal solid waste dumpsite. *World J Microbiol Biotechnol*. 2024;40(12):384.

   doi: 10.1007/s11274-024-04189-3

9. He Z, Dong H. The roles of short-chain fatty acids derived from colonic bacteria fermentation of non-digestible carbohydrates and exogenous forms in ameliorating intestinal mucosal immunity of young ruminants. *Front Immunol*. 2023;14:1291846.

   doi: 10.3389/fimmu.2023.1291846

10. Ramos Meyers G, Samouda H, Bohn T. Short chain fatty acid metabolism in relation to gut microbiota and genetic variability. *Nutrients*. 2022;14(24):5361.

    doi: 10.3390/nu14245361

11. Ahamad R, Parveen S. *Gut Microbiota and Nutrient Enrichment: Mechanism and Production of Vitamins. Probiotics*. United States: CRC Press; 2024. p. 56-75.

    doi: 10.1201/9781003452249

12. Pandit NK, Sharma P, Sharma P, Rout PR, Mohanty A, Meena SS. Valorizing agro-food waste for microbial B vitamin biosynthesis: Impacts on gut microbiota dynamics and microbial communication. *Rev Environ Sci Bio Technol*. 2026;25(1):1.

    doi: 10.1007/s11157-025-09753-3

13. Uebanso T, Shimohata T, Mawatari K, Takahashi A. Functional roles of B-vitamins in the gut and gut microbiome. *Mol Nutr Food Res*. 2020;64(18):2000426.

    doi: 10.1002/mnfr.202000426

14. Kaplan BJ, Rucklidge JJ, Romijn A, McLeod K. The emerging field of nutritional mental health: Inflammation, the microbiome, oxidative stress, and mitochondrial function. *Clin Psychol Sci*. 2015;3(6):964-980.

    doi: 10.1177/2167702614555413

15. Sahle Z, Engidaye G, Shenkute Gebreyes D, Adenew B, Abebe TA. Fecal microbiota transplantation and next-generation therapies: A review on targeting dysbiosis in metabolic disorders and beyond. *SAGE Open Med*. 2024;12:1-12.

    doi: 10.1177/20503121241257486

16. Illiano P, Brambilla R, Parolini C. The mutual interplay of gut microbiota, diet and human disease. *FEBS J*. 2020;287(5):833-855.

    doi: 10.1111/febs.15217

17. Rondanelli M, Borromeo S, Cavioni A, *et al.* Therapeutic strategies to modulate gut microbial health: Approaches for chronic metabolic disorder management. *Metabolites*. 2025;15(2):127.

    doi: 10.3390/metabo15020127

18. Shukla V, Singh S, Verma S, Verma S, Rizvi AA, Abbas M. Targeting the microbiome to improve human health with the approach of personalized medicine: Latest aspects and current updates. *Clin Nutr ESPEN*. 2024;63:813-820.

    doi: 10.1016/j.clnesp.2024.08.005

19. Feng W, Liu J, Ao H, Yue S, Peng C. Targeting gut microbiota for precision medicine: Focusing on the efficacy and toxicity of drugs. *Theranostics*. 2020;10(24):11278.

    doi: 10.7150/thno.47289

20. Chauhan NS, Kumar S. *Microbiome Therapeutics: Personalized Therapy Beyond Conventional Approaches*. Elsevier; 2023. Available from: https://www.researchwithrutgers.com/en/publications/microbiome-therapeutics-personalized-therapy-beyond-conventional [Last accessed on 2025 Jul 12].

21. Yaqub MO, Jain A, Joseph CE, Edison LK. Microbiome-driven therapeutics: From gut health to precision medicine. *Gastrointest Disord*. 2025;7(1):7.

    doi: 10.3390/gidisord7010007

22. Ebadpour N, Abavisani M, Sahebkar A. Microbiome-driven precision medicine: Advancing drug development with pharmacomicrobiomics. *J Drug Target*. 2025;33:1495-1510.

    doi: 10.1080/1061186X.2025.2509283

23. Shah JS, Scheible CE, Farris AL, Bishop KA. *Precision Medicine and its Application to Chemical and Biological Diagnostics*; 2023. Available from: https://www.ida.org/-/media/feature/publications/p/pr/precision-medicine-and-its-application-to-chemical-and-biological-diagnostics/p-33457.ashx [Last accessed on 2025 Jul 14].

24. Satya S, Sharma S, Choudhary G, Kaushik G. Advances in environmental microbiology: A multi-omic perspective. In: *Microbial Omics in Environment and Health*. Germany: Springer; 2024. p. 175-204.

    doi: 10.1007/978-981-97-1769-9_7

25. Chen XL, Sun MC, Chong SL, Si JP, Wu LS. Transcriptomic and metabolomic approaches deepen our knowledge of plant-endophyte interactions. *Front Plant Sci*. 2022;12:700200.

    doi: 10.3389/fpls.2021.700200

26. Sarsan S, Pandiyan A, Rodhe AV, Jagavati S. Synergistic interactions among microbial communities. In: *Microbes in Microbial Communities: Ecological and Applied Perspectives.*

Germany: Springer Nature; 2021. p. 1-37.

doi: 10.1007/978-981-16-5617-0_1

27. Liu XA, Li X, Shen P, Cong B, Wang L. Fundamental role of brain-organ interaction in behavior-driven holistic homeostasis. *Fundam Res*. 2024;5:2626-2638.

doi: 10.1016/j.fmre.2024.09.005

28. Chirivi M, Contreras GA. Endotoxin-induced alterations of adipose tissue function: A pathway to bovine metabolic stress. *J Anim Sci Biotechnol*. 2024;15(1):53.

doi: 10.1186/s40104-024-01013-8

29. Jin L, Xiao J, Luo Y, *et al*. Exploring gut microbiota in systemic lupus erythematosus: Insights and biomarker discovery potential. *Clin Rev Allergy Immunol*. 2025;68(1):42.

doi: 10.1007/s12016-025-09051-4

30. Grueso Navarro E, Lucendo AJ. Metabolic dysfunction-associated steatotic liver disease in inflammatory bowel disease: Prevalence, risk factors, pathophysiological pathways and clinical consequences. *Expert Rev Clin Immunol*. 2025;21:875-891.

doi: 10.1080/1744666X.2025.2514605

31. Aziz T, Khan AA, Tzora A, Voidarou C, Skoufos I. Dietary implications of the bidirectional relationship between the gut microflora and inflammatory diseases with special emphasis on irritable bowel disease: Current and future perspective. *Nutrients*. 2023;15(13):2956.

doi: 10.3390/nu15132956

32. Dixit K, Chaudhari D, Dhotre D, Shouche Y, Saroj S. Restoration of dysbiotic human gut microbiome for homeostasis. *Life Sci*. 2021;278:119622.

doi: 10.1016/j.lfs.2021.119622

33. Bajaj JS, Ng SC, Schnabl B. Promises of microbiome-based therapies. *J Hepatol*. 2022;76(6):1379-1391.

doi: 10.1016/j.jhep.2021.12.003

34. Ciernikova S, Sevcikova A, Drgona L, Mego M. Modulating the gut microbiota by probiotics, prebiotics, postbiotics, and fecal microbiota transplantation: An emerging trend in cancer patient care. *Biochim Biophys Acta Rev Cancer*. 2023;1878(6):188990.

doi: 10.1016/j.bbcan.2023.188990

35. Nawaz K, Ullah M, Yoo JW, Aiman U, Ghazanfar M, Naeem M. Role of nutrition in the management of inflammatory bowel disease. *Recent Prog Nutr*. 2025;5(1):002.

doi: 10.21926/rpn.2501002

36. Gupta N, Kachhawaha K, Behera DK, Verma VK. Next-generation probiotics as potential therapeutic supplement for gastrointestinal infections. *Pharmacol Res Rep*. 2023;1:100002.

doi: 10.1016/j.prerep.2024.100002

37. Makki K, Vidal H, Grangette C. *Targeting the Gut Microbiota in Metabolic Disorders: Potential Impact of Lactic Acid Bacteria and Next-Generation Probiotics*. Lactic Acid Bacteria. CRC Press; 2019. p. 474-498. Available from: https://www.taylorfrancis.com/chapters/edit/10.1201/9780429057465-27/targeting-gut-microbiota-metabolic-disorders-juvenile-growth-kassem-makki-martin-schwarzer-bernardo-cuffaro-hubert-vidal-emmanuelle-maguin-corinne-grangette [Last accessed on 2025 Jul 14].

38. Jan T, Negi R, Sharma B, *et al*. Next generation probiotics for human health: An emerging perspective. *Heliyon*. 2024;10:e35980.

doi: 10.1016/j.heliyon.2024.e35980

39. Singh A, Midha V, Chauhan NS, Sood A. Current perspectives on fecal microbiota transplantation in inflammatory bowel disease. *Indian J Gastroenterol*. 2024;43(1):129-144.

doi: 10.1007/s12664-023-01516-8

40. Srivastava N, Ibrahim SA, Nasr MHA. *Microbiome Engineering: The New Dimension of Biotechnology*. CRC Press; 2024. Available from: https://www.taylorfrancis.com/books/edit/10.1201/9781003394662/microbiome-engineering-nimmy-srivastava-salam-ibrahim-mohamed-hussein-arbab-nasr [Last accessed on 2025 Jul 14].

41. D'Haens GR, Jobin C. Fecal microbial transplantation for diseases beyond recurrent clostridium difficile infection. *Gastroenterology*. 2019;157(3):624-636.

doi: 10.1053/j.gastro.2019.04.053

42. Matheson JAT, Holsinger RD. The role of fecal microbiota transplantation in the treatment of neurodegenerative diseases: A review. *Int J Mol Sci*. 2023;24(2):1001.

doi: 10.3390/ijms24021001

43. Ullah M, Awan UA, Ali H, *et al*. Carbon dots: New rising stars in the carbon family for diagnosis and biomedical applications. *J Nanotheranostics*. 2024;6(1):1.

doi: 10.3390/jnt6010001

44. Lemmens G, Brouwers J, Snoeys J, Augustijns P, Vanuytsel T. Insight into the colonic disposition of celecoxib in humans. *Eur J Pharm Sci*. 2020;145:105242.

doi: 10.1016/j.ejps.2020.105242

45. Fadda HM. The route to palatable fecal microbiota transplantation. *AAPS PharmSciTech*. 2020;21(3):114.

doi: 10.1208/s12249-020-1637-z

46. Allegretti JR, Mullish BH, Kelly C, Fischer M. The evolution of the use of faecal microbiota transplantation and emerging therapeutic indications. *Lancet*. 2019;394(10196):420-431.

doi: 10.1016/S0140-6736(19)31266-8

47. Chumpitazi BP, Kearns G, Shulman RJ. The physiological effects and safety of peppermint oil and its efficacy in

irritable bowel syndrome and other functional disorders. *Aliment Pharmacol Therapeut*. 2018;47(6):738-752.

doi: 10.1111/apt.14519

48. Zhong Y, Cao J, Ma Y, Zhang Y, Liu J, Wang H. Fecal microbiota transplantation donor and dietary fiber intervention collectively contribute to gut health in a mouse model. *Front Immunol*. 2022;13:842669.

doi: 10.3389/fimmu.2022.842669

49. Wilson BC, Vatanen T, Cutfield WS, O'Sullivan JM. The super-donor phenomenon in fecal microbiota transplantation. *Front Cell Infect Microbiol*. 2019;9:430737.

doi: 10.3389/fcimb.2019.00002

50. Brown JRM, Flemer B, Joyce SA, *et al.* Changes in microbiota composition, bile and fatty acid metabolism, in successful faecal microbiota transplantation for Clostridioides difficile infection. *BMC Gastroenterol*. 2018;18:1-15.

doi: 10.1186/s12876-018-0860-5

51. Kulsoom J, Kamran HB, Ullah F, Nawaz K, Ullah M, Naeem M. Nano-Based Drug Delivery Systems in Plants. In: *Revolutionizing Agriculture: A Comprehensive Exploration of Agri-Nanotechnology*. Germany: Springer; 2024. p. 307-323.

doi: 10.1007/978-3-031-76000-6_14

52. Fassarella M, Blaak EE, Penders J, Nauta A, Smidt H, Zoetendal EG. Gut microbiome stability and resilience: Elucidating the response to perturbations in order to modulate gut health. *Gut*. 2021;70(3):595-605.

doi: 10.1136/gutjnl-2020-321747

53. Safarchi A, Al-Qadami G, Tran CD, Conlon M. Understanding dysbiosis and resilience in the human gut microbiome: Biomarkers, interventions, and challenges. *Front Microbiol*. 2025;16:1559521.

doi: 10.3389/fmicb.2025.1559521

54. Rivas-Domínguez A, Pastor N, Martínez-López L, Colón-Pérez J, Bermúdez B, Orta ML. The role of DNA damage response in dysbiosis-induced colorectal cancer. *Cells*. 2021;10(8):1934.

doi: 10.3390/cells10081934

55. Ullah M, Lee J, Hasan N, *et al.* Clindamycin-loaded polyhydroxyalkanoate nanoparticles for the treatment of methicillin-resistant *Staphylococcus aureus*-infected wounds. *Pharmaceutics*. 2024;16(10):1315.

doi: 10.3390/pharmaceutics16101315

56. Wei X, Wang F, Tan P, *et al.* The interactions between traditional Chinese medicine and gut microbiota in cancers: Current status and future perspectives. *Pharmacol Res*. 2024;203:107148.

doi: 10.1016/j.phrs.2024.107148

57. Al-Matouq J, Al-Ghafli H, Alibrahim NN, Alsaffar N, Radwan Z, Ali MD. Unveiling the interplay between the human microbiome and gastric cancer: A review of the complex relationships and therapeutic avenues. *Cancers*. 2025;17(2):226.

doi: 10.3390/cancers17020226

58. Routy B, Lenehan JG, Miller WH Jr., *et al.* Fecal microbiota transplantation plus anti-PD-1 immunotherapy in advanced melanoma: A phase I trial. *Nat Med*. 2023;29(8):2121-2132.

doi: 10.1038/s41591-023-02453-x

59. Meng Y, Sun J, Zhang G. A viable remedy for overcoming resistance to anti-PD-1 immunotherapy: Fecal microbiota transplantation. *Crit Rev Oncol Hematol*. 2024;200:104403.

doi: 10.1016/j.critrevonc.2024.104403

60. Yu H, Li XX, Han X, *et al.* Fecal microbiota transplantation inhibits colorectal cancer progression: Reversing intestinal microbial dysbiosis to enhance anti-cancer immune responses. *Front Microbiol*. 2023;14:1126808.

doi: 10.3389/fmicb.2023.1126808

61. Aftab M, Ikram S, Ullah M, Khan SU, Wahab A, Naeem M. Advancement of 3D bioprinting towards 4D bioprinting for sustained drug delivery and tissue engineering from biopolymers. *J Manuf Mater Process*. 2025;9(8):285.

doi: 10.3390/jmmp9080285

62. Safdar M, Ullah M, Hamayun S, *et al.* Microbiome miracles and their pioneering advances and future frontiers in cardiovascular disease. *Curr Probl Cardiol*. 2024;49(9):102686.

doi: 10.1016/j.cpcardiol.2024.102686

63. Zhao W, Lei J, Ke S, *et al.* Fecal microbiota transplantation plus tislelizumab and fruquintinib in refractory microsatellite stable metastatic colorectal cancer: An open-label, single-arm, phase II trial (RENMIN-215). *EClinicalMedicine*. 2023;66:102315.

doi: 10.1016/j.eclinm.2023.102315

64. Ullah M, Bibi A, Wahab A, *et al.* Shaping the future of cardiovascular disease by 3d printing applications in stent technology and its clinical outcomes. *Curr Probl Cardiol*. 2024;49(1 Pt A):102039.

doi: 10.1016/j.cpcardiol.2023.102039

65. Gattazzo F. *The Role of Gut Microbiota in the Modulation of Cancer therapy Responses from Immune Mechanisms to Clinical Implications*; 2025. Available from: https://hdl.handle.net/10807/309857 [Last accessed on 2025 Jul 14].

66. Yadav D, Sainatham C, Filippov E, Kanagala SG, Ishaq SM, Jayakrishnan T. Gut microbiome-colorectal cancer relationship. *Microorganisms*. 2024;12(3):484.

doi: 10.3390/microorganisms12030484

67. Naharro-Rodriguez J, Bacci S, Fernandez-Guarino M.

Molecular biomarkers in cutaneous photodynamic therapy: A comprehensive review. *Diagnostics (Basel)*. 2024;14(23):2724.

doi: 10.3390/diagnostics14232724

68. Zhang WH, Jin ZY, Yang ZH, *et al.* Fecal microbiota transplantation ameliorates active ulcerative colitis by downregulating pro-inflammatory cytokines in mucosa and serum. *Front Microbiol*. 2022;13:818111.

doi: 10.3389/fmicb.2022.818111

69. Ishikawa D, Nomura K, Zhang X, *et al.* P1225 The interplay of donor-derived gut microbiota correlates with the efficacy of combination therapy of fecal microbiota transplantation with antibiotics for ulcerative colitis. *J Crohn's Colitis*. 2024;18(Suppl 1):i2173.

doi: 10.1093/ecco-jcc/jjad212.1225

70. Halsey TM, Thomas AS, Hayase T, *et al.* Microbiome alteration via fecal microbiota transplantation is effective for refractory immune checkpoint inhibitor-induced colitis. *Sci Transl Med*. 2023;15(700):eabq4006.

doi: 10.1126/scitranslmed.abq4006

71. Wang Y, Varatharajalu K, Shatila M, *et al.* Effect of fecal transplantation on patients' reported outcome after immune checkpoint inhibitor colitis. *Am Soc Clin Oncol*. 2023;41:2645-2645.

doi: 10.1200/JCO.2023.41.16_suppl.2645

72. Khuat LT, Dave M, Murphy WJ. The emerging roles of the gut microbiome in allogeneic hematopoietic stem cell transplantation. *Gut Microbes*. 2021;13(1):1966262.

doi: 10.1080/19490976.2021.1966262

73. Aftab M, Ali H, Ullah M, *et al.* Biomedical applications of carbon dots: Advances in antimicrobial therapy and targeted delivery systems. *Biomedical Materials and Devices*. New York: Springer; 2025. p. 1-22.

doi: 10.1007/s44174-024-00122-7

74. Han X, Zhang BW, Zeng W, *et al.* Suppressed oncogenic molecules involved in the treatment of colorectal cancer by fecal microbiota transplantation. *Front Microbiol*. 2024;15:1451303.

doi: 10.3389/fmicb.2024.1451303

75. van der Vossen EW, Davids M, Voermans B, *et al.* Disentangle beneficial effects of strain engraftment after fecal microbiota transplantation in subjects with MetSyn. *Gut Microbes*. 2024;16(1):2388295.

doi: 10.1080/19490976.2024.2388295

76. Hemachandra S, Rathnayake SN, Jayamaha AA, *et al.* Fecal microbiota transplantation as an alternative method in the treatment of obesity. *Cureus*. 2025;17(1):e76858.

doi: 10.7759/cureus.74762

77. Jiang X, Gao X, Ding J, *et al.* Fecal microbiota transplantation alleviates mild-moderate COVID-19 associated diarrhoea and depression symptoms: A prospective study of a randomized, double-blind clinical trial. *J Med Virol*. 2024;96(8):e29812.

doi: 10.1002/jmv.29812

78. Zeb F, Mehreen A, Naqeeb H, *et al.* Nutrition and dietary intervention in cancer: Gaps, challenges, and future perspectives. In: *Nutrition and Dietary Interventions in Cancer*. Germany: Springer; 2024. p. 281-307.

doi: 10.1007/978-3-031-55622-7_11

79. Song Q, Gao Y, Liu K, Tang Y, Man Y, Wu H. Gut microbial and metabolomics profiles reveal the potential mechanism of fecal microbiota transplantation in modulating the progression of colitis-associated colorectal cancer in mice. *J Transl Med*. 2024;22(1):1028.

doi: 10.1186/s12967-024-05786-4

80. Niu X, Jin L, Liu S, Li H. The impact of fecal microbiota transplantation on the intestinal microecology of patients with colorectal cancer. *Med Health Res*. 2024;2(2):31-33.

doi: 10.18686/mhr.v2i2.4129

81. Food and Agriculture Organization of the United Nations. *Health and Nutritional Properties of Probiotics in Food Including Powder Milk with Live Lactic Acid Bacteria*; 2001. Available from: https://openknowledge.fao.org/server/api/core/bitstreams/8b1233c6-f928-4ff0-85e1-78b2e27c6e4e/content [Last accessed on 2025 Jul 14].

82. Mohamed MYA. Probiotics benefits, potential limitations and risks. *Egypt Acad J Biol Sci Physiol Mol Biol*. 2024;16(1):253-276.

doi: 10.21608/eajbsc.2024.344590

83. Ikram S, Abbasi ZW, Khan AI, Kulsoom J, Khan MA, Khan SU. Aerobes in the gut microbiota-roles, interactions, and implications for host health. *Int J Basic Med Sci Pharmacy*. 2025;11(2):40-44.

84. Mousa WK, Mousa S, Ghemrawi R, *et al.* Probiotics modulate host immune response and interact with the gut microbiota: Shaping their composition and mediating antibiotic resistance. *Int J Mol Sci*. 2023;24(18):13783.

doi: 10.3390/ijms241813783

85. Safdar M, Aftab M, Ullah M, Naeem M, Wahab A. Genetic engineering of fungi. In: *Fungal Biotechnology*. Florida: CRC Press; 2025. p. 36-44.

doi: 10.1201/9781003594840-4

86. Hossain KS, Amarasena S, Mayengbam S. B vitamins and their roles in gut health. *Microorganisms*. 2022;10(6):1168.

doi: 10.3390/microorganisms10061168

87. Ullah M, Wahab A, Khan D, *et al.* Modified gold and polymeric gold nanostructures: Toxicology and biomedical

applications. *Colloid Interface Sci Commun*. 2021;42:100412.

doi: 10.1016/j.colcom.2021.100412

88. Hyland N, Stanton C. *The Gut-Brain Axis: Dietary, Probiotic, and Prebiotic Interventions on the Microbiota*. Elsevier; 2023. Available from: https://www.sciencedirect.com/book/edited-volume/9780128023044/the-gut-brain-axis [Last accessed on 2025 Jul 14].

89. Denman CR, Park SM, Jo J. Gut-brain axis: Gut dysbiosis and psychiatric disorders in Alzheimer's and Parkinson's disease. *Front Neurosci*. 2023;17:1268419.

doi: 10.3389/fnins.2023.1268419

90. Jeong JJ, Jin YJ, Ganesan R, *et al.* Multistrain probiotics alleviate diarrhea by modulating microbiome-derived metabolites and serotonin pathway. *Probiotics Antimicrob Proteins*. 2025;17(5):2894-2908.

doi: 10.1007/s12602-024-10232-4

91. Cabral V, Oliveira R, Correia M, Pedro M, Ubeda C, Xavier K. *Novel Gut Probiotic Engages Microbiota for Recovery and Pathobiont Clearance While Preventing Inflammation* [Preprint]; 2023.

doi: 10.1101/2023.11.14.566997

92. Ahmed Z, Ullah M, Zeshan D, Khan SU, Ali F, Wahab A. Exploring the tumor microenvironment in solid cancer: From biology to therapy. *Methods Cell Biol*. 2025;198:359-385.

doi: 10.1016/bs.mcb.2025.02.020

93. Altaib H, Badr Y, Suzuki T. Bifidobacteria and psychobiotic therapy: Current evidence and future prospects. *Rev Agric Sci*. 2021;9:74-91.

doi: 10.7831/ras.9.0_74

94. Han S, Lu Y, Xie J, *et al.* Probiotic gastrointestinal transit and colonization after oral administration: A long journey. *Front Cell Infect Microbiol*. 2021;11:609722.

doi: 10.3389/fcimb.2021.609722

95. Taverniti V, Cesari V, Gargari G, *et al.* Probiotics modulate mouse gut microbiota and influence intestinal immune and serotonergic gene expression in a site-specific fashion. *Front Microbiol*. 2021;12:706135.

doi: 10.3389/fmicb.2021.706135

96. Mahesh Krishna B, Francis Luther King M, Robert Singh G, Gopichand A. 3D printing in drug delivery and healthcare. In: *Advanced Materials and Manufacturing Techniques for Biomedical Applications*. United States: John Wiley and Sons; 2023. p. 241-274.

doi: 10.1002/9781394166985.ch10

97. DiMattia Z, Damani JJ, Van Syoc E, Rogers CJ. Effect of probiotic supplementation on intestinal permeability in overweight and obesity: A systematic review of randomized controlled trials and animal studies. *Adv Nutr*. 2024;15(1):100162.

doi: 10.1016/j.advnut.2023.100162

98. Zhu X, Tian X, Wang M, Li Y, Yang S, Kong J. Protective effect of *Bifidobacterium* animalis CGMCC25262 on HaCaT keratinocytes. *Int Microbiol*. 2024;27(5):1417-1428.

doi: 10.1007/s10123-024-00419-1

99. Ullah M, Wahab A, Khan SU, *et al.* Stent as a novel technology for coronary artery disease and their clinical manifestation. *Curr Probl Cardiol*. 2023;48(1):101415.

doi: 10.1016/j.cpcardiol.2022.101415

100. Parhizgar N, Azadyekta M, Zabihi R. Effect of probiotic supplementation on depression and anxiety. *Complement Med J*. 2021;11(2):166-179.

doi: 10.32598/cmja.11.2.1073.1

101. Chung Y, Ryu Y, An BC, *et al.* A synthetic probiotic engineered for colorectal cancer therapy modulates gut microbiota. *Microbiome*. 2021;9(1):122.

doi: 10.1186/s40168-021-01067-3

102. Piątek J, Bernatek M, Krauss H, *et al.* Effects of a nine-strain bacterial synbiotic compared to simethicone in colicky babies - an open-label randomized study. *Benef Microbes*. 2021;12(3):249-258.

doi: 10.3920/bm2020.0178

103. Kwong Z. The application of probiotics in gastrointestinal diseases. *Theor Nat Sci*. 2024;74:25-34.

doi: 10.54254/2753-8818/2024.la18762

104. Aftab M, Ikram S, Ullah M, *et al.* Recent trends and future directions in 3D printing of biocompatible polymers. *J Manuf Mater Process*. 2025;9(4):129.

doi: 10.3390/jmmp9040129

105. Sepehr A, Miri ST, Aghamohammad S, *et al.* Health benefits, antimicrobial activities, and potential applications of probiotics: A review. *Medicine (Baltimore)*. 2024;103(52):e32412.

doi: 10.1097/md.0000000000032412

106. Korotko U, Biskupski M, Cygnarowicz A, *et al.* The role of probiotics in antibiotic-associated diarrhea, acute diarrhea and functional constipation in children. *J Educ Health Sport*. 2024;76:56616-56616.

doi: 10.12775/jehs.2024.76.56616

107. Wampers A, Huysentruyt K, Vandenplas Y. An update on the use of 'biotics' in pediatric infectious gastroenteritis. *Expert Opin Pharmacother*. 2024;25(11):1483-1496.

doi: 10.1080/14656566.2024.2374494

108. Lee SJ, Jeong W, Atala A. 3D Bioprinting for engineered tissue constructs and patient-specific models: Current

progress and prospects in clinical applications. *Adv Mater*. 2024;36(49):2408032.

doi: 10.1002/adma.202408032

109. Tiwari A, Ika Krisnawati D, Susilowati E, Mutalik C, Kuo TR. Next-generation probiotics and chronic diseases: A review of current research and future directions. *J Agric Food Chem*. 2024;72(50):27679-27700.

doi: 10.1021/acs.jafc.4c08702

110. Patra D. Synthetic biology-enabled engineering of probiotics for precision and targeted therapeutic delivery applications. *Exon*. 2024;1(2):54-66.

doi: 10.69936/en11y0024

111. Ullah M, Safdar M, Yoo JW, *et al.* Introduction to gastrointestinal inflammation and Gut Microbiota. In: *Gastrointestinal Inflammations and Gut Microbiota*. United States: CRC Press; 2025. p. 1-13.

doi: 10.1201/9781003493143

112. Verdugo-Meza A, Gill SK, Godovannyi A, *et al.* Bio-Engineering a Common Probiotic to Exploit Colonic Inflammation Promotes Reliable Efficacy in Translational Models of Colitis. [bioRxiv Preprint]; 2024.

doi: 10.1101/2024.10.08.617317

113. Aziz T, Naveed M, Sarwar A, *et al.* Functional annotation of *Lactiplantibacillus* plantarum 13-3 as a potential starter probiotic involved in the food safety of fermented products. *Molecules*. 2022;27(17):5399.

doi: 10.3390/molecules27175399

114. Abouelela ME, Helmy YA. Next-generation probiotics as novel therapeutics for improving human health: Current trends and future perspectives. *Microorganisms*. 2024;12(3):430.

doi: 10.3390/microorganisms12030430

115. Hasan N, Jiafu C, Mustopa AZ, *et al.* Recent advancements of nitric oxide-releasing hydrogels for wound dressing applications. *J Pharm Investig*. 2023;53(6):781-801.

doi: 10.1007/s40005-023-00651-7

116. Meng J, Liu S, Wu X. Engineered probiotics as live biotherapeutics for diagnosis and treatment of human diseases. *Crit Rev Microbiol*. 2024;50(3):300-314.

doi: 10.1080/1040841X.2023.2280197

117. Kaźmierczak-Siedlecka K, Skonieczna-Żydecka K, Hupp T, Duchnowska R, Marek-Trzonkowska N, Połom K. Next-generation probiotics-do they open new therapeutic strategies for cancer patients? *Gut Microbes*. 2022;14(1):2035659.

doi: 10.1080/19490976.2022.2035659

118. Al-Fakhrany OM, Elekhnawy E. Next-generation probiotics: The upcoming biotherapeutics. *Mol Biol Rep*. 2024;51(1):505.

doi: 10.1007/s11033-024-09398-5

119. Steidler L, Neirynck S, Huyghebaert N, *et al.* Biological containment of genetically modified *Lactococcus lactis* for intestinal delivery of human interleukin 10. *Nat Biotechnol*. 2003;21(7):785-789.

doi: 10.1038/nbt840

120. Oh JH, Van Pijkeren JP. CRISPR-Cas9-assisted recombineering in *Lactobacillus reuteri*. *Nucleic Acids Res*. 2014;42(17):e131-e131.

doi: 10.1093/nar/gku623

121. Li H, Cheng Y, Cui L, *et al.* Combining gut microbiota modulation and enzymatic-triggered colonic delivery by prebiotic nanoparticles improves mouse colitis therapy. *Biomater Res*. 2024;28:0062.

doi: 10.34133/bmr.0062

122. Ren Y, Nie L, Luo C, Zhu S, Zhang X. Advancement in therapeutic intervention of prebiotic-based nanoparticles for colonic diseases. *Int J Nanomed*. 2022;17:6639.

doi: 10.2147/IJN.S390102

123. Guo J, Li L, Cai Y, Kang Y. The development of probiotics and prebiotics therapy to ulcerative colitis: A therapy that has gained considerable momentum. *Cell Commun Signal*. 2024;22(1):268.

doi: 10.1186/s12964-024-01611-z

124. Fei Y, Chen Z, Han S, *et al.* Role of prebiotics in enhancing the function of next-generation probiotics in gut microbiota. *Crit Rev Food Sci Nutr*. 2023;63(8):1037-1054.

doi: 10.1080/10408398.2021.1958744

125. Sadiq MB, Azhar F-u-A, Ahmad I. Probiotic and prebiotic interactions and their role in maintaining host immunity. In: *Microbiome-Gut-Brain Axis: Implications on Health*. Germany: Springer; 2022. p. 425-443.

doi: 10.1007/978-981-16-1626-6_22

126. Alifah N, Palungan J, Ardayanti K, *et al.* Development of clindamycin-releasing polyvinyl alcohol hydrogel with self-healing property for the effective treatment of biofilm-infected wounds. *Gels*. 2024;10(7):482.

doi: 10.3390/gels10070482

127. Cusumano G, Flores GA, Venanzoni R, Angelini P. The impact of antibiotic therapy on intestinal microbiota: Dysbiosis, antibiotic resistance, and restoration strategies. *Antibiotics*. 2025;14(4):371.

doi: 10.3390/antibiotics14040371

128. Speckmann B, Ehring E, Hu J, Rodriguez Mateos A. Exploring substrate-microbe interactions: A metabiotic approach toward developing targeted synbiotic compositions. *Gut Microbes*. 2024;16(1):2305716.

doi: 10.1080/19490976.2024.2305716

129. Wang X, Xing Y, Ji Y, *et al.* The combination of phages and faecal microbiota transplantation can effectively treat mouse colitis caused by *Salmonella enterica Serovar* Typhimurium. *Front Microbiol*. 2022;13:944495.

doi: 10.3389/fmicb.2022.944495

130. Safdar M, Amin Z, Ullah M, Wahab A, Hasan N, Naeem M. Cancer stem cell analysis and targeting. *Methods Cell Biol*. 2025;198:251-271.

doi: 10.1016/bs.mcb.2025.02.017

131. Jennings SA, Clavel T. Synthetic communities of gut microbes for basic research and translational approaches in animal health and nutrition. *Annu Rev Anim Biosci*. 2024;12(1):283-300.

doi: 10.1146/annurev-animal-021022-025552

132. Li L, Nielsen J, Chen Y. Personalized gut microbial community modeling by leveraging genome-scale metabolic models and metagenomics. *Curr Opin Biotechnol*. 2025;91:103248.

doi: 10.1016/j.copbio.2024.103248

133. Waleed A, Hamayun S, Shaukat A, *et al.* Nanotechnology and biomedical devices used as a novel tool in biosensing and bioimaging of disease. *J Women Med Dent Coll*. 2023;1(4):13-21.

doi: 10.56600/jwmdc.v1i4

134. Biazzo M, Deidda G. Fecal microbiota transplantation as new therapeutic avenue for human diseases. *J Clin Med*. 2022;11(14):4119.

doi: 10.3390/jcm11144119

135. Li Y, Zhu W, Jiang Y, Lessing DJ, Chu W. Synthetic bacterial consortia transplantation for the treatment of *Gardnerella vaginalis*-induced bacterial vaginosis in mice. *Microbiome*. 2023;11(1):54.

doi: 10.1186/s40168-023-01454-6

136. Oliveira RA, Pandey B, Lee K, *et al.* Statistical Design of a Synthetic Microbiome that Clears a Multi-Drug Resistant Gut Pathogen. [bioRxiv Preprint]; 2024.

doi: 10.1101/2024.02.28.582635

137. Ullah M, Wahab A, Saeed S, *et al.* Coronavirus and its terrifying inning around the globe: The pharmaceutical cares at the main frontline. *Chemosphere*. 2021;275:129968.

doi: 10.1016/j.chemosphere.2021.129968

138. Zahedifard Z, Mahmoodi S, Ghasemian A. Genetically engineered bacteria as a promising therapeutic strategy against cancer: A comprehensive review. *Biotechnol Appl Biochem*. 2025;72:1458-1476.

doi: 10.1002/bab.2676

139. Ullah M, Awan UA, Muhaymin A, *et al.* Cancer nanomedicine: Smart arsenal in the war against cancer. *Inorg Chem Commun*. 2025;174:114030.

doi: 10.1016/j.inoche.2024.114030

140. Amen RA, Hassan YM, Essmat RA, *et al.* Harnessing the microbiome: CRISPR-based gene editing and antimicrobial peptides in combating antibiotic resistance and cancer. *Probiotics Antimicrob Proteins*. 2025;174:1938-1968.

doi: 10.1007/s12602-025-10169-7

141. Remington LA, Goodwin D. *Clinical Anatomy and Physiology of the Visual System E-book: Clinical Anatomy and Physiology of the Visual System E-book*. Amsterdam: Elsevier Health Sciences; 2021. Available from: https://www.elsevier.com/permissions [Last accessed on 2025 Jul 14].

142. Nawaz K, Ullah M, Yoo JW, Wahab A, Hasan N, Naeem M. *Tissue Engineering for Wound Healing: Recent Advancements and Opportunities*. *Nanotechnology in Wound Healing*. CRC Press; 2025. p. 149-167. Available from: https://www.taylorfrancis.com/chapters/edit/10.1201/9781003605966-7/tissue-engineering-wound-healing-khalid-nawaz-muneeb-ullah-jin-wook-yoo-abdul-wahab-nurhasni-hasan-muhammad-naeem [Last accessed on 2025 Jul 14].

143. Selim HMRM, Gomaa FAM, Alshahrani MY, Aboshanab KM. Role of CRISPR-Cas system as a new approach in fighting the antimicrobial resistance of bacterial and viral pathogens. *Infect Dis Immun*. 2025;5(02):127-137.

doi: 10.1097/id9.0000000000000127

144. Liu L, Zhao W, Zhang H, Shang Y, Huang W, Cheng Q. Relationship between pediatric asthma and respiratory microbiota, intestinal microbiota: A narrative review. *Front Microbiol*. 2025;16:1550783.

doi: 10.3389/fmicb.2025.1550783

145. Pantazi AC, Balasa AL, Mihai CM, *et al.* Development of gut microbiota in the first 1000 days after birth and potential interventions. *Nutrients*. 2023;15(16):3647.

doi: 10.3390/nu15163647

146. Olatunji AO, Olaboye JA, Maha CC, Kolawole TO, Abdul S. Next-generation strategies to combat antimicrobial resistance: Integrating genomics, CRISPR, and novel therapeutics for effective treatment. *Eng Sci Technol J*. 2024;5(7):2284-2303.

doi: 10.51594/estj.v5i7.1344

147. Sharon I, Quijada NM, Pasolli E, *et al.* The core human microbiome: Does it exist and how can we find it? A critical review of the concept. *Nutrients*. 2022;14(14):2872.

doi: 10.3390/nu14142872

148. Debnath N, Kumar R, Kumar A, Mehta PK, Yadav AK. Gut-microbiota derived bioactive metabolites and their functions in host physiology. *Biotechnol Genet Eng Rev*. 2021;37(2):105-153.

doi: 10.1080/02648725.2021.1930054

149. Debnath N, Yadav AK. Regulation of probiotic as a

therapeutic agent to manage gastrointestinal cancer. *Probiotic Research in Therapeutics: Modulation of Gut Flora: Management of Inflammation and Infection Related Gut Etiology*. Vol. 2. Singapore: Springer Nature; 2021. p. 167.

doi: 10.1007/978-981-33-6236-9_7

150. Mitrea L, Nemeş SA, Szabo K, Teleky BE, Vodnar DC. Guts imbalance imbalances the brain: A review of gut microbiota association with neurological and psychiatric disorders. *Front Med*. 2022;9:813204.

doi: 10.3389/fmed.2022.813204

151. Deehan EC, Zhang Z, Riva A, *et al.* Elucidating the role of the gut microbiota in the physiological effects of dietary fiber. *Microbiome*. 2022;10(1):77.

doi: 10.1186/s40168-022-01256-0

152. Wang B, Han D, Hu X, Chen J, Liu Y, Wu J. Exploring the role of a novel postbiotic bile acid: Interplay with gut microbiota, modulation of the farnesoid X receptor, and prospects for clinical translation. *Microbiol Res*. 2024;287:127865.

doi: 10.1016/j.micres.2024.127865

153. Caradonna E, Abate F, Schiano E, *et al.* Trimethylamine-N-Oxide (TMAO) as a rising-star metabolite: Implications for human health. *Metabolites*. 2025;15(4):220.

doi: 10.3390/metabo15040220

154. Nageswaran V. The Impact of Gut Microbial Imidazole Propionate on Endothelial Regeneration and the Development of Atherosclerosis [Dissertation]; 2023.

doi: 10.17169/refubium-42738

155. Luo J, Luo M, Kaminga AC, *et al.* Integrative metabolomics highlights gut microbiota metabolites as novel NAFLD-related candidate biomarkers in children. *Microbiol Spectr*. 2024;12(4):e0523022.

doi: 10.1128/spectrum.05230-22

156. Tan J, Taitz J, Nanan R, Grau G, Macia L. Dysbiotic gut microbiota-derived metabolites and their role in non-communicable diseases. *Int J Mol Sci*. 2023;24(20):15256.

doi: 10.3390/ijms242015256

157. Ferrocino I, Rantsiou K, McClure R, *et al.* The need for an integrated multi-OMICs approach in microbiome science in the food system. *Compr Rev Food Sci Food Saf*. 2023;22(2):1082-1103.

doi: 10.1111/1541-4337.13103

158. Han S, Van Treuren W, Fischer CR, *et al.* A metabolomics pipeline for the mechanistic interrogation of the gut microbiome. *Nature*. 2021;595(7867):415-420.

doi: 10.1038/s41586-021-03707-9

159. Singer F, Kuhring M, Renard BY, Muth T. Moving toward metaproteogenomics: A computational perspective on analyzing microbial samples via proteogenomics. In: *Proteogenomics: Methods and Protocols*. Germany: Springer; 2024. p. 297-318.

doi: 10.1007/978-1-0716-4152-1_17

160. Kadam A, Kadam D, Tungare K, Shah H. Probiotics and prebiotics in healthy ageing. In: *Nutrition, Food and Diet in Ageing and Longevity*. Germany: Springer; 2021. p. 85-108.

doi: 10.1007/978-3-030-83017-5_5

161. Hasan N, Luthfiyah W, Palungan J, *et al.* Nitric oxide-releasing self-healing hydrogel for antibacterial and antibiofilm efficacy against polymicrobial infection. *Future Microbiol*. 2024;19(18):1559-1571.

doi: 10.1080/17460913.2024.2415237

162. Patel PG, Patel AC, Chakraborty P, Gosai HB. Impact of dietary habits, ethnicity, and geographical provenance in shaping human gut microbiome diversity. In: *Probiotics, Prebiotics, Synbiotics, and Postbiotics: Human Microbiome and Human Health*. Germany: Springer; 2023. p. 3-27.

doi: 10.1007/978-981-99-1463-0_1

163. Van Zanten AR. Personalized nutrition therapy in critical illness and convalescence: Moving beyond one-size-fits-all to phenotyping and endotyping. *Curr Opin Crit Care*. 2023;29(4):281-285.

doi: 10.1097/MCC.0000000000001025

164. Marcos-Zambrano LJ, Karaduzovic-Hadziabdic K, Loncar Turukalo T, *et al.* Applications of machine learning in human microbiome studies: A review on feature selection, biomarker identification, disease prediction and treatment. *Front Microbiol*. 2021;12:634511.

doi: 10.3389/fmicb.2021.634511

165. Xia Y, Sun J. Applied Microbiome Statistics: Correlation, Association, Interaction and Composition. United States: CRC Press; 2024.

doi: 10.1201/9781003121572

166. Airola C, Severino A, Porcari S, *et al.* Future modulation of gut microbiota: From eubiotics to FMT, engineered bacteria, and phage therapy. *Antibiotics*. 2023;12(5):868.

doi: 10.3390/antibiotics12050868

167. Seet WT, Mat Afandi MA, Shamsuddin SA, Lokanathan Y, Ng MH, Maarof M. Current good manufacturing practice (cGMP) Facility and production of stem cell. In: *Stem Cell Production: Processes, Practices and Regulations*. Germany: Springer; 2022. p. 37-68.

doi: 10.1007/978-981-16-7589-8_3

168. Ng RW, Dharmaratne P, Wong S, Hawkey P, Chan P, Ip M. Revisiting the donor screening protocol of faecal microbiota transplantation (FMT): A systematic review. *Gut*. 2024;73(6):1029-1031.

doi: 10.1136/gutjnl-2023-331180

ACCSCIENCE PUBLISHING

Journal of Clinical and Translational Research

REVIEW ARTICLE

Hepatitis B virus X protein-targeted therapeutic strategies toward a functional cure for chronic hepatitis B infection: A review

Sunita Giri and Vijay Kumar*

Department of Molecular and Cellular Medicine, Institute of Liver and Biliary Sciences, New Delhi, Delhi, India

(This article belongs to the *Special Issue: Biomedicine and Bioinformatics Engineering*)

Abstract

Background: Chronic hepatitis B (CHB) remains a major global health challenge, with persistent covalently closed circular DNA (cccDNA) and viral integration leading to lifelong infection, cirrhosis, and hepatocellular carcinoma (HCC). Current antiviral therapies suppress replication but rarely achieve a functional cure. The multifunctional hepatitis B virus (HBV) X (HBx) protein is well known to sustain viral replication, impair host immune responses, and promote hepatocarcinogenesis, which makes it an attractive therapeutic target. **Aim:** This review synthesizes current literature supporting HBx as a promising therapeutic target to achieve a functional cure of CHB. **Conclusion:** HBx is a high-value therapeutic target with potential to accelerate progress toward a functional cure. Destabilization or downregulation of HBx would not only attenuate its oncogenic signaling but also limit relapse after treatment discontinuation and diminish the cccDNA reservoir and viral antigen load. **Relevance for patients:** Multitargeted treatment regimens incorporating HBx-directed therapies hold the potential to achieve durable viral suppression and a functional cure, and to reduce the risk of HCC. The combined strategies could transform the long-term management and outcomes for patients with CHB.

Keywords: Hepatitis B virus; Hepatitis B virus X protein; Chronic hepatitis B; Covalently closed circular DNA; Viral persistence; Furanocoumarins; Functional cure

***Corresponding author:**
Vijay Kumar
(vkumar@ilbs.in)

Citation: Giri S, Kumar V. Hepatitis B virus X protein-targeted therapeutic strategies toward a functional cure for chronic hepatitis B infection: A review. *J Clin Transl Res.* 2026;12(1):22-38. doi: 10.36922/JCTR025410069

Received: October 8, 2025

Revised: November 27, 2025

Accepted: January 13, 2026

Published online: February 9, 2026

1. Introduction

Hepatitis B virus (HBV) is a DNA virus that causes acute and chronic liver disease and remains a major global health burden.[1] Transmission occurs through contact with infected blood or bodily fluids, with perinatal, early childhood, sexual, and parenteral exposures being the primary routes.[2] In highly endemic regions, vertical and early childhood transmission perpetuates infection across generations, especially where immunization coverage is limited.[2] The World Health Organization estimated that in 2022, approximately 254 million people were living with chronic hepatitis B (CHB), with approximately 1.1 million annual deaths primarily due to cirrhosis and hepatocellular carcinoma (HCC).[3] The risk of developing CHB is strongly age-dependent, with more than 90% of infants infected at birth, approximately 50% in children aged 1–5 years, and <10% in adults.[3,4]

Structurally, HBV consists of an envelope surrounding a nucleocapsid that encloses a relaxed circular DNA genome.[5] The virus exhibits a strong affinity for hepatocytes and enters cells through interactions between the pre-S1 domain of its envelope glycoprotein and the sodium taurocholate co-transporting polypeptide receptor.[5,6] Once internalized, relaxed circular DNA is transported to the nucleus and converted into covalently closed circular DNA (cccDNA), a stable episomal minichromosome that acts as a template for the transcription of the 3.5 kb pre-genomic RNA (pgRNA), the 2.4/2.1 kb transcripts encoding three surface antigens (small, middle, and large), and the 0.7 kb RNA encoding the regulatory HBV X (HBx) protein.[6,7] pgRNA is reverse transcribed into new relaxed circular DNA and also serves as the mRNA for the capsid proteins and viral polymerase, essential for virion assembly. Mature nucleocapsids either acquire an envelope for secretion as infectious virions or are recycled to the nucleus to replenish cccDNA, sustaining persistent infection. In addition, HBV DNA can integrate into the host genome, contributing to chronic disease progression and HCC. Although integrated HBV DNA is replication-defective, it can significantly contribute to the circulating pool of hepatitis B surface antigen (HBsAg), particularly in hepatitis B e antigen (HBeAg)-negative individuals.[8] The persistent cccDNA pool enables the reactivation of HBV, particularly during periods of immunosuppression, by continuously producing viral RNA and progeny viruses even after antiviral treatments, which suppress viral replication but do not eliminate the cccDNA. The stability of cccDNA, integration events, and immune evasion mechanisms make HBV eradication challenging.[7] Current antiviral therapies suppress viral replication but rarely achieve complete clearance, underscoring the need for novel therapeutic approaches toward reducing HBV transmission and the associated global disease burden.[9,10]

Among potential therapeutic targets in the HBV life cycle, HBx is of particular interest due to its central role in regulating cccDNA transcription, viral replication, and in oncogenic processes underlying HCC development.[11-13] HBx can stimulate the expression of other viral genes by acting on the viral cccDNA template. Therefore, targeting HBx destabilization or downregulation would not only attenuate HBx-driven oncogenic signaling but also limit relapse after treatment discontinuation and diminish the cccDNA reservoir and viral antigen load. The present review comprehensively synthesizes current knowledge supporting HBx as a promising therapeutic target to achieve a functional cure for CHB.

2. Methodology

Original research and review articles were included if they provided experimental, mechanistic, or therapeutic insights into (i) *HBx* gene expression, (ii) HBx-mediated regulation of cccDNA, (iii) mechanisms governing intracellular HBx stability and degradation, or (iv) natural and synthetic compounds that modulate HBx function. Reports addressing RNA interference (RNAi), genome editing, epigenetic regulation, and immunotherapeutic modalities targeting HBx were also included. Information on bioactive compounds and small molecules promoting HBx degradation or repressing cccDNA transcription was collected from the original reports and curated databases. The academic research databases, including PubMed, ScienceDirect, Scopus, Web of Science, and Google Scholar, were queried using a combination of keywords, such as "HBx," "hepatitis B virus," "HBV," "HBx degradation," "cccDNA transcription," "HBx–host interactions," "HBx inhibitors," and "therapeutic targeting of HBx." We considered all relevant scholarly literature from database inception through August 2025, without restricting publication year. Exclusion criteria included non-English publications and articles lacking sufficient methodological clarity or direct relevance to HBx biology.

3. *HBV X* gene and its regulation

The regulatory HBx protein is encoded by the "X" open reading frame in the HBV genome. The expression of the *HBx* gene involves the transcription of the viral cccDNA in the nucleus of the infected cell, which serves as the template for producing viral RNAs, including the 0.7-kb HBx transcript. The *HBx* RNA transcript is then exported to the cytoplasm and translated into HBx protein in infected host cells (Figure 1). HBx regulates its own gene expression through transcriptional and post-transcriptional mechanisms, including interactions with host factors and epigenetic mechanisms, such as DNA methylation and chromatin accessibility. The *HBx* gene is regulated by its promoter and two enhancers (Enhancer I and Enhancer II), which are responsive to host factors, such as CCAAT/enhancer binding protein, hepatocyte nuclear factor 1, hepatocyte nuclear factor 3, and cyclic adenosine monophosphate response element binding protein (CREB)/activating transcription factor 2.[11,12,14]

4. Molecular characteristics of the HBV X protein

The HBx protein is a small (17 kDa) multifunctional regulatory protein that is well conserved across all mammalian hepadnaviruses but lacks sequence homology to known proteins.[11] Structurally, HBx comprises two major functional domains: An N-terminal negative regulatory domain and a C-terminal transactivation domain. Deletion of the amino-terminal 1–50 amino acids upregulates HBx transcriptional functions, suggesting that it is a negative

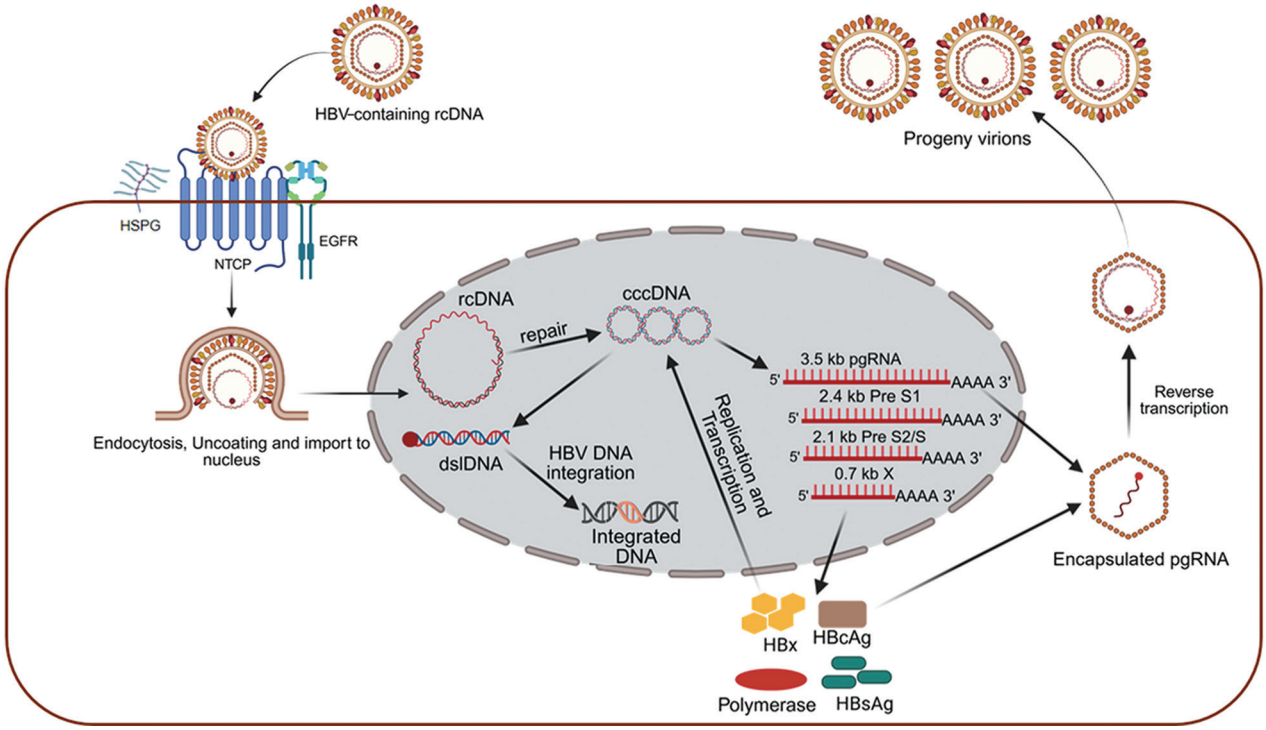

Figure 1. The hepatitis B virus (HBV) replication cycle. HBV enters hepatocytes with the help of the heparan sulfate proteoglycan (HSPG) attachment factor and sodium taurocholate co-transporting polypeptide (NTCP)/epidermal growth factor receptor (EGFR). The relaxed circular DNA (rcDNA) in virions is transported into the nucleus. rcDNA is repaired to form covalently closed circular DNA (cccDNA), which serves as a transcriptional template for pre-genomic RNA (pgRNA) and other viral mRNAs, including 0.7-kb HBV X (HBx) RNA. pgRNA is encapsidated with viral polymerase and reverse-transcribed into rcDNA within nucleocapsids. Mature nucleocapsids are either recycled to the nucleus to replenish cccDNA or enveloped and secreted as progeny virions. In parallel, HBV double-stranded linear DNA (dslDNA) can integrate into the host genome, contributing to viral persistence and pathogenesis. Created in BioRender. Giri, S. (2025) https://BioRender.com/yn90jqq. Abbreviations: HBcAg: Hepatitis B core antigen; HBsAg: Hepatitis B surface antigen.

regulatory element, whereas the C-terminal domain of HBx (amino acids 52–148) is essential for its various activities. The C-terminal region has several structural motifs, such as the H-box, Bcl-2 homology domain 3-like domain, zinc-binding motif, and alpha-helical elements.[11,12] HBx exhibits a dynamic intracellular distribution regulated by the phosphorylation of conserved residues.[15] It is predominantly cytoplasmic when highly expressed and more nuclear at lower (near-endogenous) levels.[16] HBx can directly bind to several transcription factors in the nucleus, such as activating transcription factor 2, CREB, Oct-1, p53, basic leucine zipper, and other basal transcription factors, and stimulate several cytoplasmic signal transduction pathways, such as nuclear factor kappa B (NF-κB), Janus kinase/signal transducer and activator of transcription, phosphoinositide 3-kinase/protein kinase B, Ras/Raf/mitogen-activated protein kinase, and Wnt signaling, that have a profound influence on cell proliferation, apoptosis, and viral replication.[11,14,17]

5. Regulation of intracellular HBV X protein levels

Despite its critical role in viral persistence, HBx is a short-lived protein. The intracellular abundance of HBx is tightly regulated by both the host cell's protein degradation machinery and by other viral proteins involving ubiquitination, deubiquitination, neddylation, and proteolytic degradation through proteasomal or non-proteasomal mechanisms.[7,18] These biochemical processes allow HBx to modulate various cellular processes essential for the viral life cycle and pathogenesis.

The intracellular stability of HBx protein may range from 30 min to 3 h, depending on the experimental system used. The reported half-lives of HBx range from about 30–40 min in hepatoma cells (HepG2 and Huh 7 cells) to around 1–3 h in primary human hepatocytes.[19-21] Interestingly, the woodchuck HBx protein in naturally infected hepatocytes shows a bimodal half-life—one with

a short half-life of 15–30 min and the other with a long half-life of 3 h.[22] Therefore, interference with intracellular stabilization processes or induction of destabilization mechanisms directed at HBx will open up new possibilities of developing novel therapeutic strategies for hepatitis B patients who are non-responsive to existing treatments.

5.1. Destabilization processes and promotive strategies

The destabilization of HBx protein utilizes the cellular machinery involving both viral and host factors (Figure 2). For example, the tumor suppressor p53 is known to induce degradation of HBx with the help of E3 ligase mouse double min 2 through a ubiquitin-independent proteasomal mechanism.[23] Alternatively, p53 can induce E6-associated protein-mediated ubiquitination and proteasomal degradation of HBx.[24] The intrahepatic homeobox protein muscle segment homeobox 1 acts as a restriction factor against HBV by reducing HBx protein levels through an ubiquitin-independent proteasomal degradation pathway by upregulating DnaJ heat shock protein family (Hsp40) member A4 and crystallin alpha B expression.[25] Similarly, the tumor suppressor PreS1-binding protein facilitates HBx degradation through the ubiquitin–proteasome system, resulting in the suppression of HBV DNA replication and viral gene expression.[26] Interestingly, as a part of a negative feedback mechanism to regulate viral replication, the core protein of HBV is also known to stimulate the proteasome-mediated degradation of HBx.[20]

The E3 ubiquitin ligases, such as seven in absentia homolog 1 and 2 and neuronal precursor cell-expressed developmentally downregulated gene 4, have been reported to prevent the proliferation, migration, and invasion in HBV-related HCC cell lines by promoting K48-linked polyubiquitination and proteasomal degradation of HBx.[27-29] In addition, the core protein of hepatitis C virus has been found to inhibit HBV replication by downregulating HBx levels through seven in absentia homolog 1.[30] Recent findings suggest that E3 ligase tripartite motif-containing protein (TRIM) 21 interacts with HBx and HBV DNA polymerase and triggers their ubiquitination and degradation, resulting in the downregulation of other viral antigens (HBsAg, hepatitis B core antigen, and HBeAg).[31,32] Interestingly, type I interferon (IFN)-stimulated gene TRIM5γ acts as an adaptor protein for TRIM31 and helps restrict HBV infection by targeting HBx for degradation in a multi-step process.[33] In addition, the interaction between HBx and TRIM proteins provides a new target for developing antiviral therapies for HBV. Furthermore, activating HBx-destabilizing ligases (e.g., seven in absentia homolog 2, neural precursor cell expressed developmentally downregulated protein 4, and

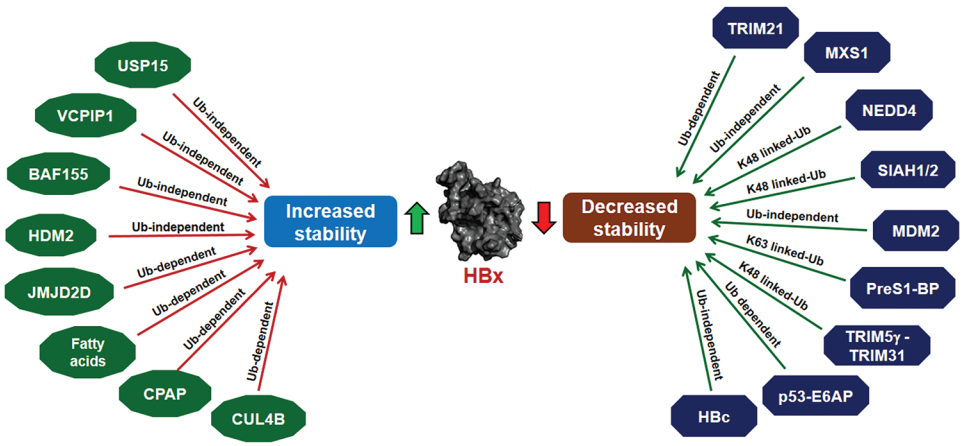

Figure 2. Regulation of the intracellular stability of hepatitis B virus X protein (HBx). Schematic representation of host and viral factors that influence the intracellular stability of HBx. Green arrows indicate HBx degradation via ubiquitin (Ub)-dependent or Ub-independent proteasomal pathways, while red arrows indicate stabilization or protection from proteolytic degradation. E3 ubiquitin ligases that mediate HBx degradation include seven in absentia homolog (SIAH) 1, SIAH2, neural precursor cell expressed developmentally downregulated protein 4 (NEDD4), tripartite motif-containing protein 5 gamma-tripartite motif-containing protein 31 (TRIM5γ–TRIM31, p53–E6-associated protein (E6AP), tripartite motif-containing protein 21 (TRIM21), PreS1-binding protein (PreS1-BP), and mouse double min 2 (MDM2), as well as non-E3 factors, such as hepatitis B virus capsid (HBc) and muscle segment homeobox 1 (MSX-1) (via DnaJ heat shock protein family member A4 [DNAJA4)] and crystallin alpha B [CRYAB]). Mechanisms include K48-linked polyubiquitination, K63-linked polyubiquitination, E6AP-mediated ubiquitination, and ubiquitin-independent proteasomal degradation. Stabilizing factors include USP15, VCPIP1, BAF155, HDM2, JMJD2D, fatty acids, CPAP, and CUL4B. Edge labels denote the specific ubiquitination type or pathway involved. These networks highlight potential therapeutic targets for regulating HBx abundance in the HBV-infected cells and viral replication. Abbreviations: BAF155: BRG1-associated factor 155; CPAP: Centrosomal P4.1-associated protein; CUL4B: Cullin 4B; Fatty acids: Fatty acids; HDM2: Human double min 2; JMJD2D: Jumonji domain–containing protein 2D; USP15: Ubiquitin-specific peptidase 15; VCPIP1: Valosin-containing protein interacting protein 1.

TRIM5γ) or mimicking their activity is likely to enhance HBx clearance, suppress HBV replication, and limit HBx-driven tumorigenesis (Figure 2).

5.2. Stabilization mechanisms and targeting strategies

Unlike the ubiquitination process, the ubiquitin moieties from the HBx protein can be removed by deubiquitinating enzymes, which prevent degradation caused by the proteasome and thereby influence its stability, function, and localization. Several deubiquitinating enzymes have been characterized that confer intracellular stability to HBx (Figure 2). For example, the ubiquitin-specific peptidase 15 is reported to prevent the proteasomal degradation of HBx, increasing its levels and augmenting its ability to activate several cellular signaling pathways, contributing to CHB.[34] Therefore, developing ubiquitin-specific peptidase 15-targeted strategies may expand the therapeutic repertoire for CHB. Similarly, the valosin-containing protein-interacting protein 1 (VCPIP1) is a novel deubiquitinating enzyme that stabilizes HBx in a ubiquitin-independent manner. VCPIP1 serves as a scaffold that promotes interactions between HBx and proteasome components (including proteasome 26S subunit adenosine triphosphate 3), thereby enhancing HBV cccDNA transcription.[35] Therefore, disrupting HBx interactions with stabilizing factors, such as VCPIP1 or proteasome 26S subunit adenosine triphosphate 3, may reduce viral persistence and provide new insights for developing ubiquitin–proteasome system-based therapeutics for HBV-mediated pathogenesis (Figure 2). In addition, understanding the ability of HBx to degrade host restriction factors also opens avenues for restoring intrinsic antiviral defense in CHB infections.

The stability and activity of HBx are also enhanced after neddylation by the human homolog of mouse double min 2 that, in turn, prevents degradation following ubiquitination by E3 ligase seven in absentia homolog 1[36] (Figure 2). Therefore, targeting the neddylation pathway holds promise for the therapy of CHB. Likewise, Jumonji C domain-containing histone demethylase protein 2D (JMJD2D) is shown to stabilize HBx protein through direct interaction, preventing TRIM14-mediated polyubiquitination and HBx degradation. JMJD2D cooperates with HBx to promote HBV cccDNA transcription by demethylating histone H3 lysine 9 (H3K9) trimethylation on the cccDNA minichromosome.[37] Therefore, targeting JMJD2D through RNAi or pharmacological inhibitors can repress HBV replication and treat CHB infection. Similarly, the scaffold protein Cullin 4B, which is a component of the Cullin-RING E3 ligase complex, interacts with HBx protein to enhance HBV replication by inhibiting HBx ubiquitination and subsequent proteasomal degradation.[38] Thus, Cullin 4B could be a potential target for inhibiting HBV replication (Figure 2).

The HBx protein is also known to promote fatty acid build-up within hepatocytes, leading to hepatic inflammation, steatosis, or fatty liver disease. Elevated levels of fatty acids subvert the ubiquitination and degradation of HBx.[39] These observations suggest new therapeutic approaches for curing CHB patients with metabolic syndrome through low-fat diet therapy. Furthermore, the interaction between centrosomal P4.1-associated protein and HBx is reported to significantly increase NF-κB activity, promoting the development and progression of HCC.[40] Altogether, these results offer opportunities to develop mechanism-based therapies. HBx protein has been shown to directly interact with the E2-EPF ubiquitin carrier protein, resulting in the stabilization of its downstream target, hypoxia-inducible factor 1 subunit alpha proteins, which promote angiogenesis and HBx-mediated tumor growth and metastasis.[41] Moreover, the chromatin remodeling factor Brg1/Brm-associated factor 155 has been found to protect HBx protein from proteolytic degradation by competing with the proteasome 20S subunit alpha 7 (Figure 2).[42] The preceding observations may help develop new strategies for treating HBV infection and chronic liver diseases.

6. Regulation of key host and viral pathways

The HBx protein modulates the host cell's signal transduction pathways, calcium and reactive oxygen species levels, and influences cell proliferation and apoptosis. It also interacts with several host transcription factors (e.g., CREB, NF-κB) to activate or repress specific host and viral genes.[11-13] HBx promotes viral replication and host cell survival, interfering with the host immune system, and epigenetically altering host gene expression (Figure 3). HBx plays a central role in viral pathogenesis by disrupting cell cycle regulation, inducing oxidative stress and DNA damage, leading to chronic infection and HCC development.[11-13] Therefore, through specific targeting of one or more regulatory pathways, it should be possible to disrupt viral replication, chronic inflammation, or disease progression as discussed in subsequent sections.

6.1. Epigenetic regulation of cccDNA

The HBx protein plays a central role in regulating the transcriptional activity of cccDNA, the persistent nuclear template of HBV.[7,43] In the absence of HBx, cccDNA exists in a repressed chromatin state, marked by hypoacetylation and H3K9 methylation, which correlates

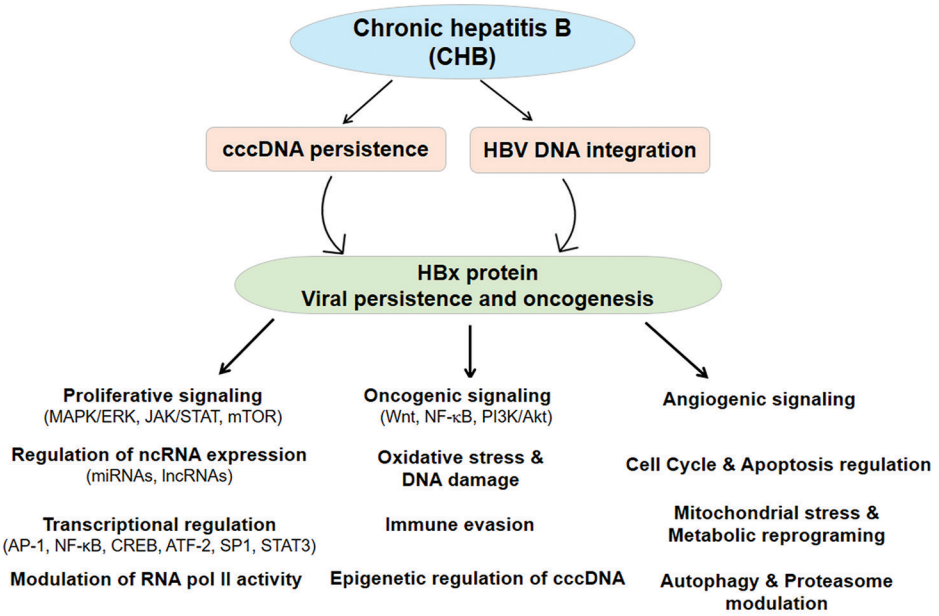

Figure 3. Role of the hepatitis B virus (HBV) X (HBx) protein in pathogenesis of chronic hepatitis B (CHB). CHB is sustained through covalently closed circular DNA (cccDNA) persistence and HBV DNA integration, both of which drive the expression of the HBx protein. HBx promotes viral persistence and hepatocarcinogenesis through multiple mechanisms, including deregulation of proliferative signaling and cell cycle, non-coding RNA expression, transcriptional regulation, epigenetic regulation of cccDNA, mitochondrial stress and metabolic reprogramming, Oxidative stress and DNA damage, immune evasion, angiogenic signaling, and many other functions. Abbreviations: Akt: Protein kinase B; AP-1: Activator protein 1; ATF-2: Activating transcription factor 2; cccDNA: Covalently closed circular DNA; CREB: Cyclic adenosine monophosphate response element binding protein; ERK: Extracellular signal-regulated kinase; JAK: Janus kinase; lncRNAs: Long non-coding RNAs; MAPK: Mitogen-activated protein kinase; miRNAs: Micro RNAs; mTOR: Mechanistic target of rapamycin; ncRNA: Non-coding RNA; NF-κB: Nuclear factor kappa B; PI3K: Phosphoinositide 3-kinase; RNA pol II: RNA polymerase II; SP1: Specificity protein 1; STAT: Signal transducer and activator of transcription.

with the recruitment of histone deacetylases, SET domain bifurcated histone lysine methyltransferase 1, and heterochromatin protein 1.[44,45] HBx binding facilitates a permissive chromatin state for viral replication and gene expression by recruiting chromatin-modifying enzymes, including p300 histone acetyltransferase and lysine-specific histone demethylase 1 to remove H3K9 methylation, and H3K4 methyltransferase Set1A to catalyze the mono-, di-, and trimethylation of lysine 4 on histone H3 (H3K4).[46-48] In addition, HBx can epigenetically alter gene expression by influencing the activity of DNA methyltransferases, which causes hypermethylation and repression of tumor suppressor genes, promoting tumorigenesis.[13]

The HBx protein also alters the epigenetic landscape of cccDNA by antagonizing host restriction factors, such as the Smc5/6 complex, and prevents transcriptional silencing.[49] One of the best-characterized HBx-host interactions involves the damage-specific DNA-binding protein 1 (DDB1), an adaptor of the cullin 4 (CUL4) A-regulator of cullins 1 E3 ubiquitin ligase complex.[50] Degradation of Smc5/6 by the HBx-DDB1-CUL4 complex removes this transcriptional block, thereby enabling productive HBV replication.[51] Consequently, these interactions are critical for persistent viral gene expression mediated by HBx.

6.2. Regulation of the host immune system

The HBx protein extensively modulates the host immune response, generally by suppressing innate immunity and evading immune destruction to promote viral persistence and disease progression. HBx can dysregulate the function of immune cells, such as dendritic cells and natural killer cells, contributing to chronic inflammation and the progression of liver disease. It achieves this through various mechanisms, including interfering with IFN signaling, altering epigenetic modifications, impairing immune cell functions, and downregulating key immune molecules such as type-1 IFN receptor and TRIM22 by suppressing tyrosine kinase 2 activity.[52] HBx can inhibit the retinoic acid-inducible gene i/melanoma differentiation-associated protein 5 pathway by interacting with essential proteins such as Sp110, thereby reducing IFN production. It can also interfere with the tumor necrosis factor receptor-associated factor 3/TANK-binding kinase 1/IFN regulatory factor 3 pathway, which is critical for initiating antiviral responses.[53,54]

The HBx protein plays a crucial role in HBV-related progression of chronic liver disease and HCC by promoting a pro-tumorigenic microenvironment, inhibiting apoptosis, and disrupting immune surveillance (Figure 3). It contributes to malignant transformation by modulating several signaling pathways, including Wnt/β-catenin, Ras/Raf/mitogen-activated protein kinase, NF-κB, Janus kinase/signal transducer and activator of transcription, phosphoinositide 3-kinase/protein kinase B, and focal adhesion kinase cascades, leading to increased proliferation, survival, invasion, and metastasis of hepatocytes.[11,14,17] In the nucleus, HBx dysregulates transcription, cell cycle checkpoints, apoptosis, and DNA repair, whereas in the mitochondria, it promotes the generation of reactive oxygen species and metabolic reprogramming.[55] HBx also induces oxidative stress, endoplasmic reticulum stress, and chronic hepatic inflammation, all of which contribute to tumor-promoting microenvironments.[56]

Furthermore, HBx also modulates immune responses by activating the NF-κB signaling pathways, protecting infected hepatocytes from apoptosis and immune-mediated clearance.[57] Its interactions with mitochondrial antiviral signaling protein can alter innate immune signaling, whereas transcriptional upregulation of host neoantigens may provoke adaptive immune responses during chronic liver disease.[58] These properties allow HBx to maintain a reservoir of infected cells, facilitating HBV persistence and increasing the risk of liver cancer. These observations suggest HBx to be a valuable therapeutic target for preventing CHB.

7. Strategies to regulate intracellular levels of HBV X protein

There are multiple strategies to regulate the intracellular HBx level and its diverse functions, which may be critical in mitigating the diverse roles of HBx in viral pathogenesis. The three main strategies are inhibiting *HBx* gene expression (RNAi, gene editing, or gene silencing); inducing proteolytic degradation of HBx protein (using small molecules); and developing therapeutic vaccines (Figure 4). The positive outcomes from new investigations could be useful in developing curative interventions for CHB.

7.1. Inhibition of the *HBV X* gene expression

As a transcriptional activator, HBx is central to HBV replication, viral gene expression, and the development of liver diseases, including hepatitis, cirrhosis, and HCC. Therefore, inhibiting HBx expression could downregulate viral load and counter HBV-associated pathogenesis. The inhibition strategies include RNAi, genome editing, and transcriptional gene silencing (Figure 4).

7.1.1. RNAi

RNAi could emerge as a preferred strategy against CHB therapy, as this could downregulate all activities associated with HBx. Small interfering RNAs (siRNAs) designed against HBx have effectively reduced HBV replication in different experimental models, confirming HBx as a critical therapeutic target for HBV.[7] Modified 5'-triphosphate siRNAs (3p-siRNAs) exhibited dual functionality, such as specific silencing of HBx and activation of the retinoic acid-inducible gene I pathway, thereby inducing type I IFN production and restoring innate immunity.[59] More broadly, siRNAs targeting all HBV transcripts suppressed HBx expression and indirectly stabilized Smc5/6, leading to the transcriptional repression of cccDNA.[51] Clinical candidates such as ALN-HBV, VIR-2218, ARC-520, and JNJ-3989 have demonstrated safe, dose-dependent HBsAg reduction, and, in some cases, prolonged suppression of viral proteins.[7,60] A phase 2 study showed that combining VIR-2218 with pegylated IFN-α2a improved HBsAg seroclearance rates.[61] GSK3389404, an antisense oligonucleotide conjugated to N-acetylgalactosamine, can also reduce HBx RNA and HBsAg levels with favorable pharmacokinetics.[62] While RNAi therapies offer strong potential, challenges remain regarding their delivery efficiency, durability, and effects on integrated HBV sequences that frequently encode HBx.[62] Early studies using hammerhead and hairpin ribozymes against HBx RNA successfully reduced HBx expression and activity, supporting the feasibility of RNA-based catalytic therapy. However, their clinical application is limited by the lack of effective delivery systems.[7]

7.1.2. Genome editing

The clustered regularly interspaced short palindromic repeats (CRISPR)/Cas9 system has been used as an alternative method for directly targeting HBx and other *HBV* genes (Figure 4). HBx-specific RNAs coupled with Cas9 nucleases have been shown to excise HBx, leading to significant reductions in HBx levels, HBsAg production, and cccDNA replication in hepatoma cells.[63] However, the off-target cleavage remains a technical limitation, although multiplexed targeting of conserved viral regions may improve the efficacy of this approach. While RNAi-based drugs are already progressing through clinical trials, ribozyme and CRISPR technologies are still in the early stages but hold long-term promise.

7.1.3. Transcriptional gene silencing

In HBV-infected hepatocytes, HBx localizes to the nucleus and hijacks the host CUL4-DDB1 E3 ubiquitin ligase complex. DDB1 typically functions as an adaptor for DDB1-CUL4-associated factors, enabling precise substrate recognition.[7] HBx mimics a DDB1-CUL4-associated

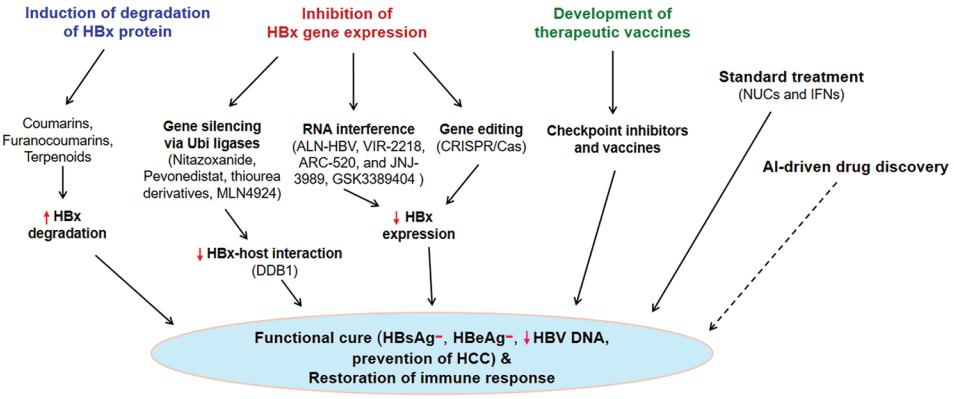

Figure 4. Therapeutic strategies targeting the hepatitis B virus X protein (HBx). Three main strategies for therapeutic targeting of HBx are the inhibition of HBx gene expression (by gene silencing, RNA interference, or gene editing), the induction of proteolytic degradation of HBx (using small molecules), and the development of therapeutic vaccines. Standard treatment for CHB infection involves antiviral medications, which are typically oral nucleos(t)ide analogs (NUCs), such as tenofovir or entecavir. Interferons (IFNs) are an alternative treatment option given to boost the host's immune system. Artificial intelligence (AI) could be considered for designing new therapeutic candidates. Abbreviations: ALN: Antisense oligonucleotide; ARC-520: RNA interference therapeutic targeting hepatitis B virus; CRISPR: Clustered regularly interspaced short palindromic repeats; DDB1: Damage-specific DNA binding protein 1; HBeAg: Hepatitis B e antigen; HBsAg: Hepatitis B surface antigen; HCC: Hepatocellular carcinoma; JNJ-3989: RNA interference therapeutic targeting hepatitis B virus; MLN4924: NEDD8-activating enzyme inhibitor; VIR-2218: RNA interference therapeutic targeting hepatitis B virus.

factor to bind to DDB1, thereby recruiting the ubiquitin ligase machinery to target the structural maintenance of Smc5/6 for proteasomal degradation. As Smc5/6 acts as a transcriptional repressor of cccDNA, its removal by HBx relieves this repression, thereby enhancing HBV transcription and replication (Figure 4).[7] Therefore, disrupting the HBx–DDB1 interaction and maintaining cccDNA in a transcriptionally repressed state could be a promising therapeutic approach for CHB.

Recently, a number of molecules that could disrupt the HBx-DDB1 interaction have been identified. For example, nitazoxanide, a thiazolide with antiparasitic activity, also exhibited an antiviral activity against HBV by disrupting this interaction and stabilizing the Smc5/6 complex. Nitazoxanide showed a significant reduction in virion production as well as potency against multiple drug-resistant HBV variants ($EC_{50:}$ 0.15–0.31 μM).[64] A pilot clinical trial in CHB showed a rapid decline in serum HBV DNA, which was consistent with its preclinical mechanism (Table 1).[65] These findings establish nitazoxanide as a proof-of-concept inhibitor for HBx–DDB1-targeted therapy. Pevonedistat, an inhibitor of the NEDD8-activating enzyme, has been found to stabilize the Smc5/6 complex by targeting the DDB1-CUL4-ROC1 E3 ligase pathway and downregulate HBV replication.[66]

More recently, thiourea derivatives (DSA-00, DSA-02, DSA-03) have been shown to enforce episomal silencing of cccDNA by stabilizing the Smc5/6 complex, resulting in the suppression of pgRNA synthesis, HBV DNA replication, and antigen secretion (HBsAg, HBeAg).[67] These agents showed antiviral potency comparable to that of entecavir without cytotoxicity, supporting their potential in functional cure strategies (Table 1). Likewise, inhibition of neddylation mediated by the E3 ligases has been found to stabilize HBx. Inhibition of neddylation by MLN4924 is able to suppress cccDNA transcription, pgRNA synthesis, HBV DNA replication, and HBsAg production.[68] Together, these findings underscore that pharmacologic stabilization of Smc5/6 achieved through interference with HBx-DDB1 binding or modulation of HBx post-translational modifications represents a targeted strategy for durable HBV suppression.

In addition, several natural bioactive compounds have been studied for their anti-HBV activities. For example, gambogic acid exhibited dose-dependent inhibition of HBx expression by upregulating the expression of the *DTX1* gene and boosting the notch signaling pathway.[69] Likewise, ursolic acid, a pentacyclic triterpenoid derived from medicinal herbs, blocked HBx-mediated autophagy and reversed HBx-driven drug resistance, cell migration, and apoptosis regulation through p38 and extracellular signal-regulated kinase signaling.[70] With its proven hepatoprotective and antitumor effects and minimal toxicity, ursolic acid should be considered as a candidate drug for further investigation and targeting *HBx-mediated* gene regulation.

7.2. Interference with HBV X protein stability and its functions

Targeting HBx for degradation has emerged as a promising curative strategy for CHB infection because HBx plays a

Table 1. Natural products and synthetic compounds known to promote hepatitis B virus X protein degradation and suppress hepatitis B virus replication

Compound/molecule	Class/source	Mechanism of HBx degradation	Effect on HBV markers	Development stage	References
Nitazoxanide	Synthetic thiazolide anti-infective agents	Disrupts DDB1–HBx interaction, restores Smc5/6	↓ HBV transcription and proteins	Clinical (Phase I)	65
Pevonedistat	Synthetic NEDD8-activating enzyme inhibitor	Blocks DDB1–CUL4–ROC1 E3 ligase activity, restores Smc5/6	↓ HBV replication	Preclinical	66
Thiourea derivatives (DSA-00, DSA-02, DSA-03)	Synthetic small molecules	Stabilizes Smc5/6 by blocking HBx–DDB1 interaction	↓ pgRNA synthesis, ↓ HBV DNA replication, ↓ HBsAg, ↓ HBeAg	Preclinical	67
Dicoumarol	Synthetic coumarin derivative; vitamin K analog; NQO1 inhibitor	Disrupts NQO1–HBx binding, promotes 20S proteasomal degradation	↓ HBx recruitment to cccDNA, ↓ HBV RNA/DNA, ↓ HBsAg, ↓ HBcAg	Preclinical (humanized liver mouse model)	71
Esculetin	Coumarin (*Microsorium fortunei*)	Reduces HBx protein levels (likely proteasome-dependent)	↓ HBx, ↓ HBsAg, ↓ HBV DNA	Preclinical (*in vitro*)	72
Sphondin	Angular furanocoumarin (*Toddalia asiatica*)	Binds HBx at Arg72, causes, 26S proteasomal degradation	↓ HBx–cccDNA binding, ↓ HBV RNA, ↓ HBsAg	Preclinical (*in vitro* and *in vivo*)	73
Furanocoumarins (Fc-20, Fc-31)	Synthetic furanocoumarin analogs	Directly binds HBx, induces allosteric change, and causes proteasomal degradation	↓ cccDNA transcription, ↓ pgRNA, ↓ HBsAg/HBeAg, ↓ virion secretion; active vs drug-resistant strains	Preclinical (*in vitro*)	74
Asiatic acid	Triterpenoid (*Centella asiatica*)	Autophagy–lysosomal degradation of HBx; alters histone markers (↓ H3K4me3, ↑ H3K9me3, H3K27me3)	↓ HBx–cccDNA binding, ↓ cccDNA transcription	Preclinical	75
All-trans retinoic acid	Natural vitamin A derivative	Antagonizes HBx-mediated suppression of p14/p16/p21 (indirect functional inhibition)	↓ HBx-driven cell proliferation	Preclinical	76
Tranilast	Antiviral (repurposed), HBx-targeting	High-affinity binding to HBx→promotes HBx degradation	↓ HBV DNA/HBsAg in cell culture	Preclinical	84
Broad-spectrum antivirals (e.g., azithromycin, domiphen, ammonium glycyrrhizinate, valsartan)	Antiviral (repurposing/ HBx-binding)	HBx binders with a low dissociation constant; antiviral activity demonstrated	Require functional validation	Experimental	84
Rapamycin	Antiviral, immunotropic	mTOR inhibitor, enhances proteasomal degradation of HBx	↓ HBx protein, ↓ HBV replication	Preclinical	85
SC75741, punicalagin, ledipasvir	Antiviral/ HBx-binders (*in silico*/ repurposed)	Strong HBx binding (by molecular docking); predicted to block HBx-interaction regions	Potential HBx inhibitors (predicted)	Experimental validation is limited or pending	86
TLR agonists (TLR7: GS-9620/vesatolimod; TLR8: GS-9688/ Selgantolimod)	Antiviral, immunotropic	Activate innate immunity; IFNα, ISGs, augment NK/ CD8 responses to counter HBx-mediated immune suppression	↓ HBV DNA/HBsAg in animal models	Clinical-stage immune modulators	87
PD-1/PD-L1 checkpoint inhibitors (e.g., nivolumab, anti-PD-L1 antibodies)	Immunotropic	Reverse HBx-exacerbated T-cell exhaustion→restore HBV-specific $CD8^+$T cells	↑ T-cell responses, ↑ viremia	Preclinical model	87

(Cont'd...)

Table 1. ***(Continued)***

Compound/molecule	Class/source	Mechanism of HBx degradation	Effect on HBV markers	Development stage	References
IL-12 (cytokine therapy)	Antiviral, immunotropic	Boosts multifunctional T cells (↑ IFN-γ, TNF-α), lowers PD-1 expression	↓ viremia, ↑ HBV-specific T cells	Preclinical model	87
Engineered HBV-specific T cells/TCR/CAR approaches	Antiviral, immunotropic,	Redirected cytotoxic T cells target HBx/HBV-expressing hepatocytes	Killing of HBV/HBx expressing cells; ↓ HBsAg in clinical cases	Preclinical, clinical	87
siRNAs/ASOs (e.g., JNJ-3989, VIR-2218, IONIS-HBVRx, ARC-520, bepirovirsen)	Antiviral, HBx-silencing (nucleic acid)	Post-transcriptional silencing of HBV transcripts, including HBx mRNA	↓ HBx expression, ↓ HBV RNAs/ HBsAg in clinical trials or preclinical studies	Preclinical/ clinical	87-89
Therapeutic vaccines (e.g., GS-4774)	Antiviral, immunotropic	Deliver HBx/core/surface antigens to stimulate HBV-specific T cells	Immune activation observed; limited HBsAg clearance as monotherapy in trials - candidate for combination therapy	Clinical	90
Curcumin (Herbal remedy)	Antioxidant, hepatoprotective	Anti-inflammatory; downregulates HBV transcriptional co-activators	↓ HBV transcription, protects hepatocytes from oxidative damage	Preclinical/ clinical	91
EGCG (epigallocatechin-3-gallate) (Herbal remedy)	Antiviral, antioxidant	Blocks HBV receptor and clathrin-mediated endocytosis; restores autophagy/lysosomal function	↓ HBV entry↓HBV markers Assists in autophagy	Preclinical	91
Punicalagin/punicalin/ geraniin (Herbal remedy)	Antiviral	Inhibit cccDNA production promote degradation	↓ cccDNA levels↓HBV markers	Preclinical *(in vitro)*	92
Rubiadin (Herbal remedy)	Natural anthraquinone	Inhibits HBx-associated functions in hepatocytes	↓ HBsAg, ↓ HBeAg, ↓ HBV DNA	Preclinical (*in vitro*)	93
Oxymatrine (Herbal remedy)	Matrine-type alkaloid (from *Sophora flavescens*)	Inhibits HBV DNA, HBsAg, HBeAg; immunomodulatory	↓ viral replication; ↑ IFN-α; activates NK cells and macrophages;	Preclinical (*in vitro*)	94

Note: ↓ refers to reduces; ↑ refers to increases.
Abbreviations: ATRA: All-trans retinoic acid; ASOs: Antisense oligonucleotides; CAR: Chimeric antigen receptor; cccDNA: Covalently closed circular DNA; CUL4: Cullin 4; DDB1: Damage-specific DNA binding protein 1; EGCG: Epigallocatechin-3-gallate; HBcAg: Hepatitis B core antigen; HBeAg: Hepatitis B e antigen; HBsAg: Hepatitis B surface antigen; HBV: Hepatitis B virus; HBx: Hepatitis B virus X protein; IFNs: Interferon; IL-12: Interleukin 12; ISGs: Interferon-stimulated genes; mTOR: Mammalian target of rapamycin; NK: Natural killer; NQO1: NAD (P) H quinone dehydrogenase 1; PD-1: Programmed cell death protein 1; PD-L1: Programmed death-ligand 1; pgRNA: Pregenomic RNA; ROC1: Ring-box protein 1; siRNAs: Small interfering RNAs; TCR: T-cell receptor; TLR: Toll-like receptor.

pivotal role in the HBV life cycle. Several natural and synthetic compounds have been reported to destabilize HBx through proteasomal or lysosomal pathways, thereby repressing HBV replication and viral gene expression. Coumarin-based compounds exhibit antiviral activity through diverse molecular targets. Dicoumarol, a vitamin K analog and inhibitor of nicotinamide adenine dinucleotide phosphate quinone oxidoreductase 1 (NQO1), was shown to disrupt the protective interaction between NQO1 and HBx, leading to HBx degradation through 20S proteasome.[71] Esculetin, another coumarin isolated from *Microsorium fortunei*, can also inhibit the expression of HBx protein and production of viral antigens in a dose-dependent manner (Figure 5 and Table 1).[72]

Natural furanocoumarins have a long history in traditional medicine with a wide array of bioactivities, including antiviral, anti-inflammatory, anti-proliferative, and photochemical properties, mediated by their structural variability (substituents, ring position, and isomerism). Natural furanocoumarins, such as sphondin from *Toddalia asiatica*, have been shown to bind to HBx and induce proteasomal degradation, resulting in suppression of viral transcription and HBsAg expression (Figure 5).[73] Synthetic furanocoumarin analogs include the systematic modification of substituents to optimize potency, selectivity, and pharmacological properties while minimizing off-target and toxic effects.[7] Recently, our team has identified two synthetic furanocoumarins, Fc-20 and

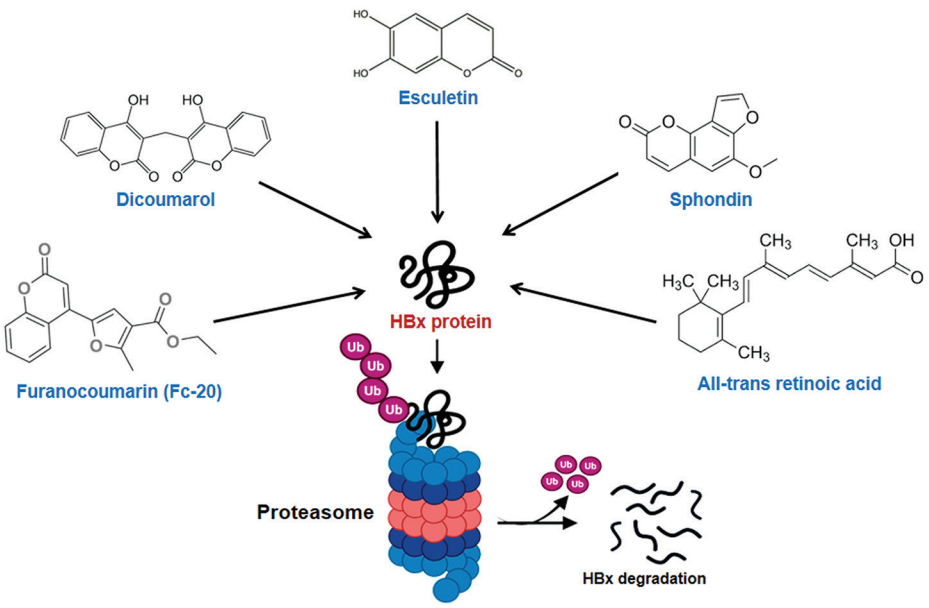

Figure 5. Inducers of hepatitis B virus X protein (HBx) destabilization. Molecular structures of some well-characterized bioactive compounds that promote proteasomal degradation of the HBx protein, including furanocoumarin (Fc-20), all-trans retinoic acid, asiatic acid, esculetin, and dicoumarol. Created in BioRender. Giri, S. (2025) https://BioRender.com/f1vc9g2.

Fc-31, that exhibited strong anti-HBV activity in cell culture by substantially reducing HBsAg and HBeAg secretion (>90%), thus outperforming the maximal reductions reported for entecavir.[74] Both compounds significantly decreased cccDNA transcriptional output, as inferred from reductions in 3.5 kb pgRNA levels, reflecting impaired replication template synthesis, and virion production, consistent with lowered intracellular viral replication intermediates (Table 1). Furthermore, these candidates retained potency against drug-resistant strains, including the tenofovir-resistant CYEI HBV mutant, positioning them as promising leads for both mono- and combination therapies.[74] Given the corroborative findings with natural analogs, such as sphondin, furanocoumarin scaffolds represent a compelling chemical series for advancing HBx-directed therapies aimed at the functional cure of CHB.

Asiatic acid, a pentacyclic triterpenoid isolated from *Centella asiatica* (a Chinese medicinal herb), can also promote HBx degradation through the autophagy-lysosomal pathway, resulting in reduced binding to cccDNA, reduced activating histone marks (H3K4 trimethylation), and increased repressive modifications (H3K9 trimethylation and H3K27 trimethylation), thereby impairing cccDNA transcription (Table 1).[75] Other natural compounds, such as all-trans retinoic acid, exhibited antiviral activity and antagonized HBx-mediated suppression of cell cycle inhibitors (p14, p16, and p21) by upregulating these proteins, suggesting indirect interference with HBx function (Table 1).[76] Collectively, these findings underscore the potential of both natural products and synthetic agents to promote HBx degradation, disrupt its interactions with host cofactors, and ultimately silence cccDNA transcription. Such strategies may complement existing antiviral efforts to achieve a functional cure for HBV.

7.3. HBV X protein-based therapeutic vaccine

One desirable goal of HBV immunotherapy has been to restore sufficient anti-HBV immunity in the CHB patients, as these patients show T cell exhaustion and a tolerogenic liver environment. HBx is considered to be a suitable immunogen for rejuvenating anti-HBV adaptive immunity in these patients. Experimental animals vaccinated with HBx demonstrated a good HBx-specific $CD4^+$ and $CD8^+$ T cell response with a significant reduction in serological biomarkers of HBV.[77] Interestingly, suppression of viral transcription, HBV replication, and viral antigen production could also be accomplished through intracellular delivery of monoclonal antibodies against HBx protein. These antibodies could also inhibit HBx–DDB1 interaction *in vitro*, suggesting their therapeutic potential.[78,79] These observations have provided proof-of-principle that targeting HBx merits further investigation.

8. Conclusion

Due to its role in viral persistence and hepatocarcinogenesis, HBx is a highly valuable therapeutic target for CHB infection.

Targeting HBx would not only mitigate both viral persistence and oncogenic transformation but also potentially improve the long-term outcomes of patients with CHB. Therefore, inclusion of HBx-directed agents within current therapeutic regimens may accelerate progress toward a functional cure. Furthermore, this could achieve durable viral suppression, limit relapse, and help restore HBV-specific immune responses.

Despite the availability of effective vaccines and nucleos(t)ide analogs as antivirals, CHB infection continues to pose a global health challenge, affecting nearly 254 million individuals and causing over 1.1 million deaths annually.[3] The persistence of cccDNA and the integration of viral genomes into host hepatocytes remain the primary barriers to cure.[80-82] Current therapeutic regimens, primarily nucleos(t)ides and IFN-α, can achieve viral suppression but rarely result in sustained HBsAg clearance.[82] Consequently, the risk of progressive liver disease and HCC persists, even with long-term therapy.[82] Recently, HBx protein has emerged as a key viral factor because of its essential role in viral replication and gene expression, as well as reprogramming of host signaling pathways to promote immune tolerance, inflammation, fibrosis, and oncogenic transformation.[11,12,17] Therefore, destabilization or downregulation of HBx would not only attenuate HBx-driven oncogenic signaling but also limit relapse after treatment discontinuation, and diminish cccDNA reservoir and viral antigen load.

Emerging approaches, such as RNAi, antisense oligonucleotides, CRISPR/Cas-based genome editing, and small molecules directed at HBx-host interactions, are being investigated as means to neutralize the oncogenic potential of HBx. Furthermore, the direct-acting antivirals that block viral entry, nucleocapsid assembly, reverse transcription, and secretion of viral antigens are at advanced stages of development.[82] While such antivirals can effectively reduce antigenemia and/or suppress viremia, none of these strategies are effective at eliminating cccDNA or integrated HBV DNA.[81,82] Therefore, combining HBx-targeted strategies into existing treatment regimens could bridge this gap. Moreover, artificial intelligence should be applied in designing therapeutic candidates with desired characteristics, such as solubility and target affinity.[83] In summary, HBx-targeting represents a critical frontier in HBV therapy with the potential to couple viral suppression with cancer prevention.

Acknowledgments

None.

Funding

This work was supported in part by a J.C. Bose National Fellowship (Grant no. SR/S2/JCB-80/2012) from the Department of Science and Technology, Government of India, New Delhi (awarded to V.K.). S.G. received a senior research fellowship from the University Grants Commission, India (grant no. 590/CSIR-UGC NET June 2017).

Conflict of interest

The authors declare that they have no competing interests.

Author contributions

Conceptualization: Vijay Kumar
Visualization: Sunita Giri
Writing – original draft: Sunita Giri
Writing – review & editing: Vijay Kumar

Ethics approval and consent to participate

Not applicable.

Consent for publication

Not applicable.

Availability of data

Not applicable.

References

1. Jeng WJ, Papatheodoridis GV, Lok ASF. Hepatitis B. *Lancet*. 2023;401(10381):1039-1052.

   doi: 10.1016/S0140-6736(22)01468-4

2. di Filippo Villa D, Navas MC. Vertical transmission of hepatitis B virus-an update. *Microorganisms*. 2023;11(5):1140.

   doi: 10.3390/microorganisms11051140

3. WHO; 2025. Available from: https://www.who.int/news-room/fact-sheets/detail/hepatitis-b [Last accessed on 2025 Sep 21].

4. CDC; 2025. Available from: https://www.cdc.gov/hepatitis-b/hcp/perinatal-provider-overview/index.html [Last accessed on 2025 Sep 24].

5. Yuen MF, Chen DS, Dusheiko GM, *et al*. Hepatitis B virus infection. *Nat Rev Dis Primers*. 2018;4:18035.

   doi: 10.1038/nrdp.2018.35

6. Seeger C, Mason WS. Molecular biology of hepatitis B virus infection. *Virology*. 2015;479-480:672-686.

   doi: 10.1016/j.virol.2015.02.031

7. Kumar V. HBx protein as a therapeutic target for functional cure of hepatitis B virus infection. *Virology*. 2025;604:110438.

   doi: 10.1016/j.virol.2025.110438

8. Zoulim F, Chen PJ, Dandri M, Kennedy PT, Seeger C. Hepatitis B virus DNA integration: Implications

for diagnostics, therapy, and outcome. *J Hepatol*. 2024;81(6):1087-1099.

doi: 10.1016/j.jhep.2024.06.037

9. Singh A, Kumar J, Kumar V. Chronic hepatitis B infection: Current and emerging therapeutic strategies. *Curr Top Med Chem*. 2023;23(18):1727-1752.

doi: 10.2174/1568026623666230413094331

10. Liu T, Wang H, Zhao Y, Wang YX, Xing X, Gao P. Drug development for chronic hepatitis B functional cure: Recent progress. *World J Hepatol*. 2025;17:105797.

doi: 10.4254/wjh. v17.i4.105797

11. Kumar V, Sarkar DP. Hepatitis B virus X protein (HBx): Structure-function relationships and role in viral pathogenesis. In: Gossen M, Kaufman J, Triezenberg SJ, editors. *Handbook of Experimental Pharmacology – Transcription Factors*. Vol. 166. Berlin/Heidelberg (Germany): Springer; 2004. p. 377-407.

doi: 10.1007/978-3-642-18932-6_12

12. Li D, Hamadalnil Y, Tu T. Hepatitis B viral protein HBx: Roles in viral replication and hepatocarcinogenesis. *Viruses*. 2024;16(9):1361.

doi: 10.3390/v16091361

13. Sivasudhan E, Blake N, Lu Z, Meng J, Rong R. Hepatitis B viral protein HBx and the molecular mechanisms modulating the hallmarks of hepatocellular carcinoma: A comprehensive review. *Cells*. 2022;11:741.

doi: 10.3390/cells11040741

14. Turton KL, Meier-Stephenson V, Badmalia MD, Coffin CS, Patel TR. Host transcription factors in hepatitis B virus RNA synthesis. *Viruses*. 2020;12(2):160.

doi: 10.3390/v12020160

15. Prieto C, Montecinos J, Jiménez G, *et al*. Phosphorylation of phylogenetically conserved amino acid residues confines HBx within different cell compartments of human hepatocarcinoma cells. *Molecules*. 2021;26(5):1254.

doi: 10.3390/molecules26051254

16. Henkler F, Hoare J, Waseem N, *et al*. Intracellular localization of the hepatitis B virus HBx protein. *J Gen Virol*. 2001;82(Pt 4):871-882.

doi: 10.1099/0022-1317-82-4-871

17. Agustiningsih A, Rasyak MR, Turyadi, Jayanti S, Sukowati C. The oncogenic role of hepatitis B virus X gene in hepatocarcinogenesis: Recent updates. *Explor Target Antitumor Ther*. 2024;5(1):120-134.

doi: 10.37349/etat.2024.00209

18. Minor MM, Slagle BL. Hepatitis B virus HBx protein interactions with the ubiquitin proteasome system. *Viruses*. 2014;6(11):4683-4702.

doi: 10.3390/v6114683

19. Hu Z, Zhang Z, Doo E, Coux O, Goldberg AL, Liang TJ. Hepatitis B virus X protein is both a substrate and a potential inhibitor of the proteasome complex. *J Virol*. 1999;73(9):7231-7240.

doi: 10.1128/JVI.73.9.7231-7240.1999

20. Kim JH, Kang S, Kim J, Ahn BY. Hepatitis B virus core protein stimulates the proteasome-mediated degradation of viral X protein. *J Virol*. 2003;77(13):7166-7173.

doi: 10.1128/jvi.77.13.7166-7173.2003

21. Kornyeyev D, Ramakrishnan D, Voitenleitner C, *et al*. Spatiotemporal analysis of hepatitis B virus X protein in primary human hepatocytes. *J Virol*. 2019;93(16):e00248-19.

doi: 10.1128/JVI.00248-19

22. Dandri M, Petersen J, Stockert RJ, Harris TM, Rogler CE. Metabolic labeling of woodchuck hepatitis B virus X protein in naturally infected hepatocytes reveals a bimodal half-life and association with the nuclear framework. *J Virol*. 1998;72(11):9359-9364.

doi: 10.1128/JVI.72.11.9359-9364.1998

23. Xian L, Zhao J, Wang J, *et al*. p53 Promotes proteasome-dependent degradation of oncogenic protein HBx by transcription of MDM2. *Mol Biol Rep*. 2010;37(6):2935-2940.

doi: 10.1007/s11033-009-9855-1

24. Lim HY, Han J, Yoon H, Jang KL. Tumor suppressor p53 inhibits hepatitis B virus replication by downregulating HBx via E6AP-mediated proteasomal degradation in human hepatocellular carcinoma cell lines. *Viruses*. 2022;14:2313.

doi: 10.3390/v14102313

25. Qiu Q, He Z, Liu J, *et al*. Homeobox protein MSX-1 restricts hepatitis B virus by promoting ubiquitin-independent proteasomal degradation of HBx protein. *PLoS Pathog*. 2025;21:e1012897.

doi: 10.1371/journal.ppat.1012897

26. Wang J, Yuan X, Wang Y, *et al*. PreS1BP mediates inhibition of hepatitis B virus replication by promoting HBx protein degradation. *Virus Res*. 2024;341:199326.

doi: 10.1016/j.virusres.2024.199326

27. Zhao J, Wang C, Wang J, *et al*. E3 ubiquitin ligase Siah-1 facilitates poly-ubiquitylation and proteasomal degradation of the hepatitis B viral X protein. *FEBS Lett*. 2011;585(19):2943-2950.

doi: 10.1016/j.febslet.2011.08.015

28. Hu Q, Liu Z, Liu Y, *et al*. SIAH2 suppresses c-JUN pathway by promoting the polyubiquitination and degradation of HBx in hepatocellular carcinoma. *J Cell Mol Med*. 2024;28:e18484.

doi: 10.1111/jcmm.18484

29. Wan T, Lei Z, Tu B, Wang T, Wang J, Huang F. NEDD4 Induces K48-Linked degradative ubiquitination of hepatitis B virus X protein and inhibits HBV-associated HCC progression. *Front Oncol*. 2021;11:625169.

doi: 10.3389/fonc.2021.625169

30. Lee S, Yoon H, Han J, Jang KL. Hepatitis C virus core protein inhibits hepatitis B virus replication by downregulating HBx levels via Siah-1-mediated proteasomal degradation during coinfection. *J Gen Virol*. 2021;102(12):e001701.

doi: 10.1099/jgv.0.001701

31. Song Y, Li M, Wang Y, Zhang H, Wei L, Xu W. E3 ubiquitin ligase TRIM21 restricts hepatitis B virus replication by targeting HBx for proteasomal degradation. *Antiviral Res*. 2021;192:105107.

doi: 10.1016/j.antiviral.2021.105107

32. Sheng X, Yang Y, Zhu M, *et al*. Non-proteolytic ubiquitination of HBx controls HBV replication. *Virol Sin*. 2024;39(2):338-342.

doi: 10.1016/j.virs.2024.01.008

33. Tan G, Yi Z, Song H, *et al*. Type-I-IFN-stimulated gene TRIM5γ inhibits HBV replication by promoting HBx degradation. *Cell Rep.* 2019;29(11):3551-3563.e3.

doi: 10.1016/j.celrep.2019.11.041

34. Su ZJ, Cao JS, Wu YF, *et al*. Deubiquitylation of hepatitis B virus X protein (HBx) by ubiquitin-specific peptidase 15 (USP15) increases HBx stability and its transactivation activity. *Sci Rep.* 2017;7:40246.

doi: 10.1038/srep40246

35. Wu Q, Zhang L, Xu X, *et al*. Hepatitis B virus X protein is stabilized by the deubiquitinating enzyme VCPIP1 in a ubiquitin-independent manner by recruiting the 26S proteasome subunit PSMC3. *J Virol*. 2022;96(13):e0061122.

doi: 10.1128/jvi.00611-22

36. Liu N, Zhang J, Yang X, *et al*. HDM2 promotes NEDDylation of hepatitis B virus HBx to enhance its stability and function. *J Virol*. 2017;91(16):e00340-17.

doi: 10.1128/JVI.00340-17

37. Kong X, Liu Z, Zhang R, *et al*. JMJD2D stabilises and cooperates with HBx protein to promote HBV transcription and replication. *JHEP Rep.* 2023;5(10):100849.

doi: 10.1016/j.jhepr.2023.100849

38. Shan H, Wang B, Zhang X, *et al*. CUL4B facilitates HBV replication by promoting HBx stabilization. *Cancer Biol Med*. 2021;19(1):120-131.

doi: 10.20892/j.issn.2095-3941.2020.0468

39. Cho HK, Kim SY, Yoo SK, Choi YH, Cheong J. Fatty acids increase hepatitis B virus X protein stabilization and HBx-induced inflammatory gene expression. *FEBS J*. 2014;281(9):2228-2239.

doi: 10.1111/febs.12776

40. Yen CJ, Yang ST, Chen RY, *et al*. Hepatitis B virus X protein (HBx) enhances centrosomal P4.1-associated protein (CPAP) expression to promote hepatocarcinogenesis. *J Biomed Sci*. 2019;26(1):44.

doi: 10.1186/s12929-019-0534-9

41. Lim JH, Kim DG, Yu DY, *et al*. Stabilization of E2-EPF UCP protein is implicated in hepatitis B virus-associated hepatocellular carcinoma progression. *Cell Mol Life Sci*. 2019;76(13):2647-2662.

doi: 10.1007/s00018-019-03066-9

42. Chen H, Zhang Y, Ye S, *et al*. Chromatin remodelling factor BAF155 protects hepatitis B virus X protein (HBx) from ubiquitin-independent proteasomal degradation. *Emerg Microbes Infect*. 2019;8(1):1393-1405.

doi: 10.1080/22221751.2019.1666661

43. Belloni L, Pollicino T, De Nicola F, *et al*. Nuclear HBx binds the HBV minichromosome and modifies the epigenetic regulation of cccDNA function. *Proc Natl Acad Sci U S A*. 2009;106(47):19975-19979.

doi: 10.1073/pnas.0908365106

44. Shon JK, Shon BH, Park IY, *et al*. Hepatitis B virus-X protein recruits histone deacetylase 1 to repress insulin-like growth factor binding protein 3 transcription. *Virus Res*. 2009;139(1):14-21.

doi: 10.1016/j.virusres.2008.09.006

45. Rivière L, Gerossier L, Ducroux A, *et al*. HBx relieves chromatin-mediated transcriptional repression of hepatitis B viral cccDNA involving SETDB1 histone methyltransferase. *J Hepatol*. 2015;63(5):1093-1102.

doi: 10.1016/j.jhep.2015.06.023

46. Chong CK, Cheng CYS, Tsoi SYJ, *et al*. HBV X protein mutations affect HBV transcription and association of histone-modifying enzymes with covalently closed circular DNA. *Sci Rep*. 2020;10(1):802.

doi: 10.1038/s41598-020-57637-z

47. Alarcon V, Hernández S, Rubio L, *et al*. The enzymes LSD1 and Set1A cooperate with the viral protein HBx to establish an active hepatitis B viral chromatin state. *Sci Rep.* 2016;6:25901.

doi: 10.1038/srep25901

48. Gómez-Moreno A, Ploss A. Mechanisms of hepatitis B virus cccDNA and minichromosome formation and HBV gene transcription. *Viruses*. 2024;16(4):609.

doi: 10.3390/v16040609

49. Decorsière A, Mueller H, van Breugel PC, *et al*. Hepatitis B virus X protein identifies the Smc5/6 complex as a host

restriction factor. *Nature*. 2016;531(7594):386-389.

doi: 10.1038/nature17170

50. Sitterlin D, Lee TH, Prigent S, Tiollais P, Butel JS, Transy C. Interaction of the UV-damaged DNA-binding protein with hepatitis B virus X protein is conserved among mammalian hepadnaviruses and restricted to transactivation-proficient X-insertion mutants. *J Virol*. 1997;71(8):6194-6199.

doi: 10.1128/JVI.71.8.6194-6199.1997

51. Bächer J, Allweiss L, Dandri M. SMC5/6-mediated transcriptional regulation of hepatitis B virus and its therapeutic potential. *Viruses*. 2024;16(11):1667.

doi: 10.3390/v16111667

52. Li A, Yi Z, Ma C, *et al*. Innate immune recognition in hepatitis B virus infection. *Virulence*. 2025;16(1):2492371.

doi: 10.1080/21505594.2025.2492371

53. Kim HR, Lee SH, Jung G. The hepatitis B viral X protein activates NF-kappaB signaling pathway through the up-regulation of TBK1. *FEBS Lett*. 2010;584(3):525-530.

doi: 10.1016/j.febslet.2009.11.091

54. Wang X, Li Y, Mao A, Li C, Li Y, Tien P. Hepatitis B virus X protein suppresses virus-triggered IRF3 activation and IFN-beta induction by disrupting the VISA-associated complex. *Cell Mol Immunol*. 2010;7(5):341-348.

doi: 10.1038/cmi.2010.36

55. Kim S, Park J, Han J, Jang KL. Hepatitis B virus X protein induces reactive oxygen species generation via activation of p53 in human hepatoma cells. *Biomolecules*. 2024;14(10):1201.

doi: 10.3390/biom14101201

56. Fu S, Zhou RR, Li N, Huang Y, Fan XG. Hepatitis B virus X protein in liver tumor microenvironment. *Tumour Biol*. 2016;37:15371-15381.

doi: 10.1007/s13277-016-5406-2

57. Lin S, Zhang YJ. Interference of apoptosis by hepatitis B virus. *Viruses*. 2017;9(8):230.

doi: 10.3390/v9080230

58. Wei C, Ni C, Song T, *et al*. The hepatitis B virus X protein disrupts innate immunity by downregulating mitochondrial antiviral signaling protein. *J Immunol*. 2010;185(2):1158-1168.

doi: 10.4049/jimmunol.0903874

59. Chen X, Qian Y, Yan F, *et al*. 5'-triphosphate-siRNA activates RIG-I-dependent type I interferon production and enhances inhibition of hepatitis B virus replication in HepG2.2.15 cells. *Eur J Pharmacol*. 2013;721:86-95.

doi: 10.1016/j.ejphar.2013.09.050

60. Gane E, Lim YS, Kim JB, *et al*. Evaluation of RNAi therapeutics VIR-2218 and ALN-HBV for chronic hepatitis B: Results from randomized clinical trials. *J Hepatol*. 2023;79:924-932.

doi: 10.1016/j.jhep.2023.05.023

61. Yuen MF, Lim YS, Yoon KT, *et al*. VIR-2218 (elebsiran) plus pegylated interferon-alfa-2a in participants with chronic hepatitis B virus infection: A phase 2 study. *Lancet Gastroenterol Hepatol*. 2024;9:1121-1132.

doi: 10.1016/S2468-1253(24)00237-1

62. Han K, Ito H, Elston R, *et al*. Comparison of pharmacokinetics of the GalNAc-conjugated antisense oligonucleotide GSK3389404 in participants with chronic hepatitis B infection across the Asia-Pacific region. *Antimicrob Agents Chemother*. 2023;67(1):e0090022.

doi: 10.1128/aac.00900-22

63. Rawal P, Tripathi DM, Hemati H, *et al*. Targeted HBx gene editing by CRISPR/Cas9 system effectively reduces epithelial to mesenchymal transition and HBV replication in hepatoma cells. *Liver Int*. 2024;44:614-624.

doi: 10.1111/liv.15805

64. Sekiba K, Otsuka M, Ohno M, *et al*. Inhibition of HBV transcription from cccDNA with nitazoxanide by targeting the HBx-DDB1 interaction. *Cell Mol Gastroenterol Hepatol*. 2019;7(2):297-312.

doi: 10.1016/j.jcmgh.2018.10.010

65. Rossignol JF, Bréchot C. A pilot clinical trial of nitazoxanide in the treatment of chronic hepatitis B. *Hepatol Commun*. 2019;3:744-747.

doi: 10.1002/hep4.1339

66. Ren J, Cheng S, Ren F, *et al*. Epigenetic regulation and its therapeutic potential in hepatitis B virus covalently closed circular DNA. *Genes Dis*. 2024;12:101215.

doi: 10.1016/j.gendis.2024.101215

67. Kumar J, Singh A, Tyagi P, Sharma D, Sarin SK, Kumar V. New thiourea derivatives that target the episomal silencing SMC5 protein to inhibit HBx-dependent viral DNA replication and gene transcription. *Virusdisease*. 2024;35(4):577-588.

doi: 10.1007/s13337-024-00895-6

68. Xie M, Guo H, Lou G, *et al*. Neddylation inhibitor MLN4924 has anti-HBV activity via modulating the ERK-HNF1α-C/EBPα-HNF4α axis. *J Cell Mol Med*. 2021;25:840-854.

doi: 10.1111/jcmm.16137

69. Wen X, Li D, Chen P, *et al*. Gambogic acid inhibits HBx-mediated hepatitis B virus replication by targeting the DTX1-Notch signaling pathway. *Virus Res*. 2024;339:199273.

doi: 10.1016/j.virusres.2023.199273

70. Chang CD, Lin PY, Hsu JL, Shih WL. Ursolic acid suppresses hepatitis B virus X protein-mediated autophagy

and chemotherapeutic drug resistance. *Anticancer Res.* 2016;36:5097-5107.

doi: 10.21873/anticanres.11079

71. Cheng ST, Hu JL, Ren JH, *et al*. Dicoumarol, an NQO1 inhibitor, blocks cccDNA transcription by promoting degradation of HBx. *J Hepatol*. 2021;74(3):522-534.

doi: 10.1016/j.jhep.2020.09.019

72. Huang SX, Mou JF, Luo Q, *et al*. Anti-hepatitis B virus activity of esculetin from *Microsorium fortunei in vitro* and *in vivo*. *Molecules.* 2019;24:3475.

doi: 10.3390/molecules24193475

73. Ren F, Hu J, Dang Y, *et al*. Sphondin efficiently blocks HBsAg production and cccDNA transcription through promoting HBx degradation. *J Med Virol*. 2023;95(3):e28578.

doi: 10.1002/jmv.28578

74. Tyagi P, Singh A, Kumar J, *et al*. Furanocoumarins promote proteasomal degradation of viral HBx protein and down-regulate cccDNA transcription and replication of hepatitis B virus. *Virology*. 2024;595:110065.

doi: 10.1016/j.virol.2024.110065

75. Li R, Wang C, Xu K, *et al*. Asiatic acid inhibits HBV cccDNA transcription by promoting HBx degradation. *Virol J*. 2024;21:268.

doi: 10.1186/s12985-024-02535-3

76. Han J, Jang KL. All-trans retinoic acid downregulates HBx levels via E6-associated protein-mediated proteasomal degradation to suppress hepatitis B virus replication. *PLoS One*. 2024;19:e0305350.

doi: 10.1371/journal.pone.0305350

77. Horng JH, Lin WH, Wu CR, *et al*. HBV X protein-based therapeutic vaccine accelerates viral antigen clearance by mobilizing monocyte infiltration into the liver in HBV carrier mice. *J Biomed Sci*. 2020;27(1):70.

doi: 10.1186/s12929-020-00662-x

78. Tao S, Pan S, Gu C, *et al*. Characterization and engineering of broadly reactive monoclonal antibody against hepatitis B virus X protein that blocks its interaction with DDB1. *Sci Rep.* 2019;9(1):20323.

doi: 10.1038/s41598-019-56819-8

79. Zhang JF, Xiong HL, Cao JL, *et al*. A cell-penetrating whole molecule antibody targeting intracellular HBx suppresses hepatitis B virus via TRIM21-dependent pathway. *Theranostics*. 2018;8(2):549-562.

doi: 10.7150/thno.20047

80. Tsounis EP, Tourkochristou E, Mouzaki A, Triantos C. Toward a new era of hepatitis B virus therapeutics: The pursuit of a functional cure. *World J Gastroenterol*. 2021;27:2727-2757.

doi: 10.3748/wjg.v27.i21.2727

81. Fanning GC, Zoulim, F, Hou, J, Bertoletti, A. Therapeutic strategies for hepatitis B virus infection: Towards a cure. *Nat Rev Drug Discov*. 2019;18:827-844.

doi: 10.1038/s41573-019-0037-0

82. Phillips S, Jagatia R, Chokshi S. Novel therapeutic strategies for chronic hepatitis B. *Virulence*. 2022;13:1111-1132.

doi: 10.1080/21505594.2022.2093444

83. Xu Y, Liu X, Cao X, *et al*. Artificial intelligence: A powerful paradigm for scientific research. *Innovation* (*Camb*). 2021;2:100179.

doi: 10.1016/j.xinn.2021.100179

84. Ma Y, Nakamoto S, Ao J, *et al*. Antiviral compounds screening targeting HBx protein of the hepatitis B virus. *Int J Mol Sci*. 2022;23:12015.

doi: 10.3390/ijms231912015

85. Zhang Y, Li L, Cheng ST, *et al*. Rapamycin inhibits hepatitis B virus covalently closed circular DNA transcription by enhancing the ubiquitination of HBx. *Front Microbiol.* 2022;13:850087.

doi: 10.3389/fmicb.2022.850087

86. Hamadalnil Y, Altayb HN. *In silico* molecular study of hepatitis B virus X protein as a therapeutic target. *J Biomol Struct Dyn*. 2024;42:4002-4015.

doi: 10.1080/07391102.2023.2217920

87. Zhang E, Kosinska A, Lu M, Yan H, Roggendorf M. Current status of immunomodulatory therapy in chronic hepatitis B, fifty years after discovery of the virus: Search for the "magic bullet" to kill cccDNA. *Antiviral Res*. 2015;123:193-203.

doi: 10.1016/j.antiviral.2015.10.009

88. Zhang L, Cao Y, Zhuang S, *et al*. Small nucleic acid drugs-the dawn of functional cure of chronic hepatitis B. *Front Pharmacol*. 2025;16:1633001.

doi: 10.3389/fphar.2025.1633001

89. Li J, Liu S, Zang Q, Yang R, Zhao Y, He Y. Current trends and advances in antiviral therapy for chronic hepatitis B. *Chin Med J* (*Engl*). 2024;137(23):2821-2832.

doi: 10.1097/CM9.0000000000003178

90. Lok AS, Pan CQ, Han SH, *et al*. Randomized phase II study of GS-4774 as a therapeutic vaccine in virally suppressed patients with chronic hepatitis B. *J Hepatol*. 2016;65:509-516.

doi: 10.1016/j.jhep.2016.05.016

91. Hao L, Li S, Hu X. Therapeutic interventions aimed at cccDNA: Unveiling mechanisms and evaluating the potency of natural products. *Front Cell Infect Microbiol*. 2025;15:1598872.

doi: 10.3389/fcimb.2025.1598872

92. Liu C, Cai D, Zhang L, *et al*. Identification of hydrolyzable

tannins (punicalagin, punicalin and geraniin) as novel inhibitors of hepatitis B virus covalently closed circular DNA. *Antiviral Res*. 2016;134:97-107.

doi: 10.1016/j.antiviral.2016.08.026

93. Peng Z, Fang G, Peng F, *et al*. Effects of Rubiadin isolated from Prismatomeris connata on anti-hepatitis B virus activity *in vitro*. *Phytother Res*. 2017;31(12):1962-1970.

doi: 10.1002/ptr.5945

94. Lin M, Yang LY, Li WY, Peng YP, Zheng JK. Inhibition of the replication of hepatitis B virus *in vitro* by oxymatrine. *J Int Med Res*. 2009;37(5):1411-1419.

doi: 10.1177/147323000903700515

ACCSCIENCE PUBLISHING

Journal of Clinical and Translational Research

ORIGINAL ARTICLE

Diagnostic delay in very early-onset inflammatory bowel disease: A tertiary single-center retrospective study

Juliana Tedesco Dias, Debora Avellaneda Penatti, Jessika Alves de Souza Costa, Gabriela Nascimento Hercos, Carine Dias Ferreira de Jesus, Mary de Assis Carvalho, and Nilton Carlos Machado*

Division of Pediatric Gastroenterology, Hepatology, and Nutrition, Department of Pediatrics, Botucatu Medical School, São Paulo State University, Botucatu, São Paulo, Brazil

Abstract

Background: Very early-onset inflammatory bowel disease (VEO-IBD) may have an aggressive clinical course. Upon suspicion, an immediate transfer to a pediatric gastroenterology clinic should be made, considering that diagnostic delay (DD) in referral can have profound implications. **Objectives:** The objectives of the study are to investigate the time, proportion, and factors associated with DD in VEO-IBD and explore the symptoms at initial presentation. **Methods:** An observational, retrospective, single-center study of consecutive patients with VEO-IBD confirmed by histopathology was conducted. We measured the time to diagnosis—the interval between symptom onset and the final VEO-IBD diagnosis. DD was defined as the time to diagnosis that exceeded the 75th percentile. **Results**: Twenty-five children with VEO-IBD—16 with ulcerative colitis (UC) and 9 with Crohn's disease (CD)—were evaluated, with a median age of 34 months. Ages at first symptoms, first visit, and diagnosis were significantly lower for the CD group. However, there was no significant difference in the time from first symptoms to diagnosis between CD and UC. Patients with weight loss, anemia, and fistulas did not meet established criteria for DD and were referred early. **Conclusion**: Our study underscores the importance of early recognition of VEO-IBD, with bloody diarrhea, abdominal pain, and weight loss serving as crucial warning signs. Identifying these symptoms can aid in the early diagnosis and prompt referral to a specialist, potentially reducing the risk of DD. **Relevance for patients:** Early recognition of bloody diarrhea, abdominal pain, and weight loss in young children can speed diagnosis of VEO-IBD and ensure timely referral to specialist care.

Keywords: Very early-onset inflammatory bowel disease; Diagnostic delay; Crohn's Disease; Ulcerative colitis; Diarrhea; Blood in stools; Abdominal pain; Weight loss

***Corresponding author:**
Nilton Carlos Machado
(nilton.machado@unesp.br)

Citation: Dias JT, Penatti DA, de Souza Costa JA, *et al*. Diagnostic delay in very early-onset inflammatory bowel disease: A tertiary single-center retrospective study. *J Clin Transl Res*. 2026;12(1):39-46.
doi: 10.36922/JCTR025360059

Received: September 2, 2025

Revised: November 21, 2025

Accepted: December 4, 2025

Published online: December 16, 2025

1. Introduction

Pediatric inflammatory bowel disease (IBD) is a chronic condition, consisting of Crohn's disease (CD), ulcerative colitis (UC), and unclassified IBD.[1-3] In addition, pediatric IBD has a severe subgroup designated very early-onset IBD (VEO-IBD), which manifests

before 6 years of age, and is classified as infantile-onset IBD if diagnosed before 2 years of age and neonatal-onset if diagnosed by 28 days of age.[4,5] VEO-IBD is distinct in its clinical and therapeutic challenges and often follows an aggressive course that requires close specialist management. Upon suspicion of pediatric IBD, immediate referral to a pediatric gastroenterology clinic for investigation is not only necessary but also a professional responsibility that cannot be overstated. This rapid action can help prevent the development of severe complications,[6,7] underscoring the crucial role of early referral and diagnosis in managing VEO-IBD.

Diagnosing pediatric IBD involves several sequential time intervals, from the onset of symptoms to the final confirmation of VEO-IBD. Prolonged intervals between symptom onset and definitive diagnosis (diagnostic delay [DD]) can increase the risk of complications, such as more extensive disease, poorer treatment response, growth failure, and impaired health-related quality of life, accentuating the impact on patient outcomes.[8-10]

The overall time to diagnosis comprises distinct intervals: the time from symptom onset to the first visit to a healthcare provider, and the time from referral to endoscopy and histopathology. Reducing these delays may significantly improve patient outcomes. Identifying children who require timely referral to a specialist can reduce DD. Establishing a timely and accurate diagnosis is a key challenge in the management of IBD. Therefore, understanding and addressing these time intervals is crucial, as this can facilitate earlier diagnosis, timely initiation of effective treatment, and improved prognosis.

The objectives of this study are to thoroughly investigate the time and proportion of DD in children with VEO-IBD. In addition, we aim to categorize factors associated with DD, describe symptoms at initial presentation, investigate growth impairment, and examine the association between specific characteristics of the disease subtypes.

2. Methods

2.1. Study design, setting, and selection of participants

The study was an observational, retrospective, single-center, descriptive study that focused on consecutive patients referred with a suspicion of VEO-IBD between January 2012 and December 2022. These patients were all from the same geographic area and referred by the Brazilian Public Health System to the only regional tertiary center that treats children with VEO-IBD. The Botucatu Medical School Ethics Committee approved the study (CAAE 90158218.0.0000.5411). In addition, parents/caretakers provided informed consent.

2.2. Data collection

The data collection process was designed to extract clinical data from electronic medical records using a standardized, pre-designed protocol to ensure the comprehensive collection of sociodemographic, clinical, laboratory, radiological, and endoscopic findings. Two authors independently reviewed the medical records to ensure the completeness and accuracy of the data. The data were then stored in an Excel file (Microsoft, United States). The extracted data were entered into a database to facilitate standardized analysis.

Anthropometric measurements were obtained by trained pediatric nurses using standardized procedures. Body mass index (BMI) (kg/m^2) and corresponding BMI-for-age *z*-scores were calculated in accordance with the World Health Organization (WHO) growth assessment guidelines.[11,12] *z*-scores <−2 for any measurement were interpreted based on the WHO growth curve standards as indicative of potential growth or nutritional concerns.

2.3. Endoscopic evaluation

Biopsies of the colonic and ileal mucosa were obtained, and the extent of gross disease was based on the Paris Classification.[13,14] Information from colonoscopy and radiological examination reports was thoroughly and systematically utilized, further ensuring the reliability of the evaluation process.

2.4. Histopathological evaluation

Histopathological criteria of the European Crohn's and Colitis Organization and the European Society of Pathology were used.[15] Biopsies were fixed in buffered formalin, and 4- to 5-μm histological sections were stained with hematoxylin and eosin. Two observers performed histological examination. The histological diagnosis was based on the following characteristics: crypt (distortion, atrophy, cryptitis, and microabscesses), focal or diffuse inflammation, degree of mucosal inflammation, villiform surface, plasmacytosis, eosinophilia, presence or absence of granulomas, and lymphoid aggregates. Classifications of histological changes were performed according to a scoring system.[16] This standardized approach was used to promote reliability and consistency in histopathological evaluation.

The degrees of inflammation were recorded on a 5-point scale: 1 = no acute inflammation and no increase in chronic inflammation; 2 = only chronic inflammation; 3 = acute cryptitis, but without crypt abscesses; 4 = acute inflammation, including crypt abscesses (≤10% of crypts), and 5 = acute inflammation, crypt abscesses (>10% of crypts).

2.5. Diagnosis of IBD

The IBD diagnosis was based on clinical features and radiological, colonoscopic, and histopathological investigations, as proposed by the revised Porto Criteria.[14] VEO-IBD patients were divided into three age categories according to the Paris Classification, a widely accepted and validated system for classifying IBD patients by age and disease onset: neonate (<28 days), infantile (<2 years), and VEO (<6 years). Pediatric CD activity was calculated using the weighted Pediatric CD Activity Index.[17] For UC, a validated tool for assessing disease activity severity was used, measuring the Pediatric UC Activity Index.[18]

2.6. Time to diagnosis and DD

Signs and symptoms suggestive of IBD included diarrhea lasting ≥2–4 weeks with Bristol stool type 5–7; more than two episodes of bloody diarrhea, each lasting >1 week within the preceding 6 months; recurrent abdominal pain lasting >14 days; weight loss; and perianal diseases (abscesses, fistulas, fissures, and skin tags).[19]

The following age-related variables were used to calculate DD: age at first symptoms, age at first visit to a primary care pediatrician, duration of symptoms, age at first visit to the pediatric gastroenterology clinic, and age at diagnosis. The time interval (in months) definitions were time from the first symptoms to diagnosis and the time from the first visit to the pediatric gastroenterology clinic to diagnosis. DD in the current study was defined as the time to diagnosis in months exceeding the 75th percentile.[20-24] DD in pediatric IBD may lead to prolonged disease activity, increased complications, and poorer response to treatment.

2.7. Statistical analysis

GraphPad Prism (version 8.4.0, GraphPad Software, US) was used for statistical analysis. The Kolmogorov–Smirnov test was performed to evaluate the distribution of continuous variables. Fisher's exact test was used to analyze the categorical variables, presented as numbers and percentages. Continuous variables, expressed as medians and interquartile ranges (IQRs), were analyzed using the Mann–Whitney *U* test. All analytical tests were two-tailed, with a significance level of $p<0.05$.

3. Results

This study carefully evaluated 25 children diagnosed with VEO-IBD (16 with clinical and pathological features of UC and 9 with CD). Table 1 presents the baseline characteristics of the children and their parents at the first visit. The median age of all children was 34 months (IQR = 18.5–56.5). Children with CD presented at a younger age (median 14 months) than those with UC (median 48 months). This age difference was statistically significant ($p<0.001$), suggesting different disease progression or severity. Most children received breastfeeding and age-appropriate complementary feeding. However, 44% of the patients had been treated for food allergy, and 60% had been delivered by cesarean section.

Table 2 presents the signs and symptoms at the first visit. Diarrhea and blood in the stools were the most prevalent, with half of the children experiencing weight loss. Perineal fistulas were present in 20% of children with

Table 1. Baseline characteristics of children and their parents at the first visit

Variables	Value (*n*=25)
Child characteristics	
Sex: Female/male, *n* (% female)	21/04 (84)
Child age (months)	34 (18.5–56.5)
Firstborn, *n* (%)	13 (52)
Breastfeeding (months)	6 (4–9)
Complementary diet (months)	6 (5–6)
Previous treatment for FA, *n* (%)	11 (44)
Antibiotic use in UC/CD (%)	69/100
Parental characteristics	
Mother's age (years)	34.5 (28–38.5)
Father's age (years)	38 (30–42.5)
Mother's education (years)	8 (8–12)
Father's education (years)	8 (8–12)
Family history of IBD, *n* (%)	4 (16)
Birth characteristics	
Vaginal/cesarean (Cesarean %)	10/15 (60)
Term, *n* (%)	16 (64)
Preterm, *n* (%)	9 (36)
Birth weight (g)	3,280 (2,520–3,520)
Birth length (cm)	49 (47.75–50)
Anthropometric variables at first visit	
Weight (kg)	12.9 (7.79–19.15)
Weight (*z*-score)	−0.87 (−1.680–0.215)
Height (cm)	87.5 (75.25–108.00)
Height (*z*-score)	−0.84 (−2.22–0.23)
BMI/A (kg/m^2)	15.5 (14.7–15.9)
BMI/A (*z*-score)	−0.23 (−0.88–0.42)

Note: Continuous variables are expressed as median (interquartile range) and categorical variables as number (percentage).
Abbreviations: BMI/A: Body mass index-for-age; CD: Crohn's disease; FA: Food allergy; IBD: Inflammatory bowel disease; IQR: Interquartile range; UC: Ulcerative colitis.

CD, underscoring the urgent need for effective and timely diagnosis and treatment.

Table 3 presents comparisons of the ages and time intervals between CD and UC. The ages at first symptoms, first visit, and diagnosis were all significantly lower for the CD group. In addition, the time from the first visit to the pediatric gastroenterology clinic to diagnosis was shorter for children with CD. There was no statistical difference in the time from first symptoms to diagnosis between CD and UC.

Table 4 compares clinical, laboratory, and anthropometric variables in patients with and without DD. DD (greater than the 75th percentile, i.e., 28 months) was observed in seven patients. Interestingly, the proportion of children with weight loss (67%) and low hemoglobin levels (<11 g/dL; 72%) was significantly higher in children without DD, highlighting the importance of early diagnosis in improving patient outcomes.

4. Discussion

The current study examined symptoms at initial presentation and identified factors associated with DD in children with VEO-IBD. Based on a widely accepted standard, diagnoses of IBD were made using laboratory, radiological, endoscopic, and histological criteria, as outlined in the revised Porto Criteria.[14]

Our study's main finding is that there is no significant difference in the time from the first symptoms to diagnosis between CD and UC. However, the time from first visit to the pediatric gastroenterology clinic to diagnosis was shorter for children with CD. The proportion of patients with DD at the ≥75th percentile (≥28 months) was 28%. The ages at first symptoms, first visit, and diagnosis were significantly lower for the CD group. Diarrhea and blood in stool were present in >90% of children. Previous treatment for food allergy was reported in 44% of patients, a family history of IBD in 16%, and delivery by cesarean section in 60%.

Table 2. Symptoms and signs at the first visit

Symptoms/signs	*n* (%)
Diarrhea	24 (96)
Blood in stool	23 (92)
Abdominal pain	16 (64)
Weight loss	13 (52)
Perineal disease	10 (40)
Plicoma	5 (20)
Fistulas	5 (20)
Genital fistula	3 (12)
Perineal abscess	2 (8)
Perianal fissure	9 (36)
Extraintestinal symptoms	3 (12)

Table 3. Comparisons of clinical variables between Crohn's disease and ulcerative colitis

Parameters	Median (IQR)		*p*-value
	Crohn's disease	Ulcerative colitis	
Age (months)			
At first symptoms	2.5 (1.0–12.0)	36.0 (9.0–51.0)	0.006
At the first visit	22.0 (5.0–32.0)	46.5 (33.2–69.0)	0.003
Duration of symptoms	16.0 (3.5–22.5)	10.0 (3.7–24.7)	Ns
At diagnosis	22.9 (5.0–32.7)	58.1 (34.5–71.6)	0.0006
Time interval (months)			
The first symptoms of diagnosis	16.8 (3.6-23.2)	25.3 (6.7–32.8)	Ns
The first visit to PGEC for diagnosis	0.8 (0.3–0.9)	1.2 (0.7–13.0)	0.007

Abbreviations: IQR: Interquartile range; ns: Non-significant; PGEC: Pediatric gastroenterology clinic.

Table 4. Comparisons between clinical, anthropometric, and laboratory variables based on the presence or absence of diagnostic delay

Parameters	Diagnostic delay		*p*-value
	Yes (*n*=7)	No (*n*=18)	
Family history of IBD, *n* (%)	1 (14)	3 (17)	ns
Vaginal section, *n* (%)	2 (29)	8 (44)	ns
Breastfeeding (mo), median (IQR)	7 (6–26)	5.5 (3.7–7.7)	ns
Food allergy treatment, *n* (%)	5 (71)	6 (33)	ns
Weight loss, *n* (%)	1 (14)	12 (67)	0.03
Weight-for-age *z*-score, median (IQR)	−0.87 (−1.6–0.3)	−0.7 (−2.0–0.2)	ns
Height-for-age *z*-score, median (IQR)	−0.61 (−1.8–0.3)	−0.9 (−2.7–0.1)	ns
Perineal fistula	0 (0)	5 (28)	ns
Hemoglobin <11 g/dL, *n* (%)	1 (14)	13 (72)	0.02
Positive CRP (mg/dL)	5 (71)	12 (67)	ns
Elevated ESR (mm/h)	6 (86)	16 (89)	ns
Albumin <3,5 g/dL	2 (29)	7 (39)	ns
Fecal calprotectin (µg/g), median (IQR)	242 (141–3,000)	1,107 (825–2,159)	ns

Note: Percentages are calculated relative to the *n* number of the subgroup (Yes [*n*=7]; No [*n*=18]).
Abbreviations: CRP: C-reactive protein; ESR: Erythrocyte sedimentation rate; IBD: Inflammatory bowel disease; IQR: Interquartile range.

These findings have significant implications for the management of VEO-IBD, suggesting that early diagnosis and intervention could significantly reduce disease severity and improve patient outcomes. Timely diagnosis is measured as the difference between the time of first symptom onset and the time of diagnosis. Pediatricians and pediatric gastroenterologists must be motivated to emphasize the importance of early diagnosis, as it holds the promise of better outcomes for their patients.

The time from disease onset to established IBD diagnosis in children and adults may take several months, as described in existing systematic reviews.[25-27] One systematic review in pediatric IBD has emphasized delays in diagnosis, with a median of 2–10 months (range 2–18 months) for UC and 4–24 months for CD.[25] In another recent systematic review, DD was quantified at 4.5 months for IBD overall, with medians of 5 and 3 months, respectively, for children with CD and UC.[27]

In addition, age at diagnosis is clinically important. It appears that VEO-IBD is usually considered to be more severe when diagnosed later in life. In pediatric IBD overall (not specifically VEO-IBD), the median of DD was 5.0 months.[9,10,28-30] with significantly longer delays in children with CD than in those with UC. In the current study, the DD was 16 months for CD and 25 months for UC, which are substantially higher than the median reported in the literature. Two factors may contribute to DD in IBD in our country: the low prevalence of VEO-IBD and the prioritization of more common diseases.[19]

In the current study, DD is defined as being greater than or equal to 28 months (i.e., greater than the 75th percentile). However, when comparing CD and UC, there is no significant difference in the time from the onset of first symptoms to diagnosis, differing from the published data.[10,25] The discrepancy may be related to the similar duration of symptoms between CD and UC in our cohort, suggesting that the IBD investigation is unbiased. Indeed, prior studies indicate that with access to specialty care, disparities among minority and low-income patients with IBD may be reduced or improved.[31] The Red Flags index—a set of symptoms that indicate a high likelihood of IBD—when used in conjunction with fecal calprotectin, is practical for physicians in recognizing early CD and reducing DD.[32] Investigations for the diagnosis of IBD involve a combination of clinical, hematological, endoscopic, and histological approaches, as well as imaging studies.[33] These tools provide reassurance and confidence in the diagnostic process.

In certain pediatric cohorts, DD was associated with bowel stenosis, fistulas, and decreased height-for-age.[10,22] Consequently, DD would compromise therapy.[34,35] The National Institute for Health and Clinical Excellence (NICE) recommends that IBD be considered in patients with gastrointestinal symptoms lasting at least 6 weeks, such as (a) abdominal pain or discomfort, (b) bloating, and (c) changes in bowel habits.

In children with IBD, the most common symptoms are chronic diarrhea, rectal bleeding, abdominal pain, and weight loss. Because UC classically presents with rectal bleeding, its recognition and subsequent referral for investigation may be more straightforward.[36,37] Children with VEO-IBD often present with non-specific gastrointestinal symptoms that may be associated with a DD. In this cohort, rectal bleeding was present in >90% of children and weight loss in > 50%, underscoring the need for rapid referral when these symptoms are observed.

The definition of growth failure was based on inspection of growth curves at the discretion of the treating physician (z-scores <−2, or curve crossing two major percentiles). While the z-scores for both weight and length were slightly negative, mothers reported weight loss in more than 50% of cases. Thus, avoiding the decreased weight and height is a crucial part of good patient care.[36]

Misinterpretation of symptoms, especially those attributed to infection or food allergy, is common and may delay recognition of severe colitis. In this study, previous treatment for food allergy occurred in 44% of patients, while antibiotic therapy was prescribed to 69% of children with UC and to all with CD. Similar rates (48%) of previous food allergy treatment have been reported in children with IBD-VEO. On the other hand, antibiotic therapy for diarrhea was reported in 25% of children with IBD-VEO.[38]

Extraintestinal manifestations may occur, primarily in CD patients, who are twice as likely to develop them as those with UC, potentially leading to misdiagnosis. Many patients develop at least one extraintestinal manifestation before diagnosis.[39-41]

Laboratory tests to guide referral to a specialist pediatric gastroenterologist for suspected IBD are not yet available. Published summaries of alarm symptoms highlight the most frequently reported clinical features, and recommendations are available for interpreting fecal calprotectin levels in conjunction with other diagnostic measures. In addition, symptoms and signs were assessed to identify predictors of DD by comparing patients with and without DD. Weight loss and anemia did not meet both established criteria for DD. In addition, the presence of a fistula did not indicate DD. These features may have prompted earlier consultation, leading to more timely diagnosis and initiation of treatment.

The current study has some limitations. First, the study had a limited sample size. Nonetheless, standardized data collection permitted an objective analysis of the results. Second, only children diagnosed at a single tertiary center were included, which may limit the generalizability of the results. Third, the retrospective design was an inevitable limitation that may have compromised the accurate assessment of the DD. However, these data were recorded at the time of the first visit in routinely maintained clinical records, which may have improved accuracy. Fourth, DD may result from various factors, including patients delaying healthcare seeking, healthcare professionals failing to recognize IBD promptly, and delays in conducting investigations. Finally, this study's comparison was limited by the scarcity of publications on DD in VEO-IBD.

The strengths of this study include the following: first, our hospital is the only referral site for cases with clinical suspicion of VEO-IBD. Second, the study cohort comprises well-defined, consecutive VEO-IBD patients. Third, a single center can provide more uniform diagnostic procedures. Fourth, to the best of our knowledge, this study is the first to evaluate DD in VEO-IBD in Brazilian children.

5. Conclusion

The main conclusions were:

(a) The median time to diagnosis in children with VEO-IBD in this cohort was prolonged.
(b) Children with CD or UC can experience several months of DD.
(c) Most of the DD in VEO-IBD accrued before specialist consultation.
(d) Children often wait several months for a final diagnosis.
(e) UC cases are predominant in this study cohort.
(f) Bloody diarrhea is the most common symptom among children with VEO-IBD.

Overall, DD is associated with deleterious health outcomes. Therefore, general pediatricians must recognize symptoms, laboratory parameters, and risk factors to identify cases needing referral to a pediatric gastroenterologist. Rectal bleeding, weight loss, family history of IBD, and perianal disease should prompt active case-finding. Finally, further research is needed to identify factors influencing the length of DD in VEO-IBD and to develop strategies to minimize the DD.

Acknowledgments

The authors would like to express their appreciation to the incredible children and families who have profoundly enriched our understanding of the art of medicine.

Funding

None.

Conflict of interest

The authors declare that they have no competing interests.

Author contributions

Conceptualization: Juliana Tedesco Dias, Mary de Assis Carvalho, Nilton Carlos Machado
Formal analysis: Mary de Assis Carvalho
Investigation: Debora Avellaneda Penatti, Jessika Alves de Souza Costa
Methodology: Juliana Tedesco Dias, Gabriela Nascimento Hercos, Carine Dias Ferreira de Jesus
Writing–original draft: Mary de Assis Carvalho, Nilton Carlos Machado, Juliana Tedesco Dias
Writing–review & editing: Mary de Assis Carvalho, Nilton Carlos Machado

Ethics approval and consent to participate

The Ethics Committee from Botucatu Medical School approved the study (CAAE 90158218.0.0000.5411). Written informed consent was obtained from the parents/caretaker.

Consent for publication

All authors consented to publication.

References

1. Kerur B, Benchimol EI, Fiedler K, *et al*. Natural history of very early onset inflammatory bowel disease in North America: A retrospective cohort study. *Inflamm Bowel Dis*. 2021;27(3):295-302.

   doi: 10.1093/ibd/izaa080

2. Levine AE, Mark D, Smith L, Zheng HB, Suskind DL. Pharmacologic management of monogenic and very early onset inflammatory bowel diseases. *Pharmaceutics*. 2023;15(3):969.

   doi: 10.3390/pharmaceutics15030969

3. Collen LV, Kim DY, Field M, *et al*. Clinical phenotypes and outcomes in monogenic versus non-monogenic very early onset inflammatory bowel disease. *J Crohns Colitis*. 2022;16(9):1380-1396.

   doi: 10.1093/ecco-jcc/jjac045

4. Uhlig HH, Schwerd T, Koletzko S, *et al*. The diagnostic approach to monogenic very early onset inflammatory bowel disease. *Gastroenterology*. 2014;147(5):990-1007 e3.

   doi: 10.1053/j.gastro.2014.07.023

5. Ouahed J, Spencer E, Kotlarz D, *et al*. Very early onset

inflammatory bowel disease: A clinical approach with a focus on the role of genetics and underlying immune deficiencies. *Inflamm Bowel Dis*. 2019;26(6):820-842.

doi: 10.1093/ibd/izz259

6. Kelsen JR, Conrad MA, Dawany N, *et al*. The unique disease course of children with very early onset-inflammatory bowel disease. *Inflamm Bowel Dis*. 2020;26(6):909-918.

doi: 10.1093/ibd/izz214

7. Kelsen JR, Sullivan KE, Rabizadeh S, *et al*. North American society for pediatric gastroenterology, hepatology, and nutrition position paper on the evaluation and management for patients with very early-onset inflammatory bowel disease. *J Pediatr Gastroenterol Nutr*. 2020;70(3):389-403.

doi: 10.1097/mpg.0000000000002567

8. Zaharie R, Tantau A, Zaharie F, *et al*. Diagnostic delay in romanian patients with inflammatory bowel disease: Risk factors and impact on the disease course and need for surgery. *J Crohns Colitis*. 2016;10:306-314.

doi: 10.1093/ecco-jcc/jjv215

9. Schoepfer AM, Vavricka S, Safroneeva E, *et al*. Systematic evaluation of diagnostic delay in pediatric inflammatory bowel disease. *J Pediatr Gastroenterol Nutr*. 2017;64:245-247.

doi: 10.1097/mpg.0000000000001238

10. Ricciuto A, Fish JR, Tomalty DE, *et al*. Diagnostic Delay in Canadian children with inflammatory bowel disease is more common in Crohn's disease and associated with decreased height. *Arch Dis Child*. 2018;103:319-326.

doi: 10.1136/archdischild-2017-313060

11. World Health Organization. Physical status: The use and interpretation of anthropometry. Report of a WHO expert committee. *World Health Organ Tech Rep Ser*. 1995;854:1-452.

12. De Onis M, Onyango AW, Borghi E, Siyam A, Nishida C, Siekmann J. Development of a WHO growth reference for school-aged children and adolescents. *Bull World Health Organ*. 2007;85:660-667.

doi: 10.2471/blt.07.043497

13. Levine A, Griffiths A, Markowitz J, *et al*. Pediatric modification of the Montreal classification for inflammatory bowel disease: The Paris classification. *Inflamm Bowel Dis*. 2011;17(6):1314-1321.

doi: 10.1002/ibd.21493

14. Levine A, Koletzko S, Turner D, *et al*. ESPGHAN revised Porto criteria for the diagnosis of inflammatory bowel disease in children and adolescents. *J Pediatr Gastroenterol Nutr*. 2014;58:795-806.

doi: 10.1097/mpg.0000000000000239

15. Magro F, Langner C, Driessen A, *et al*. European consensus on the histopathology of inflammatory bowel disease. *J Crohns Colitis*. 2013;7(10):827-851.

doi: 10.1016/j.crohns.2013.06.001

16. Boyle B, Collins MH, Wang Z, *et al*. Histologic correlates of clinical and endoscopic severity in children newly diagnosed with ulcerative colitis. *Am J Surg Pathol*. 2017;41(11): 1491-1498.

doi: 10.1097/pas.0000000000000939

17. Turner D, Levine A, Walters TD, *et al*. Which PCDAI version best reflects intestinal inflammation in pediatric Crohn disease? *J Pediatr Gastroenterol Nutr*. 2017;64:254-260.

doi: 10.1097/mpg.0000000000001227

18. Turner D, Otley AR, Mack D, *et al*. Development, validation, and evaluation of a pediatric ulcerative colitis activity index: A prospective multicenter study. *Gastroenterology*. 2007;133:423-432.

doi: 10.1053/j.gastro.2007.05.029

19. Martín-de-Carpi J, Jiménez Treviño S, Pujol Muncunill G, Martín-Masot R, Navas-López VM. Time to diagnosis in paediatric inflammatory bowel disease: Key points for an early diagnosis. *An Pediatr (Engl Ed)*. 2020;92:242.e1-242.e9.

doi: 10.1016/j.anpedi.2019.11.005

20. Vavricka SR, Spigaglia SM, Rogler G, *et al*. Systematic evaluation of risk factors for diagnostic delay in inflammatory bowel disease. *Inflamm Bowel Dis*. 2012;18:496-505.

doi: 10.1002/ibd.21719

21. Jiménez Treviño S, Pujol Muncunill G, Martín-Masot R, *et al*. Spanish pediatric inflammatory bowel disease diagnostic delay registry: SPIDER study from sociedad española de gastroenterología, hepatología y nutrición pediátrica. *Front Pediatr*. 2020;8:584278.

doi: 10.3389/fped.2020.584278

22. Ricciuto A, Mack DR, Huynh HQ, *et al*. Diagnostic delay is associated with complicated disease and growth impairment in paediatric Crohn's disease. *J Crohns Colitis*. 2021;15(3):419-431.

doi: 10.1093/ecco-jcc/jjaa197

23. Schoepfer A, Santos J, Fournier N, *et al*. Systematic analysis of the impact of diagnostic delay on bowel damage in paediatric versus adult onset Crohn's disease. *J Crohns Colitis*. 2019;13(10):1334-1342.

doi: 10.1093/ecco-jcc/jjz065

24. El Mouzan MI, AlSaleem BI, Hasosah MY, *et al*. Diagnostic delay of pediatric inflammatory bowel disease in Saudi Arabia. *Saudi J Gastroenterol*. 2019;25(4):257-261.

doi: 10.4103/sjg.SJG_457_18

25. Ajbar A, Cross E, Matoi S, *et al*. Diagnostic delay in pediatric inflammatory bowel disease: A systematic review. *Dig Dis Sci*. 2022;67(12):5444-5454.

doi: 10.1007/s10620-022-07452-5

26. Vernon-Roberts A, Aluzaite K, Khalilipour B, Day AS. Systematic review of diagnostic delay for children with inflammatory bowel disease. *J Pediatr Gastroenterol Nutr*. 2023;76:304-312.

doi: 10.1097/mpg.0000000000003670

27. Jayasooriya N, Baillie S, Blackwell J, *et al*. Systematic review with meta-analysis: Time to diagnosis and the impact of delayed diagnosis on clinical outcomes in inflammatory bowel disease. *Aliment Pharmacol Ther*. 2023;57:635-652.

doi: 10.1111/apt.17370

28. Sawczenko A, Sandhu BK. Presenting features of inflammatory bowel disease in Great Britain and Ireland. *Arch Dis Child*. 2003;88(11):995-1000.

doi: 10.1136/adc.88.11.995

29. Timmer A, Behrens R, Buderus S, *et al*. Childhood onset inflammatory bowel disease: Predictors of delayed diagnosis from the CEDATA German-language pediatric inflammatory bowel disease registry. *J Pediatr*. 2011;158(3):467-473.e2.

doi: 10.1016/j.jpeds.2010.09.014

30. Arcos-Machancoses JV, Donat-Aliaga E, Polo-Miquel B, Masip-Simo E, Ribes-Koninckx C, Pereda-Perez A. Description and study of risk factors for the diagnostic delay of pediatric inflammatory bowel disease. *An Pediatr (Barc)*. 2015;82(4):247-254.

doi: 10.1016/j.anpedi.2014.05.024

31. Gu P, Clifford E, Gilman A, *et al*. Improved healthcare access reduces requirements for surgery in indigent IBD patients using biologic therapy: A 'safety-net' hospital experience. *Pathophysiology*. 2022;29:383-393.

doi: 10.3390/pathophysiology29030030

32. Fiorino G, Bonovas S, Gilardi D, *et al*. Validation of the red flags index for early diagnosis of Crohn's disease: A prospective observational IG-IBD study among general practitioners. *J Crohns Colitis*. 2020;14(12):1777-1779.

doi: 10.1093/ecco-jcc/jjaa111

33. Kapasi R, Glatter J, Lamb CA, *et al*. Consensus standards of healthcare for adults and children with inflammatory bowel disease in the UK. *Frontline Gastroenterol*. 2020;11:178-187.

doi: 10.1136/flgastro-2019-101260

34. Bolia R, Rajanayagam J, Hardikar W, Alex G. Impact of changing treatment strategies on outcomes in pediatric ulcerative colitis. *Inflamm Bowel Dis*. 2019;25:1838-1844.

doi: 10.1093/ibd/izz072

35. Ihekweazu FD, Fofanova T, Palacios R, *et al*. Progression to colectomy in the era of biologics: A single center experience with pediatric ulcerative colitis. *J Pediatr Surg*. 2020;55:1815-1823.

doi: 10.1016/j.jpedsurg.2020.01.054

36. Ledder O, Catto-Smith AG, Oliver MR, Alex G, Cameron DJ, Hardikar W. Clinical patterns and outcome of early-onset inflammatory bowel disease. *J Pediatr Gastroenterol Nutr*. 2014;59:562-564.

doi: 10.1097/mpg.0000000000000465

37. Perler BK, Ungaro R, Baird G, *et al*. Presenting symptoms in inflammatory bowel disease: Descriptive analysis of a community-based inception cohort. *BMC Gastroenterol*. 2019;20:406.

doi: 10.1186/s12876-020-01526-2

38. Kammermeier J, Dziubak R, Pescarin M, *et al*. Phenotypic and genotypic characterisation of inflammatory bowel disease presenting before the age of 2 years. *J Crohns Colitis*. 2017;11:60-69.

doi: 10.1093/ecco-jcc/jjw118

39. Greuter T, Bertoldo F, Rechner R, *et al*. Extraintestinal manifestations of pediatric inflammatory bowel disease: Prevalence, presentation, and anti-TNF treatment. *J Pediatr Gastroenterol Nutr*. 2017;65:200-206.

doi: 10.1097/mpg.0000000000001455

40. Isene R, Bernklev T, Hoie O, *et al*. Extraintestinal manifestations in Crohn's disease and ulcerative colitis: Results from a prospective, population-based European inception cohort. *Scand J Gastroenterol*. 2015;50:300-305.

doi: 10.3109/00365521.2014.991752

41. Jose FA, Garnett EA, Vittinghoff E, *et al*. Development of extraintestinal manifestations in pediatric patients with inflammatory bowel disease. *Inflamm Bowel Dis*. 2009;15:63-68.

doi: 10.1002/ibd.20604

ACCSCIENCE PUBLISHING

Journal of Clinical and Translational Research

ORIGINAL ARTICLE

A dual-modal approach for detecting and classifying autism spectrum disorder using behavioral and facial features

M. S. Sankari* and **A. Kannammal**

Department of Electronics and Communication, Faculty of Electronics and Communication Engineering, PSG College of Technology, Coimbatore, Tamil Nadu, India

Abstract

Background: Autism spectrum disorder (ASD) is a neurodevelopmental condition that significantly affects social connection, behavior, and knowledge acquisition. Despite increasing global prevalence, timely diagnosis remains challenging due to heterogeneity in clinical presentation. **Aim:** The aim of this study is to develop a dual-modal framework for early detection of ASD by analyzing behavioral assessment and image data. **Methods:** The proposed framework consists of two independent yet complementary modules. In the behavioral module, questionnaire responses and assessment data were analyzed using an artificial neural network classifier to predict the likelihood of ASD. In the visual module, facial images were analyzed using a DenseNet121-based deep learning model with transfer learning to detect ASD-related traits. Each module independently estimates ASD probability and categorizes severity levels. **Results:** The DenseNet121 model achieved strong performance in image-based ASD detection, with 91.16% (95% confidence interval [CI]: 87.8–94.2) accuracy, 91.2% (95% CI: 87.8–94.2) sensitivity, and 89.8% specificity, including when trained on a relatively small dataset. Independent training of the two modules may improve robustness and reduce modality-specific bias. **Conclusion:** The proposed framework demonstrates potential for enhancing early ASD detection using dual modalities. The findings support the use of deep learning-based approaches to improve detection accuracy. **Relevance for patients:** Early screening of ASD can facilitate timely interventions and personalized care strategies. This method offers a noninvasive, data-driven approach that may support caregivers and healthcare systems in informed decision-making, ultimately benefiting individuals with ASD and their families.

Keywords: Behavioral features; Facial features; Artificial neural network; Transfer learning; Machine learning; Deep learning model; Severity prediction

***Corresponding author:**
M. S. Sankari
(227rlfx01@psgtech.ac.in)

Citation: Sankari MS, Kannammal A. A dual-modal approach for detecting and classifying autism spectrum disorder using behavioral and facial features. *J Clin Transl Res*. 2026;12(1):47-61.
doi: 10.36922/JCTR025400068

Received: September 30, 2025

1st revised: October 27, 2025

2nd revised: December 20, 2025

Accepted: January 15, 2026

Published online: February 5, 2026

1. Introduction

Autism spectrum disorder (ASD) is a neurodevelopmental condition characterized by challenges in language development, cognitive processing, social interaction, and communication,[1] along with reduced empathy and sympathy.[2] Symptoms typically emerge in early childhood, often within the first 3 years of life. A review of data from 2000 through 2014 on 8-year-old children in selected U.S. communities by the

CDC's autism and developmental disabilities monitoring Network showed that ASD prevalence estimates rose more than 150% over this period, from 6.7/1,000 in 2000 to 16.8/1,000 in 2014.[3] Traditionally, diagnostic frameworks (e.g., the international classification of diseases-11[4]) and standardized instruments (e.g., the autism diagnostic observation schedule and the childhood autism rating scale [CARS][5]) are designed for individuals across a wide range of ages and developmental levels, from toddlers to adults. The Social Communication Questionnaire,[6] intended for children aged 4 years and above, consists of 40 items completed by parents under the guidance of a trained clinician. The Autism Spectrum Quotient (AQ)[7] is used to measure autistic traits in the general population and supports the early identification of individuals who may require further assessment. However, the diagnosis remains challenging, especially for marginal case disorders.

The diagnostic statistical manual, Fifth Edition (DSM-5) is a standard classification of mental disorders and serves as a primary diagnostic reference for mental health professionals. As per the DSM-5 criteria,[8,9] ASD is categorized into three functional levels: Level 1, Level 2, and Level 3. Health professionals determine the assigned levels based on the individual's need for outside assistance in their daily routine. Additionally, individuals with ASD may experience issues related to sensory processing difficulties and cognitive challenges. Therefore, health professionals typically diagnose using multiple modalities, such as monitoring facial[10] and behavioral features, assessing motor skills, analyzing eye movements and scan paths, and conducting neuroimaging studies.[11] However, these clinical approaches are often time consuming, costly, and may also be challenging due to communication difficulties experienced by individuals with ASD.

Previous studies have indicated that certain facial features, including a broader upper facial region, increased inter-ocular distance, a pronounced philtrum, and a comparatively shorter mid-face area involving the cheeks and nose, may be associated with ASD. These insights have driven growing interest in facial image-based screening methods. Although convolutional neural networks (CNNs) pre-trained on facial landmarks are increasingly used for ASD identification, current studies present key shortcomings. In particular, limited attention has been paid to the problem of overfitting, which raises concerns about model generalization to diverse populations. Furthermore, most research remains confined to binary classification of ASD versus non-ASD, offering little information about the severity of autistic traits. However, to achieve an acknowledged outcome, relying on a single data modality, such as electroencephalography (EEG),[12] magnetic resonance imaging,[13] facial expressions,[14] or voice data attributes,[15] is insufficient. To the best of our knowledge, most existing studies employing machine learning (ML) or deep learning (DL) techniques have primarily relied on a single modality, and the exploration of ASD severity prediction remains limited. In the current study, by keeping the modalities independent, we aim to ensure that when one model performs sub-optimally on certain samples, the other can still provide reliable classification.

The primary contributions of this research are as follows:

(i) The system employs an artificial neural network (ANN) classifier for analyzing questionnaire responses based on behavioral and demographic data and a fine-tuned DenseNet121 model for image-based data, enabling early detection and classification of ASD.
(ii) The system further predicts severity levels based on both questionnaire responses and image-based features, thereby assisting in suggesting treatment plans.

The remainder of the paper is organized as follows: the next section, Literature Review, presents the foundation upon which our study is built, followed by the Methodology section that describes the dataset employed, the working environment, and the methods used for experimentation, and the Results and Discussion section presents our research findings. Finally, we conclude our paper with the Conclusion section, highlighting the importance of our findings, future directions, and key takeaways.

2. Literature review

In this section, we discuss related research performed on the detection and classification of ASD. Researchers have explored various supervised, unsupervised, and reinforcement learning approaches across diverse data modalities, including behavioral features, neuroimaging, facial expressions, eye tracking, EEG, and voice data. These studies also highlight key challenges, such as data scarcity and the need for interpretability, while emphasizing the potential of ML and DL in advancing ASD research. Moreover, several systematic reviews have examined ML and data mining techniques, as well as feature optimization strategies for ASD prediction.[16-18] Singh *et al.*[19] investigated diagnostic mechanisms for ASD by extensively evaluating various ML models to identify the most significant indicators of ASD in toddlers. Their study initially developed a neural network-based classification model, which was later complemented by experiments using a random forest (RF) classifier.

Hassan and Taher[20] analyzed data from 515 children with autism and applied multiple classification algorithms, reporting high accuracy and F1 scores, with the ANN achieving the best performance. Similarly, Uddin[21] examined different ML classifiers for ASD detection across

various age groups, incorporating feature optimization methods. The study used two datasets consisting of 292 and 704 records, respectively, each with 21 attributes. Notably, the RF model achieved 100% accuracy in early ASD diagnosis.

Talukdar *et al.*[22] evaluated ML models on toddler and adolescent datasets using the quantitative checklist for autism in toddlers-10 items and AQ-10 screening tools. The RF classifier achieved the highest accuracy, reporting 93.69% on the toddler and 93.33% on the adolescent dataset, without employing feature selection methods. Bawa *et al.*[23] evaluated various ML algorithms for ASD detection across different age groups. Logistic regression (LR) achieved 94.3% accuracy in children and 99% in adolescents, while support vector machine (SVM) reached 98.5% in adults.

Haque *et al.*[24] evaluated LR, SVM, K-nearest neighbors, decision tree, and RF for predicting ASD in children and toddlers. The results showed that the toddler dataset achieved a mean intersection over union of 100 with SVM and 99.80 with LR. Jahanara and Padmanabhan[25] explored facial feature identification in children using a CNN with a transfer learning approach, using 1,167 samples labeled as autistic or non-autistic. The CNN model, based on the Visual Geometry Group VGG19 architecture, achieved 96% accuracy.

Akter *et al.*[26] proposed a model based on 2,936 facial images using a transfer learning architecture. The evaluation included performance metrics, such as accuracy, sensitivity, false positive rate (FPR), G-mean, F-measure, and false negative (FN) rate. The framework integrated 17 different classifiers, encompassing both ML and DL models. Among them, MobileNet-V1 combined with k-means clustering achieved the highest accuracy of 83%. Alam *et al.*[27] applied deep CNN-based transfer learning approaches using facial images for ASD detection. The modified Xception model achieved 95% accuracy on the test set through empirical evaluation with optimizer selection and hyperparameter tuning.

Hriti *et al.*[28] proposed a classification method that integrates both visual and behavioral data modalities, collected from the same participants, and aligned by generating common attributes and grouped into sub-classes. The ANN and MobileNet models were employed, achieving an accuracy of 97.57%. Rahman and Subashini[29] studied facial photos of autistic children, analyzing 2,936 colored facial images. Various pre-trained CNN models, including MobileNet, Xception, EfficientNet-B0, EfficientNet-B1, and EfficientNet-B2, were used as feature extractors, and a deep neural network was utilized for classification.

Anjum *et al.*[30] used MobileNet, Xception, VGG16, VGG19, and EfficientNet as feature extractors and LR as a binary classifier, achieving 88.33% test accuracy. Our study adopts a dual-modal approach to enhance ASD detection and classification by jointly analyzing image data and the questionnaire responses. The framework employs a fine-tuned DenseNet121 model and an ANN classifier model, ensuring computational efficiency while providing a comprehensive assessment.

3. Methodology

The general architecture of the proposed system, illustrated in Figure 1, leveraged both modalities to capture different aspects of ASD in children using ML techniques. This dual-pronged approach for ASD detection, classification, and severity prediction comprised two key modules: the behavioral module, which utilized questionnaire-based data, and the visual module, which employed image-based data for investigation, experimentation, and analysis.

3.1. Questionnaire data analysis sub-module

The dataset titled "ASD Children Traits"[31] was obtained from the Autism Research Group, University of Arkansas (Computer Science Department), and is publicly available via Kaggle online open-source repository (https://www.kaggle.com/code/mohammedabdelaleem/gathered-asd-datasets). It comprises 1,985 cases of children with 28 behavioral and developmental features. According to repository metadata, the dataset was last updated between 2021 and 2022. The dataset was curated and used for research purposes and contains self-reported or parent/caregiver-reported screening data. Only cases with sufficient behavioral and developmental features were considered to ensure reliable model training and evaluation, comprising several key attributes, including the AQ, assessed through columns A1 to A10, the Social Responsiveness Scale, age (in years), Q-CHAT 10 score, CARS score, speech delay disorder, learning disorder, genetic disorders, depression, global developmental delay/intellectual disability, social/behavioral issues, anxiety disorder, sex, ethnicity, jaundice, and family history of ASD. The CARS score differed from traditional survey-based measures, as it was derived from assessor observations. Each item was rated on a four-point scale from no abnormality to severely abnormal, and the total score was subsequently interpreted to determine the severity of ASD symptoms.

Children who had completed all items of the Q-CHAT 10[32] or AQ-10 behavioral screening questionnaires were included in the training. The AQ-10 scores ranged from 0 to 10; scores exceeding 6 suggested a diagnosis of ASD. Other attributes listed in the record's columns identified the factors that predominantly influenced the diagnosis

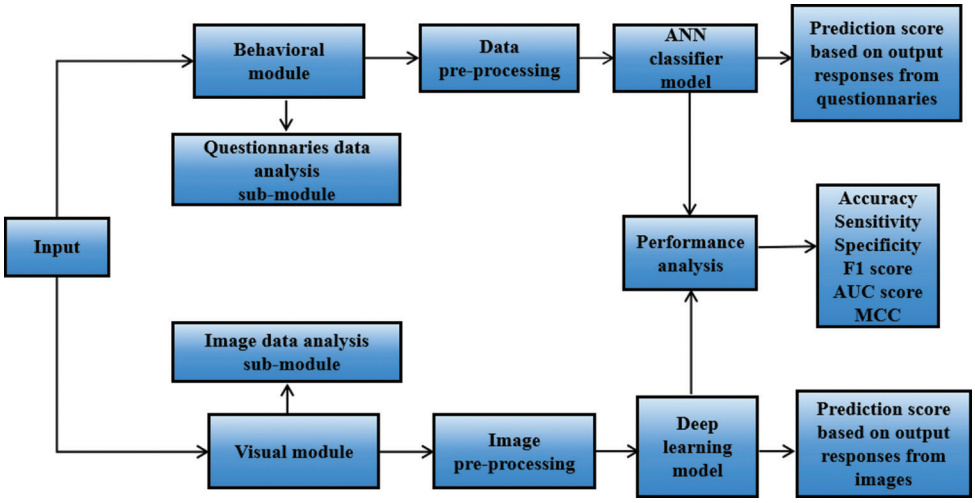

Figure 1. Proposed workflow diagram containing behavioral and visual modules for autism spectrum disorder detection and classification
Abbreviations: ANN: Artificial neural network; AUC: Area under the curve; MCC: Matthews correlation coefficient.

of ASD. The assessment was carried out by the health professional who administered the 10-item questionnaire and scored it on a 5-point scale in the Q-CHAT 10 method. Then, the points for questions 1–9 and question 10 were summed separately. A total score >3 may indicate autism, provided it is confirmed using a comprehensive assessment. During an assessment, responses to ten items (A1–A10) were recorded using five options labeled A, B, C, D, and E. For the questions Q1–Q9, 1 point was assigned if the response fell under columns C, D, or E (Somes, Rarely, or Never). For Q10, 1 point was awarded for responses in columns A, B, or C (Many s a day, A few s a day, or A few s a week), while responses in columns D and E (Rarely or Never) scored 0. A cumulative score >3 indicated potential ASD traits. Overall, the diagnostic framework emphasized two primary domains: social interaction and restricted or repetitive behaviors. Any missing values in the selected features were handled using simple imputation methods (mean or mode, as appropriate). Children with known comorbid neurological disorders unrelated to ASD (if any reported in the dataset) were excluded from the analysis.

Data preparation involved managing missing values, addressing outliers, and handling both categorical and numerical variables. The behavioral module encompassed an ANN classifier to analyze the processed questionnaire data. It predicted the likelihood of ASD by evaluating the behavioral features and responses provided. ANNs shared similarities with the interconnected neural layers of the human brain. The input layer was connected to one or more hidden layers, which in turn were connected to the output layer. During model training, the connection weights and bias terms between neurons were typically initialized with small random values drawn from a uniform or normal distribution to break the symmetry among neurons and enable effective learning through backpropagation. The dataset included a variety of behavioral attributes that were crucial for indicating the early signs of ASD. For example, items such as "Does your child point to share an interest with you?" and "The child looks at you when you call his/her name?" assess social-communication behaviors and interaction deficit among children observed with ASD. Responses to these questions and similar ones were encoded for machine analysis to support further processing and computation, enabling the identification of patterns and decision-making based on the output.

Among the 1,985 records, 1,074 were labeled as ASD and 911 as normal individuals. The participants were predominantly male, comprising 72.9% of the sample, compared to their female counterparts. Participants' ages ranged from 1 to 18 years, with an average of 9.6 years; high participation was observed between 1 and 10 years. The ASD prevalence is based on ethnicity; 16 distinct ethnic groups took part in the test, primarily originating from Europe, Asia, and the Middle East. Among them, white Europeans accounted for the highest number.

Primarily, the dataset revealed missing values in the Qchat_10_Score, social/behavioral issues, and depression columns, which were handled using simple imputation techniques. The mode was calculated and used to replace missing values in the numerical columns. The column "Who_completed_the_test" has six unique values, and the column "Ethnicity" has 16 unique values. These categorical values were converted to numerical columns using one-hot encoding. Ordinal encoding was used for categorical variables with an inherent order, such as gender specification in the dataset. Label encoding was used exclusively for the class variables. Since the dataset

attributes were measured on varying scales, normalization was performed using standard scaling techniques (*Z*-score normalization) to maintain a standard range.

A value was normalized using the standard scalar method as in Equation (1):

$$y = \frac{x - x_{mean}}{x_{std}} \quad (1)$$

Where x indicates the current value of the input x, x_{mean}, x_{std} represent the mean and standard deviation of x, respectively. The proposed system classified outcomes based on probability outputs from both the questionnaire and the visual modules, mapping them to four levels: normal, mild, moderate, and severe. We aim to ensure that the model provides meaningful results and can be used for future ASD diagnosis.

The confidence levels were derived from the prediction probabilities, and the categorization into severity levels was defined, as shown in Table 1. The severity assessment levels were aligned with DSM-5 criteria for social communication deficits, and their characteristics were defined as follows[33]: (i) Normal: A probability score ranging from 0.00 to 0.20, indicating typical developmental responses. There is no evidence of social communication impairment. (ii) Mild: A probability score between 0.21 and 0.50, indicating a mild likelihood of ASD. Some symptoms, such as unusual social responses or atypical attempts to make friends, may be present. Minimal support may be required. (iii) Moderate: A probability score between 0.51 and 0.7, indicating a moderate likelihood of ASD. This level is characterized by noticeable deficits in verbal and non-verbal social communication skills, and substantial support is required. (iv) Severe: Probability score >0.7, indicating a high likelihood of ASD. This stage is associated with severe deficits, including very limited initiation of social interaction, and requires very substantial support.

The ANN is a multi-layer feed-forward network,[34] where signals propagate from the input layer to the output layer during the forward pass. During this phase, the weights and biases were assigned random values to begin training,

Table 1. Classification of autism spectrum disorder severity levels based on prediction probability thresholds, aligned with Diagnostic Statistical Manual-5 criteria for social communication deficits and support requirements

Probability range	Severity level
0.00–0.20	Normal
0.21–0.50	Mild
0.51–0.70	Moderate
>0.70	Severe

and the output was generated as a probability-based prediction. These parameters were iteratively updated using optimization techniques to minimize prediction error during backpropagation. ANN played a central role in analyzing questionnaire data to predict and classify ASD within the proposed system.

The algorithm of the ANN classifier comprised seven steps:

(i) Input: Training dataset: $D = \{(xi, yi)\}_{i=1}^{M}$, where x_i are input features, $y_i \in \{0,1\}$, and y_i are class labels

(ii) Initialize sequential model:

Add a dense layer with 128 neurons, rectified linear unit (ReLU) activation

Input dimension d, L2 regularization

Add a dense layer with 64 neurons, ReLU activation

L2 regularization

Add dense output layer, sigmoid activation

(iii) Define evaluation metrics:

(True positive [TP], true negative [TN], false positive [FP], FN, Accuracy, Precision, Recall, F1 score, Matthews correlation coefficient [MCC], area under the curve [AUC])

(iv) Configure early stopping:

Monitor accuracy with patience, *p*, restores best weights when stopping

(v) Compile model: Optimizer = Adam(η), Loss = Binary Crossentropy

(vi) Train model:

Fit model on (X_{train}, Y_{train})

For up to E epochs, with validation split ratio v

Shuffle data each epoch, apply early stopping

(vii) Evaluate model:

Evaluate trained model on (X_{test}, Y_{test})

Output performance metrics and loss

Output: Tested the ANN model and evaluation results.

The model design required tuning several hyperparameters, including network architecture, learning rate, optimizer, batch size, and number of epochs. Among these hyperparameters, batch size played a crucial role, as it directly affects the overall training, the length of each epoch, and the quality of the trained model.

3.2. Image data analysis sub-module

The dataset titled "Autism image data" was obtained from Kaggle online open repository and comprises 2,940 images of children labeled as ASD or non-ASD (https://

data.mendeley.com/datasets/f9dycfvwbt/3).[35] Only facial images of children aged 2–8 years, with sufficient quality, correct face orientation, and distinct facial visibility, were included to support accurate feature extraction and classification. The facial images are available in JPEG format, each with a resolution of 224 × 224 pixels. Approximately 89% of the images represent white children, while the remainder depict Black, East Asian, and other ethnic groups. Duplicated or mislabeled instances were eliminated to maintain dataset integrity. The sample exhibited a male-to-female ratio of approximately 3:1, which aligned with the higher prevalence of ASD reported in males. The distribution between the autistic and non-autistic categories was nearly balanced, ensuring the model was trained on a dataset with minimal class imbalance and supporting fair and reliable classification performance. The image analysis sub-module processed children's facial images to identify key features associated with ASD. The images underwent several pre-processing steps, including cropping and resizing to standardize dimensions for model compatibility while preserving the aspect ratio to avoid distortion. Additional steps, such as normalization and consistent face region detection, were applied to improve uniformity across images. A fine-tuned CNN was employed to analyze the facial images. It was pre-trained on large image datasets, like ImageNet, and was exceptionally adept at recognizing patterns in visual data. It extracted significant facial features, such as a flatter midface, a broader upper face, a shortened philtrum, wider-set eyes, and facial expressions, which were crucial for identifying early signs of ASD. The model predicted the likelihood of ASD by comparing the extracted features against those features typically observed in individuals diagnosed with ASD. The normalization process was used to address inconsistencies and involved scaling pixel values from general ranges, such as (0, 255), to a specific range, such as (0, 1). This specification stabilized and accelerated the training process and ensured uniformity across the dataset. The normalized pixel value of the image is defined as Equation (2).

$$I'(x,y) = \frac{I(x,y) - \text{mean}(I)}{\text{std dev}(I)} \quad (2)$$

Where I (x,y) is the pixel value at position (x, y), and the mean and standard deviation of pixel values are considered. We used a fine-tuned DenseNet121 model, pre-trained on a large image dataset using deep facial features, to enhance performance.

The DenseNet121 architecture was built using dense blocks, in which each layer received inputs from a preceding layer and contributed its own feature maps to subsequent layers.[36] It began with a convolutional layer comprising 64 filters of size 7 × 7 with a stride of 2, followed by a 3 × 3 max-pooling layer with a stride of 2 to reduce spatial dimensions. Non-linearity was introduced through the ReLU activation function. The fully connected head was replaced with a global average pooling layer, which transformed the feature maps into a single feature vector. A softmax activation function was then applied to generate class probabilities. Then, the DenseNet121 model was fine-tuned on a dataset of children's facial images. The early convolutional layers were frozen to preserve low-level feature extraction, while the backbone layers were updated during training to adapt to the classification task. The model's parameters were optimized using the cross-entropy loss function, as shown in Equation (3):

$$L = -\sum_{I=1}^{c} yilog(pi) \quad (3)$$

Where *yi* is the true label, and *pi* is the predicted probability for class *i*.

The model parameters were updated using the root mean squared propagation (RMSprop) optimization algorithm, as defined in Equation (4):

$$\theta_{t+1} = \theta_t - \frac{\eta}{\sqrt{v_{t+\varepsilon}}} \cdot g_t \quad (4)$$

Where η is the learning rate, and ε is a small constant, v_t is the accumulated moving average of squared gradients at t, and $v_t = \beta v_{t-1} + (1-\beta) g_t^2$, β is the decay rate, g_t indicates the gradient at t.

Table 2 illustrates the layer-wise architecture of the DenseNet121 model for prediction and classification. The model began with an input layer (224 × 224 × 3), followed by an initial convolution and pooling stage. The input first passed through an initial convolution layer with a 7 × 7 kernel and a stride of 2, followed by a 3 × 3 max pooling layer to reduce spatial dimensions and capture low-level features. The network then proceeded through four dense blocks, each comprising multiple convolutional layers with 1 × 1 and 3 × 3 kernels, where each layer received inputs from all preceding layers to encourage feature reuse and mitigate the vanishing gradient problem. Between dense blocks, transition layers performed convolutional and pooling operations to reduce spatial resolution while preserving essential feature information. Then, the global average pooling condensed the feature maps into a fixed-length vector. This vector was flattened and fed into fully connected layers with ReLU activations, batch normalization, and regularization to improve

Table 2. Layer-wise architecture of the proposed DenseNet121 model with modifications for autism spectrum disorder image detection

Layer	Output size	Description
Input	224×224×3	RGB image input
Convolution	112×112	7×7 convolution, stride 2
Pooling	56×56	3×3 max pool, stride 2
Dense block (1)	56×56	(1×1 convolution, 3×3 convolution)×6
Transition layer (1)	56×56	1×1 convolution
	28×28	2×2 average pool, stride 2
Dense block (2)	28×28	(1×1 convolution, 3×3 convolution)×12
Transition layer (2)	28×28	1×1 convolution
	14×14	2×2 average pool, stride 2
Dense block (3)	14×14	(1×1 convolution, 3×3 convolution)×24
Transition layer (3)	14×14	1×1 convolution
	7×7	2×2 average pool, stride 2
Dense block (4)	7×7	(1×1 convolution, 3×3 convolution)×16
Global average pooling	1×1 × 1024	Reduces feature maps to a 1D vector
Batch normalization	1024	Normalize activations
Flatten	1024	Converts to a 1D vector
Dense (ReLU)	512	Fully connected layer, L2 regularization
Batch normalization	512	Normalize activations
Dense (ReLU)	512	Fully connected layer, L2 regularization
Dense (Softmax)	Num_classes	Output classification layer

Abbreviations: 1D: One-dimensional; ReLU: Rectified linear unit; RGB: Red, Green, Blue.

generalization. A softmax layer produced class probability scores for classification, enabling the model to assign confidence levels to each predicted class. The DenseNet121 model generated class probability scores, and the class with the highest probability was chosen as the final prediction for each test image.

3.3. ASD severity prediction

The ASD severity prediction was performed using two complementary models applied to independent datasets.[37] The fine-tuned DenseNet121 model processed each input image through convolutional, dense, and pooling layers, generating hierarchical feature representations that were transformed into softmax probabilities. These probabilities were then mapped into predefined severity categories (normal, mild, moderate, and severe). The predicted label, true label, probability score, and severity level were compiled into a result table and exported as a comma-separated values (CSV) file for further analysis. This workflow provided both a quantitative and interpretable assessment of ASD detection and severity estimation, while the model's dense connectivity enhanced accuracy through collective decision-making.

3.4. Experimental results evaluation

The experimental assessment of the proposed framework was performed using a publicly available dataset across different modalities. The findings reveal significant improvements in ASD detection, with greater predictive accuracy compared to existing state-of-the-art methods. The dataset employed in this study comprised two independent sources: children's questionnaire responses and facial image data. While the questionnaire responses capture behavioral attributes, the facial images provide visual features, enabling a dual-modal analysis.

3.5. Performance metrics

The performance evaluation employed several metrics, including accuracy, precision, recall (sensitivity), specificity, F1 score, MCC,[38,39] and AUC. Both the classification report and confusion matrix were analyzed to evaluate the model's predictions. The confusion matrix comprises four outcomes: TP, where an autistic individual is correctly identified; TN, where a non-autistic individual is correctly classified; FP, where a non-autistic person is incorrectly predicted as autistic; and FN, where an autistic individual is mistakenly classified as non-autistic. Quantitative evaluation was performed on the test dataset using the aforementioned metrics, along with receiver operating characteristic (ROC) analysis, as presented in Equations (5-10). Accuracy, in particular, represented the overall correctness of the model's predictions:

$$Accuracy = \frac{TP + TN}{(TP + FP + TN + FN)} \quad (5)$$

Precision measured the accuracy of positive predictions, primarily in autistic cases.

$$Precision = \frac{TP}{TP + FP} \quad (6)$$

Sensitivity measured the model's ability to correctly identify people with ASD symptoms.

$$Recall\,or\,sensitivity = \frac{TP}{TP + FN} \quad (7)$$

The F1 score is the harmonic mean of precision and recall. This metric balanced the importance of both precision and recall. Specificity indicated how effectively

the model avoided classifying non-autistic individuals as autistic.

$$Specificity = \frac{TN}{TN + FP} \quad (8)$$

MCC served as a comprehensive metric that evaluated model performance across all classes.

$$MCC = \frac{(\mathrm{TP} \times \mathrm{TN} - \mathrm{FP} \times \mathrm{FN})}{\sqrt{(\mathrm{TP} + \mathrm{FP}) \times (\mathrm{TP} + \mathrm{FN}) \times (\mathrm{TN} + \mathrm{FP}) \times (\mathrm{TN} + \mathrm{FN})}} \quad (9)$$

The MCC incorporated all elements of the confusion matrix, providing a more comprehensive and reliable evaluation. The ROC curve was generated by plotting the TP rate (TPR) against the FPR, with TPR on the y-axis and FPR on the x-axis.

$$\text{AUC score} = \frac{TPR + FPR + 1}{2} \quad (10)$$

4. Results and discussion

The DenseNet121 model achieved 91.16% accuracy in detecting ASD, highlighting its capability to identify ASD-related traits from facial image attributes. The ANN classifier achieved 85.1% accuracy in predicting ASD, demonstrating its effectiveness in leveraging behavioral attributes for ASD detection.

4.1. ANN model on questionnaire data

The ANN model was selected for analyzing questionnaire response data for its ability to capture complex nonlinear relationships among behavioral features that other models might overlook. Additionally, the architecture allowed the customization of hidden layers, activation functions, and dropout, offering flexibility to accommodate dataset growth or the inclusion of additional features. The experimentation and analysis were conducted in Google Colab, a cloud-based Jupyter Notebook service that provides access to graphics processing units. For reference, the local system specifications were as follows: Windows 10 operating system, Intel(R) Core(TM) i7-7700 CPU @ 3.6 GHz, 16 GB RAM, and a 64-bit ×64-based processor. Google Colab, an interactive cloud-based platform, was employed to facilitate data analysis. This interactive tool, powered by Python (version 3.12.12, Python Software Foundation, Netherlands) and operated on Microsoft Windows, facilitated data analysis and exploration. It was enhanced with Python libraries, including Numpy, Pandas, Matplotlib, Scikit Learn, Seaborn, and TensorFlow.

The data were processed with appropriate encoding methods, with randomization applied to select data points for training and testing, which were 1,588 and 397, respectively, by following a train and test dataset split ratio of 80:20. The dataset, consisting of 27 input features, was used to perform binary classification of instances into ASD or non-ASD categories. The model was trained for 30 epochs. The sequential application programming interface in Keras was used to define fully connected layers with Dense, specifying input and output dimensions, along with activation functions. ReLU was used for the input and hidden layers, while "sigmoid" was applied to the output layer. The Adam optimizer with a learning rate of 0.0001 was employed, and the binary cross-entropy loss function was used; L2 regularization was considered. Once the model was fine-tuned, its predicted output was compared with the actual target to evaluate performance metrics using the classification report.

The results of the prediction model across epochs for the training and validation sets are shown in Figure 2. Figure 2 illustrates how accuracy changed over epochs for training, validation, and test data, with accuracy scores on the y-axis and the number of training iterations on the x-axis. Similarly, in the loss plot, the y-axis indicates the loss value, and the x-axis denotes the number of training iterations.

The training accuracy (blue) began at approximately 0.55 and steadily increased, reaching above 0.85 by the 30th epoch. Validation accuracy (orange) followed a similar upward trend, starting around 0.65 and improving to about 0.81 by the 30th epoch. The narrow gap between the training and validation curves indicated minimal overfitting, while the flattening of both curves after 20 epochs suggested model convergence. Both training and validation loss decreased consistently across epochs, dropping from about 13.0 to 2.5 by epoch 30. The close alignment of the two loss curves further demonstrated good generalization and stable learning. Overall, the model achieved reasonable accuracy with consistent loss reduction, indicating effective training.

4.2. DenseNet121 model on image data

The DenseNet121 architecture was employed for image data owing to its effectiveness in alleviating the vanishing gradient problem. All experiments were implemented in Python using the Keras framework and executed in the Google Colab environment. Image pre-processing was followed by data augmentation through Keras's "Image Data Generator" to improve model generalization. Data augmentation strategies included random rotations (±5°), horizontal and vertical translations (up to 10% of image dimensions), and horizontal flipping. The dataset was partitioned into training, validation, and test subsets at 75:15:10. Model training was performed for 50 epochs

using the RMSprop optimizer with a learning rate of 0.0001 and a batch size of 32. The results of the prediction model, based on accuracy and loss over the number of epochs for the training and validation sets, are shown in Figure 3.

The training accuracy increased rapidly, reaching approximately 99% by epoch 20, while the validation accuracy improved steadily during the first 10 epochs to 85–90%. The gap between training and validation accuracy widened significantly after about 15 epochs, indicating that the model memorized the training data but did not generalize well to unseen validation data. The training loss decreased smoothly, approaching zero by epoch 50. In contrast, the validation loss decreased until epoch 30, then stabilized and fluctuated around 1.0, showing no further improvement. The combination of near-zero training loss and plateaued validation loss indicates slight overfitting, as the model continued to improve on the training data without corresponding gains on the validation data.

The analysis of the ROC curve highlighted how the model balanced the trade-off between the TPR and the FPR. The AUC values presented in Figure 4 provide a comprehensive evaluation of the model's effectiveness. The graphical representation illustrates the performance of the classifiers, where the ANN model achieved an AUC of 0.9152, while the DenseNet121 model attained a higher AUC of 0.96, demonstrating reliable performance with an AUC well above 0.5.

The ROC curve of DenseNet121 shows better classification performance, as reflected in its higher AUC score of 0.96, compared to the ANN model. The model maintained a high TPR while minimizing FP, indicating a strong ability to distinguish between the two classes.

Table 3 presents the performance comparison of the ANN and DenseNet121 models on behavioral questionnaire responses and facial image data. The ANN model achieved a reasonable balance, with high specificity (90.4%) but lower sensitivity (80.5%), leading to more missed ASD cases. In contrast, the DenseNet121 model substantially improved sensitivity (91.2%) while maintaining specificity at 89.8%, resulting in higher overall accuracy (91.16%) and a stronger MCC (0.824). The improvement in MCC from 0.709 to 0.824 indicates that the model effectively distinguished between the ASD and non-ASD categories. All statistical analyses were performed in Python using libraries including

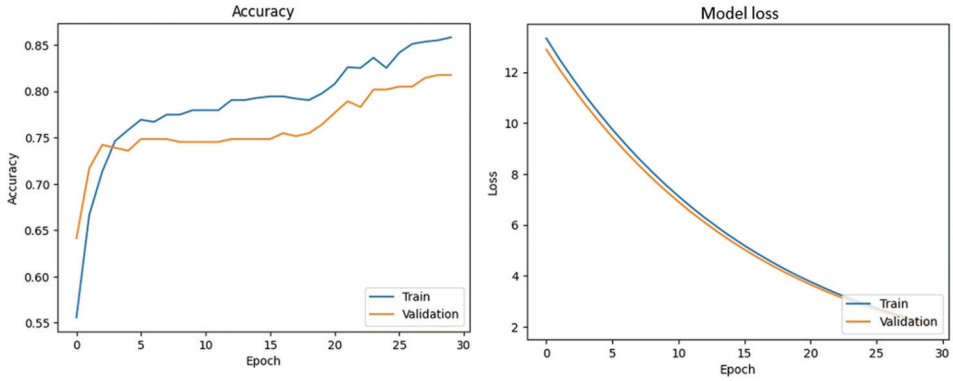

Figure 2. Accuracy and loss curves during artificial neural network training and validation, highlighting learning dynamics and model fit

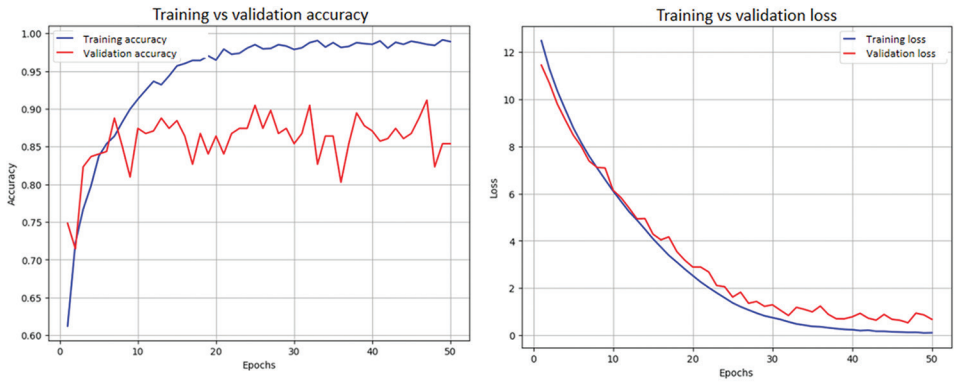

Figure 3. Training and validation accuracy and loss across epochs for the DenseNet121 model, illustrating performance trends

Table 3. Performance comparisons of the artificial neural network and DenseNet121 models on behavioral questionnaire responses and facial image data, showing key evaluation metrics

Dataset/features	Model	Key metrics			
		Precision (%)	Recall (%)	F1 score (%)	MCC
Behavioral questionnaire response	ANN accuracy: 85.1% (95% CI: 82.1–88.7)	90.4 (95% CI: 86.7–93.8)	80.5 (95% CI: 75.7–85.7)	85.4 (95% CI: 81.7–88.8)	0.709 (95% CI: 0.645–0.777)
Facial images	DenseNet121 accuracy: 91.16% (95% CI: 87.8–94.2)	91.1 (95% CI: 87.8–94.3)	91.2 (95% CI: 87.8–94.2)	91.1 (95% CI: 87.7–94.2)	0.824 (95% CI: 0.755–0.885)
Statistical significance	p=0.017 (p<0.05), improvement in accuracy~6% (95% CI: 1.1–10.9)				

Abbreviations: ANN: Artificial neural network; CI: Confidence interval; MCC: Matthews correlation coefficient.

numpy, scipy, and statsmodels. A two-sample Z-test for proportions was conducted to compare the performance of DenseNet121 and ANN. The key assumptions to consider are independence of observations, sufficient sample size, and adequate expected counts. It was used to compare the classification accuracy of two independent models and determine if the observed differences were statistically significant. This test relied on the normal approximation to the binomial distribution, which was valid when the sample sizes were sufficiently large (typically $n > 30$). The diagnostic accuracy of Densenet121 (91.16%, 268/294) was significantly higher than that of the ANN model (85.1%, 338/397). A two-sample Z-test for proportions showed that this improvement was statistically significant (Z = 2.38, p=0.017). Specifically, the effect size based on Cohen's h was small (h = 0.189), and the absolute improvement in diagnostic accuracy was approximately 6.0% (95% confidence interval: 1.1–10.9). As the DenseNet121 model demonstrated a marked reduction in FN, thereby enhancing early detection reliability, it is an essential factor in ASD screening. The higher precision (91.1%) and recall (91.2%) achieved by the DenseNet121 model further support its clinical utility. In addition to the statistically significant improvement, the DenseNet121 model demonstrated clinically meaningful gains, particularly through a 10.7% increase in recall (91.2% vs. 80.5%), indicating a marked reduction in FN. This implies enhanced sensitivity to ASD traits, which is critical for minimizing missed diagnoses and promoting timely clinical assessment.

4.3. Result of ASD severity prediction based on ANN and DenseNet121 models

The predicted label, true label, probability score, and severity category were compiled into a result table and exported as a CSV file for further analysis. This workflow offered a systematic, quantitative, and interpretable assessment of both ASD classification and severity estimation. By incorporating the model's collective decision-making process, the approach enhanced both predictive accuracy and interpretability. In the results, the dataset labels "1" and "0" denote ASD and non-ASD individuals, respectively, following the convention provided by the dataset source.

Table 4. Artificial neural network-based autism spectrum disorder prediction and severity assessment results

Index	True label	ASD probability	Predicted label	Severity level
795	1	0.803926	1	Severe
800	1	0.838478	1	Severe
127	0	0.305518	0	Mild
921	1	0.829160	1	Severe
1572	1	0.508315	1	Moderate
801	1	0.749940	1	Severe
304	1	0.846468	1	Severe
1925	0	0.357174	0	Mild
1135	1	0.519837	1	Moderate
200	1	0.903300	1	Severe

Abbreviation: ASD: Autism spectrum disorder.

The sample predictions in Table 4 show that the model not only classified ASD reasonably well, but also assigned severity level (normal, mild, moderate, and severe) depending on the model's probability scores. The DenseNet121 model utilized dense layers to generate hierarchical feature representations, which were subsequently transformed into softmax probabilities. For example, extremely low probabilities were labeled normal, moderate as mild, and extremely high as severe, and the results were saved to a CSV file. The predicted ASD probabilities were used to assign severity levels, and the results were displayed both in a table and on randomly selected test images. Figure 5 illustrates the ASD severity estimation using the DenseNet121 model for random test images.

Table 5 shows ASD prediction results: the model outputs a probability (ASD probability), predicts a class (Predicted label), and assigns a severity level (normal, mild, severe) based on the probability value. The images show a sample output of an ASD classification model, where children's faces are labeled with predicted severity levels. The model

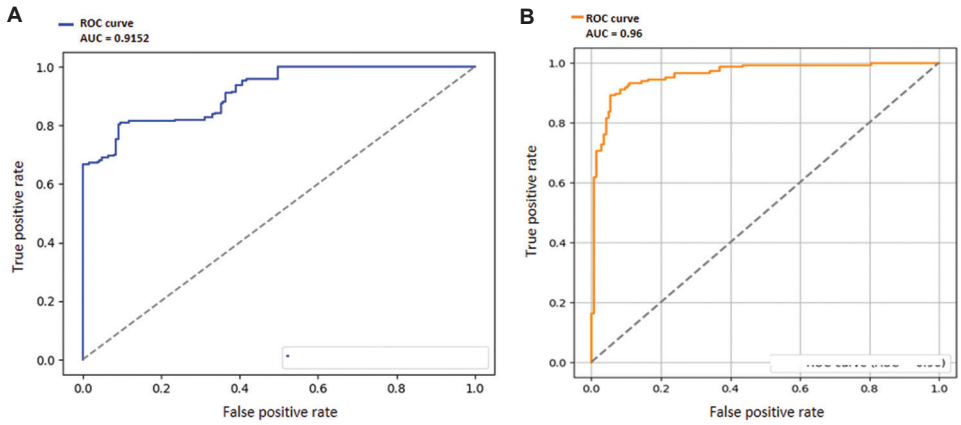

Figure 4. Receiver operating characteristic (ROC) curve with Area under the curve (AUC) illustrating the classification performance of the (A) Artificial neural network and (B) DenseNet121 model

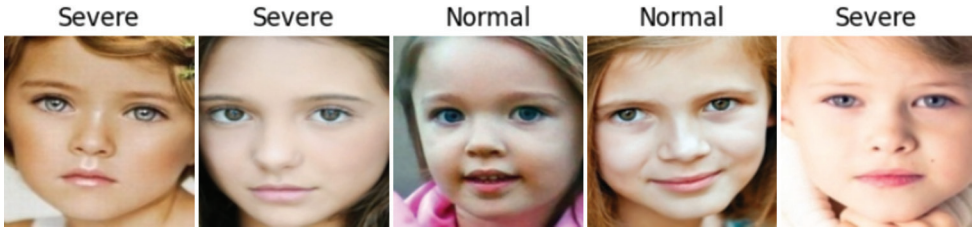

Figure 5. Autism spectrum disorder severity assessed using the DenseNet121 model. Results are presented as test-image predictions illustrated with corresponding confidence levels.

Table 5. DenseNet121-based autism spectrum disorder classification and severity assessment results

Index	True label	ASD probability	Predicted label	Severity level
0	Autistic	0.000230	0	Normal
1	Autistic	0.003804	0	Normal
2	Autistic	0.000059	0	Normal
3	Autistic	0.297353	0	Normal
4	Autistic	0.000020	0	Normal
5	Autistic	0.176527	0	Normal
6	Autistic	0.000212	0	Normal
7	Autistic	0.999946	1	Severe
8	Autistic	0.000032	0	Normal
9	Autistic	0.000438	0	Normal

Abbreviation: ASD: Autism spectrum disorder.

categorizes them into severe (high ASD probability) or normal (low ASD probability). It visually illustrates how the system interprets different faces and assigns severity levels of ASD risk.

Table 6 presents the findings of our approach compared with several existing studies reported in the literature. Previous studies on ASD detection, ML, and DL models have primarily focused on a single modality. Studies based on behavioral features (e.g., Vakadkar *et al.*,[40] Mohanty *et al.*,[42]) achieved accuracy ranging between 81% and 90%, with Mohanty *et al.*[42] reporting perfect specificity (100%). Image-based approaches proposed by Awaji *et al.*,[43] Khan *et al.*,[44] and Nawghare and Prasad[45] have achieved a competitive accuracy of 82–88%. However, these works typically lacked comprehensive reporting of sensitivity and specificity. In contrast, in our proposed dual-pronged method, the behavioral and facial image data processed with ANN and DenseNet121 demonstrated improved performance consistency. DenseNet121 achieves 91.16% accuracy, 91.2% sensitivity, and 89.8% specificity, surpassing most single-modality approaches. This finding highlights the advantage of leveraging complementary data modalities to enhance ASD detection and reduce biases inherent in individual feature spaces.

The current study evaluated behavioral and facial features independently. Each modality provided complementary insights: behavioral traits reflected self-reported or observed tendencies, while facial features offered objective visual cues. Importantly, our severity-based categorization approach extended beyond binary classification. The ANN model, trained on behavioral questionnaire responses, achieved an accuracy of 85.1%, precision of 90.4%, sensitivity of 80.5%, specificity of 90.4%, and an MCC of 0.709. The DenseNet121 model, trained on facial images, demonstrated superior performance with

Table 6. Comparative analysis of various classifier models with existing studies for autism spectrum disorder detection and classification

Reference	Type of data	Methodology	Metric value		
			Accuracy (%)	Sensitivity(%)	Specificity(%)
40	Behavioral attributes	KNN	90.52	NR	NR
		RF	81.52	NR	NR
41	Video data	VGG16	80.90	85.4	NR
42	Behavioral attributes	DNN	85.20	70.4	100.0
43	Facial image data	MobileNet	85.20	85.3	84.7
44	Facial image data	ResNet50	82.00	82.0	NR
		MobileNetV2	85.00	85.0	NR
45	Facial image data	Hybrid-model VGG16, RF	88.34	NR	NR
Proposed method	Behavioral data	ANN	85.10	80.5	90.4
	Facial image data	DenseNet121	91.16	91.2	89.8

Abbreviations: ANN: Artificial neural network; DNN: Deep neural network; KNN: K-nearest neighbors; NR: Not reported; RF: Random forest; VGG: Visual geometry group.

an accuracy of 91.16%, precision of 91.2%, recall of 91.2%, specificity of 89.8%, and an MCC of 0.824. The statistical analysis further confirmed the significance of this improvement, with a p=0.017 (p<0.05) and an approximate 6% increase in accuracy when using facial image features compared to behavioral features. These findings highlight that while both modalities provide valuable insights, facial image analysis contributes more strongly to ASD prediction. The observed increase in accuracy from 85.1% to 91.16% (p=0.017) highlights the improved performance of the facial image-based DenseNet121 model.

Clinically, this improvement reflects a substantial reduction in FN, ensuring that fewer at-risk children are overlooked during early screening and thereby supporting more timely intervention. The increased precision and recall also strengthen confidence in positive detection, enabling pediatricians and psychologists to effectively prioritize children for comprehensive diagnostic evaluation. Importantly, the proposed facial image model is not intended to replace behavioral assessments but to complement them. While behavioral questionnaires capture subjective, parent-reported traits, facial image models analyze objective, phenotype-related indicators. Furthermore, facial image-based systems hold promise for early, accessible screening, with deployment in mobile environments. Such automation may extend ASD screening to rural or resource-limited settings and reduce clinician workload.

We acknowledge potential limitations that may influence the generalization of our findings. The current study was conducted on a small sample drawn from a single dataset, which may not fully represent broader demographic diversity. Factors such as variations in ethnicity, lighting conditions, facial image resolution, and behavioral reporting bias could be confounding variables. The interpretation of the potential dual-pronged approach using behavioral and visual modalities is presented as a prospective direction rather than a definitive conclusion. At present, integrating both modalities may risk bias amplification. However, in our approach, if one modality exhibits bias or reduced sensitivity in certain cases, the other can provide compensatory evidence, thereby enhancing robustness. Furthermore, the use of severity-based thresholds enabled classification into normal, mild, moderate, and severe levels, extending the system beyond binary outcomes.

5. Conclusion

The proposed framework for ASD detection and classification in children demonstrates that DenseNet121 achieved 91.16% accuracy, 91.2% sensitivity, and 89.8% specificity in image-based prediction. While DenseNet121-based deep feature learning demonstrates better performance than other models, issues such as overfitting persist. DenseNet121 mitigates vanishing gradients by reusing features and reducing parameter complexity, thereby improving learning efficiency. By evaluating behavioral and facial modalities independently, this study enhances interpretability and identifies multimodal integration as a promising direction. Importantly, the framework progresses beyond binary ASD detection to include severity stratification, increasing its clinical applicability. However, the current evaluation is limited to a single publicly available dataset. Broader validation using larger, more diverse datasets with subject-independent

testing will be essential to strengthen robustness and generalization. Future work should also investigate fusion strategies at the feature or decision level to achieve a unified multimodal prediction. The next step involves interpretable artificial intelligence techniques, such as gradient-weighted class activating mapping or attention roll-outs, to visualize which facial features influence classification. Clinicians can then better trust and understand how model predictions relate to observable ASD markers. Overall, our study provides a strong foundation for hybrid ASD screening systems that support early detection and intervention, demonstrating the potential of ML to deliver accessible and noninvasive clinical decision support.

Acknowledgments

None.

Funding

None.

Conflict of interest

The authors declare that they have no competing interests.

Author contributions

Conceptualization: All authors
Formal analysis: Sankari M.S
Investigation: All authors
Methodology: Sankari M.S
Writing – original draft: Sankari M.S
Writing – review & editing: All authors

Ethics approval and consent to participate

This study was conducted retrospectively using publicly available human-subject data from the Kaggle open repository. Ethical approval was not required, as confirmed by the license provided with the open-access data.

Consent for publication

Not applicable.

Availability of data

The dataset used in this study is publicly available through the Kaggle open repository:
(i) https://www.kaggle.com/code/mohammedabdelaleem/gathered-asd-datasets.
(ii) https://data.mendeley.com/datasets/f9dycfvwbt/3.

References

1. Lord C, Cook EH Jr., Leventhal BL, Amaral DG. Autism spectrum disorders. *Neuron*. 2000;28(2):355-363.
doi: 10.1016/S0896-6273(00)00115-X

2. Verywell Health Staff. *Do People with Autism Lack Empathy*? Verywell Health; 2011. Available from: https://www.verywellhealth.com/do/people/with-autism-lack-empathy-259887 [Last accessed on 2025 Jul 10].

3. Baio J, Wiggins L, Christensen DL, *et al*. Prevalence of autism spectrum disorder among children aged 8 years - autism and developmental disabilities monitoring network, 11 sites, United States, 2014. *MMWR Surveill Summ*. 2018;67(SS-6):1-23.
doi: 10.15585/mmwr.ss6706a1

4. Sujatha R, Aarthy SL, Chatterjee J, Alaboudi A, Jhanjhi NZ. A machine learning way to classify autism spectrum disorder. *Int J Emerg Technol Learn*. 2021;16(6):182-200.
doi: 10.3991/ijet.v16i06.21575

5. Randall M, Egberts KJ, Samtani A, *et al*. Diagnostic tests for autism spectrum disorder (ASD) in preschool children. *Cochrane Database Syst Rev*. 2018;7(7):CD009044.
doi: 10.1002/14651858.CD009044.pub2

6. Mashudi NA, Ahmad N, Noor NM. Classification of adult autism spectrum disorder using a machine learning approach. *IAES Int J Artif Intell*. 2021;10(3):743-750.
doi: 10.11591/ijai.v10.i3.743

7. Bala M, Ali MH, Satu MS, Hasan KF, Moni MA. Efficient machine learning models for early stage detection of autism spectrum disorder. *Algorithms*. 2022;15(5):166.
doi: 10.3390/a15050166

8. Wiggins LD, Rice CE, Barger B, *et al*. DSM-5 criteria for autism spectrum disorder maximizes diagnostic sensitivity and specificity in preschool children. *Soc Psychiatry Psychiatr Epidemiol*. 2019;54(6):693-701.
doi: 10.1007/s00127-019-01674-9

9. Ramana KS. Machine learning-based novel autism spectrum disorder screening. *Turk J Comput Math Educ*. 2021;12(3):4866-4879.
doi: 10.17762/turcomat.v12i3.4132

10. Is it Autism? *Facial Features that Show Disorder*. *CBS News*; 2011. Available from: https://www.cbsnews.com/pictures/is/it/autism/facial/features/that/show/disorder/9 [Last accessed on 2024 Jul 11].

11. Bhat S, Acharya UR, Adeli H, Bairy GM, Adeli A. Autism: Causative factors, early diagnosis and therapies. *Rev Neurosci*. 2014;25(6):841-850.
doi: 10.1515/revneuro-2014-0033

12. Ardakani HA, Taghizadeh M, Shayegh F. Diagnosis of autism disorder based on deep network trained by augmented EEG signals. *Int J Neural Syst*. 2022;32(11):2250046.
doi: 10.1142/S0129065722500461

13. Khodatars M, Shoeibi A, Sadeghi D, *et al*. Deep learning for neuroimaging-based diagnosis and rehabilitation of

autism spectrum disorder: A review. *Comput Biol Med*. 2021;139:104949.

doi: 10.1016/j.compbiomed.2021.104949

14. Tamilarasi FC, Shanmugam J. Convolutional neural network-based autism classification. In: *Proceedings of the 5th International Conference on Communication and Electronics Systems (ICCES)*. Coimbatore, India: IEEE; 2020. p. 1208-1212.

    doi: 10.1109/ICCES48766.2020.9137926

15. Mohanta A, Mittal VK. Analysis and classification of speech sounds of children with autism spectrum disorder using acoustic features. *Comput Speech Lang*. 2022;72:101287.

    doi: 10.1016/j.csl.2021.101287

16. Ahmed M, Hussain S, Ali F, *et al*. Summarizing recent developments in autism spectrum disorder detection using machine learning and deep learning techniques. *Appl Sci*. 2025;15(14):8056.

    doi: 10.3390/app15148056

17. Poonia A, Kumar S, Raghuwanshi G. Machine learning and deep learning for autism spectrum disorder discovery: A descriptive review. *J Comput Cogn Eng*. 2025;4(3):267-283.

    doi: 10.47852/bonviewJCCE52024757

18. Ding Y, Zhang H, Qiu T. Deep learning approach to predict autism spectrum disorder: A systematic review and meta-analysis. *BMC Psychiatry*. 2024;24(1):739.

    doi: 10.1186/s12888-024-05388-7

19. Singh A, Farooqui Z, Sattler B, Usua U, Helde M. Using Machine Learning Optimization to Predict Autism in Toddlers. In: *Conference: 11th Annual International Conference on Industrial Engineering and Operations Management*. 2021. p. 69206931.

    doi: 10.46254/an11.20211201

20. Hassan MM, Taher SA. Analysis and classification of autism data using machine learning algorithms. *Sci J Univ Zakho*. 2022;10(4):206-212.

    doi: 10.25271/sjuoz.2022.10.4.1036

21. Uddin KMM. A machine learning approach to predict autism spectrum disorder for children and adults using feature optimization. *Netw Biol*. 2023;13(2):37-46.

    doi: 10.17323/1996-7845.2023.2.37

22. Talukdar J, Gogoi D, Singh TP. Comparative assessment of machine learning classifiers for autism spectrum disorder detection. *Healthc Anal*. 2023;3:100178.

    doi: 10.1016/j.health.2023.100178

23. Bawa P, Kadyan V, Mantri A, Vardhan H. Investigating multiclass autism spectrum disorder classification using machine learning techniques. *e-Prime Adv Electr Eng Electron Energy*. 2024;8:100602.

    doi: 10.1016/j.eprime.2024.100602

24. Haque N, Islam T, Erfan M. An exploration of machine learning approaches for early autism spectrum disorder detection. *Healthc Anal*. 2025;7:100379.

    doi: 10.1016/j.health.2025.100379

25. Jahanara S, Padmanabhan S. Detecting autism from facial images. *Int J Adv Res Ideas Innov Technol*. 2021;7(2):219-225.

    doi: 10.13140/RG.2.2.35268.35202

26. Akter T, Ali MH, Khan MI, *et al*. Improved transfer learning-based facial recognition framework for early autism detection. *Brain Sci*. 2021;11(6):734.

    doi: 10.3390/brainsci11060734

27. Alam MS, Rashid MM, Roy R, Faizabadi AR, Gupta KD, Ahsan MM. Empirical study of autism spectrum disorder diagnosis using facial images and transfer learning. *Bioengineering (Basel)*. 2022;9(11):710.

    doi: 10.3390/bioengineering9110710

28. Hriti NS, Shaer K, Momin FMN, Mahmud H, Hasan MK. *Autism Classification using Visual and Behavioral Data*. medRxiv. [Preprint]; 2022.

    doi: 10.1101/2022.10.12.22281002

29. Rahman KK, Subashini MM. Identification of autism in children using static facial features and deep neural networks. *Brain Sci*. 2022;12(1):94.

    doi: 10.3390/brainsci12010094

30. Anjum J, Hia NA, Waziha A, Kalpoma KA. Deep Learning-Based Feature Extraction from Children's Facial Images for Autism Detection. In: *Proceedings of the Cognitive Models and Artificial Intelligence Conference*; 2024. p. 155-159.

    doi: 10.1145/3660853.3660888

31. Bargrizan A. *ASD Final [Dataset]*. Kaggle; 2025. Available from: https://www.kaggle.com/datasets/afarinbargrizan/asd-final [Last accessed on 2025 Jul 16].

32. Allison C, Matthews FE, Ruta L, *et al*. Quantitative checklist for autism in toddlers (Q-CHAT). A population screening study with follow-up: the case for multiple -point screening for autism. *BMJ Paediatr Open*. 2021;5:e000700.

    doi: 10.1136/bmjpo-2020-000700

33. Irmak E. COVID-19 disease severity assessment using CNN model. *IET Image Process*. 2021;15(8):1814-1824.

    doi: 10.1049/ipr2.12175

34. Madhiarasan M, Louzazni M. Artificial neural networks: Architecture, types, and forecasting applications. *J Electr Comput Eng*. 2022;2022:5416722.

    doi: 10.1155/2022/5416722

35. Thillaikarasi R, Kumaresan P. Autism spectrum disorder detection using facial traits: DFDK framework. *Mendeley Data*. 2025;2:V3.

doi: 10.17632/f9dycfvwbt.3

36. Zhou Q, Zhu W, Li F, Yuan M, Zheng L, Liu X. Transfer learning of the resnet-18 and densenet-121 model used to diagnose intracranial hemorrhage in CT scanning. *Curr Pharm Des*. 2022;28(4):287-295.

doi: 10.2174/1381612828666220208165622

37. *Levels of Autism: ASD Levels of Severity*. Autism Speaks. Available from: https://www.autismspeaks.org/levels-of-autism [Last accessed on 2025 Sep 12].

38. Jacob SG, Sulaiman MMBA, Bennet B. Feature signature discovery for autism detection: An automated machine learning based feature ranking framework. *Comput Intell Neurosci*. 2023;2023:6330002.

doi: 10.1155/2023/6330002

39. Raj S, Masood S. Analysis and detection of autism spectrum disorder using machine learning techniques. *Procedia Comput Sci*. 2020;167:994-1004.

doi: 10.1016/j.procs.2020.03.402

40. Vakadkar K, Purkayastha D, Krishnan D. Detection of autism spectrum disorder in children using machine learning techniques. *SN Comput Sci*. 2021;2(5):386.

doi: 10.1007/s42979-021-00773-8

41. Kojovic N, Natraj S, Mohanty SP, Maillart T, Schaer M. Using 2D video-based pose estimation for automated prediction of autism spectrum disorders in young children. *Sci Rep*. 2021;11(1):15069.

doi: 10.1038/s41598-021-94555-0

42. Mohanty AS, Parida P, Patra KC. Identification of autism spectrum disorder using deep neural network. *J Phys Conf Ser*. 2021;1921(1):012006.

doi: 10.1088/1742-6596/1921/1/012006

43. Awaji B, Senan EM, Olayah F, *et al*. Hybrid techniques of facial feature image analysis for early detection of autism spectrum disorder based on combined CNN features. *Diagnostics (Basel)*. 2023;13(18):2948.

doi: 10.3390/diagnostics13182948

44. Khan B, Bhatti SM, Akram A. Autism spectrum disorder detection in children using deep learning and facial images. *Bull Bus Econ (BBE)*. 2024;13(1):557-572.

doi: 10.61506/01.00241

45. Nawghare P, Prasad J. Hybrid CNN and random forest model with late fusion for detection of autism spectrum disorder in toddlers. *MethodsX*. 2025;14:103278.

doi: 10.1016/j.mex.2025.103278

ACCSCIENCE PUBLISHING

Journal of Clinical and Translational Research

ORIGINAL ARTICLE

The efficacy and safety of acupuncture combined with ranibizumab in the treatment of macular edema secondary to retinal vein occlusion

Yan Shi[1], Yimeng Ruan[1], Pengyao Lin[1], Manhua Shi[2], and Bo Li[1]*

[1]Department of Ophthalmology, The First Affiliated Hospital of Ningbo University, Ningbo, Zhejiang, China

[2]Department of Traditional Medicine, The First Affiliated Hospital of Ningbo University, Ningbo, Zhejiang, China

Abstract

Background: Macular edema secondary to retinal vein occlusion (RVO-ME) impairs vision. Intravitreal ranibizumab is commonly used, but the adjunctive value of acupuncture remains unclear. **Objective:** To evaluate the clinical efficacy and safety of acupuncture combined with intravitreal ranibizumab injection for RVO-ME. **Methods:** Patients with RVO-ME (n = 45) were randomized into a control group (ranibizumab monotherapy) and an acupuncture group (ranibizumab and acupuncture). Both groups received monthly intravitreal ranibizumab (0.5 mg/0.05 mL) for 3 months, with a total follow-up of 6 months. Best-corrected visual acuity (BCVA), central macular thickness (CMT), macular vessel density (MVD) of superficial vascular complex (SVC), and deep vascular complex (DVC), foveal avascular zone (FAZ) area, and safety outcomes were assessed. **Results:** At 3 and 6 months post-treatment, BCVA, CMT, SVC-MVD, and DVC-MVD improved significantly in both groups (p<0.05). The acupuncture group showed significant reductions in SVC-FAZ and DVC-FAZ at 6 months (p<0.05), whereas the control group showed no such changes. Between-group differences at 6 months were significant for BCVA, CMT, DVC-MVD, and DVC-FAZ (p<0.05), with DVC-MVD differing significantly at 3 months (p<0.05). Adverse events (subconjunctival hemorrhage, elevated intraocular pressure, subcutaneous hemorrhage) were mild and comparable between groups (p>0.05). **Conclusion:** Acupuncture combined with ranibizumab effectively reduces RVO-ME, improves the microvascular structure of the macula, and is safe and reliable, with no serious adverse reactions. **Relevance for patients:** Patients with vision loss from RVO-ME may benefit from this combined treatment, which improves visual acuity, reduces retinal edema, and supports better long-term macular health with a favorable safety profile.

Keywords: Acupuncture; Ranibizumab injection; Retinal vein occlusion; Macular edema; Optical coherence tomography angiography

***Corresponding author:**
Bo Li
(nblibo@foxmail.com)

Citation: Shi Y, Ruan Y, Lin P, Shi M, Li B. The efficacy and safety of acupuncture combined with ranibizumab in the treatment of macular edema secondary to retinal vein occlusion. *J Clin Transl Res*. 2026;12(1):62-71.
doi: 10.36922/JCTR025410071

Received: October 12, 2025

Revised: December 10, 2025

Accepted: January 19, 2026

Published online: February 6, 2026

1. Introduction

Retinal vein occlusion (RVO) is a common retinal vascular disease characterized by disrupted retinal vein circulation, increased vascular permeability, and macular edema (ME). ME is the primary cause of visual impairment in patients with RVO and is a prevalent cause of unilateral blindness, particularly in middle-aged and elderly individuals.[1] Persistent and recurrent ME can result in irreversible vision loss. Currently, the first-line treatment for ME secondary to RVO involves intravitreal injections of anti-vascular endothelial growth factor (VEGF) drugs. These treatments are known for their rapid effect and ease of administration, yet persistent and recurrent ME remains a frequent clinical challenge.[2,3] In traditional Chinese medicine (TCM), RVO is classified under the conditions of "sudden blindness" or "collateral damage sudden blindness." TCM suggests that the condition often arises from stagnation of qi and blood stasis, or from qi deficiency combined with blood stasis, leading to venous obstruction in the fundus and causing ischemia and edema in the retina and macula. Acupuncture, a core therapy in TCM, functions by unblocking meridians, promoting the flow of qi and blood, and restoring normal physiological function in blocked areas, aligning with the treatment principles for sudden blindness. This study aimed to observe the efficacy and safety of combining acupuncture with intravitreal ranibizumab injections in treating ME secondary to RVO.

2. Data and methods

2.1. Data

The clinical data of 45 patients (45 eyes) with RVO-ME admitted to the First Affiliated Hospital of Ningbo University from 2020 to 2023 were retrospectively analyzed and divided into the control group (26 cases, 26 eyes) and the acupuncture group (19 cases, 19 eyes), according to the treatment received. The control group included 12 males and 14 females, with a mean age of (57.38 ± 8.87) years. In the acupuncture group, there were 7 males and 12 females, with a mean age of (55.21 ± 9.98) years. This study was approved by the Ethics Committee of the First Affiliated Hospital of Ningbo University (Ethics batch number: 2023 Research No. 083RS-01). All patients provided written informed consent before participation in this study.

2.2. Inclusion and exclusion criteria

The patients were selected according to specific inclusion and exclusion criteria to ensure accurate assessment of RVO-ME:

Inclusion criteria: Patients with newly diagnosed RVO-ME meeting the 2019 Diagnostic and Treatment Guidelines for European Society of Retina Specialists Venous Obstruction,[4] confirmed through optical coherence tomography (OCT; Heidelberg Engineering, Germany).

Exclusion criteria: (i) Patients with diabetic retinopathy identified during post-mydriatic fundus examination; (ii) patients unable to cooperate with necessary examinations; (iii) history of glaucoma or uveitis; (iv) previous intraocular surgeries, such as cataract surgery, retinal photocoagulation, or vitrectomy, or cloudy refractive media. All participants and their families were informed about the study, and signed informed consent forms were obtained.

2.3. Methods

2.3.1. Control group

The control group received intraocular injections of ranibizumab. Specifications: 0.20 mL (10 mg/mL) per vial, registration number SJ20170004, manufactured by Novartis Pharma Schweiz AG, Switzerland. To prevent infection, levofloxacin eye drops were administered 3 times daily for 3 days before the procedure. During the procedure, the patient was placed in the supine position, and after achieving satisfactory topical anesthesia, the area was disinfected and covered with sterile drapes. The injection site was located 3.5 mm to 4.0 mm posterior to the temporal corneal limbus. A vertical injection was made into the sclera, delivering 0.5 mg/0.05 mL of ranibizumab. After the procedure, levofloxacin ointment was applied to the affected eye, which was then covered. This treatment was administered once a month for 3 months.

2.3.2. Acupuncture group

In addition to the treatments provided to the control group, the acupuncture group received acupuncture therapy. Local (eye) acupuncture points were primarily selected, with whole-body points included. Two to three point groups were chosen based on the patient's constitution and disease severity, with point selection rotated regularly. The body acupuncture points included *Jingming*, *Chengwei*, *Sibai*, *Touwei*, *Qiuhou*, *Guangming*, *Taichong*, *Zhaohai*, and *Sizhukong*. The technique used was mild reinforcing and attenuating, with needles retained for 30 min, once daily. Points were alternated, with 10 sessions constituting one course of treatment. Ear point pressure with the bean method, targeting Shen Gate, liver, spleen, kidney, and eye areas (Eye 1, Eye 2), was applied once daily for 10 sessions per treatment course. The treatment included a 3-day rest period, and a total of three courses were administered.

2.3.3. Examination methods and observation indicators

Before treatment, and at 3 and 6 months after treatment, best-corrected visual acuity (BCVA) was assessed using

a standard visual acuity chart and recorded as decimal acuity, and intraocular pressure (IOP) was measured with a non-contact tonometer. The same skilled ophthalmologist performed OCT examinations. Pupils were dilated to at least 5 mm for 30 min before the examination. Central macular thickness (CMT) was measured using OCT. A 3 mm × 3 mm section of the retinal macular area was scanned in OCT angiography (OCTA) mode, and foveal avascular zone (FAZ) images were obtained. The macular superficial and deep retinal blood flow charts were analyzed using ImageJ (version 1.52 p, National Institutes of Health, USA). Superficial vascular complex (SVC) macular vessel density (MVD) data were calculated for the FAZ area, and retinal MVD was measured at the deep vascular complex (DVC) level. Adverse reactions, including subconjunctival hemorrhage, elevated IOP, and subcutaneous hemorrhage, were assessed at 1, 3, and 6 months post-treatment.

2.4. Statistical analysis

All data were analyzed using the Statistical Package for the Social Sciences (25.0, IBM, United States). Variables were expressed as mean ± standard deviation. Paired-samples *t*-tests were used for intra-group comparisons, and one-way analysis of variance for comparisons between the two groups. The χ^2 test was used for count data. A value of $p<0.05$ was considered statistically significant.

3. Results

3.1. Baseline characteristics

The study included complete and consistent follow-up data for 45 patients (45 eyes), with 26 patients (26 eyes) in the control group and 19 patients (19 eyes) in the acupuncture group. There were no statistically significant differences between the two groups in terms of gender, age, disease duration, weight, or blood pressure ($p>0.05$), making the groups comparable, as shown in Table 1.

3.2. Visual, anatomical, and optical coherence tomography angiography outcomes

We compared BCVA, CMT, SVC-MVD, DVC-MVD, SVC-FAZ, and DVC-FAZ between the two patient groups. The BCVA, CMT, SVC-MVD, and DVC-MVD of the two groups showed significant improvement at 3 and 6 months after treatment compared to pre-treatment values ($p<0.05$). In the control group, there were no statistically significant differences in SVC-FAZ and DVC-FAZ between pre-treatment and 3 or 6 months post-treatment ($p>0.05$). Similarly, in the acupuncture group, no significant differences in SVC-FAZ and DVC-FAZ were observed between pre-treatment and 3 months post-treatment ($p>0.05$). However, both parameters showed statistically significant improvement at 6 months post-treatment ($p<0.05$). There were statistically significant differences between the two groups in BCVA, CMT, DVC-MVD, and DVC-FAZ at 6 months post-treatment ($p<0.05$). In contrast, at 3 months post-treatment, only DVC-MVD showed a significant difference between the groups ($p<0.05$), indicating that the deep blood flow density in the acupuncture group recovered more quickly than in the control group. Other indicators did not show significant differences between the groups. The results are shown in Table 2 and Figure 1.

3.3. Safety outcomes

There were no significant differences in adverse reactions between the two groups at 1, 3, and 6 months post-treatment, including subconjunctival hemorrhage, elevated IOP, and subcutaneous hemorrhage ($p>0.05$). Subconjunctival and subcutaneous hemorrhages fully resolved after a week of topical hot compress treatment, while patients with elevated IOP returned to normal after using anti-glaucoma eye drops. The results are shown in Table 3.

4. Discussion

Currently, integrated traditional Chinese and Western medicine is widely used in the clinical treatment of RVO, yielding positive results through classification, staging, and individualized treatment approaches.[5] In TCM, RVO is categorized as "sudden blindness," first described in Criteria for Syndrome and Treatment, Miscellaneous Diseases, Seven Tips. The pathogenesis is attributed to the combined effects of water retention and blood stasis.[6] In modern times, researchers have sought to verify acupuncture's actual clinical value and to clarify its physiological and biological mechanisms. Since the establishment of the World Federation of Acupuncture-Moxibustion Societies in 1987, acupuncture research has developed rapidly worldwide. The 1997 National Institutes of Health Consensus Conference on Acupuncture reviewed

Table 1. Comparison of demographic data between the two groups (mean±standard deviation)

Groups	Number of eyes	Gender (male/female)	Age (years)	Duration (days)	Weight (kg)	Systolic blood pressure (mmHg)	Diastolic blood pressure (mmHg)
Control group	26	12/14	57.38±8.87	27.04±25.86	61.19±10.80	137.58±19.63	83.65±8.21
Acupuncture group	19	7/12	55.21±9.98	22.00±23.54	65.95±11.44	136.16±16.76	85.79±9.41

Table 2. Comparison of BCVA, CMT, MVD, and FAZ between the two groups

Parameters	Control group			Acupuncture group			Comparison between groups at the same time point (*p*-value)	
	Before the treatment	After the treatment		Before the treatment	After the treatment			
		3 months	6 months		3 months	6 months	3 months	6 months
BCVA	0.32±0.15	0.50±0.22*	0.42±0.15*	0.36±0.19	0.59±0.25*	0.57±0.14*[a]	0.205	0.002
p-value		<0.001	<0.001		<0.001	<0.001		
CMT (μm)	376.62±77.44	268.15±30.83*	302.35±38.37*	407.58±75.29	289.32±50.88*	280.05±28.36*[a]	0.090	0.038
p-value		<0.001	<0.001		<0.001	<0.001		
SVC-MVD (%)	46.23±8.36	59.93±7.34*	52.65±7.39*	50.93±9.22	58.07±8.91*	57.21±8.20*	0.096	0.057
p-value		<0.001	<0.001		<0.001	<0.001		
DVC-MVD (%)	40.46±4.14	45.04±3.37*	43.91±3.03*	43.77±7.27	52.97±6.28*[a]	52.41±6.51*[a]	<0.001	<0.001
p-value		<0.001	<0.001		<0.001	<0.001		
SVC-FAZ (mm^2)	0.32±0.10	0.33±0.10	0.31±0.09	0.33±0.09	0.32±0.08	0.29±0.07*	0.773	0.480
p-value		0.496	0.152		0.237	0.012		
DVC-FAZ (mm^2)	0.29±0.11	0.30±0.10	0.29±0.08	0.28±0.04	0.27±0.05	0.25±0.04*[a]	0.203	0.049
p-value		0.165	0.753		0.300	*p*<0.001		

Notes: Data are expressed as mean±standard deviation. *p<0.05 versus before treatment within the same group; [a]p<0.05 versus the control group at the same time point.
Abbreviations: BVCA: Best-corrected visual acuity; CMT: Central macular thickness; DVC: Deep vascular complex; FAZ: Foveal avascular zone; MVD: Macular vessel density; SVC: Superficial vascular complex.

Table 3. Comparison of adverse reactions between the two groups

Adverse reaction (number of occurrences)	Control group (26 eyes)			Acupuncture group (19 eyes)		
	1 month (%)	3 months (%)	6 months (%)	1 month (%)	3 months (%)	6 months (%)
Subconjunctival hemorrhage	2 (7.69%)	1 (3.85%)	0 (0)	2 (10.53%)	2 (10.53)	0 (0)
Elevated IOP	1 (3.85%)	0 (0)	0 (0)	0 (0)	0 (0)	0 (0)
Subcutaneous hemorrhage	0 (0)	0 (0)	0 (0)	2 (10.53%)	0 (0)	0 (0)

Abbreviation: IOP: Intraocular pressure.

the available scientific evidence and the therapy's efficacy for a wide range of disorders. Studies at that time focused largely on pain-related conditions and on the nature of meridians and acupoints, providing a firm foundation for the subsequent growth and acceptance of acupuncture.

Today, research interests have expanded well beyond pain control: In 2002, the World Health Organization listed 106 conditions for which acupuncture is indicated. Although some categories overlap, they are not identical.[7] The steadily accumulating evidence of benefit across diverse disorders has greatly advanced our understanding of this therapeutic approach.[8] By manually stimulating points along the meridians, acupuncture promotes the free flow of qi and blood and rebalances yin and yang.

Acupuncture treatment focuses on promoting blood circulation, removing blood stasis, and unblocking meridians. Wang and Kong[9] demonstrated that acupuncture combined with compound Xueshuantong significantly improves visual acuity in RVO patients with qi stagnation and blood stasis, and effectively regulates the expression levels of various cytokines in the body. Ranibizumab, a high-affinity recombinant monoclonal antibody fragment, inhibits neovascularization, reduces blood exudation, and promotes the absorption of edema, making it effective in treating RVO-ME.[10] It primarily promotes the absorption of intraretinal fluid and improves ME by inhibiting neovascularization, reducing vascular permeability, and regulating the permeability of the blood–retinal barrier through antagonistic mechanisms. Among these, ranibizumab is currently the most widely used anti-VEGF biologic agent. The 2010 European guidelines for the treatment of RVO recommend ranibizumab as a Grade A treatment for RVO-ME. Its overall efficacy, safety, and intravitreal injection route have been well-established in numerous studies.[11] However, the half-life of ranibizumab

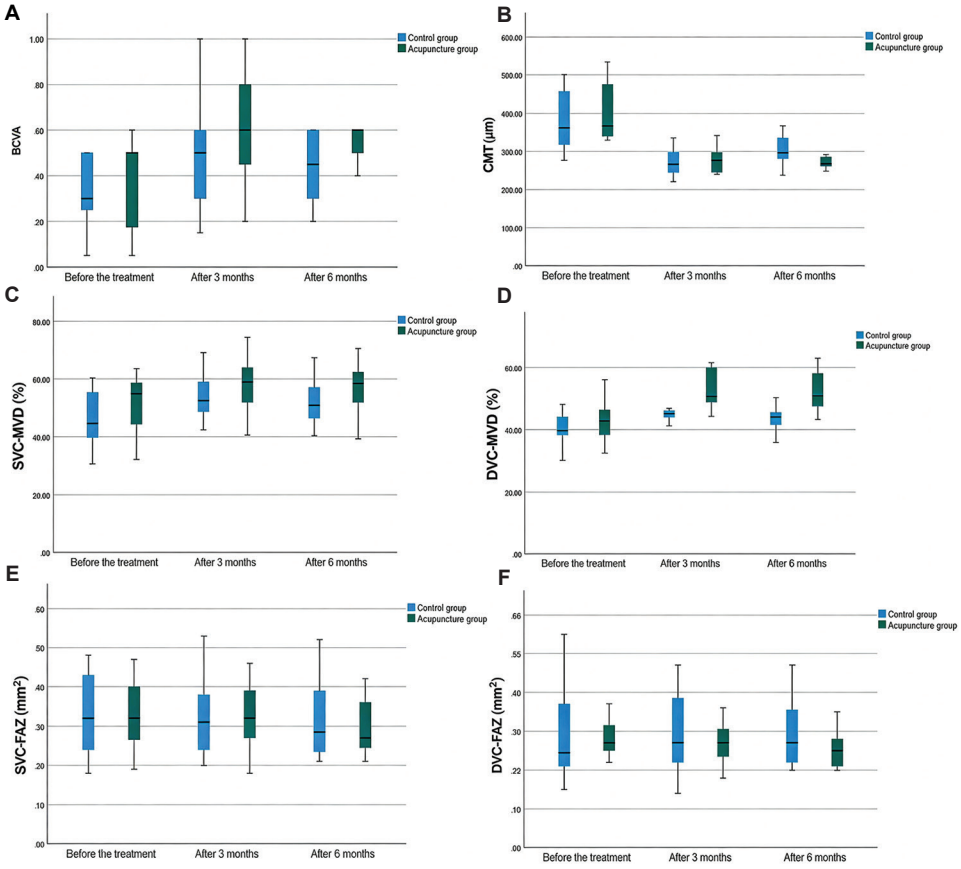

Figure 1. The box plot comparisons of (A) BCVA, (B) CMT, (C) SVC-MVD, (D) DVC-MVD, (E) SVC-FAZ, and (F) DVC-FAZ within-group (before and after treatment) and between the two groups
Note: *$p<0.05$.
Abbreviations: BVCA: Best-corrected visual acuity; CMT: Central macular thickness; DVC: Deep vascular complex; FAZ: Foveal avascular zone; MVD: Macular vessel density; SVC: Superficial vascular complex.

in the vitreous cavity is less than nine days, limiting its long-term efficacy. Studies show that on average, 8–9 injections are required annually. Due to ranibizumab's relatively short intravitreal half-life, repeated injections are required to sustain its therapeutic effect once the effective concentration declines. Data from pivotal trials show that monthly dosing for the first 6 months produces the maximal visual gain.[12] Thereafter, vision can be maintained with either monthly or *pro re nata* (PRN) injections, with no statistically significant difference between the two regimens. Consequently, a loading phase of 6 monthly injections followed by PRN retreatment (the "6 + PRN") is now regarded as the optimal anti-VEGF dosing strategy for RVO. This implies that every RVO patient should receive at least six injections, and on average, 8–9 ranibizumab injections are given within the first 12 months. Such frequent intravitreal injections not only carry the potential risk of endophthalmitis but also impose a significant financial burden on patients, limiting the widespread adoption of this therapy in China. The repeated intraocular injections increase the risk of cataracts, endophthalmitis, elevated IOP, and vitreous hemorrhage.[13,14] As a result, combining acupuncture with pharmacological treatment for RVO-ME has become a topic of increasing interest.

In this study, *Taichong* is selected as the source point of the liver meridian, while *Guangming* belongs to the gallbladder meridian. The combination of these two points, known as the *Yuan-Luo* acupoint pairing, helps regulate the liver and gallbladder, clear qi, promote blood circulation, and restore vitality. The combination of *Jingming* and *Sibai* helps to open the orifices and clear the eyes. *Chengqi*, which belongs to the stomach meridian of foot *Yangming*, works to dispel wind, clear heat, improve vision, and prevent tearing. *Qiuhou* is used to clear heat and enhance vision, while *Zhaohai* helps absorb heat and restore vitality. *Sizhukong* helps reduce turbidity and remove dampness. The combination of *Qiuhou* and *Guangming*, along with these other points, works to activate blood circulation and

improve vision. Auricular acupoint pressure therapy is an extension of auricular acupuncture. By stimulating specific points on the ear, it activates the body's bidirectional regulation functions, balances the qi in the eye meridians, and improves the local blood supply to the eyeball.

4.1. Efficacy outcomes and temporal dynamics

The results of this study showed that the acupuncture group experienced a statistically significant reduction in the FAZ area after 6 months of treatment, whereas the control group showed no significant change in the FAZ area before and after treatment. These findings remain a subject of debate,[15-17] with possible reasons for the discrepancies including differences in race, sample size, and measurement methods. Apart from the change in FAZ area, significant improvements were observed in other indicators before and after treatment in both groups, indicating that both ranibizumab intravitreal injection alone and the combination of acupuncture and medication were effective in treating RVO-ME. In a prospective case-series study,[9] 78 eyes with RVO attributed to qi stagnation and blood stasis were investigated. Control subjects received only oral compound xueshuantong capsules, whereas the intervention cohort received additional acupuncture treatment at *Touwei*, *Jingming*, *Chengqi*, *Sibai*, *Taichong*, and *Guangming*. The acupuncture-augmented regimen achieved a 97.4% clinical response rate and demonstrated significant superiority over monotherapy in visual function recovery and modulation of VEGF and serum endothelin-1 levels. These findings provide robust evidence that acupuncture is an effective adjunctive intervention for RVO and should be considered when standard pharmacotherapy alone proves insufficient. The improvement in DVC-MVD in the acupuncture group was significantly greater than in the control group at both 3 and 6 months after treatment. This may be attributed to acupuncture's ability to increase retinal blood flow and improve circulation,[18] possibly linked to glucocorticoids' effects on the DVC layer. Glucocorticoids may inhibit the production of inflammatory factors in this layer and help regulate the function of the blood–retinal barrier, contributing to similar improvements in visual function.[19] Regarding the underlying mechanisms, a previous study suggested that acupuncture stimulates parasympathetic nerve responses, thereby increasing choroidal and retinal blood flow,[20] whereas another study proposed that acupuncture inhibits sympathetic nervous system activity and raises endorphin levels to enhance retinal blood circulation.[21] When comparing other indicators between the two groups, the acupuncture group did not show significantly better results than the control group after 3 months of treatment, suggesting that acupuncture may not have an immediate effect on increasing retinal blood circulation. However, after 6 months of treatment, the differences became statistically significant, which may be due to the slower onset of acupuncture in treating RVO-ME. In a clinical trial evaluating the combined use of acupuncture and retinal laser photocoagulation for RVO,[22] visual acuities improved in both the treatment and control groups after 1 month, although the between-group difference did not achieve statistical significance. By the 6-month endpoint, however, the acupuncture-plus-laser cohort exhibited a significantly greater gain in BCVA than the laser-only controls ($p<0.05$). Parallel analyses of CMT revealed a statistically significant reduction in both arms. Nevertheless, the magnitude and velocity of CMT decrease were more pronounced in the acupuncture-augmented group, with the divergence becoming increasingly evident over time. Although the study did not incorporate pharmacotherapy, its longitudinal profile aligns with our observations: the therapeutic impact of acupuncture accumulates gradually, becoming demonstrably superior only after an extended observation period.

4.2. Hemodynamic-structural chronology and clinical implications

The temporal relationship between retinal hemodynamic alteration and microstructural injury remains a pivotal yet unresolved issue in the pathogenesis of retinal vascular disorders. Although glaucoma and RVO represent distinct clinical entities, they demonstrate remarkably similar perfusion anomalies—namely, reduced capillary density, patchy non-perfusion, and compromised blood–retinal barrier integrity—implying a shared "microcirculatory derangement–structural remodeling" cascade. Whether hemodynamic change precedes structural damage, or vice versa, is still vigorously debated. Several reports documented significant peripapillary vessel-density decline in glaucomatous eyes before any measurable alteration in retinal nerve fiber layer thickness,[23] whereas others observed prompt post-therapeutic rebound of flow density without concurrent change in macular ganglion-cell complex thickness, indirectly suggesting that vascular alteration antedates structural modification.[24] Conversely, another study argued that structural loss may precede detectable hemodynamic disturbances, proposing structural impairment as the primary driver of subsequent microvascular dysfunction.[25]

Optical coherence tomography angiography is a non-invasive imaging modality that enables high-speed scanning and layer-by-layer visualization of the retinal microvasculature, permitting quantitative assessment of retinal blood-flow parameters.[26,27] Previous investigations have demonstrated that eyes with RVO exhibit significantly reduced vessel density in both the

superficial capillary plexus (SCP) and the deep capillary plexus (DCP), accompanied by an enlargement of the FAZ.[27,28] In the present study, we longitudinally compared macular thickness and layer-specific vessel densities in both control and acupuncture-treated cohorts. Macular thickness decreased significantly in both groups within the early treatment phase; however, acupuncture eyes did not exhibit a measurable change in flow-density indices, such as FAZ area, until 6 months after initiation, implying that structural modification may precede hemodynamic improvement—a sequence that contradicts several previous observations. This finding not only expands the "flow-versus-structure" timeline debate but also provides fresh empirical evidence for clarifying microcirculation–tissue interactions across disparate retinal disorders. SVC-MVD and DVC-MVD in both groups were significantly improved at 3 and 6 months post-treatment compared to baseline (all $p<0.05$). Although there is no significant difference between the control and acupuncture group in SVC-MVD recovery, the acupuncture group demonstrated superior restoration of DVC-MVD. This divergence is presumably attributable to the vasoconstrictive effect of anti-VEGF agents. The pronounced impairment of the deep capillary layer may reflect the absence of pericytes and smooth-muscle cell coverage in the deep capillary plexus, rendering it more vulnerable than the superficial plexus.[29] Anti-VEGF can effectively alleviate leakage caused by SCP destruction, and disruption of DCP microcirculation may be a key factor for the persistence of ME after anti-VEGF treatment.[30] Consequently, we hypothesize that adjunctive acupuncture may exert a preferential protective effect on the retinal deep vascular network.

ME secondary to RVO is typically evaluated by the degree of macular thickening. However, if hemodynamic normalization is the inciting factor, early flow parameters may be more sensitive biomarkers to guide the timing and frequency of anti-VEGF therapy. On the other hand, should structural alteration precede vascular improvement, it implies that retinal tissue injury is already entrenched at baseline, mandating earlier neuroprotective or structural rescue strategies. Therefore, clarifying this chronology deepens our understanding of RVO pathobiology and furnishes a theoretical framework for individualized treatment algorithms centered on microvascular assessment. Our data further imply that early initiation of anti-VEGF therapy—followed by adjunctive acupuncture in later phases—may constitute a rational, sequential treatment paradigm for RVO-ME.

4.3. Safety profile and technique considerations

Needle withdrawal is the final step of an acupuncture treatment. Because it seems simple and technically undemanding, clinicians often pay little attention to it. In practice, however, numerous patients leave the couch with pain, bleeding, subcutaneous hematoma, or bruising; they become anxious and restless, and their satisfaction with acupuncture drops. These minor injuries are the most common complications of needling. A standardized withdrawal technique can greatly reduce discomfort and prevent conflict between doctors and patients. Research shows that the subcutaneous layer is rich in vessels and nerves.[31] If direction and digital pressure are ignored as the needle is pulled out, the tip or shaft can scrape the vessel wall or surrounding tissue; any additional force immediately increases pain and may further damage the vessel. Therefore, before the needle is removed, a sterile cotton swab is placed gently on the skin beside the puncture site. Pressure is light at first, so the skin is not dragged by the needle, and trauma is minimized. The needle is then slowly withdrawn back to the subcutaneous level against the line of insertion; pressure is increased slightly, and the shaft is briskly removed with one smooth, even motion, but not with excessive force. On the scalp and face, where vessels are denser than on the trunk or limbs, compression is maintained for a few extra seconds to limit bleeding. These simple measures reduce injury to vessels, nerves, and muscle, and they lessen post-treatment pain, bleeding, and bruising. Research suggests that subcutaneous hemorrhage can be absorbed by applying cold compresses within 48 h and hot compresses after 48 h.[32,33] Rare yet documented ocular complications of acupuncture include direct injury to the oculomotor nerve, manifesting as ptosis, mydriasis, and restricted extraocular motility, and to the optic nerve, resulting in sudden monocular blindness.[34] Imprecise needle angulation may traumatize the extraocular muscles, producing diplopia and gaze limitation.[35] Moreover, misdirection or inexperience can lead to globe perforation, retinal vessel rupture, intraocular hemorrhage, and even retinal detachment.[36] Systemic reactions have also been reported: approximately 10% of subjects experience intense anxiety or pain during periocular needling,[37] and arrhythmias, including atrial fibrillation. Given the anatomical vulnerability of the orbital region, clinicians must maintain continuous visual and verbal contact with the patient, employ pre-procedural counseling to mitigate apprehension, and be prepared to institute emergency measures should an adverse event occur.

Throughout the entire follow-up period, adverse events in both groups were limited to mild subconjunctival hemorrhage, subcutaneous hemorrhage, and transient IOP elevation; no severe anterior segment infection, vitreous hemorrhage, or systemic complications were observed. All hemorrhagic cases resolved completely within 1 week with local warm compresses, and IOP returned to baseline after

a single hypotensive eye drop. These findings indicate that adjunctive acupuncture therapy in addition to conventional anti-VEGF treatment does not pose additional safety risks and is well tolerated, meeting the safety requirements for further clinical dissemination. Although the bleeding entirely resolved after a week of hot compress treatment, this highlights the need for careful monitoring of patients' systemic conditions during acupuncture. It is essential to prevent potential bleeding, pay close attention to the technique and pressure applied during acupuncture, and avoid areas prone to bleeding to minimize the occurrence of adverse reactions.

5. Conclusion

Both acupuncture combined with ranibizumab and ranibizumab alone are effective treatments for patients with RVO-ME. However, compared to ranibizumab alone, the combination of acupuncture and medication more effectively reduces ME and improves the microvascular structure in the macular region, without causing serious adverse reactions, making it a safe and reliable option. Nevertheless, this study has several limitations. OCTA is not suitable for all patients with RVO-ME, as it requires clear refractive media and patient cooperation for accurate results. In addition, the sample size was relatively small (n = 45), which may limit statistical power and increase the risk of errors. The small cohort may affect the generalizability of our findings to the broader RVO-ME patient population. The follow-up duration was limited to 6 months, a relatively short period to assess the long-term efficacy and safety of the combined therapy. A longer observation period is needed to evaluate sustained treatment benefits and potential delayed adverse events. Future studies with larger sample sizes, multi-center collaboration, and extended follow-up periods are warranted to validate our results and improve external validity.

Acknowledgments

The authors would like to thank Dr. Wei Gao at Ningbo University of Technology for providing valuable assistance with the study and field tests.

Funding

This work was supported by The Zhejiang Province Traditional Chinese Medicine Science and Technology Plan (Award Number: 2023ZL647), The Zhejiang Province Medical and Health Science and Technology Plan (Award Number: 2024KY1496), and The Ningbo Public Welfare Research Project (Award Number: 2024S160).

Conflict of interest

The authors declare that they have no competing interests.

Author contributions

Conceptualization: Yan Shi, Bo Li
Data curation: Yimeng Ruan
Formal analysis: Yan Shi
Funding acquisition: Yan Shi
Investigation: Yan Shi, Manhua Shi
Methodology: Yan Shi
Resources: Manhua Shi, Bo Li
Software: Pengyao Lin
Supervision: Bo Li
Visualization: Pengyao Lin
Writing-original draft: Yan Shi, Yimeng Ruan
Writing-review & editing: Bo Li

Ethics approval and consent to participate

All included patients provided their oral and written informed consent. The data of this study were published with the approval of the Ethics Committee of the First Affiliated Hospital of Ningbo University (Ethics batch number: 2023 Research No. 083RS-01).

Consent for publication

Written informed consent for publication was obtained from all participants.

Availability of data

All data included in this study are available upon request from the corresponding author.

References

1. Costa JV, Moura-Coelho N, Abreu AC, Neves P, Ornelas M, Furtado MJ. Macular edema secondary to retinal vein occlusion in a real-life setting: A multicenter, nationwide, 3-year follow-up study. *Graefes Arch Clin Exp Ophthalmol*. 2021;259(3):343-350.

   doi: 10.1007/s00417-020-04932-0

2. Hirano T, Toriyama Y, Iesato Y, *et al*. Effect of leaking perifoveal microaneurysms on resolution of diabetic macular edema treated by combination therapy using anti-vascular endothelial growth factor and short pulse focal/grid laser photocoagulation. *JPN J Ophthalmol*. 2017;61(1):51-60.

   doi: 10.1007/s10384-016-0483-8

3. Li XR, Zhou HY. Special attention to the cause, treatment and prevention of macular edema. *RAO*. 2019;39(7):601-605.

doi: 10.13389/j.cnki.rao,2019.0139

4. Schmidt-Erfurth U, Garcia-Arumi J, Gerendas BS, *et al*. Guidelines for the management of retinal vein occlusion by the European society of retina specialists (EURETINA). *Ophthalmologica*. 2019;242(3):123-162.

   doi: 10.1159/000502041

5. Chen XD, Bu JP. Observation of differentiation of syndrome on ischemic retinal vein occlusion after laser photocoagulation. *IES*. 2011;11(3):461-463.

   doi: CNKI: SUN:GJYK.0.2011-03-033

6. Li X, Zhuang ZY, Bai M. Thinking mode of disease, etiology, syndrome type and treatment of macular edema in retinal vein occlusion. *Chin J Ophthalmol*. 2020;30(2):135-139.

   doi: 10.13444/j.cnki.zgzyykzz.2020.02.014

7. Sierpina VS, Frenkel MA. Acupuncture: A clinical review. *South Med J*. 2005;98(3):330-337.

   doi: 10.1097/01.SMJ.0000140834.30654.0F

8. Zhuang Y, Xing JJ, Li J, Zeng BY, Liang FR. History of acupuncture research. *Int Rev Neurobiol*. 2013;111:1-23.

   doi: 10.1016/B978-0-12-411545-3.00001-8

9. Wang Y, Kong DN. Clinical efficacy of acupuncture plus compound xueshuantong for retinal vein occlusion and its effect on the expressions of VEGF and ET-1 in peripheral blood. *Shanghai J Acu-Mox*. 2019;38(8):883-887.

   doi: 10.13460/j.issn.1005-0957.2019.08.0883

10. Zhao J, Bi XD, Si YF, Zhou L. Clinical trial of ranibizumab injection in the treatment of macular edema in non-ischemic branch retinal vein occlusion. *Chin J Clin Pharmacol*. 2021;37(11):1330-1332.

    doi: 10.13699/j.cnki.1001-6821.2021.11.007

11. Pieramiei DJ, Avery RL. Ranibizumab: Treatment in patients with neovascular age-related macular degeneration. *Expert Opin Bio Ther*. 2006;6(11):1237-1245.

    doi: 10.1517/14712598.6.11.1237

12. Liu W. Advances in the treatment of macular edema secondary to retinal vein occlusion. *Chin J Ophthalmol Otorhinolaryngol*. 2015;15(4):236-239.

    doi: 10.14166/j.issn.1671-2420.2015.04.004

13. Wan SS, Yang YN, Xing YQ, Man ZH, Rao ZQ. Efficacy and safety of Ranibizumab for macular edema due to retinal vein occlusion: A systematic review. *China Med Herald*. 2013;10(27):62-64,67.

    doi: 10.3969/j.issn.1673-7210.2013.27.022

14. Gao W, Yi XL. Meta-analysis of efficacy of ranibizumab and laser treatment for diabetic macular edema. *J Xinjiang Med Univ*. 2014;37(10):1321-1325.

    doi: 10.3969/j.issn.1009-5551.2014.10.020

15. Khalil GF, Iafe NA, Jean-Pierre H, Irena T, Sadda SR, David S. Optical coherence tomography angiography analysis of the foveal avascular zone and macular vessel density after anti-VEGF therapy in eyes with diabetic macular edema and retinal vein occlusion. *IOVS*. 2017;58(1):30-34.

    doi: 10.1167/iovs.16-20579

16. Feucht N, Schnbach EM, Lanzl I, Kotliar K, Lohmann CP, Maier M. Changes in the foveal microstructure after intravitreal bevacizumab application in patients with retinal vascular disease. *Clin Ophthalmol*. 2013;7(1):173-178.

    doi: 10.2147/OPTH.S37544

17. Balaratnasingam C, Inoue M, Ahn S, Mccann J, Dhrami-Gavazi E, Yannuzzi LA. Visual acuity is correlated with the area of the foveal avascular zone in diabetic retinopathy and retinal vein occlusion. *Ophthalmology*. 2016;123(11):2352-2367.

    doi: 10.1016/j.ophtha.2016.07.008

18. Leszczynska A, Ramm L, Spoerl E, Pillunat LE, Naim T. The short-term effect of acupuncture on different ocular blood flow parameters in patients with primary open-angle glaucoma: A randomized, clinical study. *Clin Ophthalmol*. 2018;12(1):1285-1291.

    doi: 10.2147/OPTH.S170396

19. Giuffre C, Cicinelli MV, Marchese A, Coppola M, Parodi MB, Bandello F. Simultaneous intravitreal dexamethasone and aflibercept for refractory macular edema secondary to retinal vein occlusion. *Graefes Arch Clin Exp Opthalmol*. 2020;258(4):787-793.

    doi: 10.1007/s00417-019-04577-8

20. Naruse S, Mori K, Kurihara M, *et al*. Chorioretinal blood flow changes following acupuncture between thumb and forefinger. *JPN J Ophthalmol*. 2001;45(2):205.

    doi: 10.1016/S0021-5155(00)00371-3

21. Chu TC, Potter DE. Ocular hypotension induced by electroacupuncture. *J Ocul Pharmacol Ther*. 2002;18(4):293-305.

    doi: 10.1089/10807680260218461

22. Wang TH. *Clinical Efficacy of Acupuncture Combined with Laser in the Treatment of Retinal Vein Obstruction Macular Edema*. Jinan: Shandong University of Traditional Chinese Medicine; 2024.

    doi: 10.27282/d.cnki.gsdzu.2024.000442

23. Chen CL, Bojikian KD, Wen JC, *et al*. Peripapillary retinal nerve fiber layer vascular microcirculation in eyes with glaucoma and single-hemifield visual field loss. *JAMA Ophthalmol*. 2017;135(5):461-468.

    doi: 10.1001/jamaophthalmol.2017.0261

24. Wang AL, Li YJ, Hou XL, *et al*. Effects of acupuncture therapy on macular blood flow and structure in glaucoma.

CJTCMP. 2023;38(3):1374-1378.

25. Akagi T, Iida Y, Nakanishi H, *et al*. Microvascular density in glaucomatous eyes with hemifield visual field defects: An optical coherence tomography angiography study. *Am J Ophthalmol*. 2016;168:237-249.

    doi: 10.1016/j.ajo.2016.06.009

26. Seknazi D, Coscas F, Sellam A, *et al*. Optical coherence tomography angiography in retinal vein occlusion: Correlations between macular vascular density, visual acuity, and peripheral nonperfusion area on fluorescein angiography. *Retina*. 2017;38(8):1562-1570.

    doi: 10.1097/IAE.0000000000001737

27. Wemer JU, Bohm F, Lang GE, Dreyhaupt J, Lang GK, Enders C. Comparison of foveal avascular zone between optical coherence tomography angiography and fluorescein angiography in patients with retinal vein occlusion. *PLoS One*. 2019;14(6):e0217849.

    doi: 10.1371/journal.pone.0217849

28. Ouedemi M, Assi H, Nefaa F, *et al*. Anatomo-functional study in branch retinal vein occIusion using swept source optical coherence tomography angiography. *J Fr Ophtalmol*. 2019;42(3):255-261.

    doi: 10.1016/j.jfo.2018.09.010

29. Taku W, Tatsuhiko S, Chikako HU, *et al*. Retinal microvasculature and visual acuity in eyes with branch retinal vein occlusion: Imaging analysis by optical coherence tomography angiography. *Invest Ophthalmol Vis Sci*. 2017;58(4):2087-2094.

    doi: 10.1167/iovs.16-21208

30. Deng Y, Zhong QW, Zhang AQ, *et al*. Microvascular changes after conbercept therapy in central retinal vein occlusion analyzed by optical coherence tomography angiography. *Int J Ophthalmol*. 2019;12(5):802-808.

    doi: 10.18240/ijo.2019.05.16

31. Qin WX, Zhao YR, Xu JF, Wang PF, Yang T. Clinical observation of pressing while removing filiform needles to reduce adverse reactions. *Shanghai J Acu-Mox*. 2024;43(11):1269-1274.

    doi: 10.13460/j.issn.1005-0957.2024.11.1269

32. Yang CX, Wang YY, Ma Y. Causative analysis of a case with buccinator diastem hematocele caused by retrobulbar injection and her nursing care. *Chin Nurs Res*. 2007;21(13):1219.

    doi: 10.3969/j.issn.1009-6493.2007.13.041

33. Zhang J, Zhang R. Two cases of accidental bleeding induced by acupuncture near eyes. *Zhongguo Zhen Jiu*. 2014;34(2):186-188.

    doi: 10.13703/j.0255-2930.2014.02.024

34. Gross A, Cestari DM. Optic neuropathy following retrobulbar injection: A review. *Semin Ophthalmol*. 2014;29(5-6):434-439.

    doi: 10.3109/08820538.2014.959191

35. Kim CH, Kim US. Large exotropia after retrobulbar anesthesia. *Indian J Ophthalmol*. 2016;64(1):91-92.

    doi: 10.4103/0301-4738.178148

36. Dikci S, Yılmaz T, Gök ZE, Demirel S, Genc O. Choroidal neovascularization secondary to ocular penetration during retrobulbar anesthesia and its treatment. *Oman J Ophthalmol*. 2017;10(1):44-46.

    doi: 10.4103/0974-620X.200695

37. Mimouni M, Abualhasan H, Mtanes K, Mazzawi F, Barak Y. Patients' experience of anxiety and pain during retrobulbar injections prior to vitrectomy. *J Ophthalmol*. 2019;2019:8098765.

    doi: 10.1155/2019/8098765

ACCSCIENCE PUBLISHING

Journal of Clinical and Translational Research

ORIGINAL ARTICLE

Metabolic improvements associated with low-carbohydrate diet in overweight and obese adults: Contributions to public health nutrition

Laryssa Rosa de Sousa Franckilin[1], Ludmila Lizziane de Souza Lima[1,2], Flávio Eduardo Dias Araújo Freitas[1,3], Maria Vitoria Cota de Abreu[1], Carlos Eduardo de Freitas Jorge[4], Daniela Godoy Neri[5], Janaina Koenen[6], and Giselle Foureaux[1]*

[1]Department of Morphology, Translational Biology Laboratory, Institute of Biological Sciences, Federal University of Minas Gerais, Belo Horizonte, Minas Gerais, Brazil

[2]Department of Food Microbiology, Faculty of Pharmacy, Federal University of Minas Gerais, Belo Horizonte, Minas Gerais, Brazil

[3]Department of Health, Faculty of Biomedicine, College Anhanguera, Contagem, Minas Gerais, Brazil

[4]Department of Nutrition, Angiogold Institute of Education and Research, Belo Horizonte, Minas Gerais, Brazil

[5]Hospital of The Clinics, Faculty of Medicine, University of São Paulo (USP), São Paulo, Brazil

[6]The Clinic, Integrated Medicine, Belo Horizonte, Minas Gerais, Brazil

***Corresponding author:**
Giselle Foureaux
(gifoureaux@icb.ufmg.br)

Citation: de Sousa Franckilin LR, de Souza Lima LL, Freitas FEDA, *et al*. Metabolic improvements associated with low-carbohydrate diet in overweight and obese adults: Contributions to public health nutrition. *J Clin Transl Res*. 2026;12(1):72-87.
doi: 10.36922/JCTR025310050

Received: July 31, 2025

Revised: October 9, 2025

Accepted: December 22, 2025

Published online: February 6, 2026

Abstract

Background: Overweight (OW) and obesity (OB) are major public health challenges associated with metabolic disorders, chronic diseases, and rising healthcare costs. Low-carbohydrate diets (LCDs) have emerged as cost-effective strategies for prevention and treatment. **Objective:** The objective of the study is to evaluate the effects of an LCD (≤130 g/day) on anthropometric, metabolic, hepatic, and renal parameters in OW and obese adults over 12 months. **Methods:** This open-label, non-randomized, self-controlled clinical trial included 34 adults with body mass index (BMI) ≥ 25 kg/m^2 who received individualized nutritional counseling and followed an LCD for up to 12 months. Clinical and laboratory parameters were assessed at baseline and during follow-up (3–6 months and 7–12 months). Statistical analyses included generalized estimating equations and non-parametric tests with Bonferroni correction. **Results:** Participants achieved a mean weight loss of 10%, with reductions in BMI (−2.9 kg/m^2), waist circumference (−5.4 cm), and body fat percentage. Glycated hemoglobin decreased at 7–12 months (p<0.05), while insulin levels and insulin resistance declined at 3–6 months (p=0.0497 and p=0.037). Fasting glucose remained stable. Low-density lipoprotein cholesterol increased modestly at 7–12 months (p=0.035), whereas other lipid parameters showed no significant changes. Gamma-glutamyl transferase levels decreased (p=0.0341), with no adverse effects on renal or hepatic markers. **Conclusion:** An LCD was associated with improvements in glycemic control, body composition, insulin sensitivity, and liver enzymes without compromising renal function or lipid profiles, supporting its role in OB management and cardiometabolic risk reduction in primary care.

Keywords: Low-carbohydrate diet; Overweight; Obese; Metabolic health; Nutrition; Diet

1. Introduction

Obesity (OB) and overweight (OW) are global epidemics associated with adverse health outcomes and high healthcare costs.[1,2] According to the World Health Organization (WHO), more than 2.5 billion adults are OW, of whom 890 million are living with OB.[3] Approximately one in eight people globally has OB.[3] In the United States, the prevalence of OB is currently estimated at 41.9%,[4] and OB-related conditions have reached unprecedented levels. Nearly one in 10 Americans has type 2 diabetes (T2DM), and approximately 48.6% of adults live with some form of cardiovascular disease (CVD).[5] In Brazil, data from the Telephone-based Survey on Risk and Protective Factors for Chronic Diseases, coordinated by the Ministry of Health, revealed a striking 96% increase in OB prevalence over a 15-year period—from 11.8% in 2006 to 22.4% in 2021.[6]

This burden also extends to children and adolescents. In the Americas, the prevalence of OW and OB among this population is approximately 20–25%.[7] A survey by the Brazilian Institute of Geography and Statistics from 2008 to 2009 reported that the prevalence of OW and OB in the Brazilian population increased by about 50%.[8] In 2019, the Brazilian Ministry of Health reported that 55.4% of the population had excess weight and 20.3% were obese.[9] Globally, over 390 million children and adolescents aged 5–19 years were OW in 2022, including 160 million with OB, and in 2024, 35 million children under five were OW.[3] Moreover, the sustained prevalence of OB may reduce life expectancy in future generations.[10]

OB is a multifactorial condition influenced by biological, genetic, historical, economic, and sociocultural factors.[3] This epidemic represents one of the greatest public health challenges of the 21st century and is the fastest-growing nutritional problem globally.[11,12] It affects both developed and developing countries and contributes to the rise in non-communicable diseases (NCDs), increasing overall morbidity and mortality.[12,13] OW and OB are commonly classified using body mass index (BMI), which is applied to adults,[14] children and adolescents,[15] elderly individuals,[16] and pregnant women.[17] A high BMI is a well-established risk factor for NCDs, mental health disorders such as depression, and reduced quality of life. The global rise in OB is multifactorial, driven by a complex interplay of sociodemographic, economic, environmental, physiological, and psychosocial determinants. In Latin America, particularly in Brazil, these factors are compounded by rapid urbanization, increasing sedentary lifestyles, and shifts in dietary patterns toward greater consumption of ultra-processed foods. Such dynamics have significantly contributed to the acceleration of OB prevalence in recent decades.[1]

The major consequences of OB include a heightened risk of developing NCDs, many of which are directly associated with poor dietary habits. In Brazil, NCDs linked to inadequate nutrition have a substantial impact on mortality and morbidity, accounting for approximately 71% of all deaths. Among these, the four primary categories of nutrition-related NCDs were responsible for 55% of total deaths.[18] NCDs also remain the leading cause of premature mortality (ages 30–69), accounting for 37% of deaths in the 30–49 age group and 65% in individuals aged 50–69 years.[18] The main NCDs associated with OB and poor metabolic health include T2DM, non-alcoholic fatty liver disease (NAFLD), gout, obstructive sleep apnea, CVDs, musculoskeletal and orthopedic disorders, Alzheimer's disease, and various types of cancer.[19,20]

Between 2011 and 2022, Brazil implemented the National Plan for Tackling Non-Communicable Diseases, which established 12 strategic goals aimed at promoting the development and implementation of effective, integrated, and evidence-based public policies for the prevention and control of NCDs and their main risk factors, including OB. Building on this initiative, the current Plan for the Prevention and Control of Chronic Non-Communicable Diseases in Brazil (2021–2030) outlines 226 strategic actions to be implemented at the federal, state, and municipal levels. These actions include reducing alcohol and tobacco consumption, promoting healthy eating habits, and encouraging physical activity.[21] Given the substantial personal, social, and economic burden of NCDs, especially in low- and middle-income countries, prioritizing preventive measures is imperative. In Brazil, a country marked by pronounced regional and territorial inequalities, strengthening preventive strategies is not only a matter of public health efficiency but also a critical step toward reducing inequities in access to health services and opportunities for well-being. Investments in early intervention and health promotion are therefore essential to mitigate the growing impact of chronic diseases and to build more resilient and equitable health systems.

OB is characterized by chronic, low-grade inflammation of white adipose tissue (WAT), which plays a central role in the development of systemic metabolic dysfunctions (Figure 1). Excessive expansion of WAT leads to structural and functional alterations that compromise local oxygen supply. As adipocytes undergo hypertrophy, the decreased distance between cells and capillaries results in tissue hypoxia. This hypoxic microenvironment activates hypoxia-inducible factor 1-alpha, which promotes fibrotic remodeling and induces the expression of pro-inflammatory genes.[22,23] These processes facilitate the infiltration of immune cells, particularly macrophages,

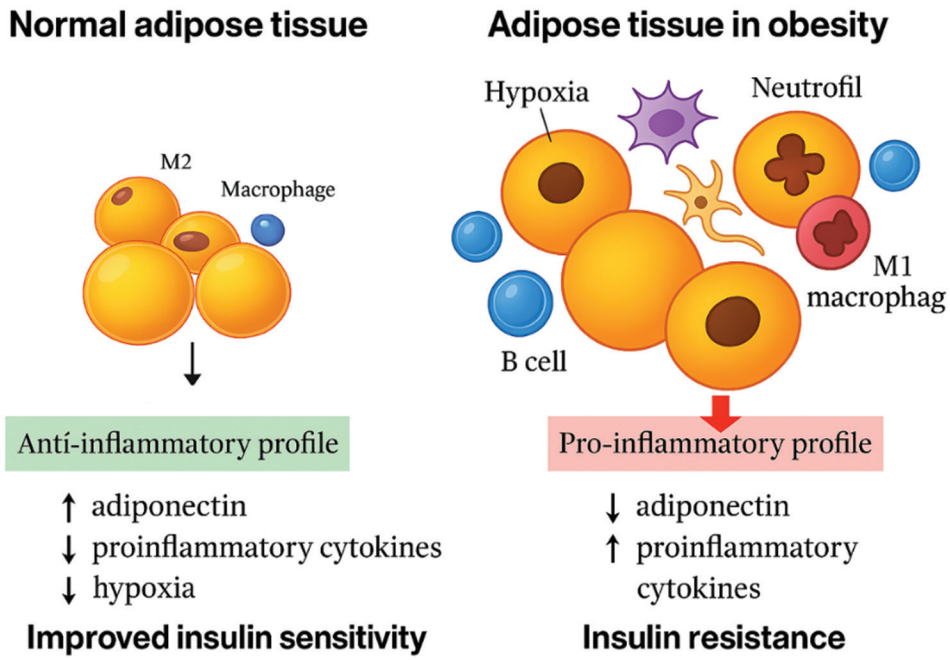

Figure 1. Comparison of normal and obese adipose tissue and their effects on insulin sensitivity. Left: Normal adipose tissue exhibits an anti-inflammatory profile characterized by the predominance of M2 macrophages, higher adiponectin levels, lower leptin levels, and minimal hypoxia, contributing to improved insulin sensitivity. Right: Obese adipose tissue is characterized by hypertrophied and necrotic adipocytes, infiltration of neutrophils and B cells, and a predominance of pro-inflammatory M1 macrophages. These alterations are associated with reduced adiponectin levels, increased hypoxia, chronic inflammation, and the development of systemic insulin resistance.

which shift from an anti-inflammatory M2 phenotype to a pro-inflammatory M1 profile, contributing to the sustained production of cytokines such as tumor necrosis factor-α, interleukin-6, and monocyte chemoattractant protein-1. This inflammatory response is further amplified by elevated levels of triglycerides (TG) and free fatty acids, which exacerbate cytokine expression and insulin resistance.[24-26] A hallmark of dysfunctional adipose tissue in OB is the increased rate of adipocyte death through multiple mechanisms, including apoptosis, necrosis, pyroptosis, and ferroptosis.[27] Dying adipocytes release damage-associated molecular patterns and lipids, which further stimulate immune cell recruitment. Macrophages surround these dead cells, forming crown-like structures, where they facilitate lipid clearance while amplifying local inflammation through the release of pro-inflammatory mediators. The resulting activation of innate immune pathways and sustained shift toward a pro-inflammatory cellular environment establishes a self-perpetuating inflammatory loop. This loop not only impairs adipose tissue homeostasis but also contributes to systemic insulin resistance, T2DM, and hepatic steatosis.[27]

Nutritional therapy remains the cornerstone of managing OW and OB, with the primary goals of preventing associated complications such as liver damage, chronic kidney disease, and cardiovascular events. Numerous dietary strategies have been explored, with particular focus on carbohydrate and fat restriction—approaches that have gained popularity over the past few decades for both disease management and weight control.[28,29] Low-carbohydrate diets (LCDs) have been studied since at least 1872, when limiting foods rich in starch and sugar was first recommended for individuals with OB.[30] In 1943, Cutting[31] demonstrated the effectiveness of restricting bread, potatoes, and sweets in promoting weight loss. The Atkins diet, which emphasizes carbohydrate restriction alongside increased protein and fat intake to stimulate fat mobilization, has been in use for more than 45 years.[32,33] Although dietary recommendations vary, multiple studies have consistently demonstrated the effectiveness of LCDs in promoting weight loss and improving glycemic control.[34-36] Recent consensus among nutrition and health experts highlights the growing body of evidence supporting LCD patterns as effective strategies for improving key risk factors associated with insulin resistance and CVD. Given the high prevalence of nutrition-related chronic conditions, particularly among adults, experts have proposed the inclusion of lower-carbohydrate approaches into official dietary recommendations as a means of broadening preventive strategies and promoting health equity at the population level.[37]

Currently, there is no universally accepted definition of a "low-carbohydrate" diet within the scientific community. While the Acceptable Macronutrient Distribution Range recommends that carbohydrates make up 45–65% of total daily energy intake,[38] and the Recommended Dietary Allowance establishes a reference intake of 130 g/day for all age and sex groups. This recommendation is primarily based on the estimated average glucose requirement of the brain. However, scientific evidence shows that the brain is metabolically adaptable and capable of utilizing alternative energy substrates, such as ketone bodies, and that glucose can be synthesized endogenously through gluconeogenesis.[34-36] These findings challenge the notion that dietary carbohydrate is essential in fixed amounts, and the absence of a standardized definition continues to hinder the development of consistent dietary recommendations for low-carbohydrate dietary patterns.

LCDs typically involve reducing carbohydrate intake and increasing protein and fat intake in appropriate proportions.[39,40] Such diet patterns have been associated with reductions in TG, abdominal fat, glycated hemoglobin (HbA1c), and circulating insulin levels, as well as increases in high-density lipoprotein (HDL) cholesterol levels.[41,42] Alterations in macronutrient distribution lead to lower serum insulin and higher serum glucagon levels.[43,44] This promotes gluconeogenesis[44] and mobilization of fatty acids from adipose tissue, with potential downstream effects on hepatic metabolism.[44] Overall, these metabolic adaptations favor reduced insulin secretion, enhanced fat oxidation, and the use of fat as a primary energy source while preserving lean body mass.[45] Although protein can also raise insulin levels, it concurrently increases glucagon levels, thereby supporting lipolysis.[46] This study aims to generate evidence on the practical implementation of LCDs in primary care settings, focusing on their medium-term effects (12 months) on metabolic health in the absence of pharmacological interference. Specifically, we evaluated the effects of an LCD (≤130 g/day) on anthropometric, metabolic, hepatic, and renal parameters in OW and OB adults over a 12-month intervention period.

2. Materials and methods

2.1. Study design and subjects

This study was designed as an open-label, non-randomized, self-controlled clinical trial, conducted according to a prespecified protocol between March 2019 and January 2021. Participants were recruited from a single integrated healthcare center located in Belo Horizonte, Brazil.

Inclusion criteria included men and women aged 18 years or older with a BMI classified as OW (25.0–29.9 kg/m^2) or obese (≥30.0 kg/m^2). To be eligible, participants were required to attend at least two of the three clinical visits and corresponding laboratory assessments scheduled throughout the study period.

Three evaluation time points were defined for the assessment of clinical and laboratory parameters: Time 0 (baseline), Time 1 (3–6 months), and Time 2 (7–12 months). The first re-evaluation involved a comparison of data between baseline and time 1. The second re-evaluation included comparisons across all three time points (baseline, time 1, and time 2).

Exclusion criteria included individuals under 18 years of age, BMI < 25 kg/m^2, diagnosed with thalassemia or type 1 diabetes mellitus, current participation in other nutritional intervention programs, or prior adherence to a LCD (<130 g/day) before enrollment. In addition, participants who reported non-adherence to the dietary recommendations or who failed to complete the scheduled anthropometric and biochemical evaluations were also excluded. All physical examinations were conducted at the clinic located in Belo Horizonte. Blood samples were analyzed by certified laboratories within the same city, each operating under standardized quality protocols established by regulatory authorities.

All participants provided written informed consent before participation. The study was approved by the local research ethics committee and conducted in accordance with the Brazilian National Health Council guidelines under the CEP/CONEP system (approval number: 4.961.640; CAAE: 49593220.4.0000.5149). This study was registered at the Brazilian Registry of Clinical Trials (ReBEC) (registration no.: RBR-107jk4tn, UTN no.: U1111-1270-4313, registry link: https://ensaiosclinicos.gov.br/rg/RBR-107jk4tn) before participant enrollment.

2.2. Dietary interventions

A preliminary set of dietary education materials was collaboratively developed by the research physician and the registered dietitian involved in the study. These materials were designed to support participants in adopting an LCD pattern and included a structured meal planner, practical dietary recommendations, sample menus, nutritional information on commonly consumed foods, and specific guidance on foods to limit or avoid. During the baseline visit, each participant received individualized dietary counseling tailored to their specific needs, preferences, and metabolic profile. This counseling session served to clarify the objectives of the dietary intervention and to ensure understanding and adherence.

Given that the three macronutrients—carbohydrates (4 kcal/g), fat (9 kcal/g), and protein (4 kcal/g)—contribute differently to total energy intake, LCDs have been defined

either by the percentage of total daily energy derived from carbohydrates or by absolute daily carbohydrate intake. Accordingly, they are commonly categorized as follows: Very LCDs (<10% of daily energy from carbohydrates or 20–50 g/day); LCDs (<26% of daily energy from carbohydrates or <130 g/day); moderate-carbohydrate diets (26–44% of daily energy from carbohydrates); and high-carbohydrate diets (≥45% of daily energy from carbohydrates) (Figure 2).

In this study, dietary guidance emphasized the inclusion of healthy, minimally processed fat sources as part of the low-carbohydrate approach. Participants were encouraged to consume olive oil, avocado, nuts, seeds, whole-fat dairy products such as yogurt, and naturally fatty fish as primary components of their meals, while limiting or avoiding industrial seed oils and ultra-processed fats. This strategy prioritized fat quality and natural origin of fats rather than restricting specific fat subtypes, with the aim of promoting satiety, metabolic flexibility, and long-term adherence to the dietary plan. Participants were instructed to maintain this dietary pattern throughout the study period and to report any difficulties or deviations during follow-up visits.

2.3. Biochemical parameters and anthropometric measurements

Biochemical and anthropometric data were collected at all three evaluation points: baseline (pre-intervention), Time 1 (3–6 months), and Time 2 (7–12 months). Biochemical analyses included fasting glucose, HbA1c, fasting insulin, total cholesterol (TC), low-density lipoprotein cholesterol (LDL cholesterol), HDL cholesterol, TG, creatinine, urea, gamma-glutamyl transferase (GGT), aspartate aminotransferase (AST), and alanine aminotransferase (ALT). Blood samples were obtained after an overnight fast and analyzed in certified laboratories using standard methods. Insulin resistance was estimated using the homeostatic model assessment of insulin resistance (HOMA-IR), calculated as follows:

$$\text{HOMA-IR} = (\text{fasting insulin } [\mu U/mL] \times \text{fasting glucose } [mg/dL])/405 \quad (1)$$

Anthropometric assessments included body weight, height, and waist circumference. BMI was calculated as weight in kilograms divided by height in meters squared (kg/m^2). All measurements were conducted by trained professionals using standardized procedures to ensure consistency and accuracy throughout the study period. Body fat percentage was assessed using bioelectrical impedance analysis with an InBody 270 body composition analyzer (InBody Asia, South Korea). Measurements were performed with participants standing upright and barefoot, according to the manufacturer's instructions. The resulting data were used to estimate body composition.

2.4. Risk evaluations

Risk assessments were performed to estimate potential comorbidities associated with OW and OB, with a particular focus on renal and CVD. Renal function was evaluated by estimating the glomerular filtration rate (eGFR), calculated using the Chronic Kidney Disease Epidemiology Collaboration formula, as implemented in

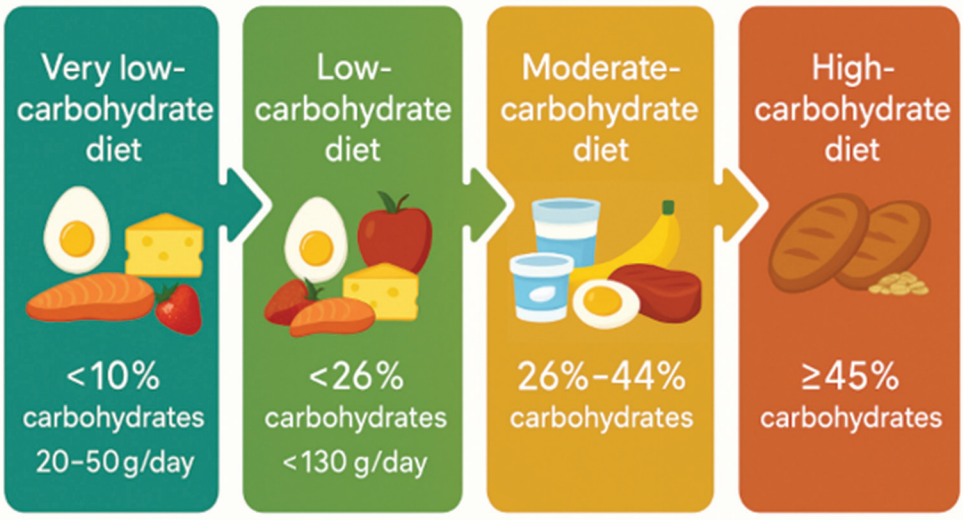

Figure 2. Classification of low-carbohydrate diets. A very low-carbohydrate diet provides <10% of daily energy or 20–50 g/day; a low-carbohydrate diet provides <26% of daily energy or <130 g/day; a moderate-carbohydrate diet provides 26–44% of daily energy; a high-carbohydrate diet provides ≥45% of daily energy, illustrated by the presence of large bread portions and grains. The progression visually demonstrates the increase in carbohydrate content and associated food choices across diet types.

the National Kidney Disease Education Program calculator (nkdep.nih.gov).

Cardiovascular risk was assessed using lipid profile-derived ratios, including the TC to HDL cholesterol ratio (TC/HDL) and the TG to HDL cholesterol ratio (TG/HDL), which serve as surrogate markers of atherogenic risk. In addition, the risk of atherosclerotic CVD (ASCVD) was estimated using the ASCVD Risk Estimator Plus, developed by the American College of Cardiology (available at www.acc.org). For participants younger than 40 years, the tool provided an estimate of lifetime ASCVD risk, while for those aged 40 years or older, the estimate reflected the 10-year ASCVD risk. Together, these tools allowed for a comprehensive evaluation of cardiometabolic health and long-term disease risk within the study population.

2.5. Statistical analysis

Data were analyzed using Python version 3.11 with the SciPy and Matplotlib libraries. The normality of continuous variables was assessed using the Shapiro–Wilk test. As most variables did not follow a normal distribution, non-parametric tests were applied. Comparisons across the three time points—Time 0 (baseline), Time 1 (3–6 months), and Time 2 (7–12 months)—were performed using the Friedman test for repeated measures. Although the timing of Time 1 assessments varied slightly among participants, with most evaluations occurring at months 5 or 6 and a small number at month 3, this variability was addressed using statistical methods robust to within-subject timing differences. When overall statistical significance was observed ($p<0.05$), *post hoc* pairwise comparisons were conducted using the Wilcoxon signed-rank test with Bonferroni correction. Generalized estimating equations were also used to support longitudinal analyses. Results are presented as mean ± standard deviation, and statistical significance was defined as $p<0.05$. Graphical representations were generated as box plots displaying individual data points, mean lines, and significance bars marked with asterisks, where applicable.

3. Results

The baseline characteristics of the enrolled participants are presented in Table 1. 203 individuals were excluded based on the predefined inclusion and exclusion criteria, and a total of 34 participants (10 men and 24 women), with a mean age of 44.8 ± 10.5 years, were included in the study. By the second follow-up, 15 participants were unable to complete the protocol within the defined schedule. Endocrinology clinic follow-up visits occurred, on average, at approximately 5 and 12 months after baseline.

Data are presented as mean ± standard deviation and median. A total of 34 participants (10 men and 24 women) were included after applying the inclusion and exclusion criteria. The mean age of the cohort was 44.8 ± 10.5 years. Fifteen participants did not complete the second follow-up within the defined study period.

Table 1. Baseline biochemical and anthropometric characteristics of study participants

Biochemical and anthropometric characteristics	Results	
	$\bar{x}$ ±SD	Median
Fasting glucose (mg/dL)	88.3±8.7	88.7
HbA1c (%)	5.3±0.3	5.3
Serum insulin (μU/mL)	9.9±4.6	8.8
HOMA-IR	2.1±0.9	2.1
TC (mg/dL)	215.0±53.0	221.0
LDL (mg/dL)	133.7±33.8	134.0
HDL (mg/dL)	58.8±17.2	54.0
TG (mg/dL)	106.9±73.5	82.0
TC/HDL	3.8±0.9	3.8
TG/HDL	2.0±1.4	1.6
Creatinine (mg/dL)	0.8±0.1	0.8
Urea (mg/dL)	34.6±8.2	34.5
GGT (U/L)	30.8±30.7	16.5
AST (U/L)	23.5±9.7	20.0
ALT (U/L)	25.2±12.9	21.5
BMI (kg/m^2)	30.6±4.6	28.8
Weight (kg)	84.9±15.8	81.1
WC (cm)	98.2±13.2	94.5

Abbreviations: ALT: Alanine aminotransferase; AST: Aspartate aminotransferase; BMI: Body mass index; GGT: Gamma-glutamyl transferase; HbA1c: Glycated hemoglobin; HDL: High-density lipoprotein; HOMA-IR: Homeostatic model assessment of insulin resistance; LDL: Low-density lipoprotein; TC: Total cholesterol; TG: Triglycerides; WC: Waist circumference; $\bar{x}$±SD: Mean±standard deviation.

Throughout the 12-month follow-up period, a consistent and statistically significant reduction in body weight (Figure 3A) was observed across all time points. Median body weight decreased progressively from baseline to Time 1 (3–6 months), and further to Time 2 (7–12 months), with statistically significant differences between each consecutive time point ($p<0.05$) for all comparisons. Similarly, body fat percentage also showed a sustained decline over time, with significant reductions from baseline to both Time 1 and Time 2. Notably, a statistically significant difference was also observed between Time 1 and Time 2 ($p=0.0421$), indicating continued improvement beyond the initial 6 months. BMI decreased by an average of 2.9 points, corresponding to an average weight loss of 8.24 kg (Figure 3B). By the end of the

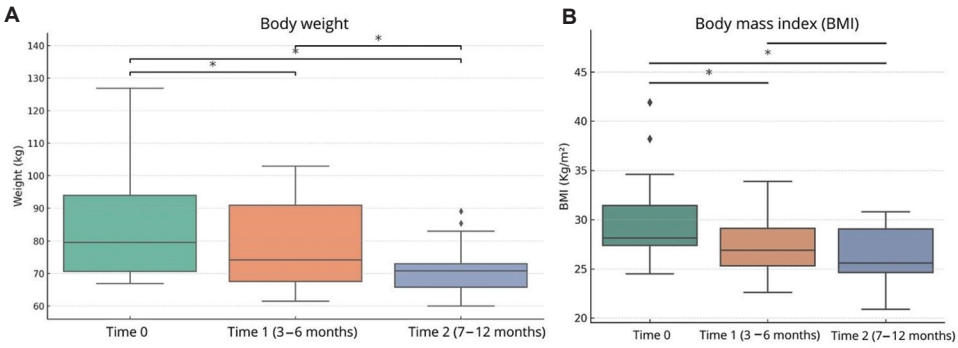

Figure 3. Anthropometric outcomes at three time points: Time 0 (baseline), Time 1 (3–6 months), and Time 2 (7–12 months). (A) Body weight: Significant reduction was observed between Time 0 and Time 1 (p=0.0004), Time 0 and Time 2 (p<0.0001), and Time 1 and Time 2 (p=0.0022). (B) Body mass index: Significant reduction was observed between Time 0 and Time 1 (p=0.0156), Time 0 and Time 2 (p=0.0022), and Time 1 and Time 2 (p=0.0421).
Notes: Statistical analysis was performed using the Friedman test followed by pairwise comparisons with Bonferroni correction. ♦ indicates the outliers. * denotes statistically significant at p<0.05.

study, participants achieved an average weight loss of 10% compared with baseline. At baseline, 29.2% of participants were classified as OB and 70.8% as OW. After 12 months, only 4.2% remained OB, 58.3% were OW, and 37.5% had reached a normal (eutrophic) weight range.

Fasting glucose levels remained relatively stable throughout the study period, with no statistically significant differences among the three time points (p=0.139) (Figure 4A). In contrast, HbA1c levels showed a statistically significant reduction between Time 0 and Time 2 (p=0.042), indicating improved long-term glycemic control (Figure 4B). Serum insulin levels also decreased significantly between Time 0 and Time 2 (p=0.0497), suggesting enhanced insulin sensitivity (Figure 4C). Notably, HOMA-IR, a surrogate marker for insulin resistance, exhibited a significant decline as early as between Time 0 and Time 1 (p=0.037), with a trend toward further improvement by time 2 (p=0.053) (Figure 4D). Collectively, these findings suggest that the intervention exerted a favorable effect on metabolic markers related to glycemic regulation and insulin resistance.

The lipid profile analysis is summarized in Figure 5. No statistically significant changes were observed in TC, HDL cholesterol, or TG levels throughout the study period (Figure 5A, B, and D), suggesting that the intervention did not adversely affect these major lipid parameters. However, a modest but statistically significant increase in LDL cholesterol level was detected between Time 0 and Time 2 (7–12 months; p=0.035), as shown in Figure 5C. Importantly, lipid ratios, including TC/HDL cholesterol and TG/HDL cholesterol, which are often considered stronger predictors of cardiovascular risk than individual lipid parameters, did not differ significantly across the time points (Figure 5E and F). Overall, these findings indicate a relatively stable lipid profile and suggest that, despite the observed increase in LDL cholesterol, the dietary or therapeutic intervention did not negatively impact cardiovascular lipid risk markers.

Renal and hepatic function markers are presented in Figure 6. No statistically significant changes were observed in serum creatinine (p=0.626; Figure 6A) or urea levels (p=0.517; Figure 6B) across the three time points, as determined by the Friedman test followed by Bonferroni-corrected pairwise comparisons. These findings suggest that the dietary intervention did not adversely affect renal function. Regarding hepatic biomarkers, GGT levels showed a statistically significant reduction from baseline to 12 months (p=0.0341; Figure 6C), which may indicate a reduction in hepatic metabolic stress. In contrast, no significant changes were observed in AST or ALT levels (p=0.958 and p=0.9854, respectively; Figure 6D and E), suggesting preservation of hepatocellular integrity throughout the intervention period.

Finally, at Time 1 (3–6 months), the proportion of patients using antihypertensive medications decreased from 20.6% to 11.8%. This reduction suggests a potential improvement in blood pressure control, possibly related to lifestyle modifications or metabolic benefits associated with the intervention. Although blood pressure measurements were not the primary endpoint of the study, the reduced reliance on pharmacological treatment may reflect a clinically meaningful response. This observation is particularly relevant in the context of OB-related hypertension, which is commonly associated with insulin resistance, chronic low-grade inflammation, and endothelial dysfunction. Improvements in dietary habits, weight loss, and reductions in visceral adiposity may have contributed to enhancing vascular function and blood pressure regulation, thereby reducing the need for antihypertensive agents in a subset of participants.

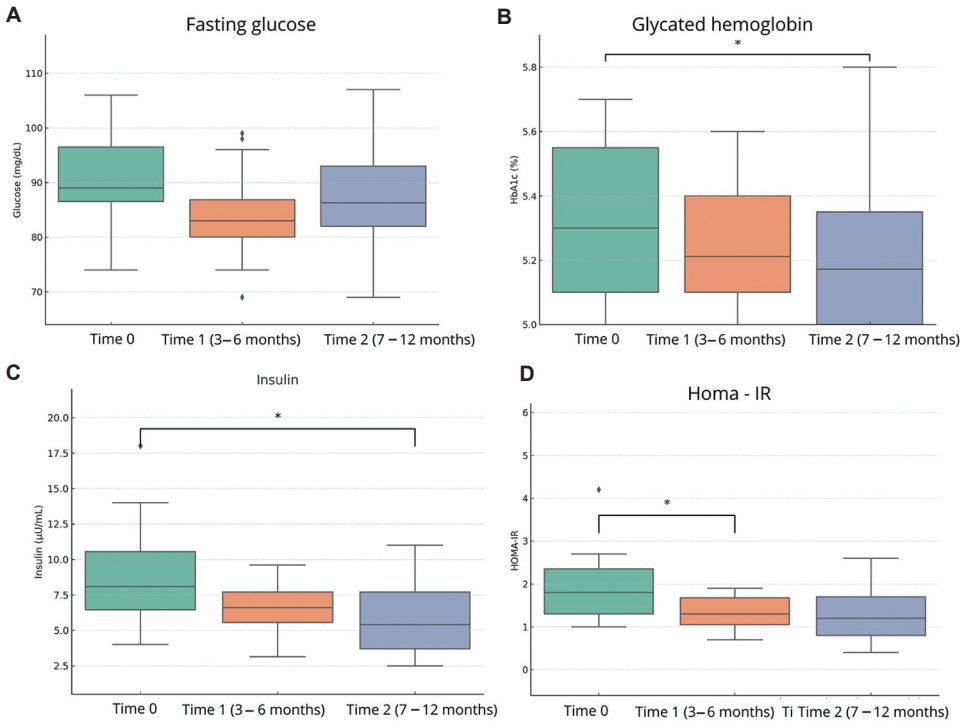

Figure 4. Variations in fasting glucose, glycated hemoglobin (HbA1c), insulin, and homeostatic model assessment of insulin resistance (HOMA-IR) levels in obese patients. Analyses were conducted on fasting samples obtained from participants at three time points: Time 0 (pre-intervention), Time 1 (3–6 months after intervention), and Time 2 (7–12 months after intervention). (A) Fasting glucose: Fasting glucose levels remained stable throughout the study period. (B) HbA1c: HbA1c levels showed a statistically significant reduction between Time 0 and Time 2 (p<0.05; Friedman test followed by pairwise comparisons with Bonferroni correction). (C) Insulin: A significant reduction in insulin levels was observed between Time 0 and Time 2 (p=0.0497; Wilcoxon test with Bonferroni correction). (D) HOMA-IR: A statistically significant reduction in HOMA-IR was observed between Time 0 and Time 1 (p=0.037; Wilcoxon test with Bonferroni correction). No other comparisons reached statistical significance, although a trend toward reduction was observed between Time 0 and Time 2 (p=0.053).
Notes: ♦ denotes the outliers. * denotes statistically significant at p<0.05.

Collectively, these findings reinforce the potential role of non-pharmacological strategies in the management of cardiometabolic risk factors. CVD risk was assessed using the TC/HDL cholesterol and TG/HDL cholesterol ratios, with no significant differences observed over the study period. ASCVD risk was also estimated based on age: A 10-year CVD risk for individuals over 40 years old and a lifetime CVD risk for those under 40 years. No statistically significant changes in ASCVD risk were detected in either group over the study period.

4. Discussion

Given its increasing prevalence and its strong association with elevated morbidity and mortality, OB represents one of the most critical public health challenges of the 21st century. Beyond its detrimental effect on individual health and well-being, OB contributes to social vulnerability and imposes a substantial burden on healthcare systems. These burdens encompass not only direct medical and non-medical expenses but also indirect costs, such as loss of productivity, and intangible consequences, including diminished quality of life.[47] In Brazil, direct costs attributable to OB within the Unified Health System (SUS) were estimated at approximately BRL 378 million (USD 75 million) in 2018. When OB is considered as a contributing factor to other chronic conditions, such as hypertension and diabetes mellitus, the economic impact becomes even more significant, reaching an estimated BRL 1.39 billion (USD 278 million).[48] This scenario highlights the urgent need to strengthen cross-sectoral coordination and promote integrated policy planning. Alignment between economic strategies and health initiatives is essential to build a coherent budgetary framework that supports food and nutrition security and enables effective nationwide prevention and control of OB.

Dietary interventions have long been recognized as effective tools for the management of chronic diseases, with historical records of their application dating back nearly 200 years. LCDs, including ketogenic approaches, were initially established for the treatment of epilepsy

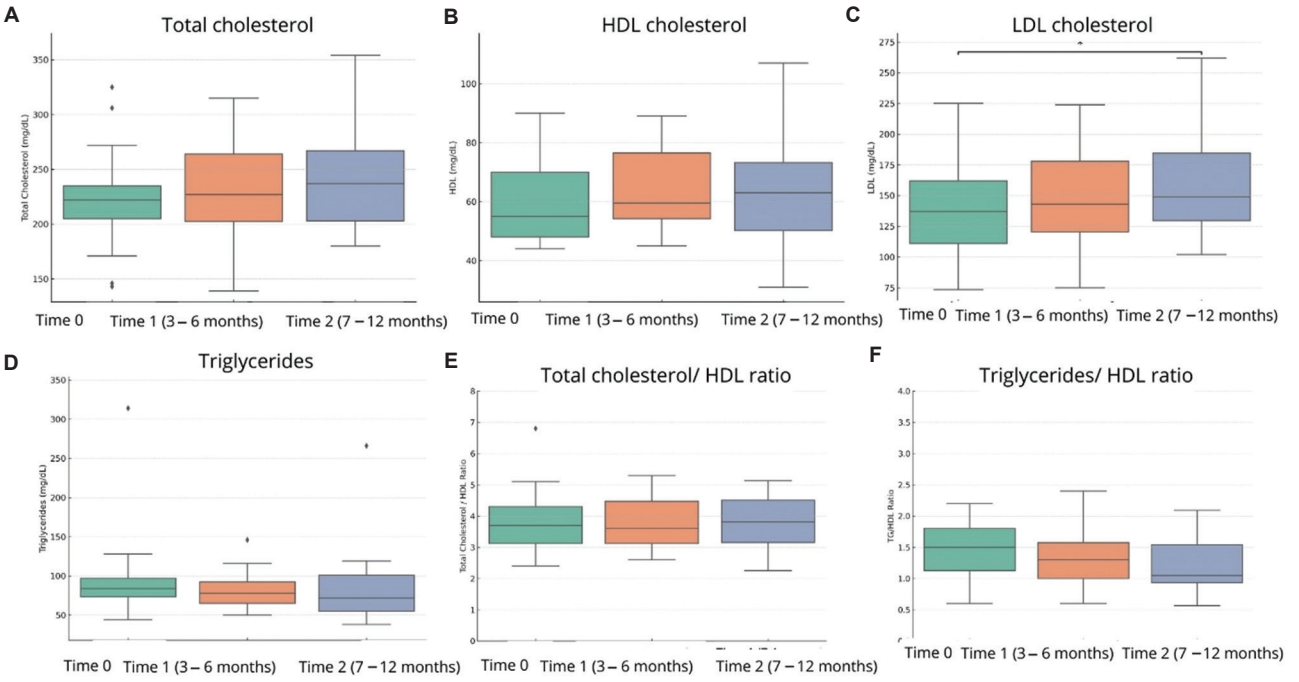

Figure 5. Lipid profile of obese patients evaluated at three different time points: Time 0 (pre-intervention), Time 1 (between 3 and 6 months), and Time 2 (between 7 and 12 months). (A) Total cholesterol: No statistically significant differences were observed between time points (p=0.141; Friedman test). (B) High-density lipoprotein (HDL) cholesterol: No statistically significant differences were observed between time points, according to the Friedman test (p=0.676) and pairwise comparisons after Bonferroni correction (p>0.05 for all pairs). (C) Low-density lipoprotein (LDL) cholesterol: A statistically significant increase in LDL levels was observed between Time 0 and Time 2 (p=0.035; Wilcoxon test with Bonferroni correction). (D) Triglycerides: No statistically significant differences were observed across time points, according to the Friedman test (p=0.692) and pairwise comparisons after Bonferroni correction (p>0.05 for all pairs). (E) Total cholesterol/HDL cholesterol ratio: No statistically significant differences were observed across time points, according to the Friedman test (p=0.759) and pairwise comparisons after Bonferroni correction (p>0.05 for all pairs). (F) Triglycerides/HDL cholesterol ratio: No statistically significant differences were observed across time points, according to the Friedman test (p=0.200) and pairwise comparisons after Bonferroni correction (p>0.05 for all pairs).
Notes: ♦ denotes the outliers. * denotes statistically significant at p<0.05.

but have since been extensively investigated in a wide range of metabolic and neurological conditions such as glucose transporter type-1 deficiency syndrome, pyruvate dehydrogenase deficiency, migraine, Alzheimer's disease, multiple myeloma, amyotrophic lateral sclerosis, NAFLD, non-alcoholic steatohepatitis, Parkinson's disease, and certain cancers.[49] More recently, LCDs have gained prominence as a promising public health strategy to address the growing burden of OB and its associated cardiometabolic consequences. Diets providing <130 g of carbohydrates per day have demonstrated superior outcomes in average weight loss and improvements in selected cardiovascular risk markers compared with traditional low-fat diets.[50,51] A systematic review and meta-analysis of 38 clinical trials involving 6,499 adults showed that LCDs were more effective in promoting weight loss and enhancing HDL cholesterol and triglyceride levels over 6–12 months.[50] In addition, a meta-analysis of long-term randomized controlled trials (lasting from 8 weeks to 24 months) in individuals with OW and OB found that LCDs led to significantly greater reductions in body weight and estimated ASCVD risk, based on pooled cohort equations developed by the National Heart, Lung, and Blood Institute.[51]

In the present cohort of OW and OB adults, the LCD resulted in significantly improvements in anthropometric and metabolic indicators, including insulin sensitivity, HOMA-IR, HbA1c, and pancreatic insulin regulation.[42,52] Reduced circulating insulin level facilitates lipolysis, fat oxidation, and glycogenolysis in muscle and liver, key metabolic mechanisms underlying effective OB intervention. By restricting carbohydrate intake and leveraging fat and protein for energy, LCDs may also support beta (β)-cell preservation and lean body mass retention.[53] In addition, these diets promote greater satiety and reduced caloric intake, bolstering weight loss.[42]

Avoidance of hyperglycemia is crucial to prevent the activation of reactive oxygen species (ROS), T cells, inflammatory cytokines, and lipid peroxidation pathways.[53] OB is associated with chronic low-grade inflammation,

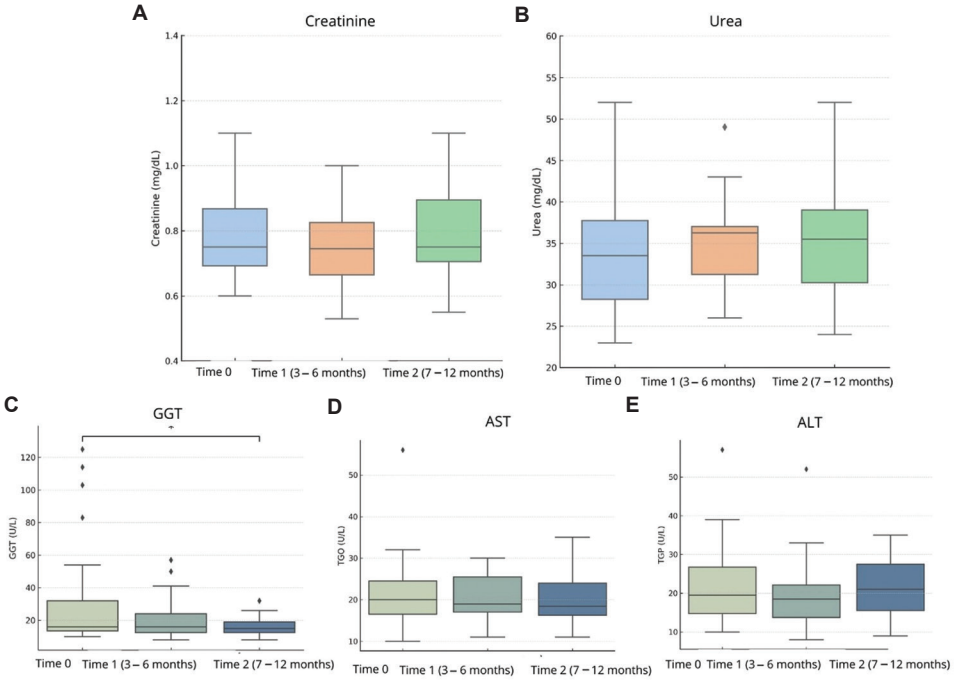

Figure 6. Evaluation of renal (panels A and B) and hepatic function (panels C-E) in obese patients at three time points: Time 0 (pre-intervention), Time 1 (3–6 months after intervention), and Time 2 (7–12 months after intervention). (A) Creatinine: Serum creatinine levels did not differ significantly across time points (Friedman test, p=0.626), and all pairwise comparisons were non-significant after Bonferroni correction (p>0.05). (B) Urea: No statistically significant differences were observed across the three time points (p=0.517; Friedman test), confirmed by pairwise comparisons with Bonferroni correction (p>0.05 for all pairs). (C) Gamma-glutamyl transferase (GGT): A statistically significant reduction was observed between Time 0 and Time 2 (p=0.0341; Wilcoxon test with Bonferroni correction). (D) Aspartate aminotransferase (AST): AST levels remained stable over time, with no statistically significant changes (global p=0.958; Friedman test). (E) Alanine aminotransferase (ALT): No statistically significant variations were observed in ALT levels across time points (global p=0.9854; Friedman test).
Notes: ♦ indicates the outliers. * denotes statistically significant at p<0.05.

which, when coupled with hyperglycemia, may induce oxidative stress, leading to vascular damage.[54] The significant reduction in anthropometric measures observed in the present study demonstrates the effectiveness of LCDs in achieving weight loss, a cornerstone of OB management. Weight loss is fundamental to the prevention of severe complications.[55,56] A 10% decrease in body weight has been linked to an approximate 20% reduction in CVD risk.[57]

In patients with OW and OB, weight loss is an effective strategy for reducing the risk of T2DM. A study by Hamman *et al.*[58] found a 16% reduction in diabetes risk per kilogram of weight lost, suggesting that a 5–7% reduction in body weight could translate into a diabetes risk reduction exceeding 90%. Beyond BMI reduction, additional anthropometric measures should be considered. Ross *et al.*[59] highlighted waist circumference as a key clinical sign associated with increased cardiometabolic risks and mortality with the risk of death increasing by 13–17% for every 5 cm increase in waist circumference. In addition, data from the Framingham Study showed that weight loss of 6.8 kg or more was associated with a 21–29% reduction in the long-term hypertension risk.[55]

The assumption that high-fat diets negatively impact cardiovascular health is largely based on the notion of a linear association between fat intake and increased cardiovascular events. However, a large-scale study by Dehghan *et al.*[60] found a significant association between high carbohydrate consumption and increased mortality risk, while no significant association was observed between total fat intake and adverse cardiovascular outcomes. In fact, isocaloric substitution of carbohydrates with fats was associated with an 11% reduction in mortality risk. Rather than focusing solely on total LDL cholesterol, emerging evidence emphasizes the importance of assessing the presence of small dense LDL particles (sdLDL), which are considered the most atherogenic subclass of LDL and are associated with phenotype B. This lipid profile is typically linked to elevated TG, reduced HDL cholesterol, metabolic disorders, OB, T2DM, and increased coronary risk.[60,61] Lipid ratios such as TC/HDL and TG/HDL are increasingly recognized as robust predictors of CVD, with values below 4 mg/dL generally considered desirable due to their inverse association with sdLDL levels.[62,63]

One randomized, parallel-group trial that compared a very-LCD (<40 g/d) with a low-fat diet (<30% fat;

<7% saturated fat) reported significant reductions in the estimated 10-year Framingham risk score in the very-low-carbohydrate group at both 6 and 12 months, whereas no significant changes were observed in the low-fat group.[64] This risk score integrates multiple cardiovascular risk factors, such as TC and HDL cholesterol and systolic blood pressure, thereby providing a more comprehensive assessment of coronary heart disease risk than reliance on a single biomarker such as LDL cholesterol, to determine the risk. The results of these studies indicate that lower-carbohydrate dietary patterns result in significant reductions in weight and improvements in risk markers for CVD. In the present study, both the TC/HDL and TG/HDL ratios, commonly regarded as more reliable predictors of cardiovascular risk than isolated lipid values, remained stable over time. These findings suggest that, despite the observed increase in LDL levels, the dietary intervention did not adversely affect overall lipid-related cardiovascular risk markers. TG levels reflect both hepatic production and intestinal absorption, although current laboratory methods cannot distinguish between these sources. Evidence suggests that TG can accumulate in the arterial wall, and lower levels are associated with a reduced risk of cardiovascular events. In addition to pharmacological interventions, such as statin use, which remain central to CVD prevention, dietary strategies are also well-established as effective interventions for reducing CVD risk and related comorbidities.[65] Moreover, TGs are capable of crossing the blood-brain barrier and can induce leptin and insulin resistance, potentially affecting cognition and appetite regulation. Hypertriglyceridemia is commonly observed in individuals with OB and T2DM; thus, reducing TG levels represents a key therapeutic target in weight management and cardiometabolic risk reduction.[66]

A protein intake considered "higher" relative to conventional dietary guidelines has been associated with multiple metabolic benefits, including reduced insulin demand, enhanced fat oxidation, improved satiety, and preservation of lean body mass.[56] It is important to note that these intake levels do not represent excess protein consumption, but rather an adjustment toward physiologically appropriate amounts, particularly for individuals with OW or OB. Despite longstanding concerns regarding the potential impact of higher protein consumption on kidney function, especially in relation to glomerular filtration rate (GFR), current scientific evidence does not support a detrimental effect. Studies comparing diets with varying protein contents have found no significant differences in GFR, a finding that is consistent with the results observed in the present study. Moreover, physiological adaptations such as the 65% increase in GFR observed during pregnancy occur without elevating the risk of kidney damage, suggesting that moderate elevations in protein intake are well tolerated by the kidneys.[67] Additional support for the renal safety of higher-protein, low-carbohydrate dietary patterns comes from the 2-year Dietary Intervention Randomized Controlled Trial, which demonstrated comparable improvements in eGFR among participants adhering to low-fat, Mediterranean, and LCDs. These findings indicate that a properly formulated low-carbohydrate dietary pattern, often accompanied by adequate protein intake, is not only safe but may also be effective in maintaining or enhancing kidney function in individuals with OB, irrespective of the presence of TD2M.[68] Collectively, these results reinforce the renal safety and clinical viability of LCDs that incorporate physiologically appropriate protein levels, particularly when guided by healthcare professionals.

Hepatic health is another important concern due to risk factors such as NAFLD, hepatic steatosis, and cirrhosis. Elevated levels of GGT and ALT may be linked to impaired insulin response and an increased risk of T2DM, particularly among individuals with a BMI above 27 kg/m^2. Previous studies have associated these enzymes with a higher incidence of T2DM over follow-up periods of up to 9 years. GGT, in particular, has been implicated in the development of β-cell dysfunction and is considered an indirect marker of elevated hepatic insulin resistance and impaired insulin secretion. Mechanistically, GGT plays a role in ROS production and the maintenance of intracellular glutathione levels.[69,70] Although GGT is also related to biliary tract function, AST and ALT are considered more specific indicators of hepatocellular health, with ALT being primarily elevated in liver damage. Despite differing degrees of hepatic association, all three enzymes are linked to excessive fat accumulation in the liver.[69] In the present study, GGT levels showed a significant reduction, suggesting a potential decrease in hepatic metabolic stress. In contrast, AST and ALT levels remained stable, indicating preservation of hepatocellular integrity throughout the intervention period. Beyond liver enzyme monitoring, dietary interventions have gained prominence in the context of metabolic dysfunction–associated fatty liver disease (MAFLD). A recent international expert consensus emphasized the central role of nutritional strategies in the prevention and management of MAFLD, particularly in individuals with OB or metabolic syndrome.[71] These recommendations emphasize low-glycemic, nutrient-rich diets and the avoidance of ultra-processed foods, added sugars, and alcohol. Although hepatic imaging and fibrosis markers were not assessed in the present study, the observed improvements in metabolic parameters—including

reduced waist circumference, HOMA-IR, and GGT—highlight the potential translational relevance of carbohydrate-restricted diets for improving hepatic health. Additional reductions in alcohol intake may further enhance these benefits, especially in high-risk populations.

The perception that LCDs are financially inaccessible has often been cited as a barrier to their widespread adoption, particularly when considering health equity. While the cost of lower-carbohydrate dietary patterns can vary substantially depending on food choices and preferences, emerging evidence suggests that these diets can be both affordable and nutritionally adequate when properly planned. A study by Zinn *et al.*[72] challenges the assumption of high cost by demonstrating that a low-carbohydrate and healthy-fat diet had only a modest cost difference compared with New Zealand's national dietary guidelines (NZ$ 51.67 vs. NZ$ 43.42/day for a family of four), representing an additional expense of just NZ$ 2.06/person/day. Zinn *et al.*[72] emphasize that this gap can be further minimized through practical substitutions, such as using sardines instead of salmon, without compromising nutritional quality. Staples like eggs, meats with natural fat, frozen vegetables, and nuts can be incorporated economically into an LCD when consumed in appropriate portions.

Moreover, recent assessments indicate that well-formulated LCDs can be compatible with budget-conscious dietary frameworks. These insights support the notion that cost should not be viewed as an intrinsic barrier to the implementation of low-carbohydrate strategies, particularly given their potential to improve metabolic health and reduce long-term healthcare expenditures. Nonetheless, more detailed analyses are needed to assess affordability and accessibility across diverse socioeconomic groups, ensuring that such dietary approaches are equitably available within public health systems.

In light of the growing body of scientific evidence, current dietary guidelines, which continue to prioritize calorie restriction as the central strategy for weight management, should be critically reassessed.[60,73] Interventions based on LCDs have demonstrated significant benefits for individuals with OB, including improvements in weight, metabolic markers, and cardiovascular risk, often surpassing the outcomes observed with conventional low-fat or calorie-restricted approaches. An important limitation of this study is the reduced number of participants who completed all follow-up assessments. Although 34 individuals were initially enrolled and evaluated at baseline, only 19 completed the full protocol through the second follow-up. This loss to follow-up, while anticipated in real-world outpatient settings, limits statistical power and generalizability of our findings. Nevertheless, as a self-controlled pilot trial, the study was designed to explore feasibility and generate preliminary effect estimates, rather than to provide definitive conclusions. These initial findings reinforce the need for future randomized controlled trials with larger and more diverse populations to validate and expand upon these results.

5. Conclusion

Addressing the global epidemic of OW and OB remains a critical public health priority, as emphasized by the WHO. In Brazil, the high and rising prevalence of OB highlights the urgent need for comprehensive, sustained, and culturally relevant strategies. Nutritional interventions that are accessible, evidence-based, and behaviorally sustainable represent non-invasive and cost-effective approaches for reducing the burden of NCDs. In the present study, implementation of an LCD resulted in clinically meaningful improvements in metabolic and anthropometric parameters, including reductions in HbA1c, waist circumference, and body weight. These improvements were accompanied by favorable shifts in BMI classification, with several participants transitioning from OB to OW or normal weight. Such changes have important implications for reducing chronic disease risk at the population level.

From a public health perspective, LCDs may offer a scalable and adaptable tool for the prevention and management of NCDs, especially when implemented with professional guidance and aligned with local dietary practices. Their relative simplicity, affordability, and potential for integration into primary care and community-based health promotion support their viability for large-scale adoption. Moreover, to strengthen the impact of nutritional strategies, Brazil should also advance regulatory policies—such as controlling the marketing of ultra-processed foods, expanding access to fresh and healthy food, and implementing fiscal measures like taxation on unhealthy products—drawing on successful examples from other countries. In contexts marked by limited resources and territorial inequalities, structured and culturally sensitive dietary interventions, such as LCDs, can support the reorientation of health systems toward prevention, equity, and the promotion of long-term well-being. Future research should further investigate their long-term safety, sustainability, and equity in access, particularly within the framework of Brazil's SUS and national food and nutrition policies. It is important to note that this was a pilot study with a limited sample size. Although the findings are promising, they should be interpreted with caution and considered exploratory. Larger studies involving more

diverse populations are necessary to confirm and expand these results.

Acknowledgments

The authors would like to thank the Coordination for the Improvement of Higher Education Personnel (CAPES) for their support in this study.

Funding

None.

Conflict of interest

The authors declare that they have no competing interests.

Author contributions

Conceptualization: Giselle Foureaux, Laryssa Rosa de Sousa Franckilin, Janaina Koenen, Daniela Godoy Neri

Formal analysis: Janaina Koenen, Carlos Eduardo de Freitas Jorge, Daniela Godoy Neri, Giselle Foureaux

Investigation: Giselle Foureaux, Laryssa Rosa de Sousa Franckilin, Janaina Koenen

Methodology: Giselle Foureaux, Laryssa Rosa de Sousa Franckilin, Janaina Koenen, Maria Vitoria Cota de Abreu

Writing – original draft: Giselle Foureaux, Laryssa Rosa de Sousa Franckilin, Ludmila Lizziane de Souza Lima, Flávio Eduardo Dias Araújo Freitas

Writing – review & editing: Janaina Koenen, Carlos Eduardo de Freitas Jorge

Ethics approval and consent to participate

The study was approved by the local Research Ethics Committee and conducted in accordance with the Brazilian National Health Council's guidelines under the CEP/CONEP system (approval number: 4.961.640; CAAE: 49593220.4.0000.5149). This study was registered at the Brazilian Registry of Clinical Trials (ReBEC) (registration no.: RBR-107jk4tn, UTN no.: U1111-1270-4313, registry link: https://ensaiosclinicos.gov.br/rg/RBR-107jk4tn) before participant enrollment. All participants provided written informed consent before undergoing any study-related procedures.

Consent for publication

All participants provided written informed consent for the publication of anonymized data and results.

Availability of data

The datasets used and/or analyzed during the current study are available from the corresponding author upon reasonable request.

References

1. Garcia CAB, Meira KC, Souza AH, Oliveira ALG, Guimarães NS. Obesity and associated factors in Brazilian adults: Systematic review and meta-analysis of representative studies. *Int J Environ Res Public Health*. 2024;21(8):1022.

   doi: 10.3390/ijerph21081022

2. National Obesity Forum; Public Health Collaboration. *Eat Fat, Cut The Carbs and Avoid Snacking To Reverse Obesity and Type 2 Diabetes*. London: National Obesity Forum, Public Health Collaboration; 2016. Available from: https://phcuk.org/wp/content/uploads/2016/05/eat/fat/cut/the/carbs/and/avoid/snacking/to/reverse/obesity/and/type/2/diabetes/national/obesity/forum/public/health/collaboration.pdf [Last accessed on 2025 May 13].

3. World Health Organization. *Obesity and Overweight*. Geneva: World Health Organization; 2025. Available from: https://www.who.int/news/room/fact/sheets/detail/obesity-and-overweight [Last accessed on 2025 May 13].

4. Centers for Disease Control and Prevention (CDC). *Adult Obesity Facts (NHANES, 2021)*. Atlanta, GA: CDC; 2023. Available from: https://www.cdc.gov/obesity/adult/obesity-facts/index.html [Last accessed on 2025 Dec 08].

5. Tsao CW, Aday AW, Almarzooq ZI, *et al*. Heart disease and stroke statistics-2023 update: A report from the American heart association. *Circulation*. 2023;147(8):e93-e621.

   doi: 10.1161/CIR.0000000000001123

6. Brazilian Ministry of Health. Secretariat of Health Surveillance. Department of Health Analysis and Surveillance of Noncommunicable Diseases. *Vigitel Brazil 2006-2021: Surveillance of Risk and Protective Factors for Chronic Diseases by Telephone Survey*. Brasília, DF: Ministry of Health; 2022. Available from: https://www.gov.br/saude/pt/br/centrais/de/conteudo/publicacoes/svsa/vigitel/vigitel/brasil/2006/2021/vigilancia/de/fatores/de/risco/e/protecao/para/doencas/cronicas/por/inquerito-telefonico.pdf [Last accessed on 2025 Apr 24].

7. Pan American Health Organization (PAHO). *Country Profile of Capacity and Response to Noncommunicable Diseases and Their Risk Factors in the Region of the Americas. Country Capacity Survey Results of 2015*; 2018. Washington, DC. Available from: https://www.paho.org/sites/default/files/9789275119273_eng.pdf [Last accessed on 2025 Apr 24].

8. Brazilian Ministry of Health. *National Food and Nutrition Policy*. 2nd ed. Brasília, DF: Ministry of Health; 2017. (Series B. Basic Health Texts). [Em Português] Available from: https://bvsms.saude.gov.br/bvs/publicacoes/politica_nacional_alimentacao_nutricao.pdf [Last accessed on 2025 May 13].

9. Brazilian Ministry of Health. *National Food and Nutrition Policy*. Brasília, DF: Ministry of Health. [Em Português]; 2020. Available from: https://www.gov.br/saude/pt/br/

composicao/saps/pnan [Last accessed on 2025 May 13].

10. World Health Organization. *Obesity and Overweight*. Geneva: World Health Organization; 2020. Available from: https://www.paho.org/en [Last accessed on 2025 May 04].

11. Zylke JW, Bauchner H. The unrelenting challenge of obesity. *JAMA*. 2016;315(21):2277-2278.

    doi: 10.1001/jama.2016.6190

12. Mariath AB, Grillo LP, Silva RO, *et al*. Obesity and risk factors for the development of chronic non-transmissible diseases among consumers in a foodservice unit. *Cad Saude Publica*. 2007;23(4):897-905.

    doi: 10.1590/s0102-311x2007000400017

13. Cordeiro R, Salles MB, Azevedo MB. Benefits and risks of the low-carbohydrate diet. *Health Focus J*. 2017;9:714-722.

14. World Health Organization (WHO). *Physical Status: The Use and Interpretation of Anthropometry*. Geneva: World Health Organization; 1995. Available from: https://www.who.int/publications/i/item/9241208546 [Last accessed on 2025 May 04].

15. De Onis M, Onyango AW, Borghi E, Siyam A, Nishida C, Siekmann J. Development of a WHO growth reference for school-aged children and adolescents. *Bull World Health Organ*. 2007;85(9):660-667.

    doi: 10.2471/blt.07.043497

16. Tavares EL, Anjos LA. Perfil antropométrico da população idosa brasileira. Resultados da Pesquisa Nacional sobre Saúde e Nutrição. *Cad Saude Publica*. 1999;15(4):759-768.

    doi: 10.1590/S0102-311X1999000400010

17. Institute of Medicine (US). *Weight Gain during Pregnancy: Reexamining the Guidelines*. Washington, DC: National Academies Press; 2009.

    doi: 10.17226/12584

18. Brazilian Ministry of Health. *Health in Brazil 2020-2021; 2021. An Analysis of the Health Situation*. Brasília, DF: Ministry of Health. [Em Português] Available from: https://www.gov.br/saude/pt/br/centrais/de/conteudo/publicacoes/svsa/vigilancia/saude_brasil_2020_2021_situacao_saude_web.pdf/view [Last accessed on 2025 Mar 08].

19. DeFronzo RA, Abdul-Ghani MA. Treatment of prediabetes. *World J Diabetes*. 2015;6(12):1207-1222.

    doi: 10.4239/wjd.v6.i12.1207

20. Leite L, Rocha ED, Brandão-Neto J. Obesity: An inflammatory disease. *J Health Sci*. 2009;2(2):85-95.

    doi: 10.15448/1983-652X.2009.2.6238

21. Brazilian Ministry of Health. Secretariat of Health Surveillance. Department of Health Analysis and Surveillance of Noncommunicable Diseases. *Strategic Action Plan for Coping with Chronic Noncommunicable Diseases and Conditions in Brazil 2021-2030*. Brasília, DF: Ministry of Health; 2021b. Available from: https://www.gov.br/saude/pt/br/centrais/de/conteudo/publicacoes/svsa/doencas/cronicas/nao-transmissiveis-dcnt/09-plano-de-dant-2022_2030.pdf [Last accessed on 2025 May 19].

22. Wood IS, De Heredia FP, Wang B, Trayhurn P. Cellular hypoxia and adipose tissue dysfunction in obesity. *Proc Nutr Soc*. 2009;68(4):370-377.

    doi: 10.1017/S0029665109990206

23. Neels JG, Olefsky JM. Inflamed fat: What starts the fire? *J Clin Invest*. 2006;116(1):33-35.

    doi: 10.1172/JCI27280

24. Prado WL, Lima LC, Caranti DA, *et al*. Obesity and inflammatory adipokines: practical implications for exercise prescription. *Brazilian J Sports Med*. 2009;15(5):378-383.

    doi: 10.1590/S1517-86922009000600012

25. Saad MJA. Obesity, diabetes, and endothelium: Molecular interactions. In: *Endothelium and Cardiovascular Diseases*. Cham: Springer; 2018. p. 639-652.

    doi: 10.1016/B978-0-12-812348-5.00044-1

26. Sippel CA, Bastian RMA, Giovanella J, Faccin C, Contini V, Dal Bosco SMD. Inflammatory processes of obesity. *J Health Care*. 2014;12(42):48-56.

    doi: 10.13037/rbcs.vol12n42.2310

27. Hildebrandt A, Ibrahim M, Peltzer N. Cell death and inflammation during obesity: "Know my methods, WAT(son)". *Cell Death Differ*. 2022;30(2):279-292.

    doi: 10.1038/s41418-022-01062-4

28. Papadopoulou SK, Nikolaidis PT. Low-carbohydrate diet and human health. *Nutrients*. 2023;15(8):2004.

    doi: 10.3390/nu15082004

29. Hu T, Yao L, Reynolds K, *et al*. The effects of a low carbohydrate diet on appetite: A randomized controlled trial. *Nutr Metab Cardiovasc Dis*. 2016;26(6):476-488.

    doi: 10.1016/j.numecd.2015.11.011

30. Harvey W. *On Corpulence in Relation to Disease: With Some Remarks on Diet*. London: Henry Renshaw; 1872.

31. Cutting W. The treatment of obesity. *J Clin Endocrinol Metab*. 1943;3(2):85-88.

    doi: 10.1210/jcem-3-2-85

32. Betoni F, Zanardo VPS, Ceni GC. Evaluation of the use of fad diets by patients attending a specialized nutrition outpatient clinic and their implications for metabolism. *Health Sci Commun*. 2010;9(3):430-440.

    doi: 10.5585/conssaude.v9i3.2322

33. Sampaio LPB. Ketogenic diet for epilepsy treatment. *Arq Neuropsiquiatr*. 2016;74(10):842-848.

doi: 10.1590/0004-282X20160116

34. Goldenberg JZ, Day A, Brinkworth GD, *et al*. Efficacy and safety of low and very low carbohydrate diets for type 2 diabetes remission: Systematic review and meta-analysis of published and unpublished randomized trial data. *BMJ*. 2021;372:m4743.

doi: 10.1136/bmj.m4743

35. Skytte MJ, Samkani A, Petersen AD, *et al*. A carbohydrate-reduced high-protein diet improves HbA1c and liver fat content in weight-stable participants with type 2 diabetes: A randomised controlled trial. *Diabetologia*. 2019;62(11):2066-2078.

doi: 10.1007/s00125-019-4956-4

36. Wang LL, Wang Q, Hong Y, *et al*. The effect of low-carbohydrate diet on glycemic control in patients with type 2 diabetes mellitus. *Nutrients*. 2018;10(6):661.

doi: 10.3390/nu10060661

37. Volek JS, Yancy WS Jr., Gower BA, *et al*. Expert consensus on nutrition and lower carbohydrate diets: An evidence- and equity-based approach to dietary guidance. *Front Nutr*. 2024;11:1376098.

doi: 10.3389/fnut.2024.1376098

38. Trumbo P, Schlicker S, Yates AA, Poos M, Food and Nutrition Board of the Institute of Medicine, The National Academies. Dietary reference intakes for energy, carbohydrate, fiber, fat, fatty acids, cholesterol, protein and amino acids. *J Am Diet Assoc*. 2002;102(11):1621-1630.

doi: 10.1016/S0002-8223(02)90346-9

39. Kuo JC. Ketogenic diet and epigenetic modulation: Role in weight loss and metabolic disease. *Nutrients*. 2019;11(9):2163.

doi: 10.3390/nu11092163

40. Noakes TD, Windt J. Evidence that supports the prescription of low-carbohydrate high-fat diets: A narrative review. *Br J Sports Med*. 2017;51(2):133-139.

doi: 10.1136/bjsports-2016-096491

41. Perna S, Spadaccini D, Rondanelli M, *et al*. Effectiveness of a hypocaloric and low-carbohydrate diet on visceral adipose tissue and glycemic control in overweight and obese patients with type 2 diabetes. *Bahrain Med Bull*. 2019;41(3):159-166.

42. Petrisko M, Brownlow B, DeLuca M, *et al*. Biochemical, anthropometric, and physiological responses to carbohydrate-restricted diets versus a low-fat diet in obese adults: A randomized crossover trial. *J Med Food*. 2020;23(3):206-211.

doi: 10.1089/jmf.2019.0059

43. Koppel S, Swerdlow RH. Neuroketotherapeutics: A modern review of a century-old therapy. *Neurochem Int*. 2018;117:114-125.

doi: 10.1016/j.neuint.2017.10.003

44. Manninen AH. Metabolic effects of the very-low-carbohydrate diets: Misunderstood "villains" of human metabolism. *J Int Soc Sports Nutr*. 2004;1(2):7-11.

doi: 10.1186/1550-2783-1-2-7

45. Phinney SD. Ketogenic diets and physical performance. *Nutr Metab (Lond)*. 2004;1:2.

doi: 10.1186/1743-7075-1-2

46. Ranjan A, Schmidt S, Madsbad S, *et al*. Low-carbohydrate diet impairs the effect of glucagon in the treatment of insulin-induced mild hypoglycemia: A randomized crossover study. *Diabetes Care*. 2017;40(1):132-135.

doi: 10.2337/dc16-1694

47. Kjellberg J, Tange Larsen A, Ibsen R, Højgaard B. The socioeconomic burden of obesity. *Obes Facts*. 2017; 10(5):493-502.

doi: 10.1159/000480404

48. Nilson EAF, Andrade RDC, Brito DA, Oliveira ML. Costs attributable to obesity, hypertension, and diabetes in the Unified Health System, Brazil, 2018 costos atribuibles a la obesidad, la hipertensión y la diabetes en el sistema único de salud de Brasil, 2018. *Rev Panam Salud Publica*. 2020;44:e32.

doi: 10.26633/RPSP.2020.32

49. Kossoff EH, Zupec-Kania BA, Amark PE, *et al*. Optimal clinical management of children receiving dietary therapies for epilepsy: Updated recommendations of the international ketogenic diet study group. *Epilepsia Open*. 2018;3(2):175-192.

doi: 10.1002/epi4.12225

50. Chawla S, Silva FT, Medeiros SA, Mekary RA, Radenkovic D. The effect of low-fat and low-carbohydrate diets on weight loss and lipid levels: A systematic review and meta-analysis. *Nutrients*. 2020;12(12):3774.

doi: 10.3390/nu12123774

51. Sackner-Bernstein J, Kanter D, Kaul S. Dietary intervention for overweight and obese adults: Comparison of low-carbohydrate and low-fat diets. A meta-analysis. *PLoS One*. 2015;10(10):e0139817.

doi: 10.1371/journal.pone.0139817

52. Pogozelski W, Arpaia N, Priore S. The metabolic effects of low-carbohydrate diets and incorporation into a biochemistry course. *Biochem Mol Biol Educ*. 2005;33(2):91-100.

doi: 10.1002/bmb.2005.49403302091

53. Stentz FB, Brewer A, Wan J, *et al*. Remission of pre-diabetes to normal glucose tolerance in obese adults with high-protein versus high-carbohydrate diet: Randomized control trial. *BMJ Open Diabetes Res Care*. 2016;4(1):e000258.

doi: 10.1136/bmjdrc-2016-000258

54. Peiró C, Romacho T, Azcutia V, *et al*. Inflammation, glucose,

and vascular cell damage: The role of the pentose phosphate pathway. *Cardiovasc Diabetol*. 2016;15(1):82.

doi: 10.1186/s12933-016-0406-2

55. Moore LL, Visioni AJ, Qureshi MM, Bradlee ML, Ellison RC, D'Agostino R. Weight loss in overweight adults and the long-term risk of hypertension. *Arch Intern Med*. 2005;165(11):1298-1303.

doi: 10.1001/archinte.165.11.1298

56. Pfeiffer AFH, Kraus A, Albrecht S, *et al*. The effects of different quantities and qualities of protein intake in people with diabetes mellitus. *Nutrients*. 2020;12(2):365.

doi: 10.3390/nu12020365

57. Gregg E, Jakicic J, Blackburn G, *et al*. Association of the magnitude of weight loss and changes in physical fitness with long-term cardiovascular disease outcomes in overweight or obese people with type 2 diabetes: A post-hoc analysis of the look AHEAD randomised clinical trial. *Lancet Diabetes Endocrinol*. 2016;4(11):913-921.

doi: 10.1016/S2213-8587(16)30162-0

58. Hamman RF, Wing RR, Edelstein SL, *et al*. Effect of weight loss with lifestyle intervention on risk of diabetes. *Diabetes Care*. 2006;29(9):2102-2107.

doi: 10.2337/dc06-0560

59. Ross R, Neeland IJ, Yamashita S, *et al*. Waist circumference as a vital sign in clinical practice: A consensus statement from the IAS and ICCR working group on visceral obesity. *Nat Rev Endocrinol*. 2020;16(3):177-189.

doi: 10.1038/s41574-019-0310-7

60. Dehghan M, Mente A, Zhang X, *et al*. Associations of fats and carbohydrate intake with cardiovascular disease and mortality in 18 countries from five continents (PURE): A prospective cohort study. *Lancet*. 2017;390(10107):2050-2062.

doi: 10.1016/S0140-6736(17)32252-3

61. Ivanova E, Myasoedova VA, Melnichenko AA, Grechko AV, Orekhov AN. Small dense low-density lipoprotein as biomarker for atherosclerotic diseases. *Oxid Med Cell Longev*. 2017;2017:1273042.

doi: 10.1155/2017/1273042

62. Feoli AMP, Muniz LC, Dorneles GP, Duarte MM, Andrade VM. Melhora do estilo de vida reduz o Índice de Castelli 1 em indivíduos com síndrome metabólica. *Saúde Pesqui*. 2018;11(3):467-472.

doi: 10.17765/1983-1870.2018v11n3p467-474

63. Da Luz PL, Favarato D, Faria-Neto JR Jr., Lemos P, Chagas AC. High ratio of triglycerides to HDL-cholesterol predicts extensive coronary disease. *Clinics (Sao Paulo)*. 2008;63(4):427-432.

doi: 10.1590/S1807-59322008000400003

64. Bazzano LA, Hu T, Reynolds K, *et al*. Effects of low-carbohydrate and low-fat diets: A randomized trial. *Ann Intern Med*. 2014;161(5):309-318.

doi: 10.7326/M14-0180

65. Wiesner P, Watson KE. Triglycerides: A reappraisal. *Trends Cardiovasc Med*. 2017;27(6):428-432.

doi: 10.1016/j.tcm.2017.01.001

66. Banks WA, Farr SA, Salameh TS, *et al*. Triglycerides cross the blood-brain barrier and induce central leptin and insulin receptor resistance. *Int J Obes (Lond)*. 2018;42(3):391-397.

doi: 10.1038/ijo.2017.274

67. Devries MC, Sithamparapillai A, Brimble KS, *et al*. Changes in kidney function do not differ between healthy adults consuming higher- compared with lower- or normal-protein diets: A systematic review and meta-analysis. *J Nutr*. 2018;148(11):1760-1775.

doi: 10.1093/jn/nxy196

68. Tirosh A, Golan R, Harman-Boehm I, *et al*. Renal function following three distinct weight loss dietary strategies during 2 years of a randomized controlled trial. *Diabetes Care*. 2013;36(8):2225-2232.

doi: 10.2337/dc12-1846

69. Ahn HR, Shin MH, Nam HS, *et al*. The association between liver enzymes and risk of type 2 diabetes: The namwon study. *Diabetol Metab Syndr*. 2014;6:14.

doi: 10.1186/1758-5996-6-14

70. Gautier A, Balkau B, Lange C, *et al*. Risk factors for incident type 2 diabetes in individuals with a BMI of <27 kg/m^2: The role of gamma-glutamyltransferase. Data from the epidemiological study on the insulin resistance syndrome (DESIR). *Diabetologia*. 2010;53(2):247-253.

doi: 10.1007/s00125-009-1579-2

71. Zeng XF, Varady KA, Wang XD, *et al*. The role of dietary modification in the prevention and management of metabolic dysfunction-associated fatty liver disease: An international multidisciplinary expert consensus. *Metabolism*. 2024;161:156028.

doi: 10.1016/j.metabol.2024.156028

72. Zinn C, North S, Donovan K, Muir C, Henderson G. Low-carbohydrate, healthy-fat eating: A cost comparison with national dietary guidelines. *Nutr Diet*. 2020;77(3):283-291.

doi: 10.1111/1747-0080.12566

73. Sato J, Kanazawa A, Makita S, *et al*. A randomized controlled trial of 130 g/day low-carbohydrate diet in type 2 diabetes with poor glycemic control. *Clin Nutr*. 2017;36(4):992-1000.

doi: 10.1016/j.clnu.2016.06.014

ACCSCIENCE PUBLISHING

Journal of Clinical and Translational Research

SHORT COMMUNICATION

Evaluation of the chemical stability of succinylcholine chloride stored in syringes under room-temperature conditions

Jeffrey Klein[1], Timothy Coffey[2], and Stacy Brown[1]*

[1]Department of Pharmaceutical Sciences, Bill Gatton College of Pharmacy, East Tennessee State University, Johnson City, Tennessee, United States of America

[2]Regulatory Affairs, Ballad Health, Johnson City, Tennessee, United States of America

Abstract

Background: Succinylcholine chloride is essential for achieving neuromuscular blockade during emergency airway management. The manufacturer specifies a 14-day stability period for 20 mg/mL vials at room temperature, which limits implementation of prefilled-syringe protocols. **Aim:** This study aims to investigate the chemical stability of succinylcholine chloride after transfer from manufacturer vials to polypropylene syringes during extended room-temperature storage. **Methods:** A validated high-performance liquid chromatography with ultraviolet detection (HPLC-UV) method was developed to quantify percent recovery. Ten 20 mg/mL succinylcholine chloride vials were used: five samples were stored refrigerated (2–8°C; controls; $n = 5$), and five were transferred to polypropylene syringes and stored at room temperature (20–25°C; $n = 5$). Samples were analyzed over 90 days. The HPLC-UV method met United States Pharmacopeia criteria for accuracy, precision (<5% error and % relative standard deviation), and linearity ($R^2 > 0.99$). **Results:** Succinylcholine chloride maintained >90% of the initial concentration over 90 days in polypropylene syringes stored at room temperature (93.13% on day 90) and in refrigerated controls (93.97% on day 90). No significant differences were observed between storage conditions ($p>0.05$). All samples remained physically stable, with no visible color change or precipitate. **Conclusion:** Despite its ester bonds, succinylcholine chloride remained chemically stable in polypropylene syringes for up to 90 days at room temperature. **Relevance for Patients:** These findings support the extended stability of prefilled succinylcholine syringes, which may improve emergency preparedness; however, sterility validation remains necessary before clinical implementation.

Keywords: Succinylcholine chloride; Neuromuscular blocking agents; Drug stability; High-performance liquid chromatography–ultraviolet detection; Prefilled syringes; Emergency medicine

***Corresponding author:**
Stacy Brown
(browsd03@etsu.edu)

Citation: Klein J, Coffey T, Brown S. Evaluation of the chemical stability of succinylcholine chloride stored in syringes under room-temperature conditions. *J Clin Transl Res.* 2026;12(1):88-94. doi: 10.36922/JCTR025280039

Received: July 9, 2025

Revised: January 9, 2026

Accepted: January 12, 2026

Published online: February 3, 2026

1. Introduction

Rapid sequence intubation (RSI) is one of the most time-critical procedures in emergency medicine, requiring immediate availability of injectable neuromuscular blocking agents. Succinylcholine chloride is the preferred agent for RSI due to its rapid

onset and short duration with predictable recovery.[1] In contrast, rocuronium has a longer duration and requires a reversal agent.[2] As such, the ready availability of the preferred neuromuscular blocking agent (succinylcholine chloride) during an intubation may significantly impact patient outcomes.[1,2]

The structure of succinylcholine chloride contains two ester bonds, notorious for hydrolytic instability (Figure 1), yet several studies have indicated that succinylcholine chloride retains its chemical integrity well beyond the 14-day beyond-use date (BUD) indicated by the manufacturer.[3] This is particularly relevant given that a 14-day BUD could constrain emergency preparedness, especially when prefilled syringes would be a viable tool to ensure rapid medication availability.

Previous stability investigations of succinylcholine chloride have indicated that its chemical stability indeed exceeds 14 days. Adnet *et al.*[4] investigated the degradation rate of succinylcholine chloride using nuclear magnetic resonance spectroscopy, and reported a 1.2%/month degradation rate for the 20 mg/mL solution when stored at room temperature. Another research team examined succinylcholine chloride, among other drugs, when stored at ambient temperatures, often exceeding the United States Pharmacopeia (USP) definition of room temperature (20–25°C).[5,6] They found that succinylcholine chloride, in its manufacturer's ampule, retained 89% of the theoretical concentration after 12 months.[5] Similarly, Merlin *et al.*[7] demonstrated that succinylcholine chloride, when stored in a prehospital setting in the manufacturer's vials, protected from light, retained >90% potency, and was not significantly vulnerable to changes in temperature. However, by analyzing degradation products by mass spectrometry, they demonstrated that degradation was apparent even at the study's initiation, evidenced by detectable levels of succinyl monocholine and choline. These studies align with an earlier investigation demonstrating the resistance of succinylcholine chloride to various manipulations, including the addition of preservatives and sterilization by the hospital pharmacist.[8]

To facilitate workflow, some hospitals may desire to aliquot drug products into syringes. The ability to prefill syringes and store them at room temperature enables timely dosing and may help mitigate dosing errors that could occur when withdrawing drug product from the bulk container.[9,10] A 2024 systematic review of prefilled syringe applications reported consistent reductions in medication errors, adverse events, preparation time, and drug waste.[11] For succinylcholine chloride, these advantages are particularly pronounced given the high stress and time-sensitive scenarios that characterize its use.[1] Despite data supporting the chemical stability of succinylcholine chloride against chemical degradation, most health care systems would not authorize transferring a drug product to a secondary container without data to support such manipulation. Vials of succinylcholine chloride may be stored at 2–8°C for 30 days or at room temperature for up to 14 days, per the manufacturer's labeling.[3] Therefore, we aim to examine the stability of succinylcholine chloride when transferred from the manufacturer's container into 1-mL polypropylene syringes.

The percentage recovery of the aliquoted drug was monitored for 90 days using high-performance liquid chromatography (HPLC) with ultraviolet (UV) detection, a gold standard for drug stability analysis.[12-14] The 90-day study period was selected to support emergency department and emergency medical service (EMS) preparedness while providing data for BUD decisions.

2. Materials and methods

2.1. Equipment and chromatographic conditions

All chromatographic analyses were performed using an HPLC system with UV detection (LC-20ADXR pumps, SIL-20ACXR autosampler, CBM-20A controller, CTO-20A column oven, and SPD-20A UV detector,

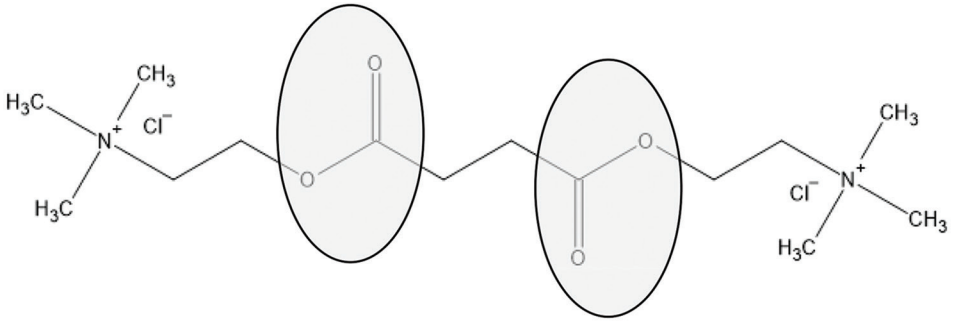

Figure 1. Chemical structure of succinylcholine chloride. The two ester bonds (circled) contribute to the compound's hydrolytic instability.

Shimadzu Scientific, Japan). The detection wavelength was optimized at 218 nm based on succinylcholine's UV absorbance characteristics.[15] The mobile phase consisted of liquid chromatography–mass spectrometry (LC–MS) grade 0.01% trifluoroacetic acid in water and LC–MS grade acetonitrile (60:40) (Honeywell Burdick and Jackson, USA) at a flow rate of 0.400 mL/min. Chromatographic separation was achieved using an HPLC column (150 × 4.6 mm; 3.5-µm particle size) (XBridge C18, Waters Corporation, USA). Succinylcholine chloride calibration standards (5–25 mg/mL) were prepared daily using a USP-grade reference standard (USP Reference Standard, USA) in a 50:50 acetonitrile: water mixture. Anectine® (succinylcholine chloride injection, 200 mg/10 mL) was used for the stability investigation (Sandoz, USA). All samples were filtered using a 13-mm 0.2-µm syringe filter (Whatman® Puradisc, Cytiva, USA) before analysis. Sample injection volume was 30 µL, with autosampler (Fisher Scientific, Waltham, USA) purging (2-propanol) between injections.

2.2. HPLC with UV detection method validation procedures

Validation was performed in accordance with USP General Chapter <1225>, focusing on system suitability, precision, accuracy, and linearity.[16] For system suitability, each 20 mg/mL calibration sample chromatogram (100% assay level) was required to meet the criteria of resolution ≥2.0, tailing factor ≤2.0, and column efficiency (theoretical plates) ≥2,000. Benchmarks for precision and accuracy were < 5% relative standard deviation (RSD) and <5% error, respectively. For these experiments, three replicates of each concentration, 15 mg/mL (75% assay level), 20 mg/mL (100% assay level), and 25 mg/mL (125% assay level), were evaluated over three days. Finally, linearity over the range of 5–25 mg/mL was evaluated on each day of the stability investigation. The linearity target was a coefficient of determination (R^2) > 0.99.

2.3. Stability study setup

The stability study was designed to encompass unit-dosing in syringes and room-temperature storage. Ten vials of succinylcholine chloride from a single lot (AA0058, expiration 04/2025) were obtained to eliminate the possibility of cross-lot variability. Vials were randomly allocated into two storage conditions: 5 vials remained in the manufacturer's original container and stored under refrigerated conditions (2–8°C) as controls, while 5 vials were aliquoted into 1-mL polypropylene syringes and stored at room temperature (20–25°C), representing the experimental group. Sampling time points (0, 24, 48 h; 7, 14, 21, 30, 60, 90 days) were selected to capture both early stability patterns and long-term degradation trends. At each time point, samples from each of the five replicate vials/syringes per condition were analyzed in triplicate. For these analyses, succinylcholine concentrations were determined by comparing peak areas to a freshly prepared calibration curve generated from reference-standard calibration solutions. Calculated concentrations were expressed as percentage recovery relative to day 0 samples (designated as 100% initial concentration). Statistical comparisons between experimental and control samples were performed using a two-way analysis of variance (ANOVA) (p<0.05) using GraphPad Prism software (Version 9.5.1, GraphPad Software, Inc., USA). These analyses did not assess bioequivalence.

3. Results

3.1. HPLC with UV detection method validation results

The HPLC–UV method was adapted from an LC–MS assay previously used for the quantification of various neuromuscular blocking agents, including succinylcholine chloride.[17] An example chromatogram of succinylcholine chloride, with a retention time of about 3.5 min at the 100% assay level, is shown in Figure 2. Validation metrics are summarized in Table 1. Notably, the tailing factor, theoretical plates, and resolution all meet the USP <1225> benchmarks, indicating symmetrical peaks well separated from other formulation components. Linearity assessment revealed excellent correlation between concentration and detector response across the 5–25 mg/mL range, with R^2 exceeding the acceptance criteria of 0.99. The calibration range was chosen so that 20 mg/mL corresponded to 100% assay concentration for the stability study, representing the concentration of the commercial product. As such, the samples could be introduced into the HPLC vials for analysis without manipulation, eliminating a source of error. Precision and accuracy evaluation demonstrated the method's suitability for stability investigations, with % RSD and % error well within the ≤5% threshold.

3.2. Chemical stability over 90 days

Analytical performance remained robust throughout the stability investigation, with all system suitability criteria consistently satisfied. The chromatogram shown in Figure 3 illustrates the typical separation quality achieved at study initiation. Complete resolution of the succinylcholine chloride peak from formulation components was maintained across all samples, ensuring accurate quantification throughout the 90 days.

All samples maintained excellent physical stability throughout the 90-day study period, with no visual

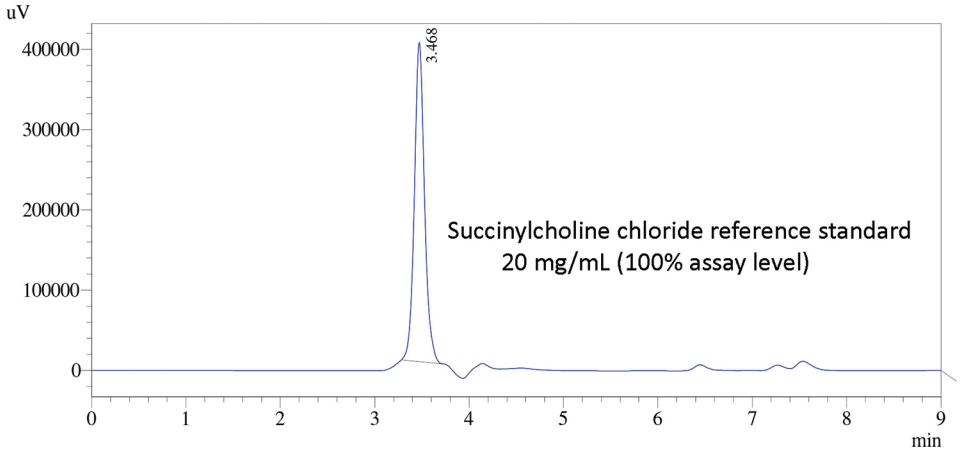

Figure 2. Representative high-performance liquid chromatography chromatogram of succinylcholine chloride reference standard

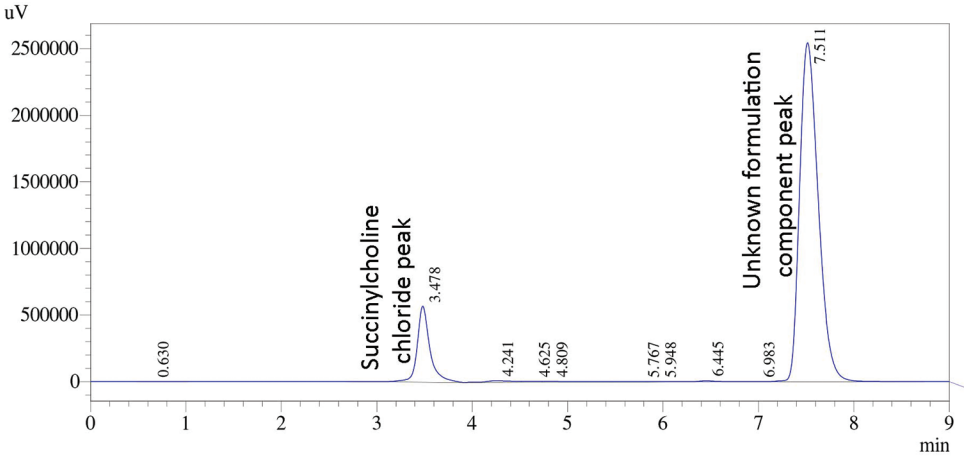

Figure 3. High-performance liquid chromatography chromatogram of the study sample at Day 0. The representative chromatogram shows separation from formulation excipients.

Table 1. High-performance liquid chromatography with ultraviolet detection method validation data

Validation criteria	Results
System suitability	Average tailing factor=1.18 Average theoretical plates (N)=4,112 Average resolution=9.275
Linearity	R^2=0.9974 Calibration range: 5–25 mg/mL
Accuracy (% error)	75% assay level=2.08 100% assay level=0.85 125% assay level=1.07
Precision (% relative standard deviation)	75% assay level=2.93 100% assay level=3.24 125% assay level=1.88

Note: Validation parameters were evaluated over three days, according to United States Pharmacopeia Chapter<1225>.

evidence of precipitation, crystallization, or discoloration. In addition, succinylcholine chloride demonstrated remarkable chemical stability throughout the 90-day study period, with both storage conditions maintaining >90% recovery (Table 2, Figure 4). Room-temperature syringe samples retained 93.13% recovery at day 90, representing only a 6.87% degradation over the 3-month period. Refrigerated controls were very similar (93.97% at day 90), indicating that the temperature differential between storage conditions had minimal impact on chemical degradation. The stability profile showed gradual, linear degradation over time, without evidence of accelerated degradation phases. This pattern supports the previously cited predictable degradation kinetics.[4]

Statistical analysis using two-way ANOVA confirmed

Table 2. Succinylcholine chloride concentration (mg/mL) data throughout the 90-day stability study

Storage period	Experimental samples (room-temperature syringe storage; 20–25°C)	Control samples (refrigerated manufacturer container; 2–8°C)
Initial concentration	20.48±0.44	20.48±0.44
24-h storage	20.31±0.63 (99.16)	20.42±0.38 (99.76)
48-h storage	20.27±0.33 (98.96)	20.43±0.43 (99.76)
7-d storage	20.11±0.40 (98.20)	20.15±0.60 (98.40)
14-d storage	19.99±0.25 (97.59)	20.06±0.18 (97.93)
21-d storage	19.82±0.28 (96.71)	19.93±0.28 (97.29)
30-d storage	19.55±0.30 (95.48)	19.66±0.22 (95.98)
60-d storage	19.12±0.36 (93.37)	19.31±0.34 (94.27)
90-d storage	19.07±0.25 (93.13)	19.25±0.26 (93.97)

Note: Values represent mean concentration (mg/mL)±standard deviation (% recovery) from n=5 replicate samples analyzed in triplicate injections at each time point. Percentages in parentheses indicate percent recovery relative to Day 0 concentration (defined as 100%).

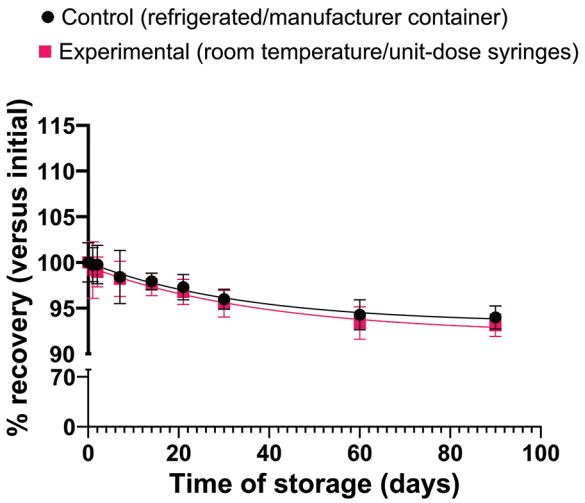

Figure 4. Succinylcholine chloride percent recovery relative to Day 0 throughout a 90-day storage period. Data are presented as mean recovery ± standard deviation (n = 5 samples with triplicate injections at each time point).

no significant differences between storage conditions at any time point (p>0.05), with confidence intervals remaining narrow throughout the study, indicating consistent performance across all replicate samples. This analysis assessed whether there were significant differences between storage conditions, but it is insufficient to demonstrate bioequivalence.

4. Discussion

Our findings show > 90% recovery of injectable succinylcholine chloride over 90 days, consistent with 89% potency after 12 months[5] and with > 90% potency in prehospital settings at elevated temperatures previously shown.[7] The degradation rate of succinylcholine chloride reported in this study is approximately 2.3% per month, similar to what was reported by Adnet *et al.*[4] Our work supplements prior findings by demonstrating that chemical stability extends to succinylcholine chloride transferred to secondary containers. These results suggest that the manufacturer's 14-day room-temperature limit may be conservative regarding chemical stability. These data support the chemical stability of succinylcholine chloride when stored in syringes for up to 90 days. In addition, collecting these data from room-temperature syringes aligns with realistic emergency department and EMS storage conditions. Demonstrating chemical stability in secondary containers is a necessary first step toward potentially extending BUD, thereby reducing medication waste. Furthermore, prefilled syringes could improve emergency response times, reducing dosing errors in critical emergencies.[9,11]

The choice of polypropylene syringes for this work was based on literature supporting this polymer's compatibility with small-molecule drugs.[18-20] The absence of a statistically significant difference between syringe-stored samples and those in the manufacturer's container (p>0.05) is consistent with polypropylene compatibility for succinylcholine chloride storage. However, alternative syringe materials, different concentrations, or different storage conditions may yield different results and would require separate validation.

Analytical validation confirmed the method's suitability for stability assessment, with all USP <1225> parameters consistently meeting acceptance criteria throughout the 90-day investigation. Unlike previous LC–MS investigations that detected early formation of succinyl monocholine and choline,[7] UV detection at 218 nm did not reveal observable degradation products. This difference likely reflects the inherent sensitivity limitations of UV detection compared to mass spectrometry, or potentially indicates that degradation product concentrations remained below the method's detection threshold. Future investigations monitoring impurity formation will require more advanced equipment, such as LC–MS, to detect low-level degradation products. Future studies should evaluate additional syringe materials and extend the study duration beyond 90 days.

Finally, the most significant limitation of this investigation is the absence of sterility testing. A recent systematic review indicates that among 24 studies involving prefilled syringes, only four (17%) evaluated sterility and

contamination.[11] Extended beyond-use dating requires both chemical stability and microbiological safety, the latter being paramount for parenteral medications. This study establishes a critical foundation, but future studies monitoring product sterility to ensure microbial integrity of the injectable product will be needed to fully implement succinylcholine in secondary containers.

5. Conclusion

This investigation demonstrates that succinylcholine chloride maintains >90% recovery when stored in 1-mL polypropylene syringes at room temperature for 90 days, exceeding the manufacturer's 14-day recommendation. The absence of significant differences between room-temperature syringe storage and refrigerated storage indicates that container transfer does not compromise drug stability. The chemical stability validation eliminates a key barrier to implementing prefilled syringe protocols, which have been shown to reduce medication errors (10–73%), decrease adverse event rates, and minimize waste (from 46–92% to 0–15%).[11] The chemical stability demonstrated here, if complemented by appropriate sterility validation, could support improvements in emergency airway management workflows while maintaining the chemical integrity essential for effective neuromuscular blockade.

Acknowledgments

The authors would like to acknowledge the provision of materials from Ballad Health.

Funding

This study was supported by the Bill Gatton College of Pharmacy, East Tennessee State University.

Conflict of interest

The authors declare that they have no competing interests.

Author contributions

Conceptualization: Timothy Coffey, Stacy Brown
Data curation: Jeffrey Klein
Formal analysis: Stacy Brown
Funding acquisition: Stacy Brown
Investigation: Jeffrey Klein
Methodology: Stacy Brown, Jeffrey Klein
Project administration: Timothy Coffey, Stacy Brown
Software: Stacy Brown
Resources: Timothy Coffey, Stacy Brown
Supervision: Stacy Brown
Validation: Stacy Brown, Jeffrey Klein
Visualization: Timothy Coffey
Writing-original draft: Stacy Brown, Jeffrey Klein
Writing-review & editing: Stacy Brown

Ethics approval and consent to participate

Not applicable.

Consent for publication

Not applicable.

Availability of data

Not applicable.

Further disclosure

The HPLC-UV method development and validation that supported this study were previously presented (prior to initiation of the stability study) as a poster at the Appalachian Student Research Forum (ASRF), April 5, 2024, Johnson City, Tennessee, United States, titled "Chemical Potency of Succinylcholine Chloride Stored in Room-Temperature Syringes."

References

1. Stollings JL, Diedrich DA, Oyen LJ, Brown DR. Rapid-sequence intubation: A review of the process and considerations when choosing medications. *Ann Pharmacother*. 2014;48(1):62-76.

   doi: 10.1177/1060028013510488

2. Mace SE. Challenges and advances in intubation: Rapid sequence intubation. *Emerg Med Clin North Am*. 2008;26(4):1043-1068, x.

   doi: 10.1016/j.emc.2008.10.002

3. Sandoz Inc. *Anectine® (Succinylcholine Chloride Injection, USP)* [Prescribing Information]. Switzerland: Sandoz Inc.; 2010.

4. Adnet F, Le Moyec L, Smith CE, Galinski M, Jabre P, Lapostolle F. Stability of succinylcholine solutions stored at room temperature studied by nuclear magnetic resonance spectroscopy. *Emerg Med J*. 2007;24:168-169.

   doi: 10.1136/emj.2006.041053

5. United States Pharmacopeial Convention. <659> packaging and storage requirements. In: *Revision Bulletin*. Maryland: United States Pharmacopeia; 2017.

6. Welter C, Roschel K, Schneider S, Marson C, Stammet P. Impact of ambient temperature on 5 emergency drugs aboard an emergency medical car over a 1-year period. *Ann Emerg Med*. 2022;80(4):358-363.

   doi: 10.1016/j.annemergmed.2022.05.001

7. Merlin MA, Marques-Baptista A, Yang H, Ohman-Strickland P, Aquina C, Buckley B. Evaluating degradation with fragment formation of prehospital succinylcholine by mass spectrometry. *Acad Emerg Med*.

2010;17(6):631-637.

doi: 10.1111/j.1553-2712.2010.00766.x

8. Schmutz CW, Muhlebach SF. Stability of succinylcholine chloride injection. *Am J Hosp Pharm*. 1991;48(3):501-506.

doi: 10.1093/ajhp/48.3.501

9. Moreira ME, Hernandez C, Stevens AD, *et al*. Color-coded prefilled medication syringes decrease time to delivery and dosing error in simulated emergency department pediatric resuscitations. *Ann Emerg Med*. 2015;66(2):97-106.e3.

doi: 10.1016/j.annemergmed.2014.12.035

10. Whitaker DK. Pre-filled syringes and safe total intravenous anaesthesia practice. *Anaesthesia*. 2019;74(5):674-684.

doi: 10.1111/anae.14591

11. Benhamou D, Weiss M, Borms M, *et al*. Assessing the clinical, economic, and health resource utilization impacts of prefilled syringes versus conventional medication administration methods: Results from a systematic literature review. *Ann Pharmacother*. 2024;58(9):921-934.

doi: 10.1177/10600280231212890

12. Hassouna MEM, Mohamed MA. UV-spectrophotometric and stability indicating RP-HPLC methods for the determination of the hepatitis C virus inhibitor Sofosbuvir in tablet dosage form. *Anal Chem Lett*. 2018;8(2):217-229.

doi: 10.1080/22297928.2017.1410441

13. Kirk LM, Brown SD. Beyond-use date determination of buprenorphine buccal solution using a stability-indicating high-performance liquid chromatographic assay. *J Feline Med Surg*. 2015;17(12):1035-1040.

doi: 10.1177/1098612x15569329

14. Pippalla S, Nekkalapudi AR, Jillellamudi SB, Reddy MP, Kumar CV. A stability-indicating, reversed-phase HPLC method for quantification of assay and organic impurities in doxycycline hyclate bulk and parenteral dosage forms. *Biomed Chromatogr*. 2023;37(6):e5626.

doi: 10.1002/bmc.5626

15. Foss PRB, Benezra SA. Succinylcholine chloride. In: Florey K, Bishara R, Brewer GA, *et al*, editors. *Analytical Profiles of Drug Substances*. Vol 10. United States: Academic Press; 1981. p. 691-704.

doi: 10.1016/s0099-5428(08)60655-3

16. US Pharmacopeia. United states pharmacopeia and national formulary (USP 37 - NF 32). In: *Validation of Compendial Procedures*. Ch. 1225. United States: US Pharmacopeia; 2014.

17. Gonzalez-Estrada A, Archibald T, Dinsmore K, Moiser G, Campbell B, Brown S. Stability of diluted neuromuscular blocking agents utilized in perioperative hypersensitivity evaluation. *Allergy*. 2018;73(12):2398-2400.

doi: 10.1111/all.13576

18. Targett PL, Keefe PA, Merridew CG. Compatibility and stability of drug adjuvants and morphine tartrate in 10 mL polypropylene syringes. *Aust J Hosp Pharm*. 1997;27:207-210.

doi: 10.1002/jppr1997273207

19. Donnelly RF. Physical compatibility and chemical stability of bupivacaine and hydromorphone in polypropylene syringes. *Can J Hosp Pharm*. 2004;57(4):230-235.

20. Ayed WB, Drira C, Soussi MA, *et al*. Physical and chemical stability of cytarabine in polypropylene syringes. *J Oncol Pharm Pract*. 2020;27(4):827-833.

doi: 10.1177/1078155220937405

Journal of Clinical and Translational Research

Journal of Clinical and Translational Research (JCTR) welcomes submissions from various research topics that are centered on solving clinically-driven issues to ultimately benefit patients.

You will benefit from the following key features of JCTR as our author:

- Open access
- Author-friendly guidelines: 'your paper, your way'
- Reputable editorial board
- No word count or reference restrictions
- Double-blind review process to minimize bias
- Rapid production and publication
- Broad scope, interdisciplinary research exchange platform

The research areas that JCTR covers include, but are not limited to:

Internal medicine (all branches)	Gastroenterology and hepatology
Vascular medicine and phlebology	Surgery and transplantation
Oncology	Hematology
Cardiology	Nephrology
Intensive care medicine	Dermatology
Ophthalmology	Endocrinology and metabolism
Neurology and neurosciences	Anesthesiology
Anatomy, physiology, and embryology	Radiology and nuclear medicine
Pathology	Clinical chemistry
Clinical physics	Genetics and epigenetics
Epidemiology	Global health
Medical devices	Nutrition
Pharmacology	Immunology
Microbiology	Virology
Parasitology	Biomedical engineering

Biomedical spectroscopy and spectrometry

Thanks for considering the Journal of Clinical and Translational Research.

Editorial team JCTR

https://accscience.com/journal/JCTR

Contact
www.accscience.com
9 Raffles Place, Republic Plaza 1 #06-00 Singapore 048619
Email: editorial@accscience.com
Phone: +65 8182 1586